C-C BOND FORMATION AND ELECTRON-PROTON TRANSFER REACTIONS IN UNUSUAL MEDIA

A THESIS SUBMITTED TO THE
SAVITRIBAI PHULE PUNE UNIVERSITY

FOR THE DEGREE OF
DOCTOR OF PHILOSOPHY
IN CHEMISTRY

BY

ARPAN MANNA

Dr. ANIL KUMAR
(RESEARCH GUIDE)

PHYSICAL AND MATERIALS CHEMISTRY DIVISION
CSIR-NATIONAL CHEMICAL LABORATORY
PUNE-411008
INDIA

SEPTEMBER 2014

CERTIFICATE

This is to certify that the work incorporated in this thesis entitled, "**C-C Bond formation and electron-proton transfer reactions in unusual media** " submitted by **Mr. Arpan Manna**, for the degree of **Doctor of Philosophy** to **Savitribai Phule Pune University**, was carried out by the candidate under my supervision in the Physical and Materials Chemistry Division, CSIR-National Chemical Laboratory, Pune-411008, India. Any material that has been obtained from other sources has been duly acknowledged in the thesis.

Date:

Place: Pune

Dr. Anil Kumar

(Research Guide)

DECLARATION

I, Mr. Arpan Manna, hereby declare that the work incorporated in the thesis entiled "**C-C Bond formation and electron-proton transfer reactions in unusual media**" submitted by me to **Savitribai Phule Pune University** for the degree of **Doctor of Philosophy** is original and has not been submitted to this or other University or Institution for the award of Degree or Diploma. Such material, as has been obtained from other sources has been duly acknowledged.

Date:

Place: Pune

Arpan Manna

DEDICATED TO

My

Treasured Baba and Ma

who paved my way towards light. . .

Contents

Acknowledgements

It is a pleasant opportunity to express my gratitude for all of them who have accompanied and supported throughout the time-scale of my doctoral studies. Although it is the helpfulness of uncountable individuals, the following personalities are those I reckon most coming out of my instant recalling.

First, I want to acknowledge my guide **Dr. Anil Kumar**, for giving me the opportunity to work under him. It has been a great learning experience both professionally and personally. He has been an excellent teacher and a great mentor. I have sensed his great power to motivate the student when he/she is down and cut him off when he/she is jumping with excitement. His personality, down to earth attitude, and his unique sense of humor has played a great deal in transforming my character during this journey from boyhood to manhood and going to keep an everlasting imprint in my life. He has guided me with his invaluable suggestions, lightened up the way in my darkest times and encouraged me a lot in the academic life. From him I have learned to think critically, to select problems, to solve them and to present their solutions.

I owe my sense of gratitude to **Prof. Haridas Pal**, Head, Molecular Photochemistry Section, Radiation and Photochemistry Division, BARC for his timely support, invaluable guidance, and encouragements during the collaboration which helped me to expose in the field of photo physics and their application in chemistry. I have always been enthralled by his expertise in the field of photophysics and photochemistry. His never-dying spirit, organized way of doing the things, attitude to always hang on with ever smiling face taught me how to face hurdles in life both in professional and personal front.

It is my great privilege to acknowledge Dr. Manoj Kumbhakar,Scientist, Molecular Photochemistry Section, Radiation and Photochemistry Division, BARC for his invaluable support in carrying out electron transfer experiments. I warmly acknowledge him for being the perpetual source of encouragement, advocacy, assurance and emotional refuelling to me during my one of the toughest time of research. My special thanks go to Dr. Mehjabeen Syed, Dr. Sukhendu Nad, Mr. Arun

Vora for their suggestions and cooperation obtained during the research works. Their diversified help and moral support will always be remembered.

I must thank Dr. Amol Kulkarni and Dr. P R. Rajamohanan for their timely help, and guidance to me to resolve complicated NMR spectra and measurement of bubble size.

I sincerely acknowledge Dr. Sourav Pal (Director, NCL) and Dr. S. Sivaram (Former Director, NCL) for providing the infrastructure and facilities for my research. Valuable suggestions and encouragements from Dr. P A Joy, Dr. B L V Prasad, Dr. C S Gopinath, Dr. Sayam Sengupta, Dr. Srinivas Hota, Dr. S K Ghosh, Dr. Pravat Kumar Singh, Dr. Sharmistha Dattagupta, Dr. (Mrs.) Vaijayanti Kumar, Dr. A K Satpati, Prof. Satyen Saha, Prof. Biswajit Maity, Prof. S K Sengupta, Prof. Chandan K Pal, and Prof. Rana Sen are gratefully acknowledged.

I am fortunate to have a number of dedicated teachers from my early education to university who have profoundly contributed to build what I am today. I pay my heart filled gratitude for their indomitable inspiration in shaping my personality.

I thank my lab seniors Dr. Promod Sonawane, Dr. Suvarna Deshpande, Mr. Sanjay Pawar, Dr. Dilip Satpute, Dr. Diganta Sarma for making life comfortable in the initial difficult phase. I have learnt a lot about the experimental and theoretical aspects of the subject from my seniors Dr. Shraeddha Tiwari, Dr. Nageshwar Khupse, Dr. Gitanjali Rai. I will cherish the comforting and jovial presence of Amitda, Shashi, Anshu, Raju, Anirban, Sachin, Preeti and Vijay in the laboratory during very difficult phase of my research works.

Friends are the essential gifts of life who rise themselves up irrespective of situation to make the life colourful. My stay on this campus has been pleasant with the association of all the research scholars at CSIR NCL. I will surely miss the company of Sumantra da, Partha da, Mrinmoy, Tamas da, Kanak, Anjan, Saikat da, Pravat, Joyashis da, Patida, Krishanu da, Animesh da, Binoy da, Anal da, DD da, Shyam da, Sajal da, Munmun, Subha, Tanaya, Preeti Sarma, Bindhu, Jayaprabha, Mangesh da, Anantha, Govinda, Sovanda, Himadri da, Saili, Ramsundar, Negi, Manoj Mane, Raja, Eldo, Rami, Yenchalwar, Kale, Sathe, Babasaheb, Anup Tathod, Prakash, Anjali, Mohan, Ashvini, Beena di, Khwaja, Lenin, Manju, Paulamidi, Arun, Pravin, Arijit, Deepa, Ravi, Jaya, Puja, Jhumur, Karthika, Balangulu, Jayesh, Prabhu, Rohan, Rupesh, Preeti, Puneet, Anupam, Nardele, Praveen, Chitanya, Rajaperumal, Mausami, Chnadrashekar, Anupamda, Late Agnimitra Banerjee, Susanta, Anirudhya, Abhik, Abhigyan, Souvik, Doss, Prithvi, Sujit da, Debasis da, Kakada, Garaida, Prathit,

Basab da, Prathit, Chandan Da, Chandan Choudhury, Nivedita di, Amrita, Swagata, Sujit, Chakadola, Soumiya, Pushpanjali, Debarati di, Smita, Sumit, Biplab, Jitu, Brijesh, P3, Mishraji, Krunal, Dama, Rustam, Doctor, Lakshman, Chinmay, Jitu, Kaushalendra, Kiran, Deepak bhaiya, Prabhakar, Pankaj, Wahid, Manjoor, Saleem, Majid, Devraj, Manoj (Sharma), Brijesh, Anand, Suneel, Yadagiri, Shantivardhan, Yogesh, Pradeep, Kachuri, Ashok, Kailash, Sujit, and Atul with whom I used to share knowledge, time, playgrounds and several joyful moments of social life.

My associations with Amitda, Anirban, Sachin, Kanak, Abhik, Anup, Hridesh, Achintya, Chini and Mishra ji have been the source of fountain of memories. I am never going to forget our bike trips, roof top parties, many triumphs and some disasters, but all enjoyed together. May be we have been brothers in some previous incarnation.

I would also like to thank my all juniors Anup, Soumen Das, Saibal, Sudip, Shantanu, Prasenjit, Atanu, Santu, Sandip, Amit, Soumen Dey, Atreyee, Monalisa, Rupa, Piyali Arunava, Shantigopal, Hridesh, Soumyojyoti, Pooja, Seema, Jenofar, Bikas, Subhra, Late Siswa, Tapas, Pranab, Santunu, Bhojgude, Bappa, Manik, Suman, Chayanika, Jagadish, Ramkrishna, Saibal Bera, Kaushik, Akram, Soumo, Ekta, Arjun, Collins, Manoj, Firoj, Tamal, Mahitosh for cheering me up and guileless support for the completion of this work.

I am fortunate to have persons like Gitanjali di, Anshu Preeti, Monalisa for their sisterly care during my stay in Pune.

My university roommate Azmeera will always have a special place in my life. Special thanks should be extended to my GJ roommate Aryya for his immense patience to tolerate my nuisances. I cordially thank Srija for being with me, the closest individual with whom I have shared every aspect of life.

It is my pleasure to acknowledge the help rendered by all staff members of Physical and Materials Chemistry Division, CSIR-NCL at different times. Financial support from CSIR, New Delhi during my doctoral learning is highly acknowledged.

It will be insufficient and injustice to document the gratitude on the small space of a paper for my parents and their selfless sacrifice to build me what I am today. On this occasion I am crouching down before my ma for the endless struggle she has accomplished to organize me ‘brick by brick’. The unflinching faith of my baba and late grandparents in my abilities and their generous patience kept me going through the most struggling times of my carrier. I am equally opportune have love and blessings from the relatives both of my paternal and maternal sides.

At last I wish to conclude with a pray to the Almighty;

"Pardon me if I feel tired – pardon me my Lord
Pardon me if ever I lag behind on the road.
If my heart trembles like this, as it does today
Ignore that pang and pardon me Lord."

Abstract

C-C bond Formation and Electron-proton Transfer Reactions in Unusual Media

In the present thesis, we focus on the delineation of the physical forces that responsible for C-C bond formation reactions and electron as well as proton transfer reactions performed in environmental benign unconventional media. The idea of ‘‘unconventional solvents’’ expresses the common concern of today’s chemists to minimize the environmental impact resulting from the use of existing obnoxious solvents in chemical production. It is known that the consequence of a chemical reaction is strongly correlated to the mutual interactions between a reacting molecule and the solvent molecules surrounding it. Physico-chemical aspects of these solute-solvent interactions i.e. solvent effect in unusual media have been studied with reference to activation energy barrier and reactivity in comparison to the existing models suitable for usual solvent available in the literature. Throughout our research work, we have concentrated on two unusual media: 1) water and 2) ionic liquid. Organic reactions have been carried out in water and mixed aqueous media to discern the mechanistic details from the perspective of a physico-organic chemist. To broaden the applicability of ionic liquids in electrochemistry and biological processes, photophysical studies have been performed to understand the efficiency and dynamics of ionic liquids. Two most fundamental processes i.e. electron transfer and proton transfer occurring in chemistry and biology have been studied in

organized viscous ionic liquid media. Since the local solute-solvent interactions in viscous media like ionic liquids substantially differ from conventional homogeneous solvents, the mechanism and dynamics of photophysical processes are expected to differ considerably in ionic liquids.

For the convenience of presentation, different features of the present research work have been discussed in eight different chapters. Brief descriptions of these chapters are given below.

Chapter 1: Current chapter describes an introduction based on critical literature survey on green chemistry, solute-solvent interactions, carbon – carbon bond forming reactions in water particularly emphasizing on Diels-Alder reactions and Wittig reactions, physico-chemical characteristics of ionic liquids, intricacies of photochemical reactions especially energetics and kinetics of electron and proton transfer reactions. A quantitative picture of thermodynamic and kinetic aspects of solute-solvent interactions has been presented here to validate essentiality of solvent to carry out chemical reactions. Efficacy of water has been described from the perspective of its use as a green solvent. Efforts have been made to briefly discuss the current understanding of the research related to organic reactions in water both in homogeneous as well as heterogeneous conditions. Particular emphasis has been given to uncover the role of water during organic reactions occurring at the oil-water interface. A brief literature review comprising physico-chemical characteristics of ionic liquids has been introduced. The dynamic response of the surrounding solvent molecules to photoinduced changes of the chromophoric solute molecules has been briefly reviewed. Much of the significance has been given to understand dynamical and energetic response of the confined geometry of an organized solvent during ultrafast

excited state proton transfer reactions. Kinetics of photo induced electron transfer (PET) reaction mechanism has been discussed in the light of Marcus theory as well as Sumi-Marcus model. Emphasis has been given on 2-D electron transfer model while discussing PET since solvation dynamic response to PET in condense phase or viscous media like ionic liquid can be appropriately rationalized by two dimensional electron transfer approach (2DET) or Sumi-Marcus model.

Chapter 2: A brief note on the objectives of the designed research as well as the motivation of the present work has been penned down in the context of literature survey.

Chapter 3: Different instrumental techniques that have been employed to carry out present investigations have been enumerated in this chapter. The instruments that have been used to provide accurate data are gas chromatography; UV-Vis spectrophotometer; steady state spectrofluorimeter; time correlated single photon counting (TCSPC) fluorescence spectrometer and Subpicosecond ultrafast fluorescence spectrometer (Up-conversion fluorimeter). The basic principles of all the instruments as well as experimental techniques to obtain data have been described precisely in the present chapter.

Chapter 4: This chapter elaborates the research on delineation of physical parameters responsible for amazing augmentation in the reactivity as well as selectivity of Diels-Alder reactions and Wittig reactions especially at the organic (oil)/water interface. In general, organic reactions at ‘on water’ condition i.e. heterogeneous condition show remarkable improvement both in reactivity and selectivity in comparison to ‘in water’ i.e. homogeneous condition as well as neat condition. However, presence of interface along with its role during reaction progress is not univocally supported in the present literature.

In the present chapter, through our systematic kinetic and thermodynamic studies we have established the presence of oil-water interface and quantified its assistance in promoting reactions keeping all other physical parameters invariant. A comparative study of the enthalpic and entropic activation parameters associated to homogeneous and heterogeneous reactions has been presented here. In the midst of unique characteristics of water promoted reactions viz. enforced hydrophobic interactions, cohesive energy density, and polarity etc., the superior role of hydrogen bonding of the interfacial water molecules during heterogeneous aqueous reactions has been reported in this chapter.

Chapter 5: Present Chapter is concerned with the widening of the solvation window of water upon introduction of ionic liquids as co-solvents to uphold its extensive application for performing organic reactions. In the present chapter reactivity of Diels –Alder reaction has been quantified by the interactions of water and co-solvent i.e. ionic liquid with the reactants and the activated complex. Hydrophobic hydration plays pivotal role in solvation of the apolar reactants in aqueous and mixed aqueous solvent. The interactions of apolar solutes and mixed aqueous solvents are mainly guided by the extent of overlap of the hydrophobic hydration shells. Concentration of ionic liquids in water has been intentionally kept low to access the one to one interactions between reactants and mixed aqueous solvent. To estimate small range hydrophobic hydration i.e. pairwise interactions 'Group Additivity Approach' and SWAG principle have been applied throughout this study. Observations come out of large variety of ionic liquids establishes quantitative efficacy of ionic liquids as co-solvents in a comparative manner.

Chapter 6: This chapter elaborates kinetics and energetics of excited state intramolecular proton transfer (ESIPT) reactions of 1, 8-dihydroxyanthraquinone (18DHAQ) in ionic

liquids specifically in protic ionic liquids, since proton transfer reaction in aprotic ionic liquids has been found to be too fast to analyze. Absence of the mirror image relationship between absorption and emission spectra related to tautomeric reactions of 18DHAQ in protic ionic liquids justifies the involvement of dissimilar energy states at the excited state in comparison to ground state. The changes in the dipole moment between normal excited form (N*) and excited tautomeric form (T*) of the dye indicate that the drastic solvation relaxation is accompanied by the excitation and the ESIPT process, which is consistent with the remarkable dynamic Stokes shift observed in the experiments. The unexpected increase in the emission of T* with the increasing viscosity of ionic liquids signifies the presence of slower reverse ESIPT along with forward ESIPT. The extent of backward ESIPT process dies away on moving towards higher viscous ionic liquids. First diffusive relaxation of the low/ moderately viscous ionic liquids causes modulation in the energy states of N* and T* and induces backward ESIPT. Direct observation of backward ESIPT in protic ionic liquids is a very important investigation of the present study.

Chapter 7: This chapter deals with indepth analysis photoinduced intermolecular electron transfer reactions between coumarin dyes and aromatic amine (*N*, *N*-dimethyl aniline) in ionic liquids. In the present study, in the steady state fluorescence measurement data, the positive deviation from Stern-Volmer (SV) linearity is generally observed even in the absence of any ground state complex formation and is ascribed to the quenching involving close vicinity donor-acceptor pairs at the moment of photo-excitation. As the closely spaced D-A pairs participate in instantaneous quenching (i.e. static quenching); they gradually contribute more as the quencher concentration is increased. In both the IL media, coumarin dyes show strong non-exponential decay

profiles from fluorescence up-conversion measurements in the presence of DMAN. The fluorescence transients were rigorously fitted by convolution method using a Gaussian shape for the instrument response function (IRF, ~ 200 fs) and a multi-exponential decay function. Correlation of the observed bimolecular quenching constant (k_q) values in ionic liquids with the free energy changes (ΔG^0) for electron transfer reactions establishes an inversion behaviour at the higher exergonic region, as predicted by Marcus outer sphere electron transfer theory.

Chapter 8: Results and principle conclusions has been summarized in the present chapter. Moreover the future prospects of research works carried out in the present thesis has been discussed in this chapter. In a nutshell, the significant contributions from investigations carried out in the present thesis are as follows:

1. The mechanistic intricacies of the 'on water' reactions have been demonstrated experimentally. The participation of the oil/water interface and contribution of extensive hydrogen bonding present at the interface to promote the reactions have been established univocally.

2. One to one interaction between ionic liquids and reactants in the mixed-aqueous solvent has been delineated by invoking pairwise interactions. Quantitative comparison of pairwise interaction values among wide range of ionic liquids will encourage researchers to design reactions with minimal use of ionic liquids.

3. Direct observation of backward ESIPT along with forward ESIPT in the low viscous protic ionic liquids is an imperative investigation.

4. The Marcus inverted region (MIR) has been demonstrated from the ultrafast electron transfer (ET) quenching experiments between coumarin derivatives and *N*, *N*-dimethylaniline in viscous ionic liquid media.

List of Abbreviations

[Emim]	1-ethyl-3-methyl imidazolium
[Bmim]	1-butyl-3-methyl imidazolium
[Hmim]	1-hexyl-3-methyl imidazolium
[Omim]	1-octyl-3-methyl imidazolium
[BMpyrr]	*N*-butyl-*N*-methylpyrrolidinium
[Bpyrr]	*N*-butyl pyrolidinium
[Py]	Pyridinium
[HmIm]	1-methyl imidazolium
$[BF_4]$	Tetra fluoroborate
$[CH_3CHOO]$	Acetate
[HCOO]	Formate
$[CH_3CH_2CHOO]$	Propionate
SCN	Thiocyanate
NO_3	Nitrate
$[NTf_2]$	(trifluoromethylsulfonyl) imide
18DHAQ	1,8-dihydroxy-9,10-anthraquinone
ESIPT	Excited state intramolecular proton transfer

Chapter 1

General Introduction

‘‘The significant problems we face today cannot be solved at the same level of thinking we were at when we created them’’

Albert Einstein

The propensity of a chemical reaction is strongly related to the mutual interactions between the reacting molecules and the solvent molecules surrounding the solutes. This chapter aims at presenting a comprehensive literature survey on how solvent can control reaction rates both thermodynamically and kinetically. During discussion of solvent effects, special emphasis has been given on the feasibility of ‘green solvents’ e.g. water, ionic liquids and aqueous mixture of ionic liquids as the replacement to conventional volatile organic solvents. Organic reactions like Diels-Alder reactions, Wittig reactions having potential application in biological sciences have been studied in the environmental benign solvents from the perspective of a physico-organic chemist. To comprehend the molecular level interactions as well as dynamics of excited states of the reactants in ‘green solvents’, photophysical aspects have also been summarized in this chapter.

1. Towards the Ideal Chemistry:

1.1 The Emerging Paradigm in Chemistry

Our environment is a multifaceted nexus of interdependent dynamic activities, closely associated to the internal and external chemistries that sustain them. It has been argued that chemists pollute this environment to a fair extent by inducing an alteration in the supporting chemistry.[1] However, chemistry reserves great responsibilities in shaping the human life in the hand of an artisan.[2] Otherwise, random as well as gratuitous introduction of chemistry in human activities would lead science to produce waste and subsequently environmental epidemic. In this context, a new initiative of shaping the modern scientific developments has been put forward and the term 'green' has been introduced to emphasise researches on the interdependence among scientific discoveries, pollution and the environment as well as to encourage innovation in reducing costs of production and waste management. Paul Anastas (American Chemical Society'95), Director of the American Chemical Society's Green Chemistry Institute (GCI) divulged "We'll need to drill down to the molecular level, where you can have the most influence".[3] As chemistry involves itself in building molecules starting from atom, 'green chemistry' is essential to wisely redirect the chemical innovations and investigations in the way of environmental sustainability and acceptability.[4] United Nations' World Commission on Environment and Development published *'Our Common Future',* defining sustainability as "meeting the needs of the present without compromising the ability of future generations to meet their own needs." [5]

'Green Chemistry' can be regarded as a 'new way of thinking' rather than a new branch of chemistry.[6] Green chemistry has been defined by IUPAC as "The invention, design and application of chemical products and processes to reduce or to eliminate the use and generation of hazardous substances."[3] The challenges to the researchers of the 'green chemistry' are to go through the entire existing processes of chemical synthesis and to discover new trail to synthesise the chemical product efficiently emphasising on toxicity reduction as well as waste minimisation. A set of 12 guiding principles advocated by Anatas and Warner abridges the vast spectrum of green chemistry.[3,4] The first principle sets the basic goal of green chemistry by propagating universal idea familiar in medical sciences i.e. 'prevention is better than cure'. The remaining 11 principles can be summarized under following four headings:

1. Atom efficiency - designing processes to maximise conversion efficiency in terms of atoms involved in the whole chemical process.
2. Energy conservation – modelling the process to consume lowest possible energy
3. Waste control – designing the strategic methodology of a process to minimise the waste or to avoid waste production.
4. Substitution – delineating the way to keep the process away from hazardous reagents and to perform the reactions in no solvent or in environmental benign solvents.

'Science is necessary but not sufficient' (Maltoni and Selikoff, 1988). The new paradigm of chemistry is to define the whole process of chemical production in light of their environmental sustainability by eliminating the conventional methods having potential to contaminate the environment.

1.2 In Quest for Green Solvent:

The word 'solvent' has been derived from the original Latin 'solvo' which signifies 'I loosen, unite, I solve'.[7] Solvent indicates the class of the substances that dissolve a solute (chemically different liquid, solid or gas), resulting in a solution. Gas, liquids or solid phases can serve as the medium of chemical reactions but in comparison to all fluids, liquid serves as a medium for carrying our most of the chemical transformations. Solvents have been used for thousands of years not only as media of the chemical reactions but also they play pivotal role during extraction, purification, separations of the products.[8] From the ancient times, water remains as popular to human being not only as a universal solvent to aid chemical transformations but also it serves as the natural reservoir to germinate and sustain life.[9] The first man-made solvents were almost certainly hydrocarbons, such as turpentine derived from wood sources, and ethanol from wine spirits. Ancient civilizations discovered that by fermenting vegetable matter, such as grapes or sugar cane, they could produce ethanol.[10a] In many ways it looked and behaved like water; in other ways it was very different and proved invaluable for dissolving oils and resins. Organic solvents became a boon to the chemists due to rapid progress in the petroleum – refinery technology since 20th century. Previously, organic solvent signifies a generic term to entail a collection of common carbon based fluids those used to serve a single purpose i.e. to dissolve grease, oil, rubber etc.[10] To a chemist, significance of a solvent

requires more attentions towards both macro- and micro-scopic point of view. Macroscopically liquids serve as the ideal medium for mass transfer and heat transfer during a chemical process. From the molecular point of view, solvent helps in dissolving solids by breaking bonds and exerts specific and non-specific forces to control the chemical reaction on passing from reactants to product through transition state.[11] Therefore, for the successful completion of the chemical reactions, a chemist can hardly develop a methodology only by concentrating on the required reactants without selecting solvent to carry out the reactions.

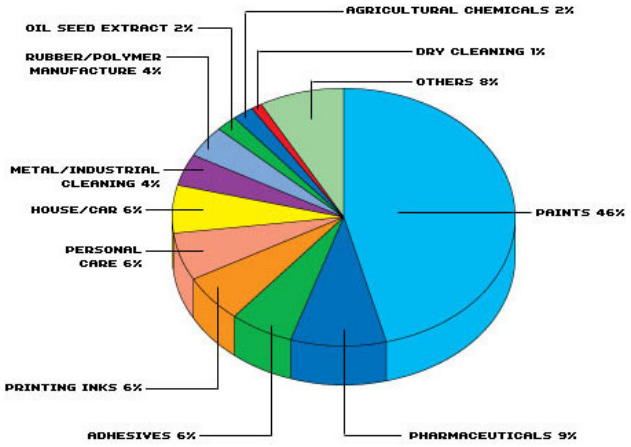

Figure 1: A pie chart displaying the percentage usage of solvent in the major areas (Obtained from: http://www.aaechemie.com/html/aae_solvent_information.html)

Solvents are often categorised as volatile organic compounds (VOCs). VOCs represent a broad group of carbon based chemicals those can easily evaporate at room temperature. Therefore, these VOCs can form low level ozone and smog by free radical oxidations in the air. Some of them are highly flammable and are also potential to cause serious health problems depending on their concentration of accumulation in environment.[12] There are thousands of VOCs are in our daily life; some of the example of VOCs is as follows: benzene, toluene, ethylene glycol, formaldehyde, acetone, methylene chloride, xylene, tetrahydrofuran etc.

Table1: E-factor of industrial production[14]

Industry sector	**Annual production (ton)**	**E-factor**
Oil refining	10^6-10^8	Ca. 0.1
Bulk chemicals	10^4-10^6	<1–5
Fine chemicals	10^2–10^4	5–50
Pharmaceuticals	10–10^3	25–100

Rapid growth in the population and fast urbanisation requires large scale industrialisation and surplus increment in the production of goods. Particularly in fine-chemical and pharmaceutical industries, major amount of solvents are used per mass of product and contribute to the heavy pollution. Recent E-factor has been used to access the actual amount of waste production during an industrial process. It is defined as E-factor = total waste (kg) / product (kg).

The new metric (E-factor) shows that production of fine chemicals and pharmaceuticals evolve highest amount of waste i.e. have the highest negative environmental impact. These statistical inferences represent a prima facie of the alarming condition of the environmental pollution roughly.[14,15] The researchers in the arena of 'green chemistry' has emphasised on development of 'green solvents' or solvent systems which reduce the intrinsic hazards associated with conventional solvents. At Green Solvents conference in Germany in October, 2010 Philip G. Jessop was asked a question "If the adoption of greener solvents over the next 20–30 years will reduce environmental damage from human activities, then the adoption of what class of solvents will be responsible for the greatest reduction in environmental damage?"[16] During selection of the green solvents, the desirable characteristics like inertness, non-flammability, cost-effectiveness, low-volatility, and non-toxic etc. serves as guiding attributes to the chemists.[3,4]

The foremost goal of the present thesis is to invoke green solvents viz. water and ionic liquids as the reaction media and to carry out a comprehensive evaluation of the 'pros' and 'cons' of the new green media in comparison to traditional organic solvents from a physical-organic chemist's perception. The knowledge of the physical forces that guide the solute-solvent interactions will be vastly beneficiary to us during the adoption of the green solvents during the performance of the chemical reactions as well as to design the new solvents or new green methodology without compromising

their environmental impacts. In this chapter, we have aimed to present a brief discussion based on the available literature on the physico-organic attributes of water as well as ionic liquids and the physical forces exerted by these green solvents during performance of the reactions. Our discussion will be focused on two important types of reactions, one is C-C bond formation reactions and another refers to the reactions evolves out of elementary particles. While discussing C-C bond formation reaction, we shall emphasise on the physical forces behind the occurrence of Diels –Alder reactions and Wittig reactions in water and ionic liquids. Again, we shall assess the photo-physics and feasibility of ionic liquids while acting as the media of photoinduced electron transfer reactions (PET) and excited state proton transfer reactions (ESIPT) during the subsequent discussion.

1.3 Thermodynamic Aspect of Solute-solvent Interactions:

1.3.1 Origin of Solvent Effects

A physical perception of solution is that it is a homogeneous liquid mixture of more than one constituent in a variable ratio. Among these components, the excess component is known as the solvent and the other quantitatively small components are known as solute. Roult's law as well as Henry's law deal with the principle criteria behind the ideality of this mixture. However, the deviation from the ideality introduces interactions among solute and solvent, originated at the molecular level. These interactions among solute and solvent molecules are too strong to be analysed by the famous 'kinetic theory of gases' and on the other hand interactions are too weak to be described by the prevailing laws that govern the physics of solid-solid interactions. Therefore, to abridge the wide gulf between 'gas model' and 'crystal model' a model pertaining to liquid phase is highly essential to interpret the characteristics of the solutions. Due to complexity in the structure and interactions in liquid contrast to that of gas and solid, development of a universal set of laws is decidedly difficult task to the chemists. In this direction, the first breakthrough was introduced by Berthelot and Saint-Gilles in 1862 through their studies on the esterification of acetic acid with ethanol.[18] While performing the reactions between trialkylamines with haloalkanes in 1890, Menschutkin had also concluded that effect of reaction medium seems to be inseparable from the reaction itself. [19] Soon after this discovery, scientific community had persuaded systematic studies to delineate the solute-solvent interactions. Claisen's study on the influence of the solvent on the

chemical equilibra directs the scientific world to concentrate on the effect of solvent properties during the reactions.[20]

The research work on the solute –solvent interactions during reaction progress can be categorized into three major tasks,

i) to dissect the solute-solvent interactions into subdivided categories to comprehend the real contribution from the individual solvent components.

ii) to define the limit of solute-solvent interactions quantitatively, and

iii) to establish connections (at least superficially) among the observed contributions to the interactions arises out of structural versatility from solvents to solvents.

1.3.2. Solute-Solvent Interactions in Terms of Solvent Properties

A solution at equilibrium is considered as a large assembly of molecules undergoing incessant collisions and exchanging energy among colliding partners and among internal degrees of freedom. These collisions among molecules and subsequent exchange in energy among the constituents follow almost similar trend as in the pure liquid. Properties of the molecules of solvent as well as that of nearby solute molecules actually decide the extent of local ordering of molecules and are responsible for introduction of both micro- and macroscopic deviation of solution from pure liquid. By considering solvent as a macroscopic continuum, we often give sufficient stress upon the macroscopic physical properties such as boiling point, cohesive pressure, refractive index, relative permittivity, surface tension, vapour pressure, viscosity, density etc. These macroscopic properties represent only classical model as here use has been made of physical classical concepts, as energy, collisions (and, implicitly, classical moments), spatial ordering (i.e., distribution of elements in the space).[17]

Similar properties play key role during specification of characteristics and boundary of pure liquid also. To understand the local ordering and mutual interactions those strongly depend on the chemical composition one should ponder over semi-classical or quantum description of the solution.[21] From the microscopic point of view, a solution is a microheterogeneous assembly guided by the molecular properties of solvent like dipole moment, electronic polarizability, hydrogen bond donor (HBD) (α) and hydrogen-bond acceptor (HBA) capability (β), electron-pair donor (EPD) and electron-pair acceptor (EPA) capability which are the consequence of individual,

mutually interacting solvent molecules, local ordering and their molecular composition.[21,23]

The interactions between solute and solvent have been explained by an age old principle 'like dissolves like' for a long time. The research workers have tried to redefine the term 'like' from time to time on the basis of updated semi-classical or quantum chemical interpretations of the microscopic parameters. However, in the present context, during the discussion of solubility of 'B' in the solvent 'A', one stresses upon the intramolecular forces (K_{AA} & K_{BB}) between 'A.....A' and 'B.....B' as well as the intermolecular attractions between A & B i.e. $K_{AB.}$ These intermolecular forces can be categorized into two types depending on their directionality and specificity. First category comprises hydrogen bonding, charge transfer, electron –proton donor acceptor forces which can be directional, specific and can be completely satisfied. The forces generally contribute towards deciding of the stoichiometry the molecule and ion interactions. The second category comprises dispersion and induction forces which are non directional as well as non specific in nature. These forces cannot be satisfied completely.[17, 23]

1.3.3 Quantification of the Solute-Solvent Interactions by Thermodynamic and Kinetic Parameters

Recent advances in spectroscopic techniques examining the dynamics and thermodynamics of solute-solvent interactions, along with the progress in computer simulations, have led to new insights into the microscopic mechanisms and solvent modes driving activated transitions.

To comprehend the influence of solvent-solute physical interactions on the enthalpy and entropy of molecular equilibrium, let us consider the equilibrium in the general form

$$\nu_1 A_1 + \nu_2 A_2 + \ldots\ldots = 0, \qquad (1)$$

where, the A_i denote electrically neutral reactants and products of the equilibrium (l), and the υ_i denote the stoichiometric coefficients, positive for products and negative for reactants. This notation is convenient for further considerations. The change in energy ΔG, or other thermodynamics functions of equilibrium (l), taking place in the solvent S can theoretically be calculated by quantum- chemical techniques. However, the accuracy of even very modern calculations is as a rule insufficient to take into

account the solvent effect. Both theoretical calculation and experimental results show that the equilibrium constants of complexation as well as equilibrium constants of tautomeric equilibra depend on the type of solvent, particularly on its polarity.[24] It can be expressed by assuming that the Gibbs free-energy change ΔG_s of equilibrium (l), in the solvent S, can be expressed by a function P of macroscopic parameters of the solvent, such as its electric permittivity ε, molar volume *V*, etc.:

$$\Delta G_s = \Delta G_o + AP(\varepsilon, V, ...), \quad (2)$$

where ΔG_o, denotes a constant which with appropriate definition of the function P, may be interpreted as the free-energy change of the equilibrium (1) in the gas phase, and A denotes a proportionality coefficient. The enthalpy change of the equilibrium (1) can be expressed by the van't Hoff equation [24,25]

$$\Delta H_s = \frac{d\left(\frac{\Delta G_s}{T}\right)}{d\left(\frac{1}{T}\right)} \quad (3)$$

where, T denotes the absolute temperature. Using assumption (2) one obtains

$$\Delta H_s = \Delta H_0 + AP\left(1 - \frac{T}{P}\frac{dp}{dT}\right) \quad (4)$$

here, ΔH_0 can be expressed as: $\Delta H_0 = \frac{d(\frac{\Delta G_0}{T})}{d(\frac{1}{T})}$

Similarly, using the assumption (2) the entropy change of the reaction can be expressed as

$$\Delta S_s = \Delta S_0 + \frac{Adp}{dT}, \quad (5)$$

where ΔS_0 can be defined as: $\Delta S_0 = \frac{\Delta G_0}{T} - \frac{\Delta H_0}{T}$

Equations (4) and (5) show that, if assumption (2) is valid, both enthalpy and entropy of the equilibrium not only depend on solvent parameters, such as ε, *V* etc. but also on the temperature. In the dipolar approximation, Onsager model provides, $A = -4\pi N^2/3$ and $P(\varepsilon, V, ...) = \Delta\mu^2 (\varepsilon-1)/(2\varepsilon-1)$.[24] In this equation, N denotes the Avogadro number, $\Delta\mu^2$ is the polarity of the reaction defined as $\Delta\mu^2 = \sum_i \frac{v_i \mu_i^2}{V_i}$ where, μ_i and V_i denote the dipole moment and molar volume of the i^{th} component of the equilibrium (1). The summation denotes all reactants and products involved in the equilibrium. From the above discussion, it is obvious that the enthalpy change ΔH_s , and entropy change ΔS_s due to solvation can be quantitatively obtained from the various form of the van't Hoff equations. This correlation among the thermodynamic parameters and

the solvation parameters implies that solvent parameters like polarity, ε, *V* etc. plays pivotal role in deciding the value of ΔG_s i.e. free energy of solvation.[17,26-27]

To realize the effect of solvent polarity on the reaction in a lucid manner, we can represent the reaction co-ordinate of S_N1 and S_N2 in both polar and apolar solvent pictorially (Figure 2),

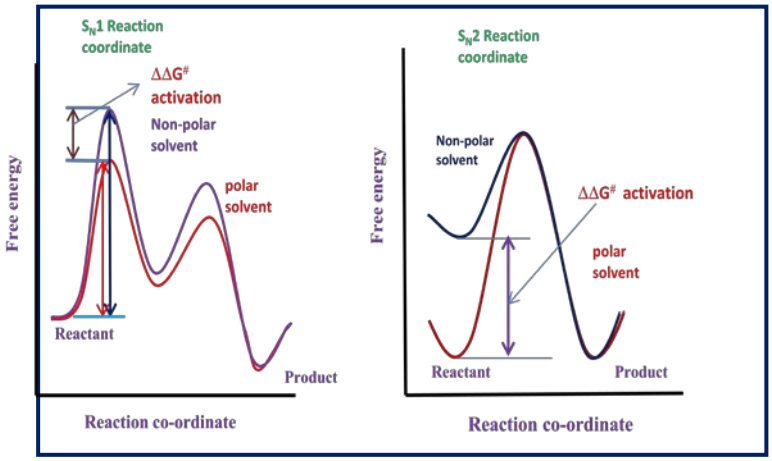

Figure 2: Diagram of free energy change during S_N1 and S_N2 in both polar and apolar solvents

As we all know that during neucleophilic substitution reactions, the polarity of the substances undergoes a wide variation in its magnitude upon moving from reactants to products through the transition state.[28] Here in the Figure 2, $\Delta\Delta G^{\#}$ represents the difference in the activation energy between polar and non-polar solvents. It is found that polar protic solvent promotes the S_N1 type reactions by stabilising the intermediate carbocation and polar aprotic solvents promotes S_N2 reactions by introducing loose solvation shell around the neucleophile.[28, 29]

If we consider the dissolution of NaCl (ionic salt) in non-polar solvent e.g. hexane and a polar solvent e.g. water, we can easily justify the relation between enthalpy change and the solvation tendency. The Na^+ and Cl^- ions are bound together in the solid through strong coulombic forces; pulling the solid apart in nonpolar solvent (hexane) is a highly endothermic process. In contrast, dissolution of NaCl in polar solvent (water) is slightly exothermic and proceeds spontaneously. This is due to the percolation of water having high dielectric permittivity (ε ~ 80) between two opposite ions, the coulombic attraction between two opposite ions lowered to 1/80 from its normal value in solid state of NaCl.[30] Thereafter, the water molecules form a

solvation shell around the ions (lower left), rendering them energetically (thermodynamically) more stable than they were in the NaCl solid.

1.4 Introduction of Green Solvents and their Effect:

Throughout the research, we have concentrated to explore the potentiality of two 'green solvents' i.e. water and ionic liquid. In the later section of our thesis we shall focus on delineating the nature of physical forces exerted by the 'green solvents' during performance of C-C bond formation as well as elementary particles transfer reactions. In this section discussion on some important properties of water and ionic liquids highlighting their uniqueness as the solvents has been made.

1.4.1 Water a Magic Solvent

Water is called as the "matrix of life", certainly with good reasons.[9] There is no other solvent offering such a wealth of possibilities for the processes nourishing life. No doubt for this reason, finding water on the moon, on other planets and generally in space has high priority to justify the existence of life in the extraterrestrial bodies for major space agencies. Apart from its stability in oxidation processes, of obvious importance in aerobic life-forms, water provides an excellent reaction medium for many types of biological reactions. Water plays a pivotal role as a mediator in communications among proteins; similar perception has also recently been used in supramolecular chemistry of let.[32] Our mother Nature has started her most complex chemistry of making life in her laboratory 'earth' by using water as a solvent.

Water has been considered as an ideal green solvent not only from the environmental standpoint but also from the economic point of view since it is most abundantly available in nature. However, though water is nature's first choice as solvent; chemists are reluctant to use water during the reactions since most of the organic/nonpolar reagents show very low solubility or simply insoluble.[33-35] In addition to these solubility problems, water promotes undesired reactions with the water-sensitive intermediates and products also.

However, in early 1980, Breslow and co-workers have revisited the concept of using water as a solvent for organic reactions. Followed by final discovery by Breslow and co-wokers, in the past about 25 years the latent potentials of using aqueous media have been recognized, and reactions including pericyclic reactions, Michael additions, and organometallic reactions have been documented and in some

cases water has increased the selectivity and reaction rate.[36,37] Compared with common organic solvents, the unique and unusual physical properties such as high specific heat, high surface tension, high dielectric constant, large cohesive energy density and unusual chemical properties like ability to form hydrogen bonds and amphoteric nature of water can in principle influence positively the reactivity and selectivity of chemical reactions.[38] The most important advantages of using water can be summarized through the following points:

i) its suppleness to form strong hydrogen bonds that give it a significant surface tension (three times that of liquid ammonia) –which could facilitate the aggregation of reactants,

ii) small structure of water molecules is advantageous for their swift orientations to form hydrogen bonding,

iii) its ability to form weak non-covalent bonds with other compounds, and

iv) its ability to engage in electron and proton transfer reactions exemplified by many biological and synthetic systems. [38, 39]

The macroscopic properties of water discussed above are the consequences of the microscopic molecular arrangement of water. Several experimental techniques as well as theoretical approaches have been used to correlate these molecular properties with the structural features of water. The most trustworthy approach of delineating the molecular structure of water is probably offered by X-ray and neutron scattering techniques. X-ray absorption spectroscopy and sum frequency generation spectroscopic studies have pointed out significant disparities among electronic structures between water and ice as well as vapour.[33, 40] In liquid state water deviates from ice as well as vapour in terms of properties due to the variation in number of broken H-bonds on the H-donating site of the water molecule. In agreement with this observed change in electronic structure upon hydrogen-bond formation, a gradual change of hydrogen bonding structure and strength towards that of bulk water was observed for clusters of water molecules going from dimers up to nonamers.[41] However, even within the liquid, not all hydrogen bonds are the same; a range of hydrogen-bonded structures with different hydrogen-bond lengths and hence different hydrogen-bond strengths exists. The relatively high molar heat capacity of water is also related to the characteristics of hydrogen bonding. Polarisation effects accompanying hydrogen bonding cause the dipole moment of water to be very different in the gas and solution phases; the gas phase dipole moment is 1.86 D (6.20

x 10^{-30} C m) whereas the dipole moment in the liquid is 2.9±0.6 D (9.67±2.0 x 10^{-30} C m) at 24.45±0.05°C. Femtosecond mid-infrared pump-probe studies indicate that the re-orientational lifetime of water molecules is longer for stronger hydrogen bonds. In fact, lengthening of the O-H···O bond is a prerequisite for reorientation.[39] These fast dynamics indicate a highly dynamic liquid whereas the relatively strong directionally-sensitive hydrogen bonds provide a certain extent of structuring.)

However, chemistry of water is a field of widespread debate. To some extent, the debate arises from the use of diverse quantum chemical calculations, [39c] different thermodynamic schemes and the various limitations in collecting definite data adhered to different techniques.[39b] Still, water remains a trendy research problem and resulting in an extraordinary large volume of reports to unfold the incredible potency of water.

1.4.2. Potentiality of Water as the Solvent for Organic Reactions

Chemists' dislike towards using water as a solvent for carrying out organic reactions has already been discussed in the previous section. Among several rationales, the very low solubility of the reactants in water has been coined as the standard hindrance next to wide acceptability of solvent water among chemists. With the pioneering research by Breslow and Guo on the enhancement of rates of Diels-Alder reactions in water, extensive works have been carried out to explore the efficacy of water in promoting organic reactions.[36,37] Spectacular enhancement in rate of the organic reactions along with enhanced regio- and stereo-selectivities has been highlighted by the researchers for major organic reactions.[42] The most abominable fact i.e. low solubility has been established as the source of the 'hydrophobic effect' which has been considered as the prime cause behind the astonishing increment in rates of the reactions in water. 'Hydrophobic effect' can be precisely defined as that property which can be highly beneficial for carrying out bimolecular or higher molecular reactions as it assists in the enhancement of local concentration of the reactants i.e. bringing reactants closer to each other for further collisions, a prerequisite for each reaction.[43] In term of thermodynamics, low solubility of apolar molecules can be ascribed as the positive Gibbs free energy of transfer deters the solution process spontaneously. However, the directional sensitivity of the strong intermolecular interactions of water molecules provides a room in water to welcome the apolar molecules, called hydrophobic

hydration, which minimises the (unfavourable) Gibbs energy change of solvation in water, and causes a pronounced thermodynamic signature. [44, 46]

The hydration has two contributions: the endothermic creation of a cavity and the exothermic addition of a molecule. The solvation entropy as well as the solvation enthalpy both are negative at room temperature water. The solvation entropy supersedes the solvation enthalpy while water remains at room temperature (298.15 K) and plays dominating role in deciding the faith of hydrophobic hydration at this temperature. With increase in the temperature of water the solvation enthalpy starts increasing and at higher temperature (~ 65 deg C) it dominates over solvation entropy.[46] The strong temperature dependence of both ΔG and ΔS is a result of the different heat capacities of the two phases. Over the whole T range there is a large positive heat capacity change upon transfer to water. The facile switch from entropy control to enthalpy dominance is the basis of the high heat capacity of hydration of non-polar molecules. This high value of negative entropy can be thought as the consequence of a packing effect (translational entropy) and is particularly large in water due to its small size.

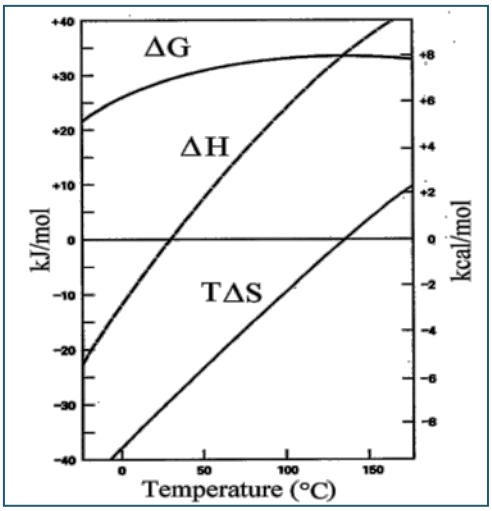

Figure 3: Free energy of transfer of pentane from the bulk liquid to aqueous solution.[47]

'Hydrophobic hydration' is the term used at the molecular level to express reorganisation among surrounding that take place in bulk water when a single non-polar molecule is transferred into it.[45] However, the size and shape of the solutes also

play major role in deciding the parameters of Gibbs energy of transfer. Additionally the dissolution of aromatic and aliphatic molecules in water also shows pronounce effect in the parameters of Gibbs energy of transfer. But convincing experimental probes of vicinal water structure around the hydrated apolar molecule are insufficient, largely because of the low solute concentrations involved.[46a,48] Subsequent to 'hydrophobic hydration', a non-covalent force operates among the hydrated molecule to drive them to form an assembly of nonpolar molecules to minimise the contact surface with water. This non-covalent force leading to inter-molecular interactions among sparingly soluble molecules in water is termed as hydrophobic interactions. Though 'hydrophobic hydration' is not a spontaneous process but 'hydrophobic interaction' is a spontaneous process. The origin of hydrophobic interaction can be thought as the consequences of the special type i.e. tangential orientation of water molecules around the hydrated apolar molecules. From thermodynamic point of view, the change in enthalpy (ΔH) is positive due to breaking of some pre-existing bonds in hydrophobic hydration shell. However, entropy of the system increases due to tearing down of the individual hydration shell of apolar molecules.[46b] Due to this favourable entropy contribution, ΔG becomes negative together with a negative heat capacity and the association process leads to spontaneity.

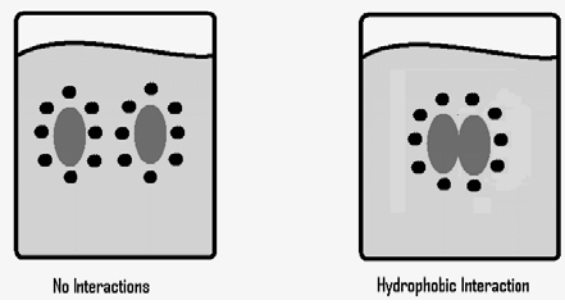

Figure 4: Comparative view of hydrophobic hydration and hydrophobic interactions

The hydrophobic interactions depend on temperature of the solution, number of carbon atoms on the hydrophobe and the shape of the hydrophobe. Hydrophobic interactions can take place in the form of solvent separated pairs and contact pairs (Fig. 5).[46]

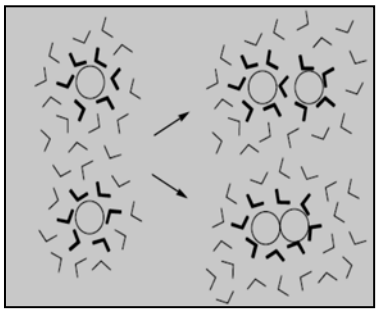

Figure 5: Cartoon displaying solvent separated pairs and contact pairs

The hydrophobic interactions have been classified into pairwise and bulk interactions.[48] Pairwise hydrophobic interactions are 1:1 interactions between individually hydrated nonpolar particles in aqueous solution where the solute concentration is below the so-called critical aggregation concentration. In aqueous solution, pairwise hydrophobic interactions occur via "hydrophobic encounters" indicating that the molecules only associate transiently. Interactions involving large clusters of nonpolar molecules for instance can be found in bilayer vesicles, micelles etc. has been categorized as 'bulk hydrophobic interaction'. Hydrophobic interactions seem to be the major force behind protein folding.[46c] Hydrophobic interactions plays pivotal role in rate enhancements of organic reaction in aqueous media

1.4.3. Ionic liquid: A Room Temperature Molten Salt Solution

Ionic Liquid, an emerging new class of solvent, continually attracting the attention from both academia and industries in this era of 'green chemistry'. Though the history of ionic liquids started with evolution of ethyl ammonium nitrate ($[EtNH_3][NO_3]$) (m.p. 13-14^{0}C) as well as subsequent studies on its property, the major scientific exploration on 'ionic liquids' flourishes since past decade only.[49] A practical definition of ionic liquid is that it is a semi organic salt with a melting temperature below the boiling point of water (373K) at ambient pressure. Ionic liquids are the substances solely composed of ions in which cation is usually of organic in nature and the anion may be of inorganic /organic in nature.[50] Besides the fact that ionic liquids enjoy high liquidus range, most of them exhibit relatively high ionic-conductivity, exceptional thermal and electrochemical steadiness, nonflammability, high heat capacity, cohesive energy density and very low vapor pressure.[51-52] In summary, most ionic liquids possess low hazard levels and are benign for environment.

Why does ionic liquids draw maximum attention of the research community in context of green chemistry, while molten salts which are known to the scientific world before 100 years for their extensive use in metallurgy and fuel cells possessing maximum of these properties? The main reason behind the popularity of ionic liquids over molten salts is that though molten salts are entirely composed of ions and do possess similar properties like Ionic liquids, they remain as liquid only at elevated temperature not at STP (Standard temperature and pressure). From the structural perspective, molten salts being entirely composed of ions shows higher order of crystalinity in their liquid state favoured by the long range coulombic interactions among ions. However, built in molecular asymmetry in the structure of Ionic liquids reduces the enormity as well as the range of coulombic interactions among the constituent ions, that results in properties more akin to normal liquids.[53-54] Moreover, presence of hydrogen bonding network among cations and anions induces *co-operative* effect and structural directionality (entropic effect) in the Ionic liquids. Hydrogen bonds are absent in molten salts. The most important property of ionic liquid is its tunability. In the synthesis of ionic-liquids, people are flexible to choose cations and anions suitable to their desired applications viz. reaction media, battery fuel, nano particle synthesis etc.[55] To be mentioned here that the first generation of ionic liquids i.e. choloroaluminate-based ionic liquids, were sensitive to water and prone to explosion through exothermic reactions with water. Due to this reason, researches on ionic liquids did not progress further until the advent of the second generation of ionic liquids. These second generation of ionic liquids are air and water stable and with their appearance in chemical literature, scientists have meticulously concentrated in exploring these ionic liquids very extensively.[49-51] Cations in these ionic liquids mainly classified into different groups e.g. five membered heterocyclic rings (imidazolium, pyrolidinium, etc.), six membered heterocyclic rings (pyridinium, pipyridinium etc.) and acyclic cations (ammonium, phosphonium and sulphonium based cations). Now a day's ionic liquids having chiral cations have been synthesised and in asymmetric synthesis these ionic liquids find potential applications.[54] Anions of these ionic liquids can be of two types depending on their miscibility with water i.e. hydrophilic and hydrophobic. Generally the anions of hydrophilic ionic liquids are $[BF_4]^-$, $[Br]^-$, $[NO_3]^-$, $[EtSO_4]^-$, $[SCN]^-$ etc. and that of hydrophobic ionic liquids are $[NTf_2]^-$, $[PF_6]^-$ etc. The efficiency of a solvent may be examined on the basis of following properties.

1.4.4. Assessment of Ionic Liquids as a Solvent

1.4.4.1. Vapour Pressure and Thermal Stability

Ionic liquids have extremely low vapor pressure. From a process engineering point of view this is an exceptional advantage due to the fact that normal distillation may be used for isolation of products following the process. The well known problem of azeotrope formation between solvent and product does not arise. The limitations of the thermal stability of ionic liquids are due to their heteroatom-carbon and heteroatom-hydrogen bonds. Ionic liquids synthesised via the direct protonation of an amine or phosphane display significantly restricted thermal stability. While 150°C has to be considered as the maximum working temperature for the vast majority of the quaternary ammonium chloride salts, [Emim]BF_4 has been reported to be stable at 300°C [50-52] and [Emim]$(CF_3SO_3)_2N$ is stable up to 400°C,[53-54] which allows for further exploration into their synthetic utility.

1.4.4.2. Polarity of Ionic Liquids

Solvent polarity is the most commonly used solvent classification. In words of Reichardt, solvent polarity is a complex issue arises during solvation of the reactants, activated complex and products as a consequence of the specific or non specific intermolecular interactions among solutes and solvent, Coulombic forces between the dipolar/charged species, inductive effect, dispersion forces, hydrogen bonding interactions, charge transfer processes etc. Due to these combinatorial effects, the quantification of "solvent polarity" by unique method is not possible. Reichardt had also pointed out that the macroscopic measurement of the dielectric constants alone does not fully reflect the polarity of the solvent.[27] Diverse solvent sensitive references have been assessed to define the polarity of the solvent. The terms polar, nonpolar and apolar are used indiscriminately to apply values of dielectric constants, dipole moments and polarizabilities, even though none of these are directly correlated in a simple way. The simplest definition of a polar solvent is a solvent that will dissolve and stabilise dipolar or charged solutes, and thus it is presumed that ionic liquids will be polar solvents. This method of assessing the solvent polarity following spectroscopic technique is known as "Solvatochromism" in the literature. [27,56] Hypsochromic and Bathochromic shifts in the peak position of the probe in the solvents are termed as "negative solvatochromism" and "positive solvatochromism" respectively.[18] The principle cause behind the occurrence of the solvatochromism is

the differential solvation of the ground state and the first excited state of the probe molecule due to disparity in their electronic arrangements by the solvent.[56b] One of the most useful probes for measuring the polarity of a solvent is the Reichardt's Dye (2,4,6-triphenylpyridinium) *N*-4-(2,6-diphenylphenoxide) betaine. $E_T(30)$ value for a given solvent is defined as the molar transition energy (in kcal mol^{-1}) of the Reichrdt's dye (**1**) at NTP, i.e., 298 K and 1 bar pressure, and can be written in the form of equation (4).[57]

$$E_T(30) = hc\nu(\mathbf{1})_{max}N_A = 2.8591\,\nu(\mathbf{1})_{max} \quad (7)$$

To avoid the use of non-SI units, in 1983 a normalized, dimensionless E_T^N scale was introduced. This scale uses water (E_T^N = 1.00) and TMS (E_T^N = 0.00) as the reference solvents and can be expressed as equation (5).[58]

$$E_T^N = [E_T(\text{solvent}) - E_T(\text{TMS})]/[E_T(\text{water}) - E_T(\text{TMS})]$$
$$= [E_T(\text{solvent}) - 30.7]/32.4 \quad (8)$$

A statistical correlation of E_T^{30} values obtained from the experiments in various solvents with the physico-chemical properties helps the researchers that the most of the solvents can be divided into two classes i.e. with acidity or anion solvating tendency and with basicity or cation solvating tendency.[59-60] According to Reichardt the dye molecule is not capable of interacting specifically and significantly with EPD (electron pair donor) solvents, i.e., the Lewis basicity of the solvents is not registered by this probe.[56] To overcome this snag Krygowski *et. al.* introduced a two parameter equation,[61] which includes a second empirical parameter, the donor number (DN) of Gutmann *et. al.*[61-63] , as a measure of the Lewis basicity of solvents. If P is the measured physicochemical property of the solvent under investigation (i.e. log *K*, log *k*, $h\upsilon$ etc.), the equation can be written as

$$P = P_0 + \alpha E_T^{30} + \beta(\text{DN}) \quad (9)$$

Here P and P_0 are the physicochemical properties under investigation obtained in solution and in gas phase or in inert solvent, respectively. α and β are the regression coefficients describing the relative sensitivity of the solute property P to electrophilic (Lewis acidic) and nucleophilic (Lewis basic) solvent properties, respectively. The acidity and basicity can also be correlated with the transfer of proton between the solute and solvent. The adduct formation between solute and solvent can be treated as a consequence of hydrogen bonding or diploe-diploe interactions without altering the chemical integrity of the solute. In this context the sum of (α + β) can be treated as a

new measure of polarity.[23] Kamlet and Taft in 1976 had introduced following equation, for correlation of the physicochemical properties on the basis of the derived from the analysis of equation to express solute-solvent interactions.[23]

$$P = P_0 + s(\pi^* + d\delta) + a\alpha + b\beta + m\delta_H^2 \quad (10)$$

The basis of this equation is the realization of Kamlet *et al.*[23] established that the effect of a solvent on the reaction rate should be dependent on the following properties: *i*) the behaviour of the solvent as a dielectric, facilitating the separation of opposite charges in the transition state, *ii*) the ability of the solvent to donate a proton in a solvent-to-solute hydrogen bond and *iii*) the ability of the solvent to donate an electron pair, by way of solute to solvent hydrogen bond. The parameter π^* in eq. 10 is an appropriate measure of the first property, while the second and the third properties are governed by the effects of the solvent acidity and basicity, quantitatively expressed by the parameters α and β, respectively. The δ term in equation 10 is a polarizability factor (equal to 0.0 for non-chlorinated aliphatic solvents, 0.5 for polychlorinated aliphatics, and 1.0 for aromatic solvents).[23,57] The equation includes a fourth term so-called cavity term, δ_H^2, which represents a physical solvent quantity called cohesive pressure (or cohesive energy density).[31] This quantity is related to Hildebrand's solubility parameter, δ_H, which is given by $\delta_H = (\triangle H° - RT/V_m)^{1/2}$ where $\triangle H°$ is the molar standard enthalpy of vaporization of the solvent to a gas of zero pressure, and V_m is the molar volume of the solvent.[32] But for solvatochromic correlations the term $m\delta_H^2$ has been dropped later from this equation as the there is no volume change during electronic transitions.[15,18] So for $E_T(30)$ values the correlation can be defined as equation (11)

$$E_T(30) = [E_T(30)]_0 + s(\pi^* + d\delta) + a\alpha + b\beta \quad (11)$$

π^* Parameter:

This parameter, a normalized scale of polarity/polarizability (using DMSO $\pi^* = 1.00$ and cyclohexane $\pi^* = 0.00$ as the reference solvents) is calculated by the solvatochromic shifts in the λ_{max} values of *N*, *N*-diethyl-4-nitroaniline dye (**2**) using equation (12).[62]

$$\nu(\mathbf{2})_{max} = 27.52 - 3.182\pi^* \quad (12)$$

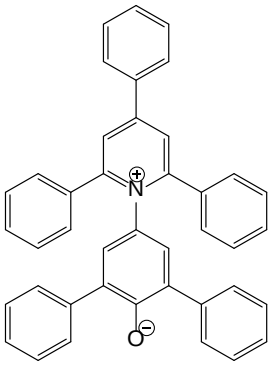

1

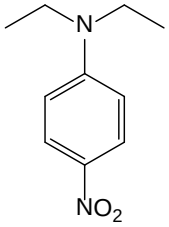

2

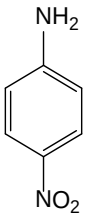

3

Figure 6: Reichardt's dye (**1**), *N*,*N*-diethyl-4-nitroaniline (**2**), and 4-nitroaniline (**3**) used as probe molecules for the determination of polarity parameters.

α Parameter:

Though number of equations have been proposed by different workers based on $E_T(30)$ and π^* values. The equation which is most accepted and applied to most number of solvents is the following.[23, 62]

$$\alpha = 0.0649\, E_T(30) - 0.72\pi^* - 2.03 \quad (13)$$

β Parameter:

The hydrogen bond acceptor or β parameter is determined by the equation (14) using the spectroscopic shift of 4-nitroaniline (**3**) with respect to *N*,*N*-diethyl-4-nitroaniline (**2**).[23]

$$\nu(\mathbf{2})_{max} = 1.035\nu(\mathbf{3})_{max} - 2.8\beta + 2.64 \quad (14)$$

Table 2: Empirical equations used to determine the polarity parameters.[58, 60, 64,65]

Polarity Parameters	**Empirical Equations**
Electronic transition energy parameter $E_T(30)$	$2.8591\ \nu(\mathbf{1})_{max}$
Normalized electronic transition energy E_T^N	$[E_T(30)\text{solvent} - 30.7]/32.4$
Hydrogen bond donor acidity (α)	$\alpha = 0.0649\, E_T(30) - 0.72\pi^* - 2.03$
Hydrogen bond acceptor basicity (β)	$\nu(\mathbf{2})_{max} = 1.035\nu(\mathbf{3})_{max} - 2.8\beta + 2.64$
Polarity/polarizability parameter (π^*)	$\nu(\mathbf{3})_{max} = 27.52 - 3.182\pi^*$

To compare the values of the solvent polarity parameter, we have tabulated values for some of the pure ionic liquids in Table 3.

Table 3: Polarity parameters of the pure ionic liquids [65]

Ionic Liquid	E_T^N	α	β	π^*
[Bmim]Br	0.62	0.42	0.70	1.17
[Bmim][BF_4]	0.69	0.64	0.64	1.08
[Bmim][PF_6]	0.68	0.64	0.19	1.04
[Bmim][NTf_2]	0.66	0.64	0.17	0.98

Here, in Table 3, α value for [Bmim]Br is significantly less than other ionic liquids. β values for hydrophilic ionic liquids ([Bmim]Br and [Bmim][BF_4]) are significantly higher than that of hydrophobic ionic liquids ([Bmim][PF_6] and [Bmim][NTf_2]). Examining at the β values of [Bmim][BF_4], [Bmim][PF_6] and [Bmim][NTf_2], it is easy to understand that there is not significant contribution of basicity to the E_T^N values, which supports the statement proposed by Reichardt.[18] The π^* values obtained for the ionic liquids follow the order of hydrophilicity in these ionic liquids. The definition of the parameter, i.e., polarity/polarizability,[62,67] suggests that more the polarizability less the value for π^* parameter, is seen in the case of the ionic liquids studied. The above discussion suggests that

1. E_T^N and α values follow the same trends in pure ionic liquids
2. Effect of β values is not significant to the E_T^N values of ionic liquids
3. β and π^* values follow the order of hydrophilicity for the given ionic liquids

1.4.4.3. Viscosity of Ionic Liquids

'Viscosity' is the property to define the resistance to flow of a liquid. It is also the consequence of intermolecular interactions among the molecules in a liquid. These intermolecular forces depend both on size as well as electronic arrangements of the involved molecules.[66] Again, from a chemical process designer point of view, processes involving heat, mass, or momentum transfer, or dissolution or absorption of compounds in liquid strongly dependent on viscosities of used fluid. Therefore, viscosity should be accurately known as a function of pressure and temperature over the full range of expected process conditions.[66-67]

Generally it has been observed that ionic liquids are much more viscous than that of conventional organic solvents, e.g. viscosities of benzene is 0.6 cP at room temperature, where as viscosity of [Emim]NTf_2 is 38 cP.[68] It is shown that one of most important property of ionic liquids is its tunability. It implies that a large number of possible judicious combinations of the cation-anion can yield a variety of ionic liquids having very different viscous behaviours. The range of these viscosities may be from very low value, analogous to organic solvents to very high values i.e. glass like viscosities. Viscosities of ionic liquids are related to the cation-anion pairing as well as the structural characteristics of ionic liquids such as size and shape of the cations, presence of flexible groups like ether on the side chain, length and branching in the substituted groups (especially alkyl groups) and stereo-nature along with size of the associated anions.[69,70] In general, the temperature and pressure dependence of viscosity of ionic liquids show non-Arrhenius nature due to its glass forming nature with respect to variation in temperature and pressure.[71c, d] However, modified Vogel-Fulcher-Tammann (VFT) equation given by, $\eta = A \exp (B/T-T_0)$ has been used to define temperature dependence of the ILs' viscosity in most of the cases.[71, 72] However, Harris et. al. have correlated their viscosity data with two-coefficient Litovitz equation given by $\eta = A \exp(B/RT^3)$. While assessing the viscous properties of ionic liquids accurately, following points should be stressed upon, i) ultra pure sample (otherwise impurities should be properly characterised for unavoidable cases) of ionic liquids are required (ii) measurements should be done for a wide range of pressure and temperature without compromising the purity of the sample and (iii) experimental results should be analysed from the molecular point of view.

It has been observed that the anions associated to ionic liquids are seemed to have much influence on the viscous nature of ionic liquids than that of the cation. Again symmetry of anions has also been regarded as an additional parameter to influence viscosity values. For imidazolium based ionic liquids, keeping cation same, changes in viscosity follow the order: $[Br]^- > [SCN]^- > [BF_4]^- > [NTf_2]^-$.

Table 4: Viscosity of ionic liquids at 298.15 K [71]

Ionic liquids	**η/cP**
[Bmim]BF_4	115
[Bmim][NTf_2]	49

The aim of gaining a deeper understanding of the interactions between the components leads researchers to delineate the change in the viscous nature of ionic liquids from pure state to its mixture with other solvents. It has been observed that there is a significant decrease in the viscosity of ionic liquids by the presence of polar and apolar solvents in it. The degree of decrease in viscosity of ionic liquids in mixed state depends on the relative permittivity of the added cosolvents. Solvents with higher dielectric constant will help in 'solvating' the constituent ions of ionic liquids and thus presence of such type of solvents in ionic liquids will hinder the process of aggregation of ions in ionic liquids. The change in the viscosity of ionic liquids turns out to be higher in magnitude in presence of acetonitrile in comparison to presence of similar quantity of benzene.[72] It is to be mentioned here that effect of water (ε~81) has been observed more for hydrophilic ionic liquids compared to hydrophobic one. Following extensive investigations on the variation of viscosities of binary or ternary mixture of ionic liquids attempts have been made to correlate the viscosity change with the amount as well as polarity of the cosolvents present. It has been found that polar solvents show greater interactions with the constituents of ionic liquids than apolar counterpart.

Along with these macroscopic properties, the extensive applicability of ionic liquids (e.g. dye sensitized solar cells, batteries etc.) cannot be justified without digging out the microscopic milieu corresponding to molecular nature of ionic liquids.[73] In this context, conscious attempt has been made to dig out the information related to microscopic mechanisms of ionic liquids in solvation as well as reactions.

1.4.5. Solvation Dynamics of Ionic Liquids

Dynamics play crucial role in determining mass and heat transport properties of ionic liquids.

Solvation dynamics can be defined as a process of molecular reorganizations in response to a perturbation in the geometric or electronic structure of a solute and are particularly important for charge-transfer reactions whose kinetic rates are determined almost exclusively by solvent reorganization. Thus, study of solvation dynamics is particularly important for charge transfer reactions whose kinetic rates and mechanisms of chemical reactions which involve polar transition states.[74] Time dependent fluorescence Stokes shift (TDFSS) of the emission spectrum of the solute

molecule has been exercised as a standard procedure to measure the instantaneous vibronic energy of solute (coumarin, Nile red or pordan).[74-75]

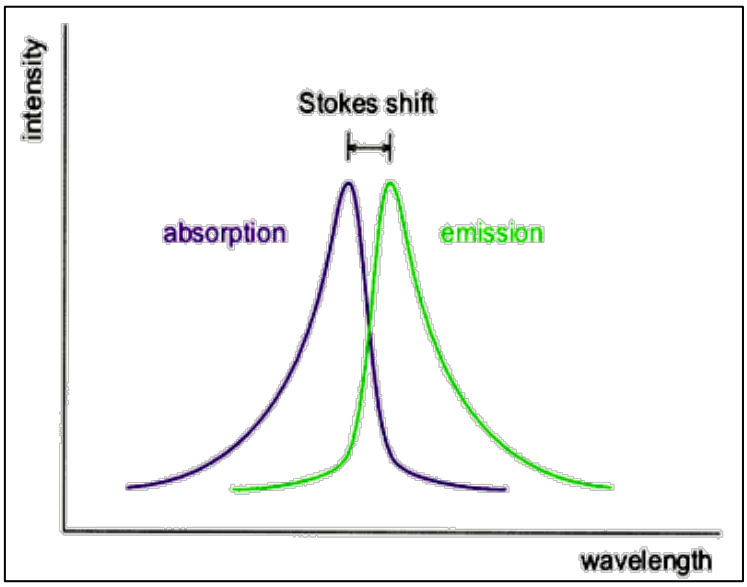

Figure 7: Schematic diagram fluorescence stokes shift

During TDFSS experiments, fluorescence probe molecules are being used to evaluate the response of the solvent to an instantaneous variation in the electronic state of probe molecule. Precisely, after electronically excitation of the probe molecule with LASER pulse [$\nu(0)$], the molecular geometry of the probe molecule remain unaffected, but its charge distribution is considerably altered. Followed by the initial excitation, the solvent in the environment begins to reorganize to accommodate the new charge distribution. The reorganization stabilizes the excited electronic state of the probe relative with respect to its ground electronic state, and subsequent to fluorescence, $\nu(t)$, is red shifted with respect to the initial fluorescence, $\nu(0)$. The time dependence of the rearrangement of the solvent environment is revealed through continuous red shift of the emission spectrum.[76]

The time scale of solvent reorganisation can be obtained by following equation:

$$S(t) = \frac{\nu(t)-\nu(\infty)}{\nu(0)-\nu(\infty)} \equiv \frac{\nu(t)}{\nu(0)} \qquad (15)$$

where, $\nu(t)$ denotes time dependent fluorescence emission frequency of solute, $\nu(0)$ is the frequency related to initial fluorescence at t=0 and $\nu(\infty)$ is the emission frequency after attainment of complete equilibrium.

The perturbation to the excited solute molecules from the surrounding solvent molecules is responded through following three factors: a) translational displacement, b) rotational motion and c) vibrational motion of the solvent molecules.

The majority of the solvation dynamics measurements on ionic liquids have been carried out by time-correlated single photon counting technique (TCSPC) subsequent to the excitation of the fluorescence probe molecule dissolved in ionic liquids.

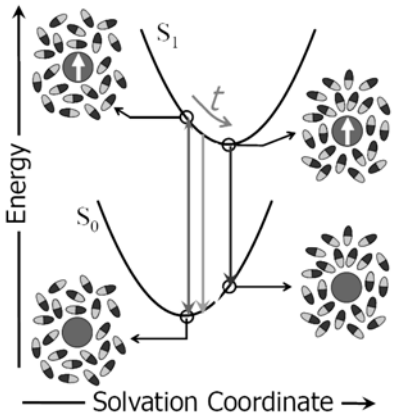

Figure 8: Schematic of solvation dynamics

TCSPC measurement is restricted to 20-50 ps; therefore the solvation dynamics lower than this limit has been investigated by employing ultrafast fluorescence upconverstion technique. It means that solvation dynamics of ionic liquids from ~10 fs to ~10 ns has been elucidated upon combining both the techniques.[77] Along with the experimental techniques, there is a number of simulation and molecular dynamics studies to reveal response of ionic liquids to the perturbation. Following the work by Maroncelli et al., on the response of ionic liquids to the solvation of coumarin 153 (C153); it can be summarized that within the region between 1 to 10 ps, kinetic profile is non-exponential in nature and do posses a plateau region.[78] Furthermore, it is obvious from the results obtained from a series of ionic liquids that slowest timescale can be correlated with the viscosity of the ionic liquids. Berg et al.[79] has reported that the solvation dynamics of ionic liquids occurs on two widely different time scales which is very analogous to the observation in imidazolium based ionic liquids by Arzhantsev et al.[80] The response was found to consist of an unresolved fast component, ascribed to 'inertial' or 'phonon-induced' motion, along with a comparatively slower component associated to 'diffusive' relaxation. Point to be mentioned here that ionic liquids having ammonium or phosphonium cations don't

show pronounce ultrafast component like imidazolium based ionic liquids. Irrespective of the nature of mathematical fit to the decay profile, Kobrak had stressed on the molecular picture of ionic liquid-probe system to delineate the solvation dynamics.[81b] Kobrak highlighted that the translational motion of the ions exhibits maximum contribution to ultrafast solvent response. However, this behaviour is highly contrasted to the short-time solvation dynamics exhibited by normal polar solvents since the dynamics is dominated by rotational motion.[81] To be mentioned here, translational motion of the constituent ions will play pivotal role in comprising solvation response since ion-dipole interactions are the most prominent interactions in case of ionic liquids. However, considering large size of ions and high polarizability, it can be predicted that orientational relaxations of free ions also have significant contribution. However, nature of physical motion and their individual contributions to the solvation response is the subject of high debate.[78, 79]

Simulation studies have indicated that the complex ionic liquid dynamics is equivalent to super cooled liquids. Presence of structural heterogeneity i.e. existence of polar and nonpolar domains, in ionic liquids has been widely accepted by the researchers. This microheterogeneous nature of ionic liquids is supposed to contribute additional complexity in mechanism of solvent reorganisation process. This structural heterogeneity is important while rationalising the existence of large solubility window (i.e. can dissolve large range of molecules) of ionic liquids. Solvatochromic studies to obtain solvent polarity parameters (E_T^{30} , E_T^{33} etc.) by using solvatochromic probes (like Reichardt's dye, Nile Red etc.) shows that polarity scale of ionic liquids (especially imidazolium, pyrolidinium based ILs) are similar to that of small chain aliphatic alcohols. Point to be mentioned here that though there are large differences in the structure of ionic liquids, the solvent polarity of ionic liquids shows small variation. This discrepancy can be rationalised if we admit the presence of micro-heterogeneity i.e. polar and nonpolar domain of local composition coexist in the ionic liquids. Normally, all liquids shows ballistic motions at short time scale and then motion shows Gaussian behaviour when time extends to perpetuity. However, on the contrary, ionic liquids display non-Gaussian diffusivity for a certain timescale depending on their individual structure and frequently this time scale coincides with that for chemical or photochemical reactivity. To pursue this abnormality, correlation of the data with van Hove correlation function reveals the existence of two dissimilar subensembles of ions in ionic liquids.[82] Van Hove equation is given by,

$$G_s(r,t) = \frac{1}{N}\langle \sum_{i=1}^{N} \delta(r - |r_i\,(t) - r_{i(0)}|)\rangle \quad (16)$$

It is found that among these subensembles one diffuses at very faster rate than expected from Fick's law and another ensemble of ions diffuse slower than predicted by Fick's law. It is to be pointed out here that diffusion of particles in normal liquid follows Fick's law. Fick's diffusion equation in standard Gaussian function can be expressed as,

$$G_{s0}(\mathrm{r,t}) = \left[\frac{3}{2\pi[r^2\,(t)]}\right]^{\frac{3}{2}} e^{-\frac{3r^2}{2\langle r^2(t)\rangle}\,2} \quad (17)$$

These local environments not necessarily related to polar/nonpolar regions of ionic liquids but may correspond to generic domains of solvent that do not significantly change on timescale relevant to chemical or optical spectroscopy. Samanta and co-workers have successfully established the presence of this local solvent heterogeneity and slow dynamics through the observation of excitation-wavelength dependent emission spectrum i.e. red edge effect which is not allowed by Kasha's rule.[77, 83] Margulis et al. observed an initial transient behaviour after photo excitation of the probe in ionic liquids.[84] Following this transient effect, there is no sign of generation of the electric field by solvent as well as change in the dipole moment of the excited probe. They have emphasised on the site specific perturbation of each molecule as well as hindered nature of the solute rotations for behaviour in ionic liquids. The red edge effect along with the presence of local heterogeneity on time scale makes properties of ionic liquid different from the conventional solvents.

1.5 Water Promoted Organic Reactions:

Indeed, about two decades ago chemists began to retrieve the benefits of water as a vivacious substitute to the conventional solvents, as far as not only is the environment concerned but also the organic reaction outcome. Solventless or neat reactions, solid state reactions, ultrasound and microwave-promoted aqueous reactions, reactions in ionic liquids, and reactions in supercritical fluids (SCF) such as the supercritical CO_2 were also conceived as friendly alternatives.[10,13-14] Rather evidently, on seeing omnipresent of water and being aware of its unique properties, chemists would have been undoubtedly enticed or wished to use it as a medium, but the persistent belief of its man-created enmity for organic reactions encumbered any attempt. This enmity may be the consequence of the detrimental effects of hydrolysis and lessons from alchemists that the reactions must be in solution for chemical reactions to occur.[33] Breslow and co-workers first resuscitated the use of water as a medium in Diels-

Alder (DA) reactions; they had carried out the cycloaddition of cyclopentadiene with methyl vinyl ketone in water and found its rate to be surprisingly enhanced by a factor of more than 100 times compared with the reaction in isooctane.[36,37] However, switching to water should be deemed not as a significant achievement but a rational and normal return to the realm of life, that is, to follow the nature lead. Therefore, we should not be surprised by the fact that water-promoted in vitro organic reactions afford better results compared with those in organic solvents, as a number of in vivo organic reactions occur entirely in water from the inception of life in earth. In fact, new terms and new reactivity coupled with some new effects that are thought to be the promoting forces for the reactions course, has cropped up in the literature. Among these effects hydrophobic effect, hydrophobic packing, antihydrophobic effect, pro-hydrophobic effect, dichotomous salts effect are predominant factors behind the water promoted organic reactions.[42,43] Rate enhancement of organic reactions in water is explained by hydrophobic effect of water.[42] Addition of organic apolar reactants in water causes repelling of water and on a reaction to these repelling forces apolar molecules tend to aggregate among themselves to reduce the contact surface area with water.[48b,33] Consequently, these aggregations cause formation of cavity inside water against high cohesive energy density of water. Thereafter, bulk water molecules try to reorient around the aggregates to form hydration layer which is often termed as hydrophobic hydration. In this hydrophobic hydration layer translational movement of water is restricted for the first layer of solvent cage but elevated hydrogen bonding potential of water directs some water molecules to reorient to maintain hydrogen bonding network around the hydration shell.[48] Hydrophobic interactions lead these aggregates to come closer and resulting into overlap of overlap of the shells as well as further abstraction of water molecules at the overlapped region to promote collisions among the reactants. The mechanism of hydrophobic hydration and hydrophobic interaction is very complicated procedure and several interpretations are available in literature to explain the phenomenon. Engberts and co-workers have designated these aggregates of organic molecules as forced aggregates i.e. these aggregates are much closer in energy with respect to activated complex compared to their unaggregated ground state energy.[43a] They have coined the term ‘enforced hydrophobic hydration’ to specify this mechanism of organic reaction accelerations. Engberts and co-workers introduced the concept of enforced hydrophobic hydration. In this process the hydrophobicity of diene and dienophile is decreased during the process of

activation.[43, 45] Diene and dienophile do not aggregate spontaneously under the reaction conditions. This observation is expressed by the term 'enforced'. To account for the large effect of water on Diels-Alder reactions, the enforced hydrophobic binding process is more favourable in water than in conventional organic solvents. On the basis of the Gibbs energy associated with the direct diene-dienophile pair potential and the rearrangement of water molecules accompanying the enforced hydrophobic hydration, it is possible to state that the reduction of the hydrophobic surface and hydrated volume during the activation process leads to a large gain of the entropy and a large loss of the enthalpy of water molecules. Addition to this hydrophobic factor, Jorgensen has pointed out that the activated complex especially in case of pericyclic reactions will be energetically stabilised if it possess hydrogen bonding acceptor sites. Polarisable nature of water as well as its extensive hydrogen bonding capability will help in reducing the activation energy of moderately polar or polar activated complex and will promote the reaction with faster rate. The separate contributions from the hydrophobic effect and hydrogen bonding effect towards rate acceleration in water vary from reaction to reactions. Breslow and follow up researches revealed that lithium chloride (LiCl) and guanidinium chloride (GnCl) acted, respectively, as pro- and anti-hydrophobic agents in the cycloaddition reaction, otherwise termed as salting-out and salting-in agents; while the former promotes the water structure by increasing the number of hydrogen bonds and accelerates the reaction, the latter disrupts it and slows down the reaction.[44] Since salting in agents increases the surface tension of water, the energy of cavitation to accommodate salt in water also increases. Therefore, these salting-in agents must be directly contributing to the solvation in water of apolar solutes likes cyclohexane, benzene etc. probably by a direct interaction. However salting out salts decreases the surface tension of the water as well as eases the cavity formation. Thus addition of salting out salts promotes direct solvation of the substrates in water by diminishing the solvation free energy. [46d]

However, arguments exist there in the literature regarding the mechanism of aqueous salt solution in promoting organic reactions. The spectroscopic studies revealed that antihydrophobic salts act as bridging agent between water and apolar solutes rather than disrupting water structure.[48c] It has been found that for most bimolecular pericyclic reactions the activation volume (i.e. difference between the molar volume of transitions state and that of ground state reactants) of the reactions is negative. The increased steroselectivity of the products in water has been thought to be a the

consequence of high internal cohesive pressure on the negative activation volume of the reactions.[43,44] Generally the transition state having less volume is stabilised more compared other possible transition states due to hydrophobic effect exerted by water. Organic reactions in water have mostly been performed using a co-solvent to stimulate solubility to some extent. A number of researches have been carried out to explain the rate enhancement of Diels-Alder reactions in aqueous solutions of alcohols by quantifying the components of the enforced hydrophobic hydration and hydrogen bonding proficiency of aqueous-alcohol mixture.[85, 86] The rate enhancements of Claisen rearrangements in water have been studied in detail and the results have also contributed to a better understanding of the aqueous acceleration of the DA reaction. The initial kinetic studies showed a rate enhancement in water up to a factor 200. This result led investigators to propose a dipolar mechanism. However, it was quickly recognised that a true dipolar mechanism would certainly lead to even more impressive rate enhancements.[87] Secondary deuterium kinetic isotope effect provided further evidence against an ionic mechanism and a meticulous analysis of the solvent effect pinpointed hydrogen bonding as the prime accelerating factor. Computational techniques have confirmed the notion that enhanced hydrogen bonding of water to the activated complex is dominant in the aqueous acceleration. Today's status, the insolubility of organic reactants in water, once considered a drawback, turns out to be advantageously a leading factor for the success of organic reactions in pure water. In 2005 Sharpless and co-workers introduced new type of reactions where water insoluble reactants endorse high yield in product at faster rate than water soluble condition.[88] Sharpless has coined term ‘on water reaction’ to describe these new type of water promoted reactions. The group had carried out some pericyclic reactions in aqueous suspension (on-water systems) and found that both kinetics and yields were extremely enhanced in most cases, compared with those in organic solvents.

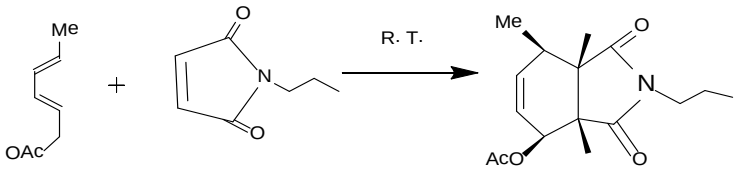

Scheme 1: Reaction of quadricyclane with dimethyl azodicarboxylate (DMAD) to yield 1, 2-diazetidines.

For the [2σ +2σ+2π] cycloaddition reaction of quadricyclane with dimethyl azodicarboxylate (DMAD) to yield 1,2-diazetidines the reaction time had been reduced from 48h to 10 min on switching from neat condition to on water condition.[88] Several reports describing the enhancement of reactivity and selectivity of the organic reactions at 'on water' condition have been available in literature. Tiwari and Kumar have reported the on-water Wittig reaction of insoluble aromatic and aliphatic aldehydes with phosphorus ylides at 298 K.[90]

Table 5: Comparative representations reaction time and yield of the reaction Scheme **1** in different solvents.*

Solvent	Time (h)	Yield (%)
Toluene	144	79
MeCN	>144	43
Neat	10	82
On water	8	81

* The table has been reproduced with permission from WILEY-VCH Verlag GmbH & Co. KGaA, Weinheim (permission number 3431340413982)

It has been found that alkali metal salts (LiCl and NaCl) decreases the rate of Wittig reaction. However, the rate of the reaction was measurable, when the same salts were utilized at 338K, and guanidinium chloride (anti-hydrophobic salt) decreased the rate of reactions in neat water. To understand the reasons behind this unusual increase in the rate of the reaction even more than 'in water' condition, several theoretical and experimental explanations are available in the literature.[42-45] Yung and Marcus had pointed that in both the homogeneous i.e. in water and heterogeneous i.e. on water reactions the reasons like hydrophobic packing, enforced hydrophobic interaction, cohesive energy density, polarity etc. act in the similar fashion since in both types of the reactions water medium is common.[91] They have theoretically advocated the presence of 'free OH' groups at the water surface and identified that the ease of hydrogen bonding with this 'free OH' groups helps in accelerating reactions. The presence of unsatisfied or unbound –OH group at the water interface has been also experimentally confirmed by surface sensitive spectroscopic techniques also.[92]

However, their contribution in promoting organic reactions at heterogeneous condition is still a matter of debate.[93] Multicomponent reactions like Passerini and Ugi reactions at on water condition have also been found faster than the homogeneous condition. Pirrung and Sarma have experimentally demonstrated that the acceleration of these organic reactions in aqueous media mainly depends on the polarity and mixing methods (stirring).[93b, 94] Beattie et al has emphasised on the possibility of acid catalysis by the strongly adsorbed hydroxide ions at the oil-water interfaces in acceleration of the reactions.[93a] Theoretically 'on water' reactions are found advantageous over their 'in water' counterpart in terms of the orientation aspect also. Interfacial anchoring of at least on the reactants will introduce compulsory relative reorientation of another reactant to form transition state of the reaction.[91, 93] Geometry of the reactants is also responsible in controlling the steroselectivity of the heterogeneous reactions. In summary, heterogeneous catalysis of the organic reactions possess several dissimilarities compared to homogeneous one. The main problem associated to the investigations of the heterogeneous reaction is that separation of the contribution of the interface from the bulk one. Moreover, maximum forces which promote the homogeneous reactions are also involved during heterogeneous reactions also. We shall exploit the mechanistic overview of the on water mechanism in the light of the presence of free OH groups at the interface through our research works in the appropriate chapter of this thesis.

1.6 Ionic liquids as Elementary Particle Transfer Reaction Medium:

1.6.1 Photophysical Process

The interaction of light and matter which may be a natural phenomenon and/or as an artificial process pervades most spectrum of science, from medicine to material science. [94] The significance of the interaction with photons in the natural world can hardly be overruled. It forms the basis for photosynthesis converting carbon dioxide and water into more complex plant-associated structures. Photophysics involves the absorption, transfer, movement, and emission of electromagnetic, light, energy without chemical reactions. By comparison, photochemistry involves the interaction of electromagnetic energy that results in chemical reactions.[95] We are encircled by substances that are produced by natural or artificial photochemical reactions. Many of the most common functions exploited in our technological environment, from signal processing, storage and display to the use of pigments, sensors and sensitizers are based on the interaction of light with matter. It was realized at the beginning of the

century that only the light that is absorbed by a chemical species can produce changes in the molecules. This could easily be explained with the advent of quantum theory. When a molecule absorbs light, only those photons (wavelengths) of the correct energy are able to produce excitation of the molecule. Thus the interaction of light with a molecular system is generally an interaction between one photon and one molecule, $A + h\nu \rightarrow A^*$, where, *A* denotes the ground state molecule, *hν* the absorbed photon, and *A** the molecule in an electronically excited state. As the equation implies, the excited molecule *A** is the molecule *A* with an extra energy *hν*.[94a]

The absorption of light to promote a ground state molecule to its singlet-excited state (S_1) is often manifested by profound changes in the electronic and nuclear configuration of the molecule, which can open up new reactive pathways not available to the ground state species. In order to be able to predict the fates of excited states, it is important to understand the basic processes that can occur during the lifetime of the excited state.[96] The most important of such processes are summarized in the Jablonski diagram presented in Figure 9.

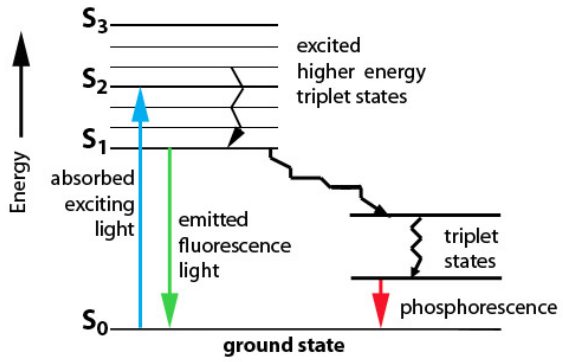

Figure 9: Jablonski diagram and photo physical processes

These pathways include intersystem crossing (ISC, a change in multiplicity), internal conversion (IC, vibrational relaxation), and fluorescence (emission of a photon). These processes are often very fast, and as a result, few excited singlet state species have lifetimes longer than 10 nanoseconds. Triplet excited states tend to be longer lived, many having lifetimes of several microseconds or longer. Of particular interest to organic chemists are chemical reactions that can occur from excited states (singlet or triplet) to give new products. Reactions from excited states must be very fast in order to compete with the other deactivation pathways, especially for singlet excited

states. There are several well studied reaction types that are known to proceed from excited states, including isomerizations, electron and proton transfers, pericyclic reactions, fragmentations, hydrogen abstractions, dimerizations, and others. A number of experimental methods exist that can offer insight into the fate of the excited states produced. Standard characterization methods (NMR, MS, IR, UV-vis, etc.) can be carried out on the products of photochemical reactions. Steady-state fluorescence spectroscopy gives information on the proportion of excited states that deactivate through emission of a photon, and provides information regarding the changes in nuclear configuration of the molecule on excitation.[97] Time-resolved fluorescence offers information regarding the rate of fluorescence and the lifetime of the excited state.

Excitation of a molecule to S_1, leads to the rapid promotion of an electron from the highest occupied molecular orbital (HOMO) to the lowest unoccupied molecular orbital (LUMO). According to the Franck-Condon (FC) principle, the motion of electrons is fast ($k \sim 10^{15}$ s^{-1}) relative to the motion of nuclei ($k \sim 10^{13}$-10^{11} s^{-1}).

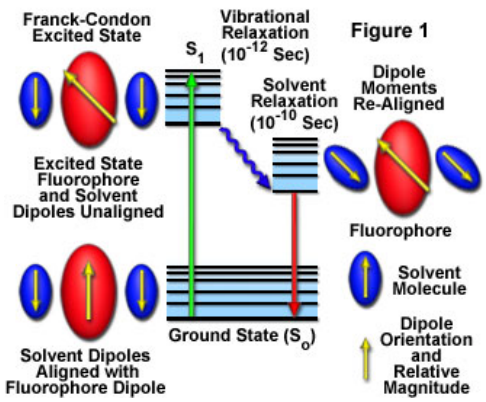

Figure 10: Frank Condon principle and progress of solvation co-ordinate

Therefore, immediately following excitation, the molecule has the same nuclear configuration and solvent cage as it did prior to excitation. A molecule in this state, termed the FC excited state, rapidly undergoes thermal relaxation to its lowest vibrational level ($k \sim 10^{13}$-10^{14} s^{-1}). This is followed by a reorganization of its nuclear geometry and solvent cage ($k \sim 10^{11}$ - 10^{13} s^{-1}) to accommodate the electronic perturbation. Once this reorganization is complete, the molecule is said to be in its equilibrium excited state, and it is this state which we refer to when we say singlet excited state or S_1. It is from the equilibrium excited state that the relevant

photophysical and photochemical processes take place. Most of the compounds show fluorescence emission maximum at energies that are at longer wavelengths (lower energies) than the corresponding absorption spectrum.[98] The magnitude of the shift in the absorption and emission maxima, termed the Stokes shift, is indicative of the extent to which the excited state geometry has changed from the ground state geometry. Inspection of the absorption and fluorescence spectra for a given molecule remains the most reliable source for information on its excited state geometry.

1.6.2 Excited state proton transfer reactions

Proton transfer reactions are the significant example of elementary particle transfer processes and they possess the relevance of solvation dynamics to reactivity.[99] It is now well established that in bulk solvents the reaction coordinate for a PT reaction is a collective solvent coordinate similar to that describing the solvation dynamics.[100] It is then not surprising that PT reactions are strongly affected by confinement of the surrounding solvent. Depending on the characteristic of the systems, various types of proton transfer reactions occur in the ground- or excited-states, either adiabatically or non-adiabatically. Among all these processes, excited-state intramolecular proton transfer (ESIPT) in particular has engrossed interest from both theoretical and experimental standpoints since it exhibits an exclusively large Stokes' shifted fluorescence emission without self-reabsorption as well as an easy population inversion in the proton transferred keto form, which are attributed to its intrinsic four-level photocycle scheme implemented by the enol (N) – keto (T) phototautomerization ($N \rightarrow N^* \rightarrow T^* \rightarrow T \rightarrow \ldots$) process.[101]

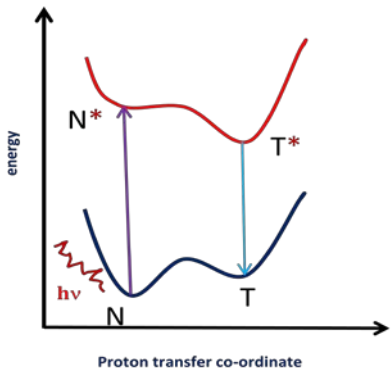

Figure 11: Illustrative diagram of ESIPT dynamics

ESIPT can be precisely defined as a phototautomerization process occurring in the electronic excited state of a molecule, where a heterocyclic ring is formed by the intramolecular hydrogen bond between a hydroxyl group and a neighboring proton acceptor. In 1950s, Weller had first reported about ESIPT process in salicylic acids, o-anicic acid.[102] We have already discussed about the unique solvation dynamics of ionic liquids and there have been many studies on solvation in relation to the use of ionic liquids as chemical reaction media. Traditional solvatochromism studies have been performed to delineate the electronic interaction parameters E_T^{30}, π^*, α, and β.[23, 62] Significant characteristics of solvation dynamics in ionic liquids is the wide distribution of solvation time scales from sub-picoseconds to nanoseconds. Since ionic liquids are composed of dipolar head group as well as non-polar tail, two types of forces predominate in ionic liquids viz. Coulombic interaction between ion-rich polar domains induced by the ions and van der Waals interactions among tails.[51-54]

From the macroscopic structural point of view heterogeneity prevails in the ionic liquids. However, solvation heterogeneity and its relation to structural heterogeneity required to be investigated properly to unearth huge applicability of ionic liquids in charge transfer devices. Permittivity of the ionic liquids is the consequences of the interplay of polar and non-polar domains as recent investigations through neutron scattering and molecular dynamics studies have confirmed the presence of small domains differing in the possessing of charges. In case of highly viscous ionic liquids observation of the red edge effect (REE) also confirm the inhomogeneity of ionic liquids. During REE, the solute is excited near the 0-0 transition or at longer wavelengths; the wavelength of the emission intensity maxima depends on excitation wavelength.[103] Although there have been several studies on charge transfer dynamics in ionic liquids available in the literature, systematic exploration of the role of heterogeneous solvation dynamics on the reaction rate in ionic liquids has been rarely investigated. Chou and his group during their study on ESIPT /ESICT dynamics of 4'-*N*, *N*-Diethylamino-3-hydroxyflavone (DEAHF) in polar and non-polar solvents noted that proton transfer occurs on two time scales (sub-ps and a few tens of ps) in polar solvents.[104] They have justified their result by invoking the idea that perturbation via solvent polarity might have played pivotal role in modifying the energetic pathway of ESIPT mechanism. It should be kept in mind that during ESIPT, considerable amount of difference in dipole moment exists between excited normal (N*) and excited tautomeric (T*) forms. Such large dipolar

change combined with solvent polarization governs the solvation dynamics of proton transfer reaction.

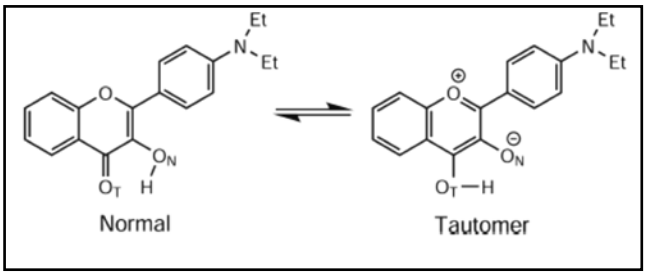

Scheme 3: Excited State Intramolecular Proton Transfer reaction of DEAHF

Ab Initio study on ESIPT reaction of DEAHF in [Bmim][PF_6] also have confirmed drastic increase in the dipole moment upon excitation the HOMO localised at aniline moiety (right hand side of DEAHF) to LUMO at chromene moiety (left hand side). This corresponds to dynamic stokes shift of the peak consigned to the excited normal form of DEAHF.[104,105] Variation in alkyl chain length or anions of the ionic liquids affects normal/tautomeric ratio and excitation wavelength dependence during tautomerization reaction. However, ion concentration of ionic liquids which is thought as one of the responsible factor for polarity of ionic liquids does not show prominent effect on proton transfer energetics.[104a] The evaluation of the proton transfer potential in ionic liquids gives following insights into the mechanism i) normal form (N) is more stable in the ground state than excited state (N*) (ii) two minima are found in the excited state which is consistent with time evolution study of the dynamics.

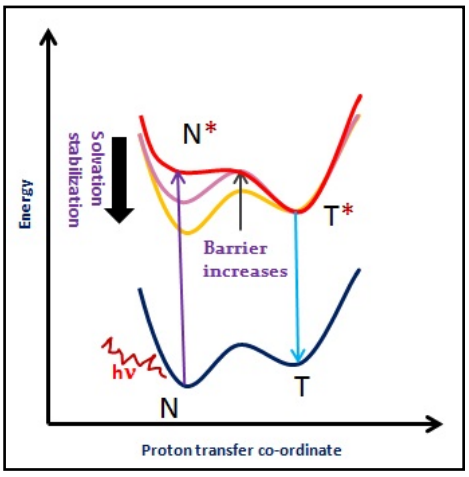

Figure 12: Proposed diagram of solvent stabilization of excited normal form of the probe

After initial excitation of the probe molecule the barrier of proton transfer process remain relatively small and thus proton transfer reactions moves forward. With time evolution, as solvation relaxation to excited normal state proceeds, the barrier of proton transfer increases to resist further transformation of N* to T*.[105a]

1.6.3. Electron Transfer Reaction

Electrons are such movable elementary particles that their spatial movement in condensed phases from one host species (donor) to another receptor species (acceptor) can either be driven by thermal fluctuations or by external photochemical excitation.[106] The most competent way to promote electron transfer is through light irradiation, wherein one of the species (donor or acceptor) is excited to a higher electronic state, depending upon the accessibility of the higher electronic excited state, followed by transfer of an electron to the acceptor through vibronic coupling.[107] The superiority of the photoinduced electron transfer over thermally activated electron transfer lies the fact that an excited molecule is more redox reactive than the ground state in the higher electronic coupling among donor excited state wave function and the ground state and the coupling of the electronic wave functions is better if one of the reactant is in excited state because the excited state wave functions are more disseminated compared to that of ground state.

1.6.3.1 Theory of Electron Transfer Reaction

As energy-rich species, excited states are, as a whole, expected to be more reactive than the corresponding ground states, deactivation of the excited state may be achieved through the following intermolecular processes in addition to the other photochemical like radioactive and non-radioactive deexcitation:

$$A^* + B \longrightarrow A^+ + B^- \quad \text{oxidative electron transfer}$$

$$A^* + B \longrightarrow A^- + B^+ \quad \text{reductive electron transfer}$$

$$A^* + B \longrightarrow A + B^* \quad \text{energy transfer}$$

Scheme 4: Probable pathways of de-excitation of excited states

Although the electron transfer or energy transfer from a donor to an acceptor apparently seems to be a very simple process, the actual intricacies involved in most of the systems involving ET reactions are so complex that the detailed understanding of the factors governing this reaction in different systems/conditions are yet to be

explored properly.[108] A substantial amount of research has been carried out in the development of ET theory, a very notable contribution to which due to Prof. R A Marcus.[109] As the electronically excited state of the species possess very different characteristics compared to that of the ground state of the molecule, both the thermodynamic and the kinetic aspects of the PET reactions must be thoroughly examined.

From the thermodynamic point of view, the free energy difference between excited and ground state of the molecule:

$$\Delta G\,(A^*, A) = \Delta E\,(A^*, A) - T\Delta S\,(A^*, A) \qquad (18)$$

The energy difference between the ground and excited state both taken at their zero vibrational levels E^{00} (A*, A) can be equated to ΔE in condensed phase such that, at 1 atm and 0 K, $\Delta E = NE^{00}$ (A*, A). This relation also holds at the room temperature if there is small difference between the vibrational partition function of the two states.[110] Change in the entropy on going from ground state to excited state can be truly calculated from the Stokes shifts between absorption and emission band. Often during electron transfer reactions, Stokes shift remains small in value since for the reaction it is necessary condition to have the excited state with longer lifetime. In this milieu, the entropy contribution can be neglected during most of the electron transfer cases. Now free energy change can be written as,

$$\Delta G^0\,(A^*, A) \approx NE^{00}\,(A^*, A) \qquad (19)$$

The redox potentials for the excited state couples can be calculated from the standard potentials of the ground state couples considering the one electron potential corresponding to the zero –zero spectroscopic energy (i.e. the E^{00} value in eV):

$$E^0\,(A^+/A^*) = E^0\,(A^+/A) - E^{00} \qquad (20a)$$

$$E^0\,(A^*/A^-) = E^0\,(A/A^-) + E^{00} \qquad (20b)$$

The excited state is both a stronger reductant and a stronger oxidant than the ground state since it possesses extra energy.[109b]

From the viewpoint of the fundamental kinetic aspects of bimolecular processes involving excited states, bimolecular electron transfer between A and B under the diffusive condition can be summarised by following scheme:

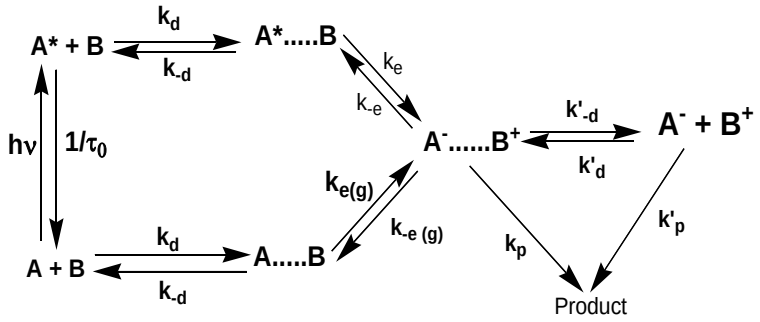

Scheme 5: Kinetic mechanism for photoinduced electron transfer reactions

In scheme **5**, k_d, k_{-d}, k'_d, and k'_{-d} are rate constants for formation and dissociation of the outer-sphere encounter complex in the ground and excited states, k_e and k_{-e} are unimolecular rate constants for the electron transfer step involving the excited state, and $k_{e(g)}$ and $k_{-e(g)}$ are the corresponding rate constants for the ground state electron transfer step.

For photoinduced processes requiring diffusion and formation of encounters, we can use the Stern–Volmer model which assumes statistical encounter between A* and B. The simplest case is that of a species A* that decays via some inherent intramolecular paths and, in fluid solution, can also encounter a quencher B. The excited state lifetimes in the absence (τ_0) and in the presence (τ) of the quencher B are then given by,

$$\tau_0 = 1/(k_r + k_{nr}) \quad (21)$$

$$\tau = 1/(k_r + k_{nr} + k_q [B]) \quad (22)$$

where, k_q is the bimolecular constant of the quenching process, leading to ET reaction in present context.

Upon dividing 21 by 22, we can write the following equation,

$$\tau_0/\tau = 1 + k_q \tau_0[B] \quad (23)$$

This is the well known Stern-Volmer equation and k_q can be calculated from the slope of the τ_0/τ *vs.* [B] plot, if τ_0 is known.

The key step of the processes depicted in Scheme **5** is the electron transfer step (k_{et}) in the encounter complex (A*.....B). Prof. Rudloph A. Marcus was awarded with the Nobel Prize in the year 1992 for his phenomenal contribution in

understanding the energetics and kinetics of the electron transfer reactions (k_{et}).[109] In the frame work of the Eyring theory of the transition state, the value of the electron transfer rate constant can be expressed both in classical as well as semi classical form as:

$$k_{et} = \left(\frac{h\nu}{k_B T}\right) \exp\left(-\frac{\Delta G^*}{k_B T}\right) \tag{24}$$

Here, ν is the product of nuclear frequency factor ν_n and the electronic transmission coefficient κ_{el}. In the classical form κ_{el} is normally considered as unity. In the semi-classical form, κ_{el} is related to V_{el} (electronic coupling at the transition state i.e. crossing point of the reactant and product surfaces) by

$$\mathcal{K}_{el} = \frac{1}{1+\left(\frac{4\pi V_{el}^2 \tau_S}{\hbar \lambda}\right)} \tag{25}$$

where, λ is the reorganisation energy, discussed below. For strong electronic coupling of the ET reaction (V_{el} >200cm^{-1}), the parameter κ_{el} closes to unity and this condition is called adiabatic electron transfer and for weak coupling cases i.e. V_{el} << 100cm^{-1} electron transfer will pass through the non-adiabatic regime, with the ET probability < 1 while reactant state passes through transition state.

The most striking feature of Marcus theory is the redefinition of the activation energy (ΔG^*) in terms of the vertical and horizontal displacements of the potential energy surfaces during the electron transfer reactions (Fig. 13). He had invoked the idea that free energies (ΔG_R^0 and ΔG_p^0) of the reactant (R) and product (P) states follow quadratic functions with the changes in the reaction co-ordinate (X).

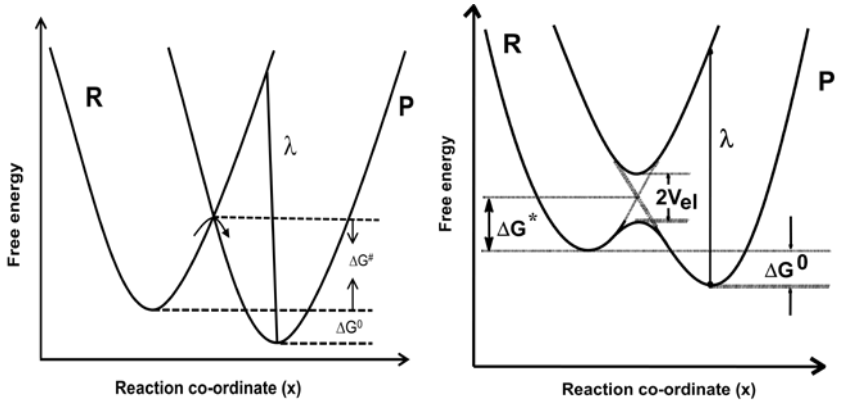

Figure 13: Schematics of the potential energy surfaces the reactant (R) and product (P) states following classical and semi-classical treatment

The free energy of activation (ΔG*) can thus be defined as:

$$\Delta G^* = \frac{(\lambda+\Delta G^0)^2}{4\lambda RT} \quad (26)$$

By using the above quadratic expression for ΔG*, the general form of the electron transfer rate constant can be rewritten as:

$$k_{et} = \left(\frac{h\upsilon}{k_B T}\right) \exp - \frac{(\lambda+\Delta G_0)^2}{4\lambda k_B T} \quad (27)$$

Here in the equation λ is the reorganisation energy required in changing the equilibrium configuration of R state to P state as shown in Fig. 13 and is the sum of combinations of solvent (λ_s) and intermolecular (λ_i) contributions i.e. $\lambda = \lambda_s + \lambda_i$. λ is a positive quantity. The driving force (ΔG_0) of the ET process can be measured experimentally or calculated theoretically. For example, when solvation after the process of producing photoinduced charge pairing is rapid, ΔG_0 can be approximately estimated by the following equation: [108]

$$\Delta G_0 = E_{D/D^+} - \left(E_{A/A^-} + E_{00}\right) - \frac{e^2}{\varepsilon}(r_{D^+} + r_{A^-}) \quad (28)$$

where E_{D/D^+} and E_{A/A^-} are the standard redox potentials of the donor and acceptor, respectively, E_{00} is the energy of the donor exited state, r_{D^+} and r_{A^-} are the radii of the donor and acceptor, respectively, and ε is the medium dielectric constant.

In summary, the classical Marcus equation is valid in the following conditions: [108, 109]

i) All reactive nuclear modes, that is, local nuclear modes, solvent inertial polarization modes, and some other kinds of collective modes, are purely classical. The electronic transition in the ET process is via the minimum energy at the crossing of the initial and final state potential surfaces.

(ii) The potential surfaces are essentially diabatic surfaces with insignificant splitting at the crossing and of parabolic shape. The latter reflects harmonic molecular motion with equilibrium nuclear coordinate displacement and a linear environmental medium response.

(iii) The vibrational frequencies and the normal modes are the same in the initial and final states

The energy gap dependence of the ET rate constant can be separated into three regions: i) $-\Delta G^0 < \lambda_s$ (normal Marcus region), the ET reaction moves faster as ΔG^0

becomes more negative. (b) $-\Delta G^0 = \lambda_s$, such a situation shows fastest ET reaction since the activation barrier of ET reaction vanishes. (c) $-\Delta G^0 > \lambda_s$ (Marcus inverted region) since ΔG^* increases with the increasing exergonicity ($-\Delta G^0$) and consequently the ET reaction rate decreases. Therefore, the ET rate constant (k_{et}) shows a bell shape dependence on the free energy gap (ΔG^0) (see fig. 14).

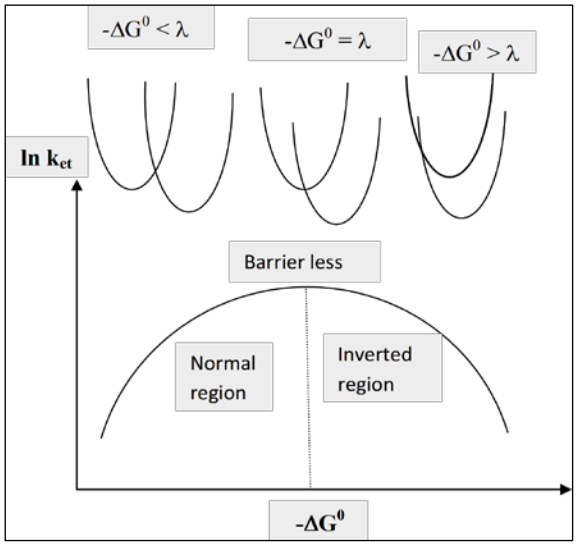

Figure 14: Free energy gap (ΔG^0) dependence of k_{et}

Since Prof. Marcus had formulated ET theory in 1956, extensive researches have been carried out to find out the experimental substantiation of the Marcus inverted region as well as the possibility of further development of the theory. In spite of tremendous efforts towards satisfying the quests, after about thirty years Miller and co-workers had successfully observed the Marcus inversion behaviour following intramolecular charge shift reaction in the donor-spacer-acceptor (D-S-A) kind of bi-functional molecules in 1984.[112] There have been a large number of follow up researches on several donor –acceptor systems to ensure the inversion behaviour at higher exergonic region i.e. $-\Delta G^0 > \lambda_s$.

It is to be mentioned here that though the experimental validation of Marcus theory on ET is proved univocally for various systems, the minutiae related to the inversion behaviour is still not well understood. For example, on the basis of Marcus' prediction on quadratic functional dependence of the free energy of activation, the k_{et} vs. ΔG^0 plots should be perfectly bell- shaped curve. However, the changes in the k_{et} vs. ΔG^0 plots are found to be relatively less stiff in the inversion region (*high*

exergonicity region) than in the normal region i.e. the curve is not symmetric with respect to $-\Delta G^0 = \lambda_s$ region. It implies that the ET reaction moves faster in the inverted region compared to that of normal region which is in contrary to the Marcus theory. Besides these anomalies, observations of inversion region are only limited to these two cases (i) the charge separation (CS) reactions in the ion pairs involving intramolecular ET systems and (ii) the charge recombination (CR) reactions involving either intramolecular or intermolecular ET systems. For bimolecular or intermolecular ET reactions, the observation of the inversion behaviour is not only rare but also not convincing in most of the studies. For CS reactions involving intermolecular or bimolecular ET systems in homogeneous condition, the observed rate constant (k_{obs}) initially increases with reaction exergonicity ($-\Delta G_0$) at the lower exergonicity region but the extent of increase gradually reduces as the ΔG_0 becomes more and more negative and finally the k_{obs} levels off at a saturation limit at the higher exergonicity region. This behaviour of the k_{et} vs. ΔG^0 plot is commonly known as Rehm-Weller behaviour followed by their first observation in 1970. k_{obs} values at the saturation limit *i.e.* at higher exergonic region are often found to be quite similar to that of bimolecular diffusion controlled rate constant (k_d). It entails that diffusion of the donor and acceptor molecules in the solutions limits the rate of electron transfer reactions at the higher exergonic region. The main reason for not observing such an inversion in intermolecular ET reactions is supposed to be due to the limiting of the bimolecular reaction rates by the diffusion of reactants, which effectively masks the expected inversion behaviour. Following the observations of the diffusion controlled electron transfer reactions, Rehm-Weller had redefined the activation energy of ET by:

$$\Delta G^* = \left(\frac{\Delta G^0}{2}\right) + \left\{\left(\frac{\Delta G^0}{2}\right)^2 + \left(\frac{\lambda}{4}\right)^2\right\}^{1/2} \qquad (29)$$

It is clear that ΔG^* defined by Rehm-Weller is drastically different than the quadratic functional form advocated by Marcus.[113] Except few cases of bimolecular ET at homogeneous condition, this Rehm-Weller equation mostly fails for the cases where quencher concentrations are not sufficiently low to avoid transient effect. Theoretical and experimental studies on ET for 40 years have ensured that all types of ET reactions irrespective of intramolecular or intermolecular can be better realized by applying Marcus ET theory, might not be in its classical form but certainly after modification following semi-classical, quantum mechanical or some other advanced

perceptions.[114] To be mentioned here that the incorporation of the factors like participation of high frequency vibrational modes and the reaction exergonicity dependent changes in reactant distributions, V_{el} and interaction distance (r), solvent polarization contributions etc. while evaluating the rate ET reactions will certainly help one in understanding the intricacies of the ET reactions in real systems.

1.6.3.2 Two Dimensional Electron Transfer theory

Following the discussions in the previous section, it is obvious that the diffusion of the reactants plays pivotal role in determining the kinetics of the bimolecular ET reaction in homogeneous solution. Intermolecular ET in the micro-heterogeneous media, e.g. in micelles, reverse micelles, ionic liquids, etc. could be a good candidate to cause the ET reaction occur effectively under non-diffusive condition such that the influence of reactant diffusion on the observed ET rates and thus to observe the predicted Marcus' inversion at higher exergonicity of the reactions.[115] Further in the restricted media, the solvent relaxation dynamics can also be much slower in comparison to that in the conventional solvents and thus can effectively shift the expected inversion at relatively lower exergonicity region, making it easier to observe experimentally. With these presumptions, we have investigated the photoinduced ET interactions of coumarin dyes with an aromatic amine donor in different ionic liquids. Our idea of delineating ET reactions in ionic liquids is being inspired by the graceful strategy adopted by Yoshihara and co-workers to investigate bimolecular ET reactions under non-diffusive condition where neat electron-donating solvents (different liquid amines, e.g. *N*-methylaniline (MAN), *N*, *N*-dimethylaniline (DMAN), etc.) had been used directly as the electron donors in combination with number of suitable chromophoric dyes (coumarin and oxazine dyes) as the electron acceptors.[116]

The two important observations made by Yoshihara and co-workers while investigating bimolecular electron transfer reactions in electron donating solvent are (i) the non-exponential ET kinetics and (ii) the ET rates faster than solvent relaxation dynamics.[115] This non-exponential nature in the ET kinetics can be understood if one applies the two-dimensional ET (2DET) model to correlate the observations where ET rates are faster than solvent relaxation. This 2DET model has been advanced by Sumi and Marcus and sometimes this model is also known as Sumi-Marcus model also.[114] In this model along with the solvation co-ordinate 'X', a second coordinate 'q' that describes the intramolecular reorganisation for the reactants (nuclear coordinate) has

also been considered to describe ET reactions the free energy surfaces of the reactant and product states as shown in Fig. 15 by contour diagrams.

Conceptually the changes in the bond lengths and bond angles for the reactants that is accompanied with the progress of the reactions is defined by normalised nuclear coordinate 'q' and the another coordinate 'X' determines the extent of solvation relaxation during ET reaction. Based on the above model, free energy functions of the reactants and products are expressed as,

$$G_r \quad (X,q) \quad = \quad \lambda_s X^2 \quad + \quad \lambda_i q^2 \tag{29a}$$

$$G_p \quad (X,q) \quad = \quad \lambda_s (X-1)^2 \quad + \quad \lambda_i (q-1)^2 \quad + \Delta G^0 \tag{29b}$$

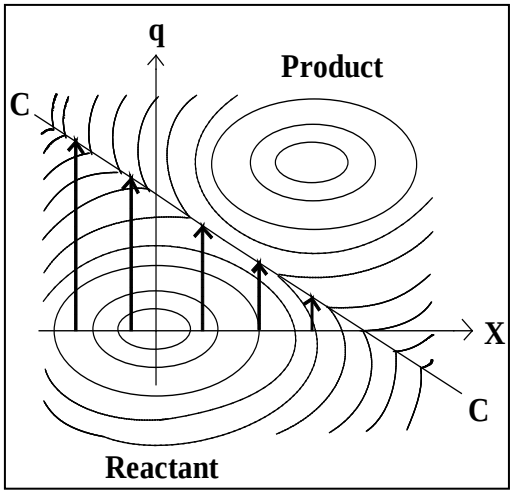

Figure 15: Isoenergy contours of potential energy surfaces drawn in two dimensional planes for reactant and product

Where, λ_s and λ_i are the solvent reorganisation energy and intramolecular reorganisation energy respectively. It is to mentioned here that the (X,q) coordinates for reactants and product states for their equilibrium configuration are (0.0) and (1,1) respectively. In 2-DET model, the relaxation across the nuclear coordinate 'q' is assumed to occur much faster than that along the solvent coordinate 'X'. It implies that the distribution of reactants and products will always maintain equilibrium along 'q' coordinate and on the contrary achieving equilibrium distribution of reactants and products will be unachievable along 'X' coordinate will be impossible during the ET reaction. Therefore, ET reaction will effectively occur along 'q' for varying 'X'

coordinate, which progressively evolve with time due to progress in solvation. By using Smoluchowski equation, the time dependent probability distribution of the reactant along 'X' coordinate can be expressed as:

$$\frac{\partial p(X,t)}{\partial t} = D\frac{\partial}{\partial X}\left[\frac{\partial}{\partial x} + \frac{1}{k_B T}\frac{\partial G_r(X)}{\partial X}\right]p(X,t) - k(x)p(X,t) \qquad (30)$$

where, D represents the solvent polarization diffusion coefficient and is given by $k_B T/(2\lambda_s \tau_s)$.The first term in the right hand side of the equation descries the diffusive motion along solvation coordinate 'X' and the last term denotes ET reaction progress along the nuclear coordinate 'q'.[116]

When the reaction is non-adiabatic, the ET rate constant at any point of 'X' can be expressed as,

$$k_{NA}(X) = \left\{\frac{2\pi V_{el}^2}{\hbar(4\pi\lambda_s k_B T)^{1/2}}\right\}\exp\left\{\frac{-\Delta G^*(X)}{k_B T}\right\} \qquad (31)$$

From the free energy functions of the reactants and products i.e. equation 29a and 29b and assuming no participation of higher frequency modes, we can write ΔG*(X) in the following way,

$$\Delta G^*(X) = \frac{\left[\lambda_s(1-2X)+\Delta G^0(X)+\lambda_i\right]^2}{4\lambda_i} \qquad (32)$$

The quasi particle on the free energy surface moves along q due to thermal fluctuations and a transition from the reactant to product occurs with some probability at a certain point of 'q' for a given solvent coordinate 'X'. In our systems of study, it is expected that the initial 'X' coordinate of the reactant state, say 'X_g' , where system is initially present after photoexciation, is quite away from the equilibrium position (X=0) for the reactant. In this situation, if the solvent relaxes very slowly (as ionic liquids are highly viscous), in the ultrafast ET process only the (1-2X_g) fraction of λ_s can contribute to G*(X).

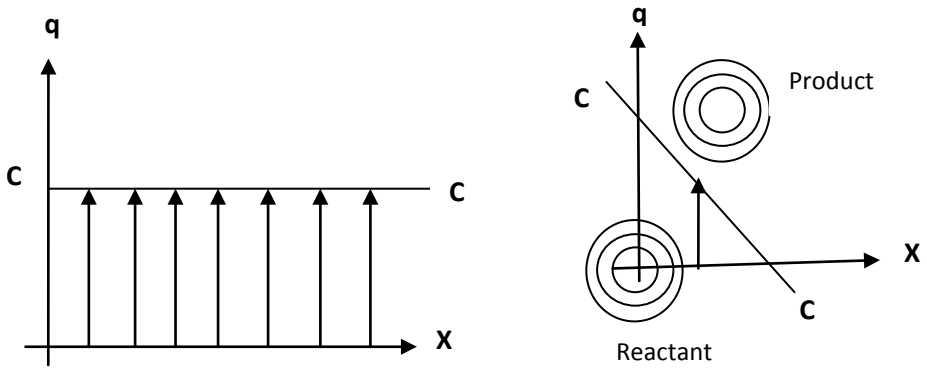

Figure 16: Wide reaction window and narrow reaction window

Fig. 16 describes typical cases for the ET reaction based on the 2DET model. If the transition curve C is parallel to the 'X' axis (for λ_i/λ_s >>1), the reaction takes place through a 'wide window'.[118] It implies that the energy barrier ΔG*(X) will be the same at any 'X' and total population of the reactant follow exponential decay kinetics. In case of λ_i/λ_s << 1, the reaction takes place through a 'narrow window'. In this case barrier ΔG*(X) varies with respect to its position on 'X' coordinate. In such cases, decay follows a non exponential kinetics.

At initial stage, the population distributed near to the low energy barrier region will react faster along 'q' coordinate, while the reactants near the bottom of the free energy surface will be left behind. These remaining reactants near the bottom of the free energy barrier will follow two pathways: (a) reactants may cross directly the high energy barrier along the nuclear coordinate 'q', or (b) they may move long the solvation coordinate 'X' first to a position with low energy barrier and then cross the activation barrier to undergo the ET reaction. In summary, in this case there will be a time dependent alteration in the distribution of the reactants and accordingly a non-equilibrium ET kinetics.

1.6.3.3 Hybrid Model for 2DET: Incorporation of High Frequency Vibrational Modes

In 'Sumi-Marcus' 2-DET model, frequency of all the vibration modes for solvent coordinate 'X' and nuclear coordinate q are considered to be much lower than the thermal energy ($h\nu$ << k_BT). In the real system, along with classical low frequency modes, some high frequency modes ($h\nu$ >> k_BT) might also participates during the ET reaction.[114-118] After incorporation of the high frequency modes in the 2-DET model the free energy function of the product can be rewritten as:

$$G_{p,n}(X,q) = \lambda_s(X-1)^2 + \lambda_i(q-1)^2 + \Delta G^0 + n h\nu_n \quad (33)$$

where n is the vibrational quantum number.

In the non-adiabatic ET process, the rate constant can be presented as,

$$k_{NA}(X) = \left\{\frac{2\pi V_{el,n}^2}{\hbar(4\pi\lambda_1 k_B T)^{1/2}}\right\} \exp\left\{\frac{-\Delta G^*(n,X)}{k_B T}\right\} \quad (34)$$

Here, crossing of the reactant and product surfaces corresponding to different vibrational levels of the high frequency modes are considered separately and ET rate

is considered as the sum of all the possible ET channels. The situation has been qualitatively described in the Figure 17, where a number of free energy surfaces for the product state have been considered for a high frequency vibrational mode.

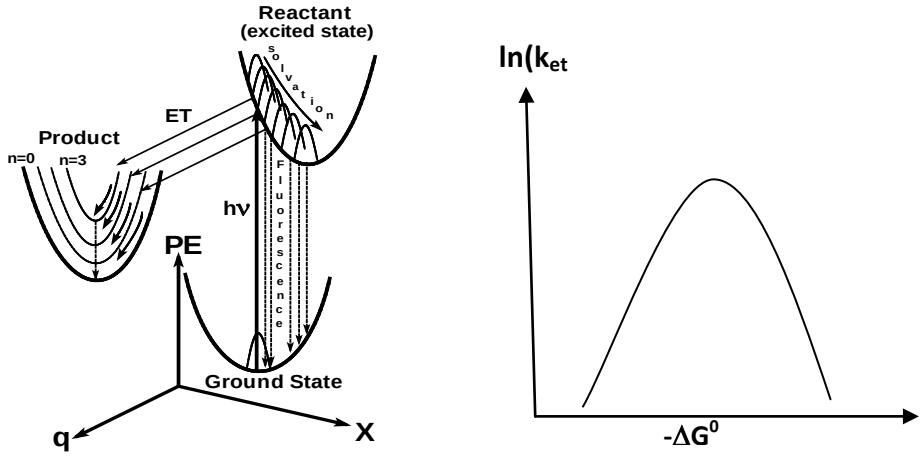

Figure 17: Solvation coordinate involving high frequency mode of solvent and asymmetric MIR plot

During ET study, the high frequency modes possess significance only at very high exergonic region *i.e.* for into the inverted region, since at this region the energy released during ET process is sufficient to excite the product to higher vibrational levels.[116] Due to the involvement of these high frequency modes, the bell-shaped k_{et} vs. ΔG^0 plots often appeared as asymmetric in nature.[117] This hybrid model of 2DET finds its significance in the situation where nuclear tunnelling is possible. At room temperature, the probability of tunnelling mechanism is significantly low.

Point to be mentioned here that this hybrid model of 2DET has been discussed here for completeness of the theoretical background of the electron transfer only. In our systems of study, incorporation of this model has been judiciously avoided since all the studies have been carried out in room temperature and at reasonably lower exergonicity region. Moreover, a rigorous quantitative calculation based upon the hybrid model of 2DET is impossible in our cases due to non-availability of many parameters associated to our systems. The Sumi-Marcus model has been incorporated during the analysis of our results.

1.7 References:

1. Carson, R. *Silent Spring, Houghton Mifflin*, Boston, **1962.**

2. Collins, T. J. *J. Chem. Edu.*, **1995**, *72*, 965.

3. Anastas, P. T.; Warner, J. C. *Green Chemistry, Theory and Practice*, Oxford University Press, **1998**.

4. Tundo, P.; Anastas, P.; Black, D. StC.; Breen, J.; Collins, T.; Memoli, S.; Miyamoto, J.; Polyakoff M.; Tumas, W. *Pure Appl. Chem.*, **2000**, *72*, 1207.

5. World Commission on Environment and Development. *Our Common Future.* Oxford: Oxford University Press. **1987**, pp-27.

6. Environment, Health and Safety Committee of the Royal Society of Chemistry '*A Note on Green Chemistry*' April, **2002.**

7. Ash, M.; Ash, I. *The Index of Solvents*, Gower Publishing Limited, Brookfield, VT, **1996**;

8. Barwick, V. J. *Trends in Analytical Chemistry*, **1997**, *16*, 293.

9. (a) Ball, P. "*H_2O A Biography of Water*" Phoenix, London, **2000**; (b) Lindstrom, U. M. *Organic Reactions in Water*, Blackwell, Oxford, **2007**.

10. (a) Sheldon, R. A. *Green Chem.* **2005,** *7*, 267; (b) Tanaka, K. *Solvent-Free Organic Synthesis;* Wiley-VCH: Weinheim, Germany, **2004**; (c) Tanaka, K.; Toda, F. *Chem. Rev.* **2000,** *100*, 1025–1074; (d) De Simone, J. M. *Science* **2002,** *297*, 799.

11. (a) Ben-Naim, A. *J. Phys. Chem.*, **1985**, *89*, 5738; (b) Ben-Naim, A.; Marcus, Y. *J. Chem. Phys.*, **1984**, *81*, 2016.

12. Minnesota Department of Health fact sheet on '*Volatile Organic Compounds (VOCs) in Your Home*' available at www.health.state.mn.us/divs/eh/air.

13. Lancaster, M. *Green Chemistry: An Introductory Text*, Royal Society of Chemistry, Cambridge, **2002**.

14. Sheldon, R.A.; Arends, I.; Hanefeld, U. *Green Chemistry and Catalysis*,Wiley-VCH, Weinheim, **2007**.

15. Clark, J. H. (Ed.), *The Chemistry of Waste Minimization*, Blackie, London, **1995**.

16**.** Jessop, P. G. *Green Chem.*, **2011**, *13*, 1391.

17. Hildebrand, J.; Scott, R. L. *Regular Solutions*, Prentice-Hall: Englewood Cliffs, NJ, **1962**.

18. (a) Berthelot, M.; de Saint-Gilles, P. L. *Ann. Phys. et Phys., 3* Ser. **1862**, *65*, 385; (b) Berthelot, M.; de Saint-Gilles, P. L. *Ann. Phys. et Phys., 3 Ser.* **1862**, *66*, 5; (c) Berthelot, M.; de Saint-Gilles, P. L. *Ann. Phys. et Phys., 3 Ser.* **1863**, *68*, 225.

19. Coetzee, J. F.; Ritchie, C. D. *Solute Solvent Interactions*; volume *1* and *2* Marcel Dekker Inc.: New York, **1976**.

20. Amis, E. S. *Solvent Effects on Reaction Rates and Mechanism*; Academic Press: New York, **1966**.

21**.** Cramer, C. J.; Truhlar, D. G. *Chem. Rev.* **1999**, *99*, 2161.

22. (a) Dimroth, K.; Reichardt, C.; Siepmann, T.; Bohlmann, F. *Leibigs Ann. Chem.* **1963**, *661*, 1; (b) Reichardt, C. *Leibigs Ann. Chem.* **1971**, *752*, 64.

23. Kamlet, M. J.; Taft, R. W. *J. Am. Chem. Soc.* **1976**, *98*, 2886.

24. Laidler, K. J. *A Century of Solution Chemistry*, *Pure Appl. Chem*. **1990**, *62*, 2221; Laidler, K. J. *The World of Physical Chemistry*, Oxford University Press, Oxford/U.K.

25. Ohtaki, H. *Coord. Chem. Rev.*, **1999**, *185/186*, 735.

26. Panayiotou, C**.** *Fluid Phase Equilibria,* **1997,** *131*, 21.

27. (a) Reichardt, C. Solvent Effects in Organic Chemistry; Verlag Chemie: Weinheim, **1979**; (b) Hansen, C.M. *Ind. Eng. Chem. Prod. Res. Dev.* **1969,** *8*, 2.

28. Uggerud, E. *J. Phys. Org. Chem.* **2006**, *19*, 461.

29. Vollhardt, K. P. C.; Schore, N., E. *Organic Chemistry Structure and Function.* New York: W. H. Freeman, **2007**.

30. (a) Arrhenius, S. *Nobel Lecture* 11 December, **1903**; (b) Rusli, I. T.; Schrader, G. L.; Larson, M. A. *J. Cryst. Growth* **1989,** *97*, 345.

31. Fischer, S.; Verma, C. S.; Hubbard, R. E. *J. Phys. Chem. B* **1998**, *102*, 1797.

32. Chaplin, M. F. *Biochem. Mol. Biol. Edu.* **2001**, *29*, 54.

33. Water, a Comprehensive Treatise, edited by F. Franks (Plenum, New York, **1982**).

34. Okhulkov, A. V.; Demianets, Y. N.; Gorbaty, Y. E. *J. Chem. Phys.* **1994**, *100*, 1578.

35. Myneni, S.; Luo, Y.; Naslund, L. A.; Cavalleri, M.; Ojamae, L.; Ogasawara, H.; Pelmenschikov, A.; Wernet, P.; Vaterlein, P.; Heske, C.; Hussain, Z.; Pettersson, L. G. M.; Nilsson, A. *J. Phys Condens. Matter* **2002**, *14*, L213.

36. Rideout, D. C.; Breslow, R. *J. Am. Chem. Soc.* **1980**, *102*, 7816.

37. (a) Grieco, P. A.; Ferrino, S.; Vidari, G. *J. Am. Chem. Soc.* **1980**, *102*, 7586; (b) Vidari, G.; Ferrino, S.; Grieco, P. A. *J. Am. Chem. Soc.* **1984**, *106*, 3539; (c) Grieco, P. A. *Organic Synthesis in Water;*, Ed.; Blackie Academic & Professional: London, **1998**; Chapter 38; (d) Keutsch, F. N.; Saykally, R. J. *Proc. Natl. Acad. Sci. U. S. A.* **2001**, *98*, 10533.

39. (a) Bakker, H. J.; Woutersen, S.; Nienhuys, H. K. *Chem. Phys.* **2000**, *258*, 233; (b) Bakker, H. J.; Nienhuys, H. K. *Science* **2002**, *297*, 587.; (b) Coe, J. V. *Int. Rev. Phys. Chem.*, 2001, **20,** 33.; (c) Rick, S. W. *J. Chem. Phys.* **2004**, *120*, 6085.

40. Badyal, Y. S.; Saboungi, M. L.; Price, D. L.; Shastri, S. D.; Haeffner, D. R.; Soper, A. K. *J. Chem. Phys.* **2000**, *112*, 9206.

41. Fu, L.; Bienenstock, A.; Brennan S. *J. Chem. Phys.* **2009**, *131*, 234702.

42. (a) Breslow, R.; Maitra, U.; Rideout, D.; *Tetrahedron Lett.*, **1983**, *24*, 1901; (b) Li, C. J., *Chem. Rev.*, **1993**, *93*, 2023; (c) Lubineau, A.; Auge, J.; Queneau, Y. *Synthesis*, **1994**, 741; (d) Chan, T. H.; Li, C. J.; Lee, M. C.; Wei, Z.Y. **1993** R.U. Lemieux Award Lecture. *Can. J. Chem.*, **1994**, *72*, 1181.; (e) Kobayashi, S., *Synlett*, **1994**, 689; (f) Engberts, J.B.F.N., *Pure Appl. Chem.*, **1995**, *67*, 823; (g) Engberts, J.B.F.N., Feringa, B.L., Keller, E. and Otto, S., *Recl. Trav. Chim. Pays-Bas*, **1996**, *115*, 457; (h) Fringuelli, F., Piermatti, O. and Pizzo, F. In: Attanasi, A.O. and Spinelli, D. (Eds.), *Targets in Heterocyclic Systems*, Vol. 1, SCI, Rome, **1997**, pp. 57;

43. (a) Otto, S.; Engberts, J.B.F.N., *Pure Appl. Chem.*, **2000**, *72*, 1365; (b) Kumar, A., *Chem. Rev.*, **2001**, *101*, 1; (c) Lindstrom, U.M., *Chem. Rev.*, **2002**, *102*, 2751. (d) Sarma, D.; Kumar, A. *Org. Lett.* **2006,** *8,* 2199**.**

44. (a) Breslow, R. and Connors, R.V., *J. Am. Chem. Soc*., **1995**, *117*, 6601; (b) Breslow, R. and Zhu, Z., *J. Am. Chem. Soc.*, **1995**, *117*, 9923; (c) Breslow, R., Connors, R. and Zhu, Z., *Pure Appl. Chem.*, **1996**, *68*, 1527.

45. (a) Otto, S.; Engberts, J.B.F.N.; Kwak, I.C.T. *J. Am. Chem. Soc*., **1998**, *120*, 9517; (b) Meijer, A.; Otto, S.; Engberts, J.B.F.N., *J. Org. Chem.*, **1998**, *63*, 8989.

46. (a) Lum, K.,; Chandler, D.; Weeks, J. D., *J. Phys. Chem. B*, **1999**, *103*, 4570; (b) Cheng, Y. K.; Rossky, P.J. *Nature*, **1998**, *392*, 696. (c) Pierotti, R.A., *J. Phys. Chem.*, **1965**, *69*, 281–288. (d) Breslow, R.; Guo, T. *Proc. Natl. Acad. Sci.* USA **1990**, *87*, 167.

47. Creighton, T. *Proteins: Structure and Molecular Properties*, New York: Freeman, **1993**.

48. (a) Israelachvili, J. N. *Intermolecular and Surface Forces*, London: Academic Press **1992**;

(b) Tanford, C. *The Hydrophobic Effect: Formation of Micelles and Biological Membranes*, New York: Wiley **1973**. (c) Bakulin, A. A.; Liang, C.; Jansen, T. l. C.; Wiersma, D. A.; Bakker, H. J.; Pshenichnikov, M. S. *Acc. Chem. Res.* **2009**, *42*, 1229.

49.(a) Walden, P. *Bull. Acad. Imper. Sci. (St. Petersburg)* **1914**, 1800; (b) Sugden, S.; Wilkins, H. *J. Chem. Soc.* **1929**, 1291.

50. (a) Welton, T. *Chem. Rev.* **1999**, *99*, 2071; (b) Earle, M. J.; Mc Cormac, P. B.; Seddon, K. R. *Green Chemistry* **1999**, *1*, 23; (c) Hussey, C. L. *Pure & Appl. Chem.* **1988**, *60*, 1763.

51. (a) Seddon, K. R. *Kinetics and Catalysis* **1996**, *37*, 693; (b) Wilkes, J. S.; Zaworotko, M. J. *J. Chem. Soc, Chem. Commun.*, **1992**, 965.

51. Wasserschied, P.; Welton, T. *Ionic Liquids in Synthesis*, Wiley-VCH, Weinheim, **2002**.

52. *An Introduction to Ionic Liquids*, ed. Freemantle,M. RSC Publishing, Cambridge, UK, **2009**, p. 281.

53 *Ionic Liquids*, ed. Kirchner, B. Springer, Heidelberg, Germany, **2010**, p. 345.

54. (a) Weingartner, H. *Angew. Chem., Int. Ed.*, **2008**, *47*, 654; (b) MacFarlane, D. R.; Seddon, K. R. *Aust. J. Chem.*, **2007,** *60*, 3.

55. Castner, Jr. E. W.; Wishart, J. F. *J. Chem. Phys*., **2010**, *132*, 120901.

56. (a) Hantzsch, A. *Ber. dtsch. Chem. Ges. A/B* **1922**, *55*, 953; (b) Reichardt, C. *Chem. Rev.* **1994**, *94*, 2319.

57. (a) Dimroth, K.; Reichardt, C.; Siepmann, T.; Bohlmann, F. *Liebigs Ann. Chem.* **1963**, *661*, 1; (b) Reichardt, C. *Chem. Soc. Rev*. **1992,** *21*, 147.

58. Reichardt, C.; Harbusch-Goernert, E. *Liebigs Ann. Chem.* **1983**, 721.

59. Swain, C. G.; Swain, M. S.; Powell, A. L.; Alunni, S. *J. Am. Chem. Soc.* **1983,** *105*, 502.

60. (a) Taft, R. W.; Abboud, J. L. M.; Kamlet, M. J. *J. Org. Chem.* **1984,** *49*, 2001; (b) Swain, C. G. *J. Org. Chem.* **1984,** *49*, 2005.

61. (a) Krygowski, T. M.; Fawcett, W. R. *J. Am. Chem. Soc.* **1976,** *97*, 2143-2148; (b) Wrona, P. K; Krygowski, T. M.; Galus, Z. *J. Phys. Org. Chem.* **1991,** *4*, 439-448.

62. Marcus, Y. *Ion Solvation;* Wiley: Chichester, **1985**. Kriegsmann, H. Z. *Phys. Chem. (Leipzig)* **1988,** *269*, 1030.

63. (a) Gutmann, V. *Coord. Chem. Rev.* **1976,** *18*, 225-255; (b) Gutmann, V. *The Donor-Acceptor Approach to Molecular Interactions*; Plenum: New York, **1978**.

64. Taft, R. W.; Abboud, J. L. M.; Kamlet, M. J. *J. Am. Chem. Soc.* **1981,** *103*, 1080.

65. (a) Shukla, S. K.; Khupse, N. D.; Kumar, A. *Phys. Chem. Chem. Phys*. **2012,** *14*, 2754. (b) Khupse, N. D.; Kumar, A. *J. Phys. Chem. B* **2010,** *114*, 376. (c) Khupse, N. D.; Kumar, A. *J. Phys. Chem. B* **2011,** *115*, 711.

66. Millat, J.; Dymond, J. H.; Nieto de Castro, C. A. *Transport Properties of Fluids: Their Correlation, Prediction and Estimation*; Cambridge University Press: Cambridge, U.K., **2005**.

67. Vesovic, V.; Wakeham, W. A. *Chem. Eng. Sci.* **1989**, *44*, 2181.

68. Nunes, V. M. B.; Lourenco, M. J. V.; Santos, F. J. V.; Nieto de Castro, C. A. *J. Chem. Eng. Data* **2003**, *48*, 446.

69. Hendriks, E.; Kontogeorgis, G. M.; Dohrn, R.; de Hemptine, J. C.; Economou, I. G.; Zilnik, L. F.; Vesovic, V. *Ind. Eng. Chem. Res.* **2010**, *49*, 11131.

70. Plechkova, N. V.; Seddon, K. R. *Chem. Soc. Rev.* **2008**, *37*, 123.

71. (a) Feng, Z.; Gang, F. C.; Ting, W. Y.; Tao, W. Y.; Min, L. A.; Bing, Z. Z. *Chem. Eng. J.* **2010**, *160*, 691; (b) Zhou, F.; Liang, Y.; Liu, W. *Chem. Soc. Rev.* **2009**, *38*,

2590. (c) Dzyuba, S.; Bartsch, R. A. *Chem. Phys. Chem.*, **2002**,*3*,161.(d) Cardo-Broch, S.; Berthhold, A.; Armstrong, D.W., *Anal. Bioanal. Chem.*, **2003**,*375*,191.

72. (a) Rogers, R. D.; Seddon, K. R. Ionic Liquids□Solvents of the Future? *Science* **2003**, *302*, 792; (b) Rooney, D.; Jacquemin, J.; Gardas, R. *Top. Curr. Chem.* **2010**, *290*, 185.

73. (a) MacFarlane, D. R.; Sun, J.; Golding, J.; Meakin, P.; Forsyth, M. *Electrochim. Acta*, **2000**, *45*, 1271. (b) Kubo, W.; Kitamura, T.; Hanabusa, K.; Wada, Y.; Yanagida, S. *Chem. Commun.* **2002**, 374. (c) Wang, P.; Zakeeruddin, S. M.; Exnar, I.; Gra¨tzel, M. *Chem. Commun.* **2002**, 2972.

73. Sumi, H.; Marcus, R. A. *J. Chem. Phys.* **1986**, *84*, 4272.

74. Jimenez, R.; Fleming, G.; Kumar, P. V.; Maroncelli, M. *Nature* **1994**, *369*, 471.

75. Stratt, R. M.; Maroncelli, M. *J. Phys. Chem.* **1996**, *100*, 12981.

76. Samanta, A. *J. Phys. Chem. B* **2006**, *110*, 13704.

77. (a) Karmakar, R.; Samanta, A. *J. Phys. Chem. A* **2002**, *106*, 4447; (b) Karmakar, R.; Samanta, A. *J. Phys. Chem. A* **2002**, *106*, 6670; (c) Wang, Y.; Voth, G. A. *J. Am. Chem. Soc.* **2005**, *127*, 12192.

78. (a) Zhang, X.-X.; Liang, M.; Ernsting, N. P.; Maroncelli, M. *J. Phys. Chem.* B **2013**, *117*, 4291; (b) Maroncelli, M.; Zhang, X.-X.; Liang, M.; Roy, D.; Ernsting, N. P. *Faraday Discuss.* **2012**, *154*, 409.

79. Khurmi, C.; Berg, M. A. *J. Chem. Phys.***2008**, *129*, 064504.

80. (a) Arzhantsev, S.; Ito, N.; Heitz, M.; Maroncelli, M. *Chem. Phys. Lett.* **2003**, *381*, 278;

(b) Shirota, H.; Funston, A. M.; Wishart, J. F. ; Castner Jr., E. W. *J. Chem. Phys.* **2005**, *122*, 184512.

81. (a) Kobrak, M. N.; Znamenskiy, V. *Chem. Phys. Lett.* **2004**, *395*, 127; (b) Kobrak, M. N. *J. Chem. Phys.* **2007**, *127*,184507; (c) Li, H.; Ibrahim, M.; Agberemi, I. ; Kobrak, M. N. *J. Chem. Phys.* **2008**, *129*, 124507.

82. (a) van Hove, L. *Phys. Rev.*, **1954**, *95*,249; (b) Hansen, J. P.; McDonald, I. R. *Theory of Simple Liquids; Academic Press*: London, U.K., **1986**; (c) Sciortino, F.; Fabbian, L.; Chen, S. H.; Tartaglia, P. *Phys. Rev. E: Stat. Phys., Plasmas, Fluids, Relat*. **1997**, 56, 5397.

83. Lakowicz, J. R. *Principles of Fluorescence Spectroscopy*, Springer. **2006**.

84. Hu, Z.; Margulis, C. J. *Proc. Natl. Acad. Sci. U.S.A.* **2006**, *103*, 831.

85. Blokzijl, W.; Engberts, J. B. F. N.; Blandamer, M. J. *J. Am. Chem. Soc.*,**1990**, *112*, 1197- 1201.

86. Blokzijl, W.; Engberts, J. B. F. N.; Jager, J.; Blandamer, M. J. *J. Phys. Chem.*, **1987**, *91*, 6022; (b) Blokzijl, W.; Jager, J.; Engberts, J. B. F. N.; Blandamer, M. J. *J. Am. Chem. Soc.* **1986**, *108*, 6411.

87. (a) Guizzetti,S.; Benaglia, M.; Raimondi, L.; Celentano, G. *Org. Lett.*, **2007**, *9*, 1247; (b) Gajewski, J. J. *Acc. Chem. Res.* **1997**, *30*, 219.

88. Narayan, S.; Muldoon, J.; Finn, M. G.; Fokin, V. V.; Kolb, H. C.; Barry Sharpless, K. *Angew. Chem. Int. Ed.*, **2005**, *44*, 3275.

89. (a) Nicolaou, K. C.; Xu, H.; Wartmann, M. *Angew. Chem., Int. Ed*., **2005**, *44*, 756; (b) Butler, R. N.; Cunningham, W. J.; Coyne, A. G.; Burke, L. A. *J. Am. Chem. Soc.* **2004**, *126*, 11923.

89. (a) Klijn, E.; Engberts, J. B. F. N. *Nature* **2005**, *435*, 746−747; (b) Shapiro, N.; Vigalok, A. *Angew. Chem., Int. Ed.* **2008**, *47*, 2849; (c) Hayashi, Y. *Angew. Chem., Int. Ed.* **2006**, *45*, 8103; (d) Butler, R. N.; Coyne, A. G.; Moloney, E. M. *Tetrahedron*

Lett. **2007**, *48*, 3501; (e) Butler, R. N.; Coyne, A. G. *Chem. Rev.* **2010**, *110*, 6302; (f) Chanda, A.; Fokin, V. V. *Chem. Rev*. **2009**, *109*, 725−748.

90. Tiwari, S.; Kumar, A. *Chem. Commun.* **2008**, 4445.

91. Jung, Y.; Marcus, R. A. *J. Am. Chem. Soc*. **2007**, *129*, 5492.

92. Du, Q.; Superfine, R.; Freysz, E.; Shen, Y. R. *Phys. Rev. Lett.* **1993**, *70*, 2313; (26) McFearin, C. L.; Richmond, G. L. *J. Phys. Chem. C* **2009**, *113*, 21162.

93. (a) Beattie, J. K.; Djerdjev, A. M. *Angew.Chem., Int. Ed.* **2004**, *43*, 3568. (b) Pirrung, M. C.; Sarma, K. D.; Wang, J. *J. Org. Chem.* **2008**, *73*, 8723; (c) Acevedo, O.; Armacost, K *J. Am. Chem. Soc.* **2010**, *132*, 1966; (d) Cozzi, P. G.; Benfatti, F.; Zoli, L. *Angew. Chem., Int. Ed.* **2009**, *48*, 1313.

94. Pirrung, M. C.; Sarma, K. D. *J. Am. Chem. Soc.* **2004**, *126*, 444.

95. Klán, P.; Wirz, J *Photochemistry of organic compounds.* Wiley, New York, **2009**

96. Dau, H.; Zaharieva, I. *Acc. Chem. Res.* **2009**, 42,1861.; (b) Ciamician, G. *Science* **1912**, *36*, 385.

97. (a) Birks, J. B. *Photophysics of Aromatic Molecules*, Wiley-Interscience: London, **1970**; (b) Parker, C. A. *Photoluminescence of Solutions*, Elsevier: Amsterdam, **1968**.

99. (a) *Chemical Dynamics in Condensed Phase*, 1st ed.; Nitzan, A., Ed. Oxford University Press: New York, **2006**; (b) *Charge and Energy Transfer Dynamics in Molecular Systems*, 3rd ed.;May, V., Kühn, O., Eds.; VCH-Wiley: Weinheim, Germany, **2011**.

100. a) Caldin , E. F.; Gold, V. Proton-transfer reactions, Chapmann and Hall, London, **1975** ; b) Douhal, A.; Kim, S. K.; Zewail, A. H. *Nature* **1995** , *378* , 260 ; c) Douhal, A.; Lahmani, F.; Zewail, A. H. *Chem. Phys.* **1996** , *207* , 477 .

101. (a) Paul, B. K.; Guchhait, N. *J. Phys. Chem. B* **2010**, *114*, 12528. (b) Wu, J. S.; Liu, W. M.; Ge, J. C.; Zhang, H. Y.; Wang, P. F. *Chem. Soc. Rev.* 2011, 40, 3483. (c) Deperasinska, I.; Gryko, D. T.; Karpiuk, E.; Kozankiewicz, B.;Makarewicz, A.; Piechowska, J. *J. Phys. Chem. A* 2012, 116, 2109. (d) Zhao, J.; Ji, S.; Chen, Y.; Guo, H.; Yang, P. *Phys.Chem. Chem. Phys.* 2012, 14, 8803. (e) Park, S.; Kwon, J. E.; Park, S. Y. *Phys. Chem. Chem. Phys.* **2012**, 14, 8878.

102. a) Weller, A. *Elektrochemie* **1952** ,*56* , 662 ; b) Weller, A. *Prog. React.Kinet.* **1961** , *1* , 187 .

103. Hu, Z.; Margulis, C. J. Proc. Natl. Acad. Sci. U. S. A. 2006, 103, 831−836.

104. (a) Chou, P. T.; Huang, C. H.; Pu, S. C.; Cheng, Y. M.; Yu, W. S.; Yu, Y. C.; Wang, Y.; Chen, C. T. *J. Phys. Chem. A* **2004**,*108*, 6452. (b) Chou, P. T.; Pu, S. C.; Cheng, Y. M.; Yu, W. S.; Yu, Y. C.; Hung, F. T.; Hu, W. P. *J. Phys. Chem. A* **2005**, *109, 3777.*

105. (a) Znamenskiy, V.; Kobrak, M. N. J. Phys. Chem. B 2004, 108, 1072−1079. (b) Crowhurst, L.; Mawdsley, P. R.; Perez-Arlandis, J. M.; Salter, P. A.;Welton, T. Phys. Chem. Chem. Phys. 2003, 5, 2790−2794.

106. (a) Bolton, J. R.; Mataga, N.; McLendon, G. L. *Electron Transfer in Inorganic, Organic and Biological Systems,* American Chemical Society, Washington, DC **1991**. (b) Fox , A. M. (Ed.), Special Issue on Electron Transfer, *Chem. Rev.*, Washington, DC, **1992**, 92 365.

107. (a) Huddleston, R. K.; Miller, J. R. *J. Phys. Chem.* **1982**, *86*, 200. (b) Strauch, S.; McLendon, G.; McGuire, M.; Guarr, T. *J. Phys. Chem.* **1983**, *87*, 3579.

108. (a) Heitele, H. *Angew. Chem. Int. Ed. Engl.* **1993**, *32*, 359. (b) Shirota, H.; Pal, H.; Tominaga, K.; Yoshihara, K. *J. Phys.Chem. A* **1998**, *102*, 3089.

109. (a) Marcus, R. A. *J. Chem. Phys.* **1956**, *24*, 966. (b) Marcus, R. A. *J. Chem.Phys.* **1956**, *24*, 979. (c) Marcus, R. A. *Can. J. Chem.* **1959**, *37*, 155. (d)Marcus, R. A. *J. Chem. Phys.* **1957**, *26*, 867. (e) Marcus, R. A. *J. Chem.Phys.* **1957**, *26*, 872. (f) Marcus, R. A. *Discuss. Faraday Soc.* **1960**, *29*,21. (g) Marcus, R. A. *J. Phys. Chem.* **1963**, *67*, 853. (h) Marcus, R. A. *Annu. Re*V. *Phys. Chem.* **1964**, *15*, 155. (i) Marcus, R. A. *J. Chem. Phys.* **1965**, *43*, 679. (j) Marcus, R. A. *Electrochim. Acta* **1968**, *13*, 995.

110. (a) Kavarnos, G. J. *Fundamentals of Photoinduced Electron Transfer*; VCH Publishers, New York, **1993**. (b) Barbara, P. F.; Meyer, T. J.; Ratner, M. A. *J. Phys. Chem.* **1996**, *100*, 13148.(c) Heitele, H. *Angew. Chem. Int. Ed. Engl.* **1993**, *32*, 359.

111. (a) Valeur, B. *Molecular Fluorescence. Principles and Applications*, Wiley-VCH: Weinheim, **2001**.(b) Niwa, T.; Kikuchi, K.; Matsusita, N.; Hayashi, M.; Katagiri, T.; Takahashi, Y.; Miyashi, T. *J. Phys. Chem.* **1993**, *97*, 11960. (c) Rice, S. A. *Diffusion Limited Reactions; Comprehensive Chemical Kinetics*, Vol. 25; Elsevier: New York, **1985**.(d) Wilemski, G.; Fixman, M. J. Chem. Phys. **1973**, 58, 4009.(e) Tachiya, M. Radiat. *Phys. Chem.* **1983**, *21*, 167.

112. (a) Miller, J. R.; Calcaterra, L. T.; Closs, G. L.*J. Am. Chem. Soc.* **1984**, *106*, 3047. (b) Miller, J. R.; Beitz, J. V.; Huddleston, R. K. *J. Am. Chem. Soc.* **1984**, *106* 5057.

113. Rehm, D.; Weller, A. *Israel J. Chem.* **1970**, *8*, 259−271.

114. (a) Shannon, C. F.; Eads, D. D. *J. Chem. Phys.***1995**, 103, 5208. (b) Dang, X., Hupp, J. T. *J. Am. Chem. Soc.* **1999**, 121, 8399. (c) Angel, S. A., Peters, K. S. *J. Phys. Chem.* **1989**,93, 713.

115. Sumi, H.; Marcus, R. A. *J. Chem. Phys.* **1986**, *84*, 4894.

116.(a) Nagasawa, Y.; Yartsev, A. P.; Tominaga, K.; Bisht, P. B.; Johnson, A. E.; Yoshihara, K. *J. Phys. Chem.* **1995**, *99*, 653; (b) Shirota, H.; Pal, H.; Tominaga, K.; Yoshihara, K. *J. Phys. Chem.A.* **1998**, *102*, 3089; (c) Shirota, H.; Pal, H.; Tominaga, K.; Yoshihara, K. *Chem. Phys.* **1998**, *236*, 355;(d) Pal, H.; Nagasawa, Y.; Tominaga, K.; Yoshihara, K. *J. Phys. Chem.* **1996**, *100*, 11964.

117. Pal, H.; Shirota, H.; Tominaga, K.; Yoshihara, K. *J. Chem. Phys.* **1999**, *110*, 11454.

118. Liu, M.; Ito, N.; Maroncelli, M.; Waldeck, D. H.; Oliver, A. M.; Paddon-Row, M. N. *J. Am. Chem. Soc.* **2005**, *127*, 17867; Liu, M.; Waldeck, D. H.; Oliver, A. M.; Head, N. J.; Paddon-Row, M. N. *J. Am. Chem. Soc.* **2004**, *126*, 10778.

Chapter 2

Aims and Objectives

"Our aim as scientists is objective truth; more truth, more interesting truth, more intelligible truth."
Karl Popper

A brief outline of the aims and objectives of the proposed research works described in the present thesis has been provided in the current chapter.

2. Aims and Objectives:

The principle objective of the studies presented through this thesis is to understand the viability of water and ionic liquid as alternative solvents to the conventional solvents through the perspective of a physico-organic chemist. The aim of this thesis is two-fold, but both objectives are inter-connected since both of them propagate the physico-chemical intricacies lie behind the employment of unusual solvents. The first endeavour of this work is to explore the origins of the aqueous accelerations of C-C bond formation reactions especially emphasising on the Diels-Alder reactions (DA), Wittig reactions etc. and to represent a comparative picture to understand the features of heterogeneous and homogeneous aqueous reactions as well as their inter-connections. Water-induced accelerations of both the Wittig reactions and the DA reactions are attributed to specific mechanistic features which are shared by other reactions as well. A number of relatively simple reacting systems have been chosen which all differ in a specific way during the whole study.

The second aim is to explore the mechanistic details of the elementary particles (e.g. photo induced electron and proton) transfer reactions in ionic liquids. To be mentioned here that a large volume of reports on photo induced electron and proton transfer reactions in conventional organic media is available in literature. However, mechanistic intricacies of these lasers induced elementary particles transfer reactions in confined and viscous media like ionic liquids are hardly studied. In the context of emergent relevance of the ionic liquids in the fields of photovoltaic cells, solar cell, fuel cell etc., it is highly significant to examine up to which extent our acquired knowledge on electron and proton transfer reactions in conventional solvents is transferrable to that in case of ionic liquids. Through the works portrayed in the present thesis, solvation dynamics in terms of energetics and kinetics of the photo-physical processes carried out in a range of protic and aprotic ionic liquids has been explored.

In view of aforementioned general features gathered from the literature survey, following were the salient objectives for the works, aimed to provide a broad outline of the future course of research:

- To discern the inevitability of presence of organic/ water interface in ‘on water’ organic reaction experimentally. Information acquired through the investigation will help researchers to comprehend the underpinnings of increased reactivity and selectivity at aqueous interface. Moreover, revelation that existence of interface with desirable characteristics instead of solubility is the prerequisite to reactivity will be a strong step towards cleaner chemistry.

- To elucidate the applicability of pairwise interactions to quantify variation in reactivity of organic reaction specifically a Diels-Alder reaction in water upon addition of ionic liquids encompassing broad difference in structure and property as co-solvents. Quantitative data of one to one interactions among reactants as well as their activated forms with co-solvent ionic liquid acquired during this study will assist researchers to tailor ionic liquids as per requirement of reactions under purview in future. Additionally, introduction of ionic liquids instead of usual organic co-solvents viz. alcohols, carbohydrates, ether etc. in water will widen the solubility window of water medium for a large variety of reactions otherwise whose reactivity seems to be negligible due to unavailability of sufficient concentration of reactants.

- To delineate the kinetics and energetics of excited state photoinduced proton transfer in ionic liquids especially in protic ionic liquids. Ionic liquids being highly viscous and moderately polar in nature is constitutionally different from the existing organic solvents. Study of excited state intramolecular proton transfer reactions which serve as key reactions in many important biological processes in confined and viscous media like ionic liquids will vividly elucidate the delicate balance between two important properties i.e. viscosity and polarity of protic ionic liquids in controlling their solvation dynamics during such type of reactions involving excited states.

- To investigate the correlation between the bimolecular photoinduced electron transfer (PET) dynamics and the associated energetics in heterogeneous media like ionic liquids. Study of bimolecular PET in viscous media like ionic liquids will attract researchers in order to comprehend the effect of topology of ionic liquids media on photochemical reactions and to assess how to control kinetics of

a reaction upon manipulating microscopic environment. Moreover, this investigation will expound the prospect of the appearance of Marcus inverted region in the restricted media like ionic liquids during bimolecular electron transfer reactions upon overcoming diffusion mediated electron transfer i.e. Rehm-Weller type of electron transfer kinetics.

Chapter 3

Instrumentation Techniques

"Experiment is the sole source of truth. It alone can teach us something new; it alone can give certainty"

Henri Poincare

In the present chapter the basic principles of different instrumental techniques used in the current investigation are briefly discussed. Instrumental performance is one of the main factors that affect the accuracy and reproducibility of measurements. The characterization and results described in this thesis have been obtained using different experimental techniques viz. gas chromatography, UV/Vis Spectrophotometer, Steady state fluorimeter (SSF), Time correlated single photon counting (TCSPC) fluorimeter, and Up-Conversion fluorimeter. Basic principles of each experimental technique have been described here followed by a common discussion to obtain desired results. Some important components of the instruments used in the present work are also briefly described in the present chapter.

3.1 Introduction:

This chapter gives an overview of the various experimental methods and instrumental techniques that have been used to carry out the research work pertaining to the present thesis. To understand the kinetic details and thermodynamic aspects of C-C bond formation reactions (e.g. Diels-Alder reaction, Wittig reaction etc.), photoinduced electron transfer reactions and ultrafast proton transfer processes in the environmentally benign solvents e.g. water and ionic liquids, several steady-state and time-resolved techniques have been used in the present study. For the estimation of the rate constants and quantification of the reactants and the products explicitly, we have also used gas chromatographic technique and UV/Vis spectroscopic techniques, based on the characteristics of the reactants and products involved. To understand the dynamical and energetic processes during proton transfer and electron transfer reactions in ionic liquids both steady-state and time-resolved photophysical measurements were carried out using absorption and fluorescence based techniques. Rotational correlation times were also evaluated using time-resolved fluorescence anisotropy measurements to understand the rotational diffusion of the probes in the ionic liquids. Basic aspects of all these techniques are briefly given in the following sections.

3.2 Basic Principle of Gas Chromatographic Analysis:

Gas Chromatography (GC) follows the main principle of chromatography that is the separation of components in a mixture based on the different distribution of the analytes between mobile and stationary phase, resulting the differences in the migration velocities of the components trough the column. Here in especially for GC techniques the mobile phase (e.g. carrier gas) is comprised of an inert gas i.e., helium, argon, or nitrogen.[1] The stationary phase consists of a packed column where the packing or solid support itself acts as stationary phase, or is coated with the liquid stationary phase (e.g. high boiling polymer). Most analytical gas chromatographs use capillary columns, where the stationary phase coats the walls of a small-diameter tube directly (i.e., 0.25 m film in a 0.32 mm tube).[2] Movement of analytes is exclusively done by mobile gas phase and separation process occurs through the stationary phase. The movement of the analytes are through the chromatographic column, is called chromatographic development. Elution development principle is generally followed in

GC technique. Elution development scheme is the continuous series of absorption-extraction processes i.e. washing of analytes through the stationary column with addition of fresh solution. The quality of the separation is basically determined by the interaction time between mobile and stationary phase. The stronger the interaction is, the longer the compound interacts with the stationary phase, and the more time it takes to migrate through the column (e.g. longer retention time).[3] The strength of interactions mainly depends on the polarity as well as boiling point of the analytes. The analytes having comparable polarity with the stationary phase will be retained for longer time. Boiling point of the component plays crucial role during separation with GC.[4] Low boiling point solutes will have high vapour pressure and will remain more in the gas phase i.e. mobile phase and will show less interactions with stationary phase.[5] Consequently these low boiling components will appear earlier in the chromatogram.

3.3 UV/Vis Absorption Spectrophotometer and Ground State Absorption Measurement:

Ultraviolet (UV) and visible spectroscopy provides information about presence and absence of unsaturated functional groups and their interactions with the environment. The UV and visible radiation encompass only a small portion (300–700 nm) of the electromagnetic spectrum, which includes other forms of radiation like radio, infrared (IR), cosmic, and X rays.[6]

During absorption of light having energy in UV/Visible range, valance electron acquires enough energy to cause transitions between different electronic energy levels. The wavelength of light absorbed is that having the energy required to move an electron from a lower energy level to a higher energy level. Energy absorption is most typically associated with transitions induced in electrons involved in bonding orbitals, and the atoms involved are, for the most part, those containing s + p electrons.[7] The full series of permitted electronic transitions (by UV/Vis absorption) are given in Figure 1:

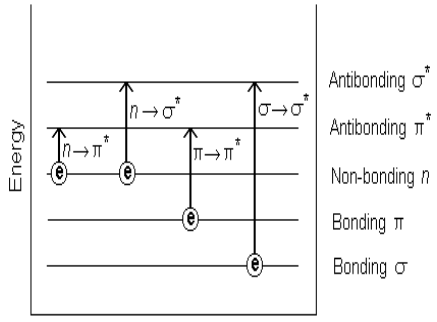

Figure 1: Electronic transitions due to absorption of light at UV/Vis region

As Figure 1 indicates, the σ ⟶ σ* and n ⟶ σ* transitions require relatively higher energy and are therefore associated with shorter wavelength radiation (ultraviolet). The lower energy n ⟶ π* and π ⟶ π* are ultraviolet or visible induced transitions. The probability that transition (and therefore absorption) will occur is closely related to molecular orbital structure. Following the Beer-Lambert law it can be written that the concentration of a substance in solution is directly proportional to the 'absorbance ', A, of the solution.[6]

Absorbance A = constant x concentration x cell length

Absorbance = A= log (I_0 / I) = log (100/T) = $\varepsilon c \ell$ and Absorption coefficient = ε

3.4 Fluorescence Spectroscopy:

The measurement of fluorescence signals provides a sensitive method to monitor various photochemical processes that occur in the excited state of the chromophoric molecules. Fluorescence is a spectrochemical method of analysis where the chromophoric molecules of the analyte are excited by light having definite wavelength and thereafter the excited molecules give off additional energy by emission of light at different wavelength.[8] Photons having energies in the ultraviolet to the blue-green region of the spectrum are needed to trigger an electronic transition. Further, since the energy gap between the excited and ground electronic states is significantly larger than the thermal energy, thermodynamics predicts that molecule predominately reside in the electronic ground state (Figure).[8,9]

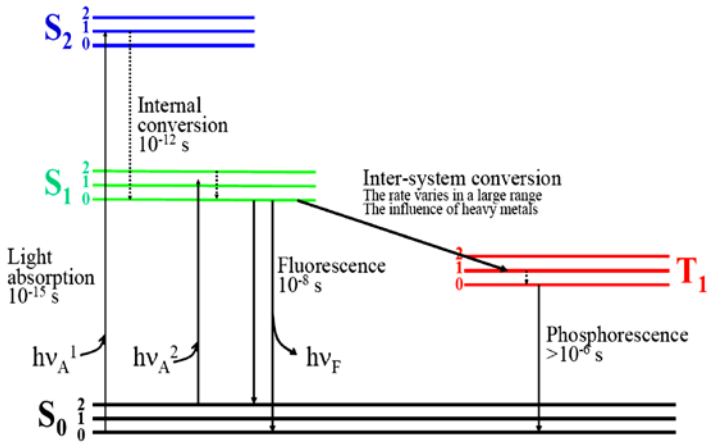

Figure 2: Jablonski diagram

It entails that external irradiation is necessary to promote molecules from ground state to excited states. The simplified Jablonski diagram conveniently represents photonic processes that involve transitions between electronic and vibronic levels at the excited state of the molecule. The emission spectrum provides information for both qualitative and quantitative analysis. The excited electronic state is usually the first excited singlet state, S1 as well as hardly for some cases the second excited singlet state, S2. Once the molecule reaches at the excited state, relaxation can occur via several processes as depicted in Figure 2. Fluorescence is one of these processes and results in the emission of light. Generally, fluorescence occurs when a molecule absorbs photons from the UV-visible light spectrum (300-700nm), causing transition to a high-energy electronic state and then emits photons as it returns to its ground state, in less than 10^{-9} sec. Some energy, within the molecule, is lost through thermal or vibrational collision so that energy of the emitted photon remains lower than that of excitation energy; i.e., the emission wavelength is always longer than the excitation wavelength. This difference between the excitation and emission wavelengths is called the Stokes shift.[9,10]

3.4.1. Steady State Fluorescence Measurement

In the present study, steady-state fluorescence measurements (either excitation spectra, emission spectra or fluorescence intensity) were carried out using a Hitachi model F-4500 fluorescence spectrometer.[9] The instrument uses a 150 watt continuous powered high pressure xenon lamp as the excitation source and R-928F (Hamamatsu) photomultiplier tube (PMT) as the photo detector. Measurement can be done for the wavelength range of 220 to 800 nm in the present instrument.[8] Samples have been

excited in a 1 mm x 1 mm quartz cuvette and fluorescence measurement has been carried out in the perpendicular geometry with respect to the excitation beam. The schematic of the steady-state spectrofluorimeter is shown in Figure 3.

.

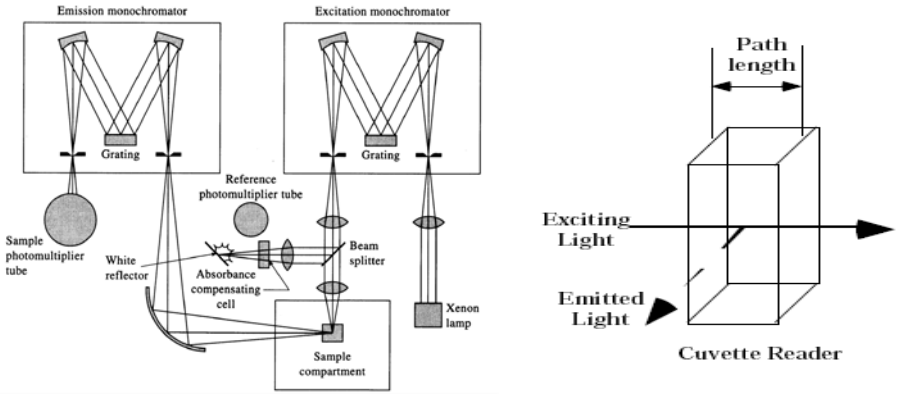

Figure 3: Schematics of steady state fluorimeter and the sample holder

3.4.2. Fluorescence Life Time Measurements

Fluorescence of a molecule mostly originates from its S_1 state and the process mostly occurs in the nanosecond time scale.[8] The average-time for which excited molecule stays in the S_1 state is defined as the lifetime of the state, which is also commonly called the fluorescence lifetime, τ_f. Measurement of τ_f not only helps one to understand different de-excitation processes of the excited molecules but also provides us the insight of different chemical and physicochemical interactions that take place in the S_1 state of the molecule, either with the environment surrounding it or with other chemical reagents present in the system. Though, in the absence of any complex photochemical processes, the fluorescence decay follows a single-exponential function, the decay often becomes multi-exponential in the presence of complex photochemical processes. Thus, in general, the fluorescence decay of a sample can be expressed as a sum of exponentials as

$$I(t) = \Sigma \; B_i \exp(-t/\tau_i)$$

where, B_i is the pre-exponential factor/fluorescence intensity at time zero and τ_i is the fluorescence lifetime of the i^{th} component of the measured decay. Present study has been carried out with TCSPC instrument obtained from Horiba Jobin Yvon IBH, UK, Model Data station Hub.

3.4.3 Basic Principle of TCSPC Technique

The best method for time-resolved fluorescence measurements in the nanosecond to picoseconds time scale is the *Time Correlated Single Photon Counting (TCSPC)* technique.[12]

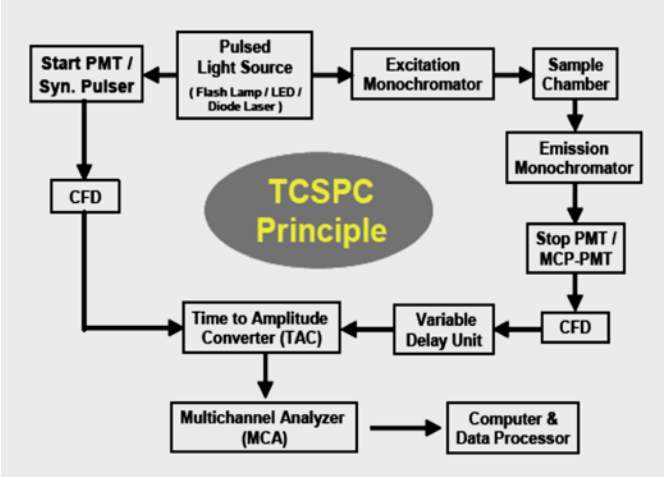

Figure 4: Schematic diagram of a time correlated single photon counting spectrometer.

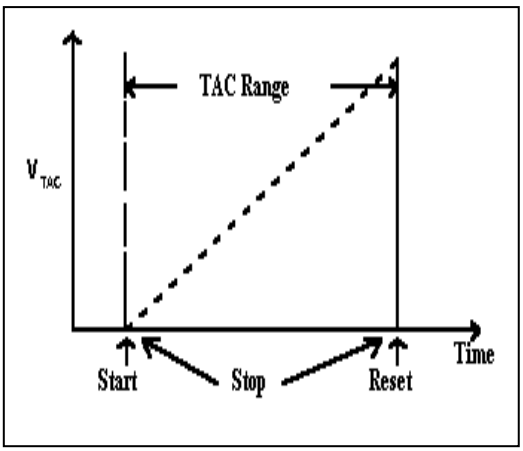

Figure 5: Functioning of TAC. start signal initiates the charging process. stop signal arrives at any time between start and reset.

The electrical signal from start PMT is fed to the START input of a Time to Amplitude Converter (TAC). On receiving this START signal the TAC starts its charging process, which increases linearly with time till the stop PMT receives a fluorescence photon and send an electrical stop signal to the STOP input of TAC.[12,14] With the latter event the charging process in TAC stops and TAC generates an

electrical output (V_{TAC}) having its amplitude proportional to the time difference (Δt) between the START and STOP pulses (*cf*. Figure 5).

The V_{TAC} signal is then fed to a Multichannel Analyzer (MCA) via an analog to digital (AD) converter. The AD converter converts V_{TAC} to a numerical value $n^{\Delta t}$ and selects a corresponding n^{th} channel in MCA where a count is just added up. Above cycle is repeated for very large number of times till a histogram is built up in MCA with about 5 to 10 thousand counts at the channel corresponding to maximum of the histogram (*cf*. Figure 6).

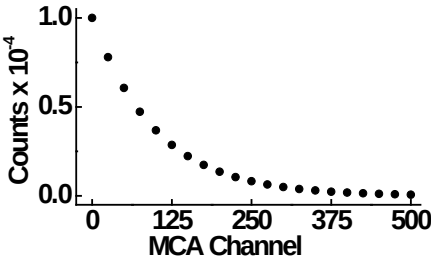

Figure 6: Histogram of counts in the MCA channels

During experiment, the data collection rate is kept very low, <0.02 photons/excitation pulse. Under this situation the histogram represents the fluorescence decay of the sample.[15] Time calibration of the MCA channels is done separately using a suitable method. TCSPC is one of the most sensitive techniques for time-resolved fluorescence measurements.

Thus, a very low intensity excitation source can be used for TCSPC detection. Samples having quite low fluorescence quantum yield can also be measured by measured by this technique. Unlike most other methods, TCSPC detection is not limited by the rise time of the PMT. TCSPC is based on a well-defined (Poison) statistics and thus fruitfulness of the data analysis can be thoroughly judged. With H_2 and D_2 filled flash lamps of having nanosecond pulse widths, the fluorescence lifetimes lower than nanosecond range cannot be measured by this technique.[13] However, by using ultrafast lasers sources in combination with MCP-PMT detector, the lifetime in the pico-second range can be measured suitably by TCSPC method.[15] Since the collection rate in TCSPC detection is to be kept very low, measurements usually take quite long time, especially for low fluorescence quantum yield samples. In the present measurements, diode lasers (~100 ps, 1 MHz repetition rate) were used as the excitation source and a special photomultiplier tube (MCP-PMT)-based

detection module supplied by Horiba Jobin Yvon IBH was used for the fluorescence detection.

3.4.4 Analysis of TCSPC Data

If the width of light pulses used to excite the sample is infinitely narrow (δ-pulse) and the response of the detection system used is exceedingly fast, the observed decay curve (the MCA histogram) would simply represent the true fluorescence decay of the sample, G(t).[16-18] However, during our experiments, the light pulses used for excitation do have a finite time width and also the detection system has its finite response time. The observed decay curve I(t) in the TCSPC measurement is thus actually a convolution of the true decay curve G(t) and the effective instrument response function P(t).[16,17] From a simple consideration it can be shown that the function I(t), G(t) and P(t) can be correlated by the following convolution integral

$$I(t) = \int_0^t P(t')G(t-t')dt'$$

Experimentally one can record both I(t) and P(t). Thus, considering a suitable functional form for G(t), a convoluted function Y(t) is calculated according to equation 1 and using the experimentally measured P(t), which is then compared with the experimentally measured decay curve I(t) for the kind of fitting. It has already been mentioned that G(t) can be expressed as the sum of exponentials given as, $G(t) = \sum_i B_i \exp(\frac{t}{\tau_i})$ where, Bi represents the pre-exponential factor of i^{th} component and τ_i signifies the corresponding fluorescence lifetime.[18] The accuracy of the analysis is defined by analysing following two statistical parameters.

3.4.4.1 Reduced Chi Square (χ_r^2) Value

We have judged the goodness of a re-convolution analysis of an observed fluorescence decay curve using TCSPC measurement by noting the reduced chi-square (χ_r^2) value for the fit, defined as[16,19-20]

$$\chi_r^2 = \frac{\sum_i W_i\{Y(i) - I(i)\}^2}{\{(n_2 - n_1 + 1) - P\}}$$

where W_i is the weighting factor of the counts I(i) in the i^{th} channel and is defined as $w_i = 1/I(i)$, n_1 and n_2 are the first and last channel numbers for the section of the

decay that is used for the analysis, and p is the number of degrees of freedom in the fitting procedure, which is equal to the number of fitting parameters involved, namely, the degrees of freedom is three for a single exponential analysis.[19] In the actual analysis the parameters B_i, τ_i and A are gradually varied following nonlinear least-square iterative re-convolution method till the minimum value for the χ_r^2 parameter is obtained. A χ_r^2 value close to unity ($\chi_r^2 \approx$ 1-1.2) represents a good fit for the observed fluorescence decay.

3.4.4.2 Distribution of Weighted Residuals

Another important statistical function that is widely used in combination with χ_r^2 values to judge the goodness of a re-convolution analysis of an observed decay is the distribution of the weighted residuals among the data channels used. The weighted residual r_i for the i^{th} channel of the fitted TCSPC data is defined as [21]

$$r_i = \sqrt{W_i}\{Y(i) - I(i)\}$$

For a good fit the weighted residuals among the data channels should be randomly distributed about zero and should also follow a Gaussian distribution such that the 68%, 95%, 99.7% and 100% of the weighted residuals should respectively be within ±1, ±2, ±3 and ±4.

3.5 Fluorescence Up-conversion Measurements:

By using time-correlated single-photon-counting (TCSPC) in conjunction with a fast photomultiplier or MCPPMT, it is possible to improve the time resolution down up to ~30 ps but in this connection a careful deconvolution is also required for accurate estimation of lifetime.[22] Another important technique for obtaining fluorescence lifetime shorter than 100 ps has been to use a streak camera.[22-23] Single shot streak cameras offer a time-resolution better than ~10 ps. One of the major disadvantages of using streak camera is the spectral response of its photocathode which cannot be used beyond 900nm. In this context, researchers rely on the use of indirect nonlinear optical detection principles to achieve highest possible resolution of fluorescence detection. The up-conversion technique is based on the principle of the optical gating of the fluorescence emission through a non linear crystal.[24] During the measurement of fluorescence up-conversion, the incoherent fluorescence photons excited by an ultrashot laser pulse is focused on a non-linear crystal. Another suitably delayed ultrashot laser pulse (probe) is focused on the same non-linear crystal, spatially overlapped with the fluorescence beam, to generate sum frequency signal. This non-

linear frequency mixing crystal acts as a sampling shutter for a very short duration of the gate pulse.

3.5.5.1 Brief Description of the Up-conversion Instrument Used

Figure 6 represents the schematic diagram of the femtosecond fluorescence up-conversion instrument assembled in house. A mode-locked Ti: sapphire oscillator (from CDP Inc. Russia), optically pumped by a diode pumped solid state laser from Coherent (Verdi, 5W at 532 nm), has been used as the source to produce ultra short laser pulses possessing the wavelength around 800nm.

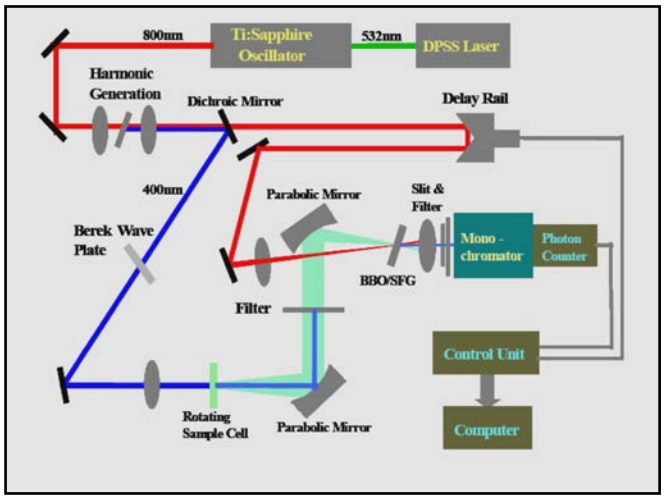

Figure 6: The diagram of the femtosecond fluorescence Up-conversion instrument developed in the department (RPCD, BARC).

The pulse duration of the present Ti: sapphire laser system is ~50 fs and it operates with a repetition rate of 82 MHz. In this up-conversion instrument the laser beam is first passed through a beta barium borate (BBO) crystals to produce 2^{nd} (~ 400nm) or 3^{rd} (~ 266nm) harmonic of the source laser through proper tuning of optical axis and required phase matching.

A dichroic mirror is used to avoid the residual of fundamental light of the Ti: sapphire source. The higher degree harmonic light is used to excite the sample of our interest. Point to be mentioned here that the intensity of this light is normally kept low to ensure the linear dependence of the fluorescence intensity with the excitation pulses. To minimize the photo-degradation of the samples during measurements of fluorescence decays, the sample solution is kept in a rotating quartz cell of 1 mm thickness in our experimental arrangement. Continuous rotation of the sample cell during measurements helps in avoidance of the localized heating of the sample and

consequently photo-decomposition is minimized. To check the residual excitation light and/or Raman light to reach the detection system a cut off filter is used just after the sample cell. Thereafter, the short-lived fluorescence originating from the samples is focused onto the non-linear frequency mixing crystal (i.e. 0.5 mm thick BBO crystal), using two elliptical mirrors.[19,20] The residual fundamental beam, used as the gate pulse, is first directed to an optical delay line and subsequently focused onto the up-conversion crystal to overlap with the fluorescence spot.[25,26] Generated up-conversion intensity is given by,

$$I_{sum}(\tau) = \int I_{fl}(\tau) I_{probe}(t-\tau) dt$$

In this equation, I_{sum} , I_{fl} and I_{probe} are the intensities of the sum-frequency, the fluorescence light and the probe beam, respectively.

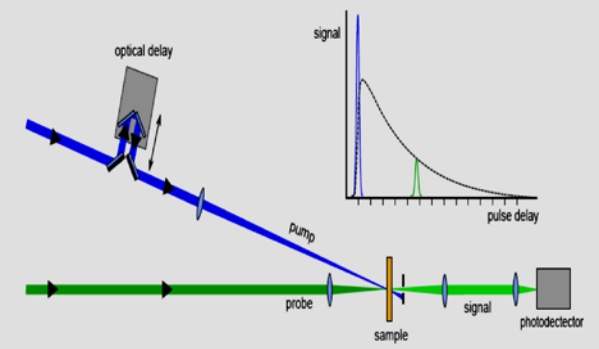

Figure 7: Collection of fluorescence data from Up-conversion instrument

This equation clearly depicts the fact that the sum-frequency signal is only present when the fluorescence photons and the probe pulse are coincident on the non-linear crystal, both spatially and temporarily. Moreover, since the intensity of the probe pulse always remains constant, the intensity of the sum-frequency light is directly proportional to the fluorescence intensity encountered by the gate pulse.

Additionally, since the probe pulse is much shorter than the time dependent fluorescence, the former acts as the optical gate to the up-conversion signal. The fineness of the time resolution of the measurement thus depends on the temporal width of the probe pulse.

3.6 References:

1. David, D. J. *Gas Chromatographic Detectors, John Wiley & Sons*, **1974**

2. Bentley, J.P., *Principles of Measurement Systems*, Longman, Singapore, **1998**

3. Moody, H.W. *Evaluation of the Parameters in the Van Deemter Equation, J. Chem. Educ.*,1982, **59**, 290.
4. Jeffery, P.G.; Kipping, P.J. *Gas Analysis by Gas Chromatography*, Pergamon, Oxford, **1972.**
5. Mark, H. *Principles and Practice of Spectroscopic Calibration, Chemical Analysis, Vol. 118*, Wiley: New York, 1991.
6. Macadam, D. L. *Colour Measurement*, Springer: Berlin, **1981**.
7. Christian, G. D.; Dasgupta, P.; Schug, K. Analytical Chemistry 7th Edition Wiley February, **2003.**
8. Lakowicz, J. R. *Principle of Fluorescence Spectroscopy;* Plenum Press: New York, 2006.
9. Turro, J. *Modern Molecular Photochemistry*, Benzamin, Menlo Park, CA, **1978.**
10. Birks, J. B. *Photophysics of Aromatic Molecules.* Wiley Interscience, New York, **1970**.
11. Gilbert, A.; Baggott, J.; Wagner, P. J. *Essentials of Molecular Photochemistry,* Blackwell Science Inc. Cambridge, USA, **1991**.
12. (a) O'Connor, D. V.; Phillips, D. *Time Correlated Single Photon Counting.* Academic Press, New York, **1984**. (b) Becker, W. *Advanced Time Correlated Single Photon Counting Technique*; Springer: New York, 2005.
13. Cundall, R. B.; Dale, R. E. eds. *Time-resolved Fluorescence Spectroscopy in Biochemistry and Biology*, Plenum, New York, **1983**.
14. Demas, J. N. *Excited State Life Time Measurements.* Academic Press, New York, **1983**.
15. Ware, W. R. *Creation and Detection of the Excited States.* Eds. Lamola, A.A.; Marcel Dekker, New York vol-1, Part A, Chap.-5,**1971**.
16. (a) G. R. Fleming, *Chemical Applications of Ultrafast Spectroscopy*. Oxford University Press, London,**1986**. (b) Kahlow, M. A.; Jarzeba, W.; DuBruil, T. P.; Barbara, P. F. *Rev. Sci. Instrum*. **1988**, *59* , 1098.
17. Singh, P. K.; Kumbhakar, M.; Ganguly, R.; Aswal, V. K.; Pal, H.; Nath, S. *J. Phys.Chem. B* **2010**, *114*, 3818.
18. Singh, P. K.; Kumbhakar, M.; Pal, H.; Nath, S. *J. Phys. Chem. B* **2008**, *112*, 7771.
19. Singh, P. K.; Kumbhakar, M.; Pal, H.; Nath, S. *J. Phys. Chem. B* **2009**, *113*, 1353.
20. Bebelaar, D. *Rev. Sci. Instrum.* **1986**, *57*, 1116.
21. Shah, J. *IEEE J. Quant. Elect.* **1988**, *24*, 276.
22. Bowers, M. J., II; McBride, J. R.; Garrett, M. D.; Sammons, J. A.; Dukes, A. D., III; Schreuder, M. A.; Watt, T. L.; Lupini, A. R.; Pennycook, S. J.; Rosenthal, S. J., *J. Am. Chem. Soc.* **2009,** *131* , 5730.
23. Garrett, M. D.; Bowers, M. J., II; McBride, J. R.; Orndorff, R. L.; Pennycook, S. J.; Rosenthal, S. J., *J. Phys. Chem. C* **2008,** *112*, 436.

24. Garrett, M. D.; Dukes, A. D., III; McBride, J. R.; Smith, N. J.; Pennycook, S. J.; Rosenthal, S. J., *J. Phys. Chem. C* **2008,** *112*, 12736.
25. Kippeny, T. C.; Bowers, M. J., II; Dukes, A. D., III; McBride, J. R.; Orndorff, R. L.; Garrett, M. D.; Rosenthal, S. J., *J. Chem. Phys.* **2008,** *128*, 084713/1.
26. Underwood, D. F.; Kippeny, T.; Rosenthal, S. J., *J. Phys. Chem. B* **2001,** *105*, 436.

Chapter 4

An Insight into the Mechanism of 'On Water' Organic Reactions

"It is life, I think, to watch the water. A man can learn so many things."

Nicholas Sparks

The exhaustive experiments described in this chapter have been performed in order to elucidate the role of interfacial water molecules in acceleration of C-C bond formation organic reactions with the emphasis on Diels-Alder reactions and Wittig reaction. Attention has been paid to justify the delicate balance between two important foundations of water promoted reactions i.e. hydrophobic interactions and hydrogen bonding prospects. Sensitive techniques have established the preferential solvation of polarizable ions at the water surface. The experimental schemes have been developed to control the molecular structure of oil−water interface in situ. Temperature-dependent analysis has also been presented to comprehend the enthalpic and entropic modifications of bonding with interfacial water molecules during a heterogeneous reaction. The systematic kinetic and thermodynamic studies described in the present chapter univocally unravel mechanistic intricacies pertaining to the participation of interfacial water during 'on water' organic reactions.

4.1 Introduction:

Synthetic organic chemists mainly focus on two principle type of reactions: one is carbon-carbon bond formation reactions and another is transformation as well as addition of functional groups to the main organic moiety. [1] C-C bond formation reactions have been termed as the foundation of organic synthesis since it gives a boon to the organic chemists to synthesise compounds having structure ranging from simple to complex.[2] Although anthropologic data as well as scientific researches confirm that water has been used by Mother Nature as a medium to nourish the synthesis of essential proteins, peptides etc. essential to germinate early sign of life in the world, chemists usually avoid water as a solvent for common organic reactions. [3] The superiority of water as solvent to promote organic reactions has been pioneered by Breslow and his group in 1980.[4] Mention should also be made of another important contribution by Grieco and co–workers who highlighted the significance of water as a solvent media in organic synthesis.[5] Since then, there have been a number of researches in this field to understand the potentiality of water as solvent during organic reactions.[6]

To unravel the principle forces behind the dramatic acceleration of Diels-Alder reactions in water, researchers have come across with a number of explanations.[6-8] Since the proposed mechanism of Diels-Alder reactions follow the suprafacial interaction of a 4π electron system with a 2π electron system through cyclic transition state without any intermediate, are usually thought to be insensitive to high polarity of water, the contribution of the polarity of water could be used to rationalize the acceleration of the reaction rate.[1,7] In the present scenario, Breslow had invoked the idea of 'hydrophobicity' to rationalize his observations related to unprecedented acceleration of Diels-Alder reactions in water.[3,9] This theory suggests that non-polar molecules/reactants i.e. molecules insoluble in water come together to increase local concentration followed by greater probability of collisions among reactants to avoid mutual repulsion to the solvent water.[6-9] A number of papers and reviews have been appeared in the literature to assess this concept of hydrophobicity and associated parameters during water promoted reactions.[2-8] Researchers have used prohydrophobic salts (GnCl, $LiClO_4$ etc.) and anti hydrophobic salts (LiCl, KCl etc.) to delineate the role of hydrophobic hydration in the water promoted reactions. [6-9] As a consequence of rigorous studies it has been revealed that along with hydrophobic acceleration,[7-9] several other properties like enforced hydrophobic interactions,[10]

enhanced hydrogen bonding capability of water,[8,11] high cohesive energy density of water,[12] and polarity of water[7] etc. are also responsible in promotion of organic reactions in water. Contribution of each property varies from reaction to reaction depending upon the molecular structure of the reactants.[5, 7] One of the significant criteria of these works is that all the reactants are taken in water in such a manner that entire reaction mixture does not exhibit any interface. This means that the reactants are completely solubilised in water. This type of reactions is termed as 'in water reaction'.[4, 5]

In 2005, Sharpless and co-workers during their study on cycloaddition of strained cyclic systems i.e. [2σ+2σ+2π] cycloaddition of quadricyclane and dimethylazodicarboxylate (DMAD) in presence of excess concentration of reactants in water observed that rate of the reaction was nearly 400 times accelerated compared to that of homogeneous reaction condition in water.[13] The yield of this reaction at heterogeneous condition was also reported very high compared to same reaction in water at homogeneous condition. It is important to be mentioned here that repetition of the same reaction in solvent free i.e. in 'neat condition' failed to show acceleration in rate at per observed that in water at heterogeneous condition. Later, the observations have been justified in the way that the excess concentration of the reactants (i.e. beyond the solubility limit of water) as well as newly created organic/ water interface play pivotal role in acceleration during these new types of reactions.[13, 14] Moreover, water appears to be the privileged medium for carrying out organic reactions, since similar reactions performed in perfluorohexane at heterogeneous condition proceeded at rates comparable to the homogeneous organic conditions. [13, 15] These new types of reaction has been categorised as 'on water' reactions.[13] Limited attention has been paid to the kinetics of organic reactions under heterogeneous aqueous conditions, when the reactants float on water. Here, the conditions being heterogeneous, with the reaction occurring on the surface of water i.e. water act here a medium to float, and so the hydrophobic effect seemingly does not play crucial role in these types of reactions.[15, 16] Importantly, vigorous mixing to form a suspension or vortex formation has been proposed to be necessary condition for the reaction to proceed further.

Yung and Marcus had emphasised on the catalysing effect of 'dangling OH' present at the water/organic interface as one of the principal factor behind the enhanced reactivity of 'on water' reactions through their DFT calculation.[16, 18]

Vigorous stirring, pressure as well as enforced hydrophobic interactions has been envisaged as necessary conditions for higher acceleration of 'on water' reactions by recent studies.[17] Some researches revealed the acidic surface of water as an accelerator of the reactions.[19,21] Though in the literature, several example of heterogeneous water promoted reactions are available, principle forces lies behind this acceleration of 'on water' conditions is not without controversy.[19-21]

In this chapter, attempts have been taken to clarify the role of 'dangling OH' by performing C-C bond forming reactions i.e. Diels-Alder reactions and Wittig reactions at the organic /water interface. These two reactions have been chosen since both of these reactions have been used to synthesise organic compounds with higher number of carbon-carbon bonds compared to that of reactants.[1,2] Moreover, Diels-Alder reactions have been proved to be an essential methodology to synthesise 6-membered or higher acyclic compounds possessing higher degree of stereo- and regio- selectivity.[1, 19a] Efforts will be focused on the delineation of physical forces responsible for promotion of rate of organic reactions at heterogeneous condition in comparison to that of homogeneous reactions in water.

4.2. Experimental Section:

4.2.1 Materials

Cyclopentadiene **1** was freshly cracked from dicyclopentadiene prior to its use, while methyl acrylate **2a**, ethyl acrylate **2b**, and butyl acrylate **2c** were distilled prior to their use. Benzaldehyde **4** was freshly distilled prior to its use. All commercially available salts –KF, KCl, KBr and KI were dried under vacuum for 6h prior to their use in the reactions. All chemicals were procured from M/S Merck Chem. Extra pure ammonia solution (30%v/v) was supplied by M/s. Loba Chemie.

4.2.2 Synthesis of Ylide

Triphenylphosphine was stirred in 50 ml water and ethyl bromoacetate was added drop wise to the solution. The resultant solution was stirred for 30 min at room temperature. The reaction mixture was then washed with ether to remove the excess reactants and then washed for several times. It was dried in vacuum for 6h to remove volatile impurities. ^{1}H NMR was taken to check the purity of the compound.

4.2.3. Kinetic Analysis

In a standard kinetic run, reaction was initiated by adding methyl acrylate (1 molar concentration) to the reaction mixture of cyclopentadiene (1 molar) in 25 ml of water

at 298 K. The temperature was controlled by a Julabo constant temperature bath with an accuracy of ± 0.01 K. The reaction progress was monitored by GC (Varian CP-3800 gas chromatograph) by withdrawing 1 ml of reaction mixture after each interval of time followed by the extraction with ether. k_2 values were measured after measuring the relative peak area of the product with respect to time. Before performance of the reaction the relative peak area was calibrated with respect to the amount of product.

10 mmol of aldehyde **4** and 10 mmol of ylide **5** (Scheme **2**) were dissolved in 1 ml of water, the mixture was subjected to vigorous stirring to avoid aggregation of ylide. The decrease in concentration of aldehyde with respect to time was observed by using UV/visible spectrophotometer. From the decrease in the absorbance value with respect to the progress of the reaction, the k_2 value was measured.

In both the cases, each experiment was carried out in triplicate with a standard error in second order rate constant, k_2 as ± 6%. The reaction was also performed at temperatures from 298 K to 318 K using the single cell Peltier supplied with spectrophotometer.

4.2.4. Drop-size Measurement

First, the size of a capillary was measured to correlate the pixel of Redlake High Speed Camera with 512 x 512 pixel in order to treat this as a reference for further measurements. The pictures were captured at the speed 230 frame per second at different rpm values. The snapshots were taken for a particular bubble at a specific rpm over few seconds and radius was measured at different points. An average of five bubbles was treated as the radious of the bubble in question.

4.3 Results and Discussion:

4.3.1 Does the Reaction Occur at Interface?

During investigation of the insights of mechanism of ‘on water’ reactions, researchers have emphasised on the presence of micro-interface in between organic reactants and water medium.[13, 16, 18] The presence of interface has been coined as a prime difference between ‘homogeneous’ or ‘in water’ type reactions and ‘heterogeneous’ or ‘on water’ type reactions.[15, 16] There were a few literature available to justify the presence of interface and its role during ‘on water’ reaction. Throughout the investigation, motive of the study is to validate the role of interface during heterogeneous water promoted reaction.

During selection of the reactants in order to carry out the desired study, preference has been given to choose those reactions where reactants show very low aqueous solubility. Selection of the reactants in terms of their aqueous solubility has been inspired from the previous investigations done by several groups.[12-15] The performance of the reaction between cyclopentadiene **1** and methyl acrylate **2a** (Scheme 1) with stirring and without stirring yields second order rate constant (k_2) as 1.21 x 10^{-5} $M^{-1}s^{-1}$ and 2.86 x 10^{-7} $M^{-1}s^{-1}$ respectively at 298.15 K.

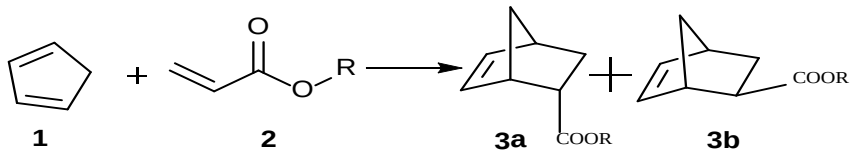

1 **2** **3a** **3b**

2a-R= Me

2b-R= Et

2c-R=Bu

Scheme 1. The reaction of Cyclopentadiene **1** and Alkyl acrylate **2**.

The value of k_2 obtained during reaction condition without stirring i.e. 2.86 x 10^{-7} $M^{-1}s^{-1}$ is almost equivalent to rate constant *(k_2)* of the same reaction at homogeneous condition in water. It should be mentioned here that micro-interface i.e. the formation of bubbles of reactants in water is not possible without vigorous stirring. Physical emergence of bubble during vigorous stirring results in formation of interface between organic reactant and water. Therefore, observations suggest that appearance of organic bubbles is one of the necessary characteristic for heterogeneous reactions. The reaction (Scheme 1) has been carried out at 'on water condition' at varying stirring speed by keeping all other physical parameters constant.

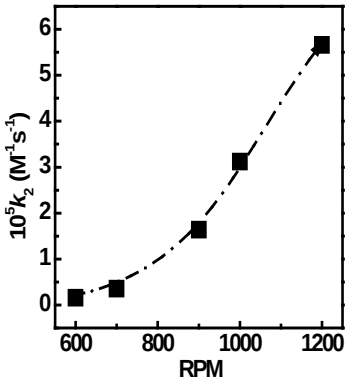

Figure 1: A plot showing the variation of the k_2 values *vs*. rpm values for the reaction of **1** with **2a**, the connecting line is shown to guide the reader eye.

Figure 1 shows that k_2 value increases with increasing RPM (Rotation per minute) value of the stirrer. It is known that increased value of rotation of the magnetic stirrer will stimulate disintegration of oil bubbles *i.e.* from a big bubble a number of smaller bubbles will be created and thus the total surface area of bubble will be increased. The area of the bubbles has been calculated from the radius value (r) obtained during each RPM value of the magnetic stirrer ($A= \pi r^2$ with A and r being the area and radius, respectively of the bubble). Total area during stirring at each RPM has been measured by fixing the volume of the added reactants to water (c/f. see experimental section for elaborate procedure). Since throughout the experiments with except RPM value all other physical parameters were kept constant, we can safely conclude that oil/water interfacial area plays certain role in promotion of the reaction during 'on water' reaction.

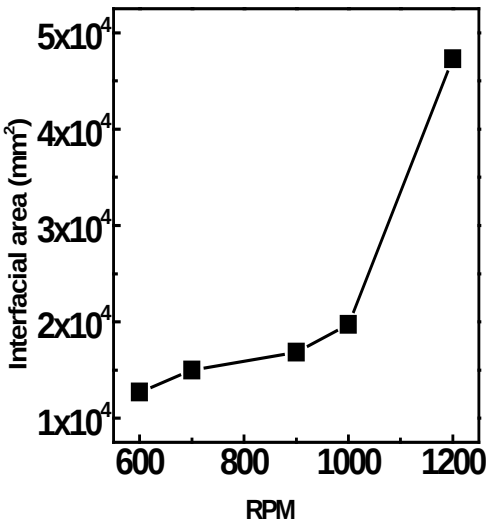

Figure 2: A plot describing the change in interfacial area against the RPM value of the stirrer for the reaction between **1** with **2a**; the connecting line is shown to guide the reader's eye.

It should be mentioned here that an introduction of interface creates asymmetry in the continuum dielectric field and interface possess large amount of energy compared to continuous field. Since water-water hydrogen bond energy is 20 kJ/mol which is 10 times higher in energy than normal thermal strength of bond at 298.15 K (kT, where k being the Boltzmann constant, invoking interface requires breaking of existing hydrogen bonds in water.[22]

To reveal the existence of interface of water, the reaction at heterogeneous condition has been carried out between **1** and **2a** (Scheme 1) in presence of hexane as a replacement of water at 298.15 K. The second order rate constant (k_2) for the reaction in hexane is 1.528 x 10^{-8} $M^{-1}s^{-1}$, which is about hundred times slower than that of under 'on water' condition. However, heterogeneous condition has been created by dissolving reactants in hexane more than its solvation capability. The k_2 value in hexane justifies the fact that not only presence of interface is necessary for promotion of the reaction but also part of interface should be comprised of water. During 'in water' reaction enforced hydrophobic interactions play pivotal role in promoting organic reactions. During enforced hydrophobic interaction, entropy driven hydrophobic hydration of the reactants turns to enthalpy driven hydrophobic interaction. Results obtained in hexane establishes the fact that hydrophobic interaction is also necessary for heterogeneous reactions, since hydrophobicity that offered by water is not present in hexane.

The reactions (Scheme 1) of **1** with **2a, 2b** and **2c** possessing varying hydrogen bonding ability has been carried out to assess the contribution of hydrogen bonding. Hydrogen bonding capacity of the alkyl acrylate decreases from **2a** to **2c**.[21] To reveal the variation in the contributions from enthalpy as well as entropy of activation, reactions have been performed (Scheme 1) both in homogeneous and heterogeneous conditions. The results shown in Table 1 throws light on the contribution of hydrogen bonding towards activated complex of the reaction in terms of change in the entropy of activation and the enthalpy of activation. A closer look of the data suggests that the hydrogen bonding ability of the reactants with the neighboring water molecules of the droplets calls upon changes at the heterogeneous conditions of the reaction. As the reactants have been varied from 2a to 2b to 2c**,** the hydrogen bonding ability of the reactants have been indirectly diminishing; the comparative values make it obvious that the enthalpy values in the case of homogeneous reactions i.e. 'in water reactions' are not too sensitive to the hydrogen bonding competence of reactants.

Table1: Activation Parameters Derived from the Reaction between **1** with **2a, 2b, 2c** (Scheme 1)

Type of reaction	1+2a		1+2b		1+2c	
	$\Delta^{\#}S$ ($Jmol^{-1}K^{-1}$)	$\Delta^{\#}H$ ($kJ\ mol^{-1}$)	$\Delta^{\#}S$ ($Jmol^{-1}K^{-1}$)	$\Delta^{\#}H$ ($kJ\ mol^{-1}$)	$\Delta^{\#}S$ ($Jmol^{-1}K^{-1}$)	$\Delta^{\#}H$ ($kJ\ mol^{-1}$)
Homogeneous	-75.65	88.32	-72.16	89.79	-66.37	88.39
Heterogeneous	-147.24	57.18	-134.52	60.74	-113.9	67.49

However, a closer look on the enthalpy and entropy values of the reactions in heterogeneous conditions establish the fact that with the decreasing potential of hydrogen bonding exothermic nature of the enthalpy is reduced. It should be stated here that the bond formation is assisted by exothermic variation in the enthalpy and the decrease in the entropy. This ascertains that our results highlight the value of the change in enthalpies i.e. the energy is effectively used in bonding in due course of the reactions to modify the activation energy diagram in favour of positive catalysis by the interface. The observation by Liang and his group concerning the accumulation of aromatics at the oil-water interface supports our experimental observation of the formation of hydrogen bonding with the reactants and the transition state at the interface.[23] The researchers have investigated that the lowering of surface tension in the presence of aromatics with the introduction of weak hydrogen bonding between water at the interface and the aromatic molecules like benzene and toluene.[23a]

4.3.2. Role of the Micro Oil-water Interface

After ascertaining the fact that aqueous interface serves as an indispensable component for promoting 'on water' reaction, focuses have been given on the participating parameters those present at the interfacial water molecules to catalyse the reaction. In this respect, experiments have been designed in such a manner that the structural arrangement and availability of water molecules in situ has been tuned.

Co-operative nature of water-water hydrogen bonding and subsequent increase in the strength of hydrogen bonding about 20% is the consequence of mutual polarization among water molecules.[24] Introduction of an external reagent in water that can modify this mutual polarization among water molecules will come out with the information of bonding at the interface. We have carried out Wittig reaction

between benzaldehyde **4** and ylide **5** at on water condition to analyse the parameters associated to the water interface in promotion of the organic reaction.

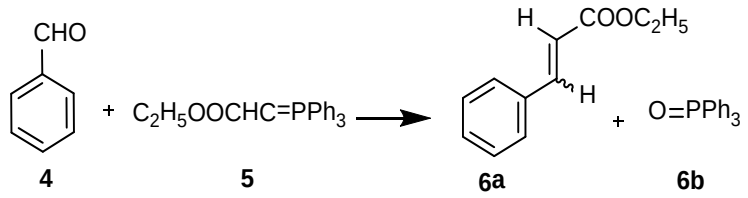

Scheme 2: A Wittig reaction between benzaldehyde **4** and phosphonium ylide **5** at 298.15k at heterogeneous condition.

4.3.4. Addition of Polarisable Salts

To perturb mutual polarization among water molecules, a series of halide salts consists of anions with increasing order of polarizability had been added to the reaction between 4 and 5 in water (Scheme 2). The polarizability and size of the halide anions increase in manner $F^- < Cl^- < Br^- < I^-$. [25, 26] The experimentally estimated rate constants in presence of potassium halide salts have been plotted against the respective polarizability of halide anions of the added salts (Figure 3).

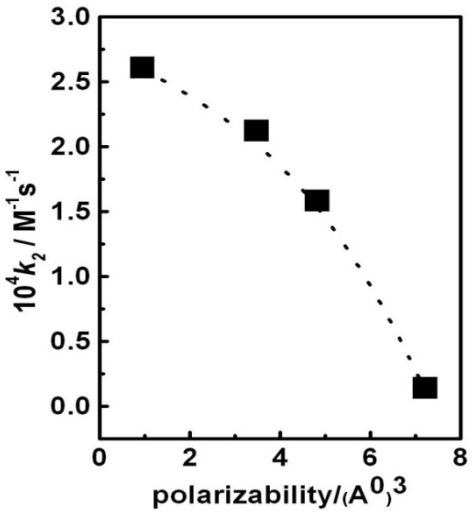

Figure 3: A plot showing the variation of k_2 *vs.* polarizability for the reaction of **4** with **5** at 298.15 K.

To comprehend a decrease in rate constants with increasing polarizability of added anions (Figure 3) in the reaction (Scheme 2), one should consider the ions' specificity at the water surface. The trend can be discussed upon correlation with the observation

made by McFearin and Richmond that the hydrophobic organic molecules experience some hydrogen bonding through the water molecules present at the interface and that the presence of monovalent and divalent anions affects the nature of hydrogen bonding.[25] According to the Gibbs adsorption equation pioneered by Onsager shows that ions are repelled from the surface since surface tension measurement exhibits that there is a net increase in the surface tension of the salt solution in water.[27] In 1990, it was recommended that the statement on repulsion of ions from the water surface should be revisited.[25, 26] Recent molecular dynamics simulation [28] and photoelectron spectroscopy and very recently SFG study on the propensity of the ions at air/water interface that alkali metal cations and halide anions have certain specificity for the air/water interface.[28, 29] The propensity of ions at the surface is a complexed function of polarity, polarizability, size of the ions of which polarizability is predominant.[30] The halide anions are soft and easily polarisable than their counter ion i.e. alkali metal cations and therefore the propensity of the halide anions for the surface is much larger than their alkali metal cations counterpart. [29]

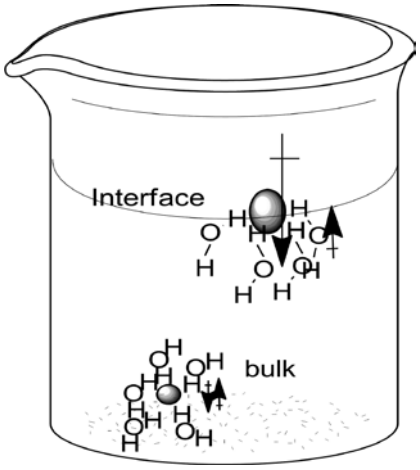

Figure 4: Diagram showing the water molecules around a small ion in bulk and large polarizable ion at interface.

The principal cause of the observed variance in the surface propensity of ions can be explained in terms of electrostatic interactions among dissolved ions and surrounding water molecules. Anions having small size and low polarizability remain at the bulk surrounded by the water molecules pointing their dipoles towards the anion.[28] The surrounding water molecules will try to induce dipole moment in the solvated anion. As the polarizability of the anion is very small, this induced effect can be safely ruled

out. If the polarizability of the solvated anion rises, the surrounding water molecules will induce large amount of dipole moment in the solvated anion. Large polarisable anions, therefore try to move towards the interface in order to get rid of the above unfavourable situation caused by dipole-induced dipole moment. The significant dipole moment present at the interface will induce an electrical interaction in the large polarisable anion. [29] This induces sufficient stabilization at the interface, which will overcome the loss of energy due to ion-water electrostatic interactions. In accordance with the polarizability and size of the halide anions, the propensity of the anions to remain near the interface increases in the order $F^- > Cl^- > Br^- > I^-$. [31] The enhancement of iodide ions at the interface layer is clearly supported by a decrease in the intensity of SFG peak the dangling OH group, which is a clear evidence of clean surface of water.[30] The same reaction (Scheme 2) has been carried out in presence of increasing molarity of KI also. Following Figure 5, it is obvious that with increasing concentration of KI the rate of the reaction decreases. The trend represented in Figure 5 implies that enhancement of iodide ions at the interface layer is clearly decrease in the intensity of the dangling OH group which is a clear notion of clean surface of water. Though the observation that k_2 values decrease with increasing concentration of KI in water confirms our explanations related to the propensity of ions at the interface, the results also had raised the concern whether our investigations are the consequences of the only salt effect instead of surface sensitive effects.[32]

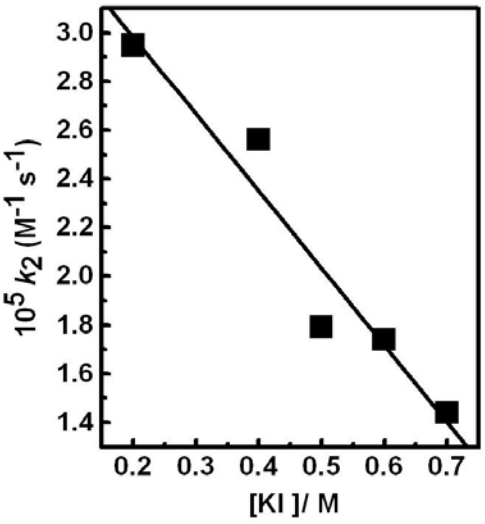

Figure 5: A Plot depicting the change in the k_2 *vs.* the concentration of ki salt for the reaction between **4** and **5**.

Since KI serves as a salting in agent, the structure breaking property of KI acts as antihydrophobic agent in the water promoted reactions.[8b]

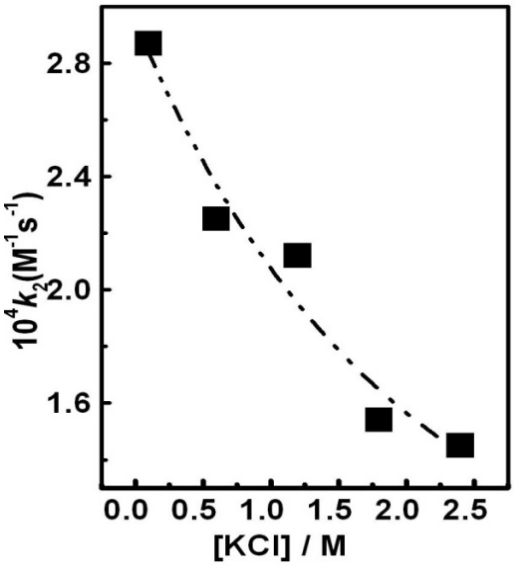

Figure 6: A plot showing the variation in values of k_2 values with addition of KCl salt for the reaction of **4** with **5**.

Therefore, the same experiment has been repeated (Scheme 2) in the presence of increasing amount of KCl, a salting out agent.[33] KCl being a prohydrophobic salt enhance the hydrophobicity of the reaction medium. If during 'on water' reactions hydrophobicity plays pivotal role, then k_2 values should increases up with the addition of increasing amount of prohydrophobic salts like KCl. Figure 6 shows the consequences on k_2 with the addition of KCl in the reaction (scheme 2). Figure 6 entails that k_2 decreases upon increasing concentration of KCl in water during heterogeneous reaction. It implies that the justification on effect of anions at the interfacial water structure presented above is mainly guided by surface sensitive factors. Here, if only the salt effect had played the guiding role to modify the oil-water interface structure then introduction of KCl salt could lead to the increase in the k_2 values instead of their decreasing. The photo detachment spectroscopic studies have recently established that with increasing concentration I^- ions accumulate at the surface in an increasing order.[32]

4.3.5. Introduction of Polarizable Cation

Important point in the present context is that not only anions show their effect at the aqueous interface, but also cations alter the structure of the interface. The presence of

polarisable cation H^+ in the form of H_3O^+ modifies the interfacial arrangement of water, but in our case added inorganic acid reacts with one of the reactant and leads to side products.[26b] To keep away from these undesired side reactions, the reaction (Scheme 2) had been repeated in the presence of ammonia-water. Here ammonium cation being large in size compared to H_3O^+ is highly polarizable and behaves as inert reagent in the studied reaction condition (Scheme 2). Choice of introduction of ammonia in the reaction medium stems from the fact that ammonia possesses high surface affinity because of high energy cost for water to solvate ammonia.[34] Formation of a surface layer of ammonia is consistent with the minimum free energy of ammonia.[34, 35] Ammonia generally bond to a surface via lone pair of nitrogen atom with C_3 molecular axis perpendicular to the surface plane.[34] The consequence of the addition of ammonia with successive increasing concentration in water has been described in Figure 6. A careful examination up of the data shows that there is disparity in terms of sensitivity of the rate of the reaction with respect to the added concentration of ammonia.

From Figure 7, a 10-fold decrease in the k_2 values at the very low concentrations of ammonia has been observed. A meticulous observation of the graph confirms that the k_2 values are insensitive to the higher concentrations of ammonia in the reaction medium. Observed result can be correlated with the data acquired from atmospheric chemistry a branch of chemistry mainly deals with the sensitivity of the air water interface towards the exposure of gas from the air.[34, 35]

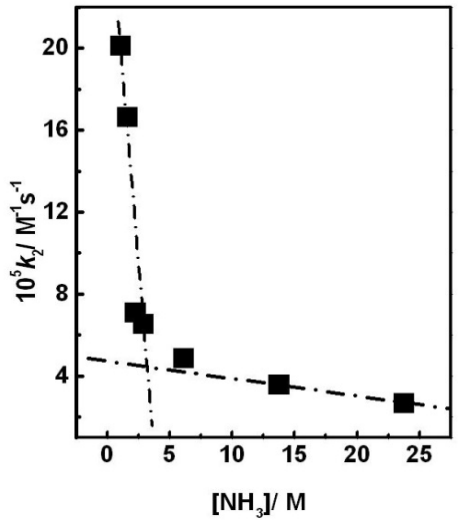

Figure 7: A plot of the k_2 values against [NH_3] for the reaction of **4** with **5**

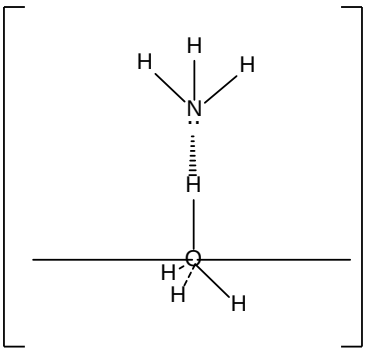

Figure 8: The diagram illustrates the capping of ammonia with the free OH groups

During adsorption of the gases, the exchanged gas modifies the thermodynamics of the surface by forming microemulsions and controls the further dynamics of the gas adsorption on water surface. At very low concentration the NH_3 molecules simply bind with a small portion of water molecule at the interface through hydrogen bonding.[35] Since ammonia molecule itself acts as weak hydrogen bond donor to the water molecule, it simply occupies the free hydrogen bonding sites of water at the oil-water interface the process. [34] The cartoon in the Figure 8 gives a vivid description to the mechanism of adsorption at low concentration of ammonia in water. The process continues till the saturation of the interface with ammonia molecules. Davidovits et al. showed that transport across the interface requires the displacement of the solvent molecules at the subsurface layer, which required a comparative mass accumulation of the ammonia molecule at the interface.[36] After saturating the surface, the hydrogen atoms of the ammonia as well as the nitrogen atoms begin to form aggregates among themselves through hydrogen bonding.[36] These ammonia molecules following aggregation up to a critical value (where the surface free energy creates a thermodynamic barrier to the growth of the nucleus initially) serve as nuclei for further clustering. High molecular density at the interfacial region indicates that the interfacial molecules are somehow interconnected and bound (Figure 9).[37] It implies that the cluster can assume various forms of arrangements at the interface of the oil−water. The recent sum frequency generation (SFG) study at the air/ water interface puts a spectroscopic justification on the above explanation.[36, 37] Consequently, the ammonia clusters form a barrier between the organic reactants and the water.

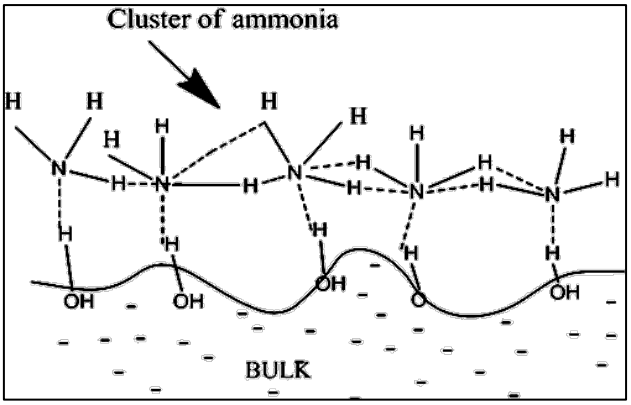

Figure 9: Diagram showing cluster of ammonia at the surface of water at moderate concentration of ammonia in water

A comparison of kinetic data experimentally obtained during carrying out of Wittig reaction (Scheme 2) upon addition of ammonia-water in reaction medium discloses the fact that the reaction in the presence of higher concentrations of ammonia is equivalent to the reaction occurring under neat conditions as ammonia clusters hinder organic droplets to come in contact with water molecules. One may note here that the organic bubbles can have the assistance from hydrogen bonding imparted by ammonia molecules, which are present as aggregates in between organic and water layers, but the trend in the values of the k_2 values for the Wittig reaction (Figure7) reveals that though ammonia molecules can stabilize the reactants as well as the transition state through hydrogen bonding, the other responsible factors essential for water promoted reactions[8-10] cannot be covered by these ammonium ions present at the oil−water interface. This experimental finding has again confirmed our previous finding with hexane regarding the essential presence of water as well as its hydrophobic property. It implies that 'on water' reactions are accelerated more than 'in water' reactions for the presence 'free OH' groups at oil/interface but the this hydrogen bonding should be accompanied by hydrophobic interactions.

4.3.6. Addition of D_2O in the Reaction Medium

Till now all the experimental criterion performed to delineate the effect of oil/water interface during heterogeneous reactions had shown that upon addition of external substances number the interfacial water molecules decreases. With the purpose of increasing probability of assistance from hydrogen bonding, D_2O has been introduced in the reaction medium (Scheme 2). Upon addition of D_2O, a smooth decrease in k_2 values with the rise of concentration of D_2O up to 1.5 M has been observed. A sharp

inversion in the k_2 values have been observed in figure 7 after 1.5 M of D_2O. The clear intersection point in this graph is at ~1.8 M corresponding to the value of k_2 as 0.97 M^{-1} s^{-1}.

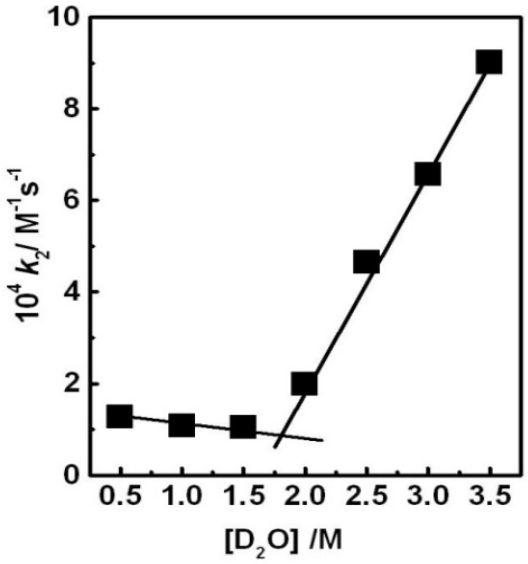

Figure 10: A plot showing the variation in the k_2 *vs.* concentration of D_2O in the reaction of **4** with **5**.

The decrease in the k_2 values at the initial stage can be easily explained by the enhanced viscosity of solution upon the addition of D_2O. [13,16, 40] However, the increment is surprising to us. To discern the reason for a sudden change in the k_2 values at about 1.8 M, we carried out temperature dependent kinetic studies in the concentration range of 1 to 2 M D_2O that is near the inversion point of Figure10.

Table 2: Activation parameters derived for the reaction of 4 and 5 in 1.0, 1.5 and 2.0 M of D_2O, respectively

Conc. of D_2O (M)	$\Delta^{\#}H$ kJmol^{-1}	$\Delta^{\#}S$ J mol^{-1} K^{-1}
1.0	51.47	-147.65
1.5	57.73	-126.78
2.0	40.66	-179.76

From the enthalpic and entropic data tubulised in Table 2, it is obvious that at the transition point enthalpy of the system favours the reaction (less endothermic). However the system becomes entropically unfavourable. Considering the concept of hydrophobic hydration which is a process of dissolution of hydrophobic molecules in water, thermodynamically it is associated with the large and negative value of $\Delta S^{\#}$.[9,10] It can be concluded that some of the degrees of freedom of the reactants and also of the transition state get restricted, leading to a rise in entropy.

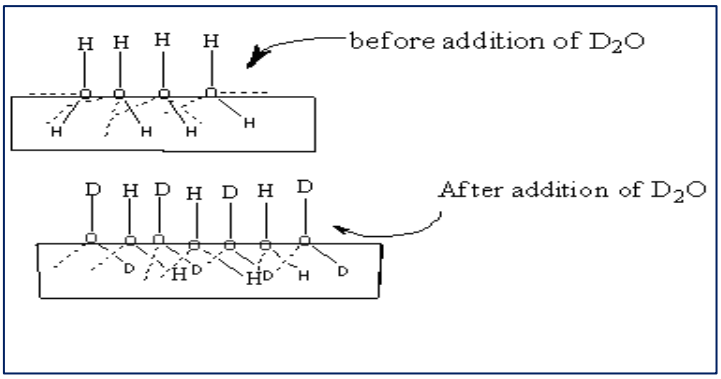

Figure 11: Diagram displaying the effect on addition of D_2O

However, on careful assessment of the activation enthalpy values (Table 2), it can safely be justified that the transition state of the Wittig reaction is stabilized through new bond formation at the water-heavy water interface. The dangling OD group actively participates together with the dangling OH group in stabilization of the transition state at the interface (Figure 11). Alternatively the exchange of hydrogen of ylide by deuterium at the higher concentration of D_2O cannot be ruled out.[41] It should be noted based upon the neutron and X-ray diffraction studies that intramolecular hydrogen bonding in D_2O can lead to OD---D bond may get stronger at the transition state. [40]

Kinetic and thermodynamic studies help us to analyze the requirement of the interface and the role of water in case of 'on water' reactions. The development of specific attributes of the polarizable salts, ammonia−water solution, and D_2O during the study of the on water reactions can be validated from their contribution in altering the interfacial structure at the molecular level. The recent observation of the support of

the ‘on water’ reaction by the adsorption of OH^- at the oil−water interface through the reaction of the reactant and surface water molecule can be argued because of the high cost of energy to adsorption and the enhanced selectivity toward hydroxide ions.[42, 43]

4.4. Conclusions:

In summary, we have attempted to demonstrate the free OH group present at the oil/water interface in promoting the reaction at “on water condition”. Our work shows experimentally the role of these unsatisfied bonds at the interface. Comparing the experimental results and subsequent discussions, the following conclusions can safely be drawn. First, the presence of micro-interface is vital criteria for the ‘on water’ reactions. Second, the nature of the interface should be figured out in a way to maximize the contact between the reactant and the water. Eventually, the most decisive conclusion of our investigations is that the ease of the hydrogen bonding with the reactants and the transition state at the interface from the water molecules due to the presence of free –OH groups at reactant/ water interface serve as imperative requirements along with hydrophobicity and cohesive energy density offered by small water molecules. This study, it is hoped, will lead to studies of complicated liquid-liquid interfaces. Such a study will help us in promoting water as the greener solvent and otherwise to design new green solvent possessing the structural features of water and large reaction window.

4.5. References:

1. Corey, E. J.; Cheng, X. M. *The Logic of Chemical Synthesis*; John Wiley & Sons: New York **1989**.

2. (a) Li, C. J. Chem. Rev. **2005**, *105*, 3095. (b) Leach, A. G.; Houk, K. N.; Reymond, J.-L. *J. Org. Chem.* **2004**, *69*, 3683. (c) Wei, C. M.; Li, C. J. *J. Am. Chem. Soc.* **2003**, *125*, 9584. (d) Lindstrom, U. M. *Chem. Rev*. **2002**, *102*, 2751.

3. (a) Kuharski, R. A.; Rossky, P. J. *J. Am. Chem. Soc.* **1984**, *106*, 5786. (b) Nozaki, Y.; Tanford, C. *J. Biol. Chem.* **1963**, *238*, 4074.

4. Rideout, D. C.; Breslow, R. *J. Am. Chem. Soc.* **1980**, *102*,7816.

5. (a) Grieco, P. A.; Ferrino, S.; Vidari, G. *J. Am. Chem. Soc*. **1980**, *102*, 7586. (b) Vidari, G.; Ferrino, S.; Grieco, P. A. *J. Am. Chem. Soc.* **1984**, *106*, 3539. (c) *Organic Synthesis in Water*; Grieco, P. A., Ed.; Blackie Academic & Professional: London, **1998**.

6. For example see (a) *Aqueous-Phase Organometallic Catalysis*; Cornils, B., Hermann, W. A., Eds.; Wiley-VCH: Weinheim, Germany, 1998. (b) *Clean Solvents: Alternative Media for Chemical Reactions and Processing*; Moens, L., Abraham, M., Eds.; ACS Symposium Series 819; American Chemical Society: Washington, DC, 2002. (c) Engberts, J. B. F. N. *Pure Appl. Chem.* **1982**, *54*, 1797. (d) Lindstrom, U. M. *Chem. Rev.* **2002**, *102*, 2751. (e) Hayashi, T.; Inoue, K.; Taniguchi, N.; Ogasawara, M. *J. Am. Chem. Soc.* **2001**, *123*, 9918. (f) Nagayama, S.; Kobayashi, S. *J. Am. Chem. Soc.* **2000**, *122*, 11531. (g) Pindur, U.; Lutz, G.; Otto, C. *Chem. Rev.* **1999**, *93*, 741. (h) Wijnen, J. W.; Engberts, J. B. F. N. *J. Org. Chem.* **1997**, *62*, 2039. (i) Muller, N. *Acc. Chem. Res*. **1990**, *23*, 23. (j) Breslow, R.; Guo, T. *J. Am. Chem. Soc.* **1988**, *110*, 5613.

7. (a) Jenner, G.; Ben Salem, R. *New J. Chem*. **2000**, *24*, 203. (b) Cativiela, C.; Garcia, J. I.; Gil, J.; Martinez, R. M.; Mayoral, J. A.; Salvatella, L.; Urieta, J. S.; Mainar, A. M.; Abraham, M. H. *J. Chem. Soc., Perkin Trans.* **1997**, *2*, 653. (c) Richardt, C, *Solvent Effects in Organic Chemistry*, Verlag Chemie, Weinheim, **1979.**

8. (a) Aggarwal, V. K.; Dean, D. K.; Mereu, A.; Williams, R. *J. Org. Chem*. **2002**, *67*, 510. (b) Kumar, A. *Chem. Rev.* **2001**, *101*, 1. (c) Van der Wel, G. K.; Wijnen, J. W.; Engberts, J. B. F. N. *J. Org. Chem.* **1996**, *61*, 9001.

9. (a) Breslow, R.; Conners, R. V. *J. Am. Chem. Soc.* **1995**, *117*, 6601. (b) Breslow, R.; Rizzo, C. J. *J. Am. Chem. Soc.* **1991,** *113***,** 4340**.**

10. (a) Engberts, J. B. F. N. *Pure Appl. Chem.* **1995**, *67*, 823. (b) Blokzijl, W.; Engberts, J. B. F. N.; Blandamer, M. J. *J. Am. Chem. Soc.* **1991**, *113*, 4241. (c) Blokzijl, W.; Engberts, J. B. F. N.; Blandamer, M. J. *J. Am. Chem. Soc.* **1990**, *112*, 1197.

11. (a) Blake, J. F.; Lim, D.; Jorgensen, W. L. *J. Org. Chem***. 1994,** *59***,** 803. (b) Blake, J. F.; Jorgensen, W. L. *J. Am. Chem. Soc.* **1991,** *113***,** 7430**.**

12. (a) Jenner, G. *J. Phys.Org. Chem*. **1999**, *12*, 619. (b) Meijer, A.; Otto, S.; Engberts, J. B. F. N. *J. Org. Chem.* **1998**, *63*, 8989. *(c)* Breslow, R.; Conners, R. V. Quantitative *J. Am. Chem. Soc.* **1995**, *117*, 6601. (d) Blokzijl, W. & Engberts, J.B.F.N. *Angew. Chem. Int. Ed. Engl.* **1993**, *32*, 1545. (e) Breslow, R. *Acc. Chem. Res.* **1991**, *24*, 159. (f) Lubineau, A.; Auge, J.; Lubin, N. *J. Chem. Soc., Perkin*

Trans.1. **1990**, 3011. (g) Brandes, E.; Grieco, P. A.; Garner, P. Garner, P. *J. Chem. Soc., Chem. Commun.* **1988**, 500.

13. Narayan, S.; Muldoon, J.; Finn, M. G.; Fokin, V. V.; Kolb, H. C.; Sharpless, K. B. *Angew. Chem.,Int. Ed.* **2005**, *44*, 3275**.**

14. Klijn, E.; Engberts, J. B. F. N. *Nature* **2005**, *435*, 746.

15. Jung, Y.; Marcus, R. A. *J. Am. Chem. Soc.* **2007**, *129*, 5492.

16. For reviews, see: (a) Butler, R. N.; Coyne, A. G. *Chem. Rev.* **2010**,*110*, 6302. (b) Chanda, A.; Fokin, V. V. *Chem. Rev.* **2009**, *109*, 725. (c) Gawande, M. B.; Bonifácio, V. D. B.; Luque, R.; Branco, P. S.; Varma, R. S. *Chem. Soc. Rev.* **2013**, 5522.

17. (a) Pirrung, M. C.; Sarma, K. D.; Wang, J. *J. Org. Chem.* **2008**, *73*, 8723. (b) Pirrung, M. C.; Sarma, K. D. *Tetrahedron* **2005**, *61*, 11456. (c) Pirrung, M. C.; Sarma, K. D. *J. Am. Chem. Soc.* **2004**, *126*, 444.

18. (a) Acevedo, O.; Armacost, K. *J. Am. Chem. Soc.* **2010**, *132*, 1966. (b) Tiwari, S.; Kumar, A. *J. Phys. Chem. A* **2009**, *113*, 13685.

19. (a) Cozzi, P. G.; Benfatti, F.; Zoli, L. *Angew. Chem., Int. Ed.*, **2009**, *48*, 1313. (b) Cozzi, P. G. ; Zoli, L. *Angew. Chem., Int. Ed.*, **2008**, *47*, 4162.

20. Beattie, J. K.; McErlean, C. S. P.; Phippen, C. B. W. *Chem. Eur. J.* **2010**, *16*, 8972.

21. (a) Tiwari, S.; Kumar, A. *Chem. Commun.* **2008**, 4445. (b) Weleski, E. T.; Silver, J. L.; Jansson, M. D.; Burmeister, J. L. *J. Organomet. Chem*. **1975**, *102*, 365.

22. Franks. F. (Ed.), *Water: A Comprehensive Treatise*, vols. *1-7*, Plenium Press, Newyork, **1973.**

23. (a) Kunieda, M; Nakaoka, K; Liang, Y; Marinda, C.R.; Ueda, Akira; Takahasi, S; Okabe, H.; Matsuoka, T. *J. Am. Chem. Soc.* **2010**, *132*, 18281. (b) Lubineau, A.; Bienayme, H.; Queneau, Y.; Scherrmann, M. C. *New J. Chem.***1994**, *18*, 279.

24. Jeffry, G. A.; Sanger, W. *Hydrogen Bonding in Biological Structure*s, Part IV Springer, Berlin, **1991.**

25. Mc Fearin, C. L.; Richmond, G. L. *J. Phys. Chem. C* **2009**, *113*, 21162.

26. (a) Santos, A. P. D.; Levin, Y. *Langmuir* **2012**, *28*, 1304. (b) Chang, T. M.; Dang, L.X. *Chem. Rev.* **2006**, *106*, 1305. (c)Vrbkaa, L.; Muchaa, M.; Minofara, B.; Jungwirth, P.; Brownb, E. C.; Tobiasb, D. J., *Current Opinion in Colloid and Interface Sci.* **2004**, *9*, 67.

27. Onsager, L; Samaras, N.N.T. *J. Chem. Phys.* **1934**, *2*, 528-536.

28. Sun, L.; Li, X.; Hede ,T.; Tu, Y.; Leck, C.; Ågren, H. *J. Phys. Chem. B* **2012**, *116*, 3198.

29. Yoo, S; Lei Y. A.; Zengb, X. C. *J. Chem. Phys.* **2003**, *119*, 6083.

30. (a) Liu, D.; Ma, G.; Lavering, L. M.; Allen, H. C. *J. Phys. Chem. B* **2004**, *108*, 2252. (b) Simonelli, D.; Baldelli, S.; Shultz, M. J. *Chem. Phys. Lett.* **1998**, *298*, 400.

31. Raymond, E. A.; Richmond, G. L. *J. Phys. Chem. B* **2004**, *108*, 5051.

32. Hiranuma, Y.; Kaniwa, K.; Shoji, M.; Mafune, F. *J. Phys. Chem. A* **2011**, *115*, 8493.

33. Deshpande, S. S.; Phalgune, U. D.; Kumar, A. *Tetrahedron* **2002**, *58*, 8759.

34. Donaldson. D. J. *J. Phys. Chem. A* **1999**, *103*, 62.

35. Simonelli, D.; Baldelli, S.; Shultz, M. J. *Chem. Phys. Lett.* **1998**, *298*, 400.

37. Davidovis, P.; Hu, J. H. ; Worsnop, D. R.; Zahniser, M. S.; Kolb, C. E. *Faraday Discussion* **1995**, *100*, 65.

38. Nathanson, G. M.; Davidovits, P.; Wornop, D. R.; Kolb, C.E. *J. Phys. Chem.* **1996**, *100*, 13007.

39. Shultz, M.J.; Baldelli, S.; Schnitzer, C.; Simonelli, D. *J. Phys. Chem. B* **2002**, *106*, 5313.

40. Soper, A. K.; Benmore, C. J. *Phys. Rev. Lett.* **2008**, *101*, 65502-1.

41. El-Batta, A.; Jiang, C.; Zhao, W.; Anness, R.; Cooksy, A.L.; M. Bergdahl, *J. Org. Chem.* **2007**, *72*, 5244.

42. Thakur, P. B.; Meshram, H. M. *RSC Adv.* **2014**, *4*, 6019. (f) Beare, K. D.; Yuen, A. K. L.; Masters, A. F.; Maschmeyer, T.; McErlean, C. S. P. *Chem. Commun.* **2013**, *49*, 8347.

43. (a) Creux, P.; Lachaise, J.; Graciaa, A.; Beattie, J. K.; Djerdjev, *J. Phys. Chem. B* **2009**, *113*, 14146.; (b) Marinova, K. G.; Alargova, R. G.; Denkov, N. D.; Velev, O. D.; Petsev, D. N.; Ivanov, I. B.; Borwankar, R. P. *Langmuir* **1996**, *12*, 2045.

Chapter 5

Pairwise Interactions to Access the Efficacy of Ionic Liquids as Co-solvents in Diels-Alder Reaction

"The meeting of two personalities is like the contact of two chemical substances: if there is any reaction, both are transformed." Carl Jung

Ionic liquids have been introduced as co-solvents during water promoted Diels-Alder reactions with the objective of increasing solubility window of solvent water. The dependence of the second order rate constants for Diels-Alder reaction between anthracene-9-carbinol and N-ethylmaleimide on the molality of added co-solvent is analyzed in terms of pairwise Gibbs function interaction parameters. Additivity of pairwise group interaction parameters (SWAG procedure) is applied, and the validity of additivity is critically examined during analysis. Pairwise Gibbs functions have been calculated for a variety of ionic liquids to comprehend the efficacy of ionic liquids as co-solvents. A comparative kinetic and thermodynamic study has been presented to guide the tailorability of ionic liquids as co-solvents during cycloaddition reaction in water.

5.1 Introduction:

Liquid water is an extraordinary solvent, both polar and apolar solutes are reasonably soluble in it.[1] Water is miscible with other liquids despite often remarkable variation in properties. From the discussion of the previous chapter, it is obvious that water supports chemical reactions involving a vast range of mechanisms and processes.[1] Though the 'on water' reactions serve as modification over the 'in water' type reaction by letting off the barrier low solubility range as in this case water does not act as solvent but as a reaction media, this type of reactions requires the criteria of presence of atoms in the reactants having the capability of hydrogen bonding.[2] Again the transition state of these heterogeneous types of the reactions in water must be more stabilized than that of the corresponding reactants.[3-6] So the letting off the barrier of the solubility in case of on water reactions invites new constraints of the essentiality of the presence of hydrogen bonding in the reactants.[7,8] Consequently, the performance of several organic reactions with structural and synthetic complications remains unsuccessful attempt in water only solvent media.[9]

The introduction of minute amount of organic liquids *viz.* alcohols, carbohydrate etc. as co-solvents to the water leads the reactions to success by promoting the solubility of the non-polar reactants.[10, 11] Interests have been concentrated on the kinetics of chemical reactions in which water and related aqueous system are used as solvents. Rate constants for chemical reactions in aqueous solutions are often particularly sensitive to the nature and mole fraction of added co-solvent.[11] This sensitivity reflects impact of added co-solvent on the initial and transition states. In fact this sensitivity is not unexpected because it is well established, that, for example, the solubilities of solutes such as rare gases and hydrocarbons are strongly dependent on the characteristics and mole fraction of added co-solvent.[11, 12]

However this method of involving alcohols or other volatile organic substances as co-solvents along with water give rises to a serious question on the retention of the green nature of solvent water as the water in the due process is being contaminated with toxic and volatile organic solvents. Our main aim through this study is to find out alternative chemical substances to the hazardous conventional organic co-solvents without sacrificing the clean and green nature of water driven reactions. Ionic liquids comprising both organic cation and organic/inorganic anion[13] can offer similar proficiency than that of usual organic co-solvents. The beneficial properties like chemical internees, non-volatility, large solubility window and wide thermal and

electrochemical stability of the ionic liquids[14] which have been appeared in several classical and quantum mechanical studies induce us to reveal their effectiveness as co-solvents in the aqueous reactions. [15]By bringing in the ionic-liquids in water two purposes can be served:

i) the solubility window widens up for a large range of polar to apolar reactants
ii) the green ionic liquids will not interfere with the eco-friendly nature of the water.

In this study a variety of ionic liquids has been employed as co-solvents in the water-promoted Diels-Alder reaction which serves as the noteworthy step in synthesizing large cyclic organic compounds.

A major problem in physical organic and physical inorganic chemistry is concerned with finding a link between kinetic data and the thermodynamic properties of aqueous solutions. Here this link is formed using transition state theory. Nevertheless quantitative descriptions of kinetic solvents effects are not straightforward.

5.1.1 Theoretical Overview

Throughout the study the concentration of the ionic liquids has been kept in a range that the ionic liquids should not interfere with the structural property of the water. It means the reaction medium is the water rich solution of ionic liquids. At low co-solvent mole fractions x_2 (where liquid-2=the co-solvent, and liquid-1 = water), water-water cooperative hydrogen bonding is enhanced. As more co-solvent is added (Le. x_2 increases, and so x_1 decreases), there is insufficient water to maintain extensive hydrogen bonded networks.[16] Nevertheless, transient domains exist where some domains arc water-rich and others co-solvent-rich. Hertz and co-workers had shown, for example, that in this composition range, aqueous mixtures are microheterogeneous.[17]

5.1.1.1 Pairwise Interactions

An interaction structure explains who interacts with whom. It denotes for each agent a set of neighbours, the set of agents with whom the agent interacts. As a consequence, an “interaction structure” is modelled as an undirected finite graph whose vertices or nodes are the members of the player population.[18] Two players are neighbours, if they form an edge of the graph. Global interaction prevails if any two players are neighbours. Otherwise, interaction is local. Very significant insights have been gained

from studying pairwise interaction under the assumption of a fixed interaction structure.[19,20]

During the application of this concept the pairwise interactions can only be restricted to very dilute region. Here, the reaction mixture is so dilute that the water molecules prevent the aggregation of apolar solutes. During bulk hydrophobic interactions, clusters of apolar molecules are formed at their higher concentrations in water. It is thermodynamically quite difficult to separate out all the interactions during bulk interactions[21].

In our present study a reaction as depicted in Scheme 1 was used. Here anthracene- 9 carbinol **1** and *N*-ethyl maleimide **2** are the two reactants and water is the medium of reaction (w) and ionic liquid is the co-solvent (c). This bimolecular Diels-Alder reaction can fairly be mimicked by using following diagrammatic representation:

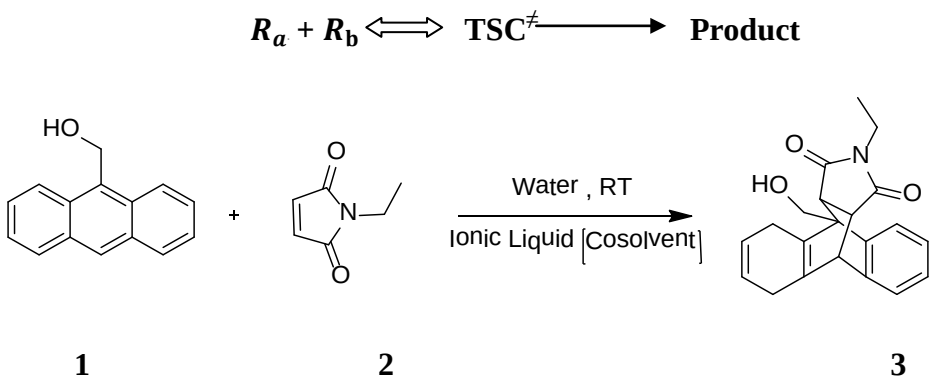

1 **2** **3**

Scheme 1: The reaction between anthracene- 9-carbinol **1** and *N*-ethyl maleimide **2**

where, 'R_a' and 'R_b' represent the reactants **1** and **2**, respectively; $TSC^{\neq}$ stands for the transition state complex of the reaction. Following the transition state theory of the reactions the reactants and activated complex are in equilibrium with each other. Then the chemical potential [22] of the above reaction follows

$$\mu_{R_a} + \mu_{R_b} = \mu_{TSC} \quad (1)$$

For chemical reaction involving solute-X proceeding through a transition state ($TS^{\#}$), the rate constant in an ideal aqueous solutions is given by eqn. (3) where $\Delta^{\neq}\mathbf{G}^{\mathbf{0}}$ is the activation Gibbs energy. (k_B refers to Boltzmann constant and h is Planck's constant).

$$k = \frac{k_B\ T}{h}\ \exp\left(-\frac{\Delta^{\neq}G^{\circ}}{RT}\right) \qquad (2)$$

where, $\Delta^{\neq}G°$ can be expressed as , [23].

$$\Delta^{\neq}G° = \mu° \text{ (TSC, aq) - } \mu° \text{ (IS}_{R_aR_b}\text{, aq)}$$

The $\Delta^{\neq}G°$ value encompasses of all the chemical potentials of all the components and their interaction present in the reaction mixture.

The ion-ion pair interaction potential in the co-sphere overlap model proposed by Friedman and co-workers is given by, [24]

$$u_{ij}\ (r) = (e_i\ e_j)/(Dr) + COR_{ij} + CAV_{ij} + GUR_{ij} \qquad (3)$$

where in the equation 3, the first term represents the Coulomb interaction of ions of charges e_i and e_j at distance r in a solvent of dielectric constant D. The second term is a repulsive core potential, and the third term is a cavity effect in a dielectric medium. The fourth term, called the Gurney potential, represents the effect of the overlap of the co-spheres when the ions come close together, and is in aqueous solution the solutes present in the reaction media can be treated as surrounded by the water molecules. In the present system, one has to look forward of four different solutes are interacting with one-another i.e. two of them are from the two reactants, another is co-solvent and the remaining one is of activated complex arises out during reaction.[17] Following cartoon (Figure 1) is the vivid representation of the model in the reaction medium.

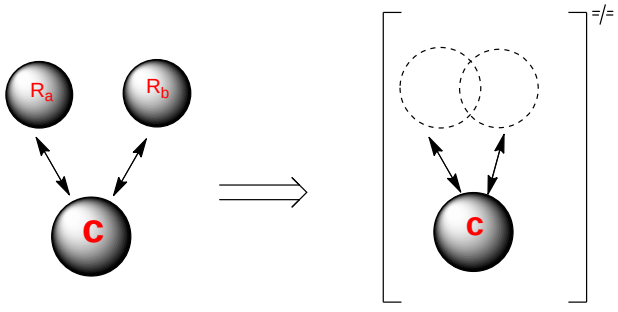

Initial state Transition state

Figure1: The cartoon of interactions between co-solvent with reactants and activated complex during the reaction.

Our main focus in this work is to establish the nature of interactions in the aqueous Diels-Alder reactions in the presence of ionic liquid as a co-solvent in very dilute region. For simplicity present system can be divided in two sections for

comparison: i) the reaction medium without the presence of co-solvents (molality (m_c=0)) and ii) in the presence of ionic liquid co-solvents ($m_c \neq 0$).

Following the equation relating rate constant (k) and equilibrium constant ($K^{\#}$), for normal aqueous reaction can be written as follows: [23]

$$k\ (m_c=0 = \frac{k_B\ T}{h}\ K^{\#} \qquad (4)$$

Since the ionic liquid is added to the reaction medium, the added ionic liquid imparts interactions with reactants and the activated complex and system will no longer behave as ideal solution. The change in the chemical potential in the presence of ionic liquids can be ascribed through the calculation of the activity coefficient of the activated complex and reactants. The term activity coefficient (γ) of the reactants and activated complex will indicate the non-ideality introduced by the addition of ionicliquids.[26, 27] This activity coefficient (γ) is related to the excess Gibbs function (G^E) of the total solution by the following differential equation:

$$\ln \gamma = \frac{1}{RT} . \frac{dG^E}{dm} \qquad (5)$$

Now in the presence of co-solvent, the rate constant (k) can be equated with

$$k(m_c \neq 0) = \frac{k_B\ T}{h} \frac{\gamma_{R_a} \gamma_{R_b}}{\gamma_{TSC}} . K^{\#} \qquad (6)$$

where γ_{R_a}, γ_{R_b} and γ_{TSC} are the activity coefficient of initial state of the reactants and transition state, respectively and have been introduced due to invoked non-ideality with the addition of ionic liquids in water. By taking logarithm of Equations (4) and (6), thereafter dividing Equation (6) by Equation (4), the following relationship between rate constant and the activity coefficient is obtained:

$$\ln[\frac{k_{m_c}}{k_{m_{c=0}}}] = \ln\gamma_{R_a} + \ln\gamma_{R_b} - \ln\gamma_{TSC} \qquad (7)$$

The excess Gibbs energy (G^E) of the solution can be equated with the expansion series of thermodynamic properties like molality of the solute using virial coefficient.[28] The arrangement of co-solvents around solutes in the solution has been quantitatively determined with the theory developed by Kirkwood and Buff [29]and which has been further modified by Newman[30] and Ben-Naim.[31] Following the equation advanced by Cassel and Wood excess Gibbs energy can be expressed in terms of pairwise Gibbs energy solute interaction parameter [32] (g_{ij}; i and j denotes any component those are interaction with each other in the dilute reaction medium) by the equation

If the solution is dilute, the excess Gibbs function, G^E (aq; T;P) can be expressed in terms of pairwise Gibbs function interaction parameters: m_0 ,m_i ,m_j , [19]

$$G^E(aq;T;p) = g_{ii}\left(\frac{m_i}{m_0}\right)^2 + \frac{2g_{ij}m_i m_j}{m_0{}^2} + g_{ij}\left(\frac{m_j}{m_0}\right)^2 \quad (8)$$

Here *i, j, k* are the interacting components present in the solutions, m_0 is the standard 1 mol/kg of water and m_i is the molality of the i^{th} solute in the solution. Here, the heterotactic interactions have been considered (g_{ij}) and the homotactic interactions (g_{ii}) are ignored to simplify the system of the study. This equation can be expanded to pairwise, triplet or higher order terms. While dealing with dilute solutions, restriction should be imposed up to first term only.

According to Savage and Wood additivity principle, the pairwise Gibbs energy solute interaction parameter can further be simplified to [20]

$$g_{ij} = \sum_x \sum_y n_x^i n_y^j \, G\,(X \leftrightarrow Y) \quad (9)$$

where, n_x^i ; n_y^j denotes the number of interacting groups in the solutes x and y in the solution G (X ↔ Y) is known as pairwise Gibbs energy group interaction parameter.[17] Following Equation 4 and taking derivative of the excess Gibbs energy (Equation 7) with respect to molality (restriction of the expansion up to first term only), the activity coefficient γ_i is given by;

$$RT \ln \gamma_i = \frac{2g_{ij}m_i}{(m_0)^2} \quad (10)$$

Since it is obvious that logarithmic comparison of rate constants of the reaction can be expressed by the following equation:

$\ln\left[\frac{k(m_i)}{k(m_i=0)}\right] = -ln\gamma(TS) + ln\gamma(IS)$, where the γ is the activity coefficients of the corresponding states. Now on comparing Equation 9 and 10, it can be written that,

$$\ln\left[\frac{k(m_i)}{k(m_i=0)}\right] = \left[\frac{2}{RT(m_0)^2}\right]\left[\sum_x \sum_y n_x^i \, n_y^{IS} \, G(X \leftrightarrow Y) - \sum_x \sum_y n_x^i \, n_y^{TS} \, G(X \leftrightarrow Y)\right] m_i \quad (11)$$

Now by replacing the value lnγ of Equation 10 in Equation 11 the following relationship is obtained:

$$\ln\left[\frac{k_{m_c}}{k_{m_{c=0}}}\right] = \frac{2}{RTm_0^2}\left(g\,[R_a \rightarrow C] + g[R_b \rightarrow C] - g[TSC \rightarrow C]\right)m_c \quad (12)$$

The equation can be rewritten as by substituting the value in Equation 9 as,

$$\ln\left[\frac{k_{m_c}}{k_{m_{c=0}}}\right] = \frac{2}{RTm_0^2} G_c \, m_c \quad (13)$$

Herein G_c is the representation of the pairwise group interaction arising out of the addition of ionic liquids as co-solvents in the water promoted Diels-Alder reaction. As the consequence of the co-solvent and solute interactions, we get a concentration dependent thermodynamic property which varies with the change in the molality of the added ionic liquid in the reaction mixture by plotting $ln\left[\frac{k}{k_0}\right]$ *vs.* molality of the co-solvent (m) [where, $k = k_{m_c}$ and $k_0 = k_{m_{c=0}}$]. As we are restricted to pairwise interaction only by keeping the solution in extremely dilute condition, we will ignore, in the interest of simplicity, the second, third i.e. any subsequent higher order interactions during experimental data analysis.

5.2 Experimental Procedure:

5.2.1 Materials and Synthesis of Ionic Liquids

N-methyl imidazole, *N*-methyl pyrrolidine, 1-bromobutane, 1-bromohexane, 1-bromoethane 1-chlorobutane and 1-iodobutane were purchased from M/s. Sigma Aldrich and were further distilled prior to their use. Analytical grade pure (99%) potassium tetrafluoroborate, sodium thiocyanide, sodium nitrate salts were used as purchased. Pyridine was obtained from M/s. Spectrochem and was distilled prior to its use. *N*-ethylmaleimide and anthracene-9-carbinol were purchased from M/s. Sigma Aldrich and was used as obtained. All the experiments were conducted using deionized water. The ionic liquids which have been used during the analysis were synthesized in our laboratory following standard reported procedures.[12, 36] The ionic liquids were synthesized following the two steps: The first step was the quaternization, which had involved the synthesis of organic cation and the second step was metathesis, where the desired anion replaces the existing one by using corresponding salt. The purity of the ionic liquids was characterized by ^{1}H-NMR spectroscopy. The ionic liquids were dried under high vacuum for at least 6 h prior to their use in reactions in order to remove excess water as well as undesired solvents. To ensure the dryness and purity, the water content of the ionic liquids was measured before making solution for reactions by a Karl Fischer coulometer which did not exceed 30 ppm for any case.

5.2.2 Kinetic Measurements

A 0.044 g of anthracene -9-carbinol **1** was dissolved in 10 mL of methanol prior to its use to give a 0.021 M stock solution. A 0.140 g of *N*-ethyl maleimide **2** was dissolved

in 10 mL of methanol to yield a 0.112 M stock solution of the reactant **2**. Methanol was used for solubilizing the reactants in turn preparing a homogeneous solution. Otherwise, anthracene-9-carbinol will remain suspended on the surface water-ionic liquid solvent medium. The reaction was monitored by UV-visible spectrophotometer. During each experiment 100 μL out of stock solution of **1** and **2** were introduced into two independent round bottom flasks each containing 0.5 mL of the binary mixture of ionic liquids in water. Methanol, which was present in very small quantity (100 μL) of each reactant dissolved in 0.5 mL of aqueous ionic liquid solution) is removed under reduced pressure at 308K. After thermal equilibration of the solution at 298K, the mixture of **2** in ionic liquid-water solution is taken into a UV-cuvette (3ml). The reaction is initiated by introducing the solution of **1**. The progress of the reaction was monitored by noting the decay in the absorbance peak of anthracene-9-carbinol at λ_{max} = 330 nm, which has the direct correlation with left over concentration of **1** with the progress of the reaction. The decay in the absorbance was used to calculate the *pseudo*-first-order rate constants, k_0. The reported rate constants here in this work are an average of at least three kinetic runs on different samples and were reproducible to within (± 5%). The temperature of the cell was controlled by using the single cell Peltier accessory having an accuracy of (± 0.01^{o}C).

The surface pressure, which is a difference of the net downward forces on the Whilmay plate experienced in contact with pure water and aqueous -ionic liquid solutions was measured at 298.15 K with KSV NIMA Langmuir Trough instrument for each molal solution of the aqueous- ionic liquid mixtures The surface pressure was determined by partially dipping the Whilmay plate into the aqueous- ionic liquid solutions. During the measurement the area of the Whilmay Plate was calibrated with 156.2 cm^2. The accuracy of the measurements remains within ± 0.2 mN/m.

5.3 Results and Discussion:

5.3.1 Addition of Ionic Liquids in the Reaction Media

5.3.1.1 Effect of Substituted Alkyl Groups Attached to Cation of the Ionic Liquids

With the addition of ionic liquids with increasing alkyl chain length adhered to the imidazolium moiety in the reaction between anthracene-9-carbinol **1** and *N*-ethylmaleimide (**2**) (Scheme 1), the pairwise interactions values acquire progressive negative values (*c. f.* Table 4 in the discussions section). It implies that the rate of the

reaction decreases with ionic liquids having higher alkyl chain length in their cations compared to that of lower one. If we scrutinize the graph (Figure 2), it can be noted that at very low concentrations (≤ 0.04 m) of the ionic liquids i.e. [Bmim]Br, [Hmim]Br and [Omim]Br the effect of the alkyl groups does not show visible distinction in the rate constant values. But at the higher concentration the ionic liquids, rate decreasing effect is prominent (Figure 2) with increase in alkyl chain length. The viscosity may have detrimental effect as the alkyl chain length is increasing[34]. But in our reaction medium the concentration of ionic liquids used remain extremely small (maximum 0.1 M only), therefore the possibility of alteration in viscosity cannot modify the reaction rates can be obviated. On the other hand the addition of alkyl groups in the chain contributes to the hydrophobicity of the corresponding ionic liquids, keeping all other effects unaltered.

One of the reasons for the decrease in the rate constants can be thought as destabilization of the transition state compared to initial state of the reactants. The transition state of the Diels Alder reaction possesses somewhat polar in nature compared to complete non-polar [35].

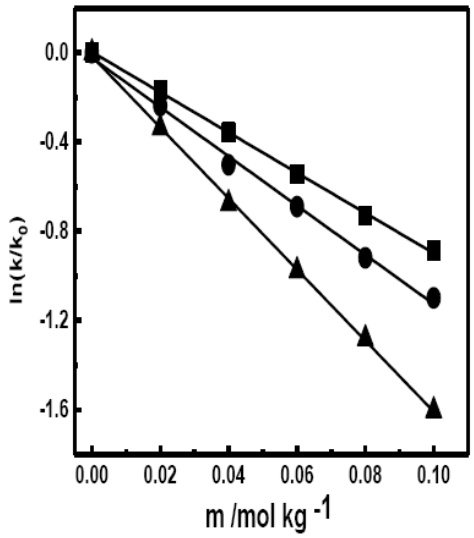

Figure 2: A comparative plot showing the ln (k/k_0) variation with molality of ionic liquids having variation in alkyl chain length at imidazolium cations i.e. [■] [Bmim]Br; [●] [Hmim]Br; [▲] [Omim]Br.

The rationale behind the drop in the rate constants with increasing chain length in the ionic liquid cations is that the alkyl groups in the cationic part interacts more with the initial state of the reactants which are apolar in nature compared to the

transition state of the reaction as the cations with higher alkyl chain lengths posses more hydrophobicity[36].

5.3.1.2 Influence of Anions of the Ionic Liquids in Deciding Pairwise Interactions

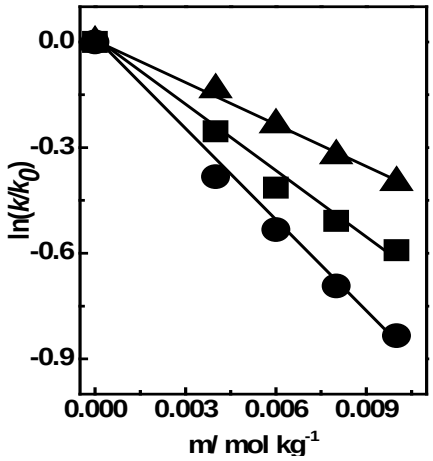

Figure 3: The concentration dependence of $\ln(k/k_0)$ data for [■] [Bmim]Br, [●] [Bmim]I , [▲] [Bmim]Cl , [▼][Bmim][CH_3COO], [♦][Bmim][BF_4], [◄] [Bmim][NO_3], [►] [Bmim][SCN]

From Figure 3, it is clear that the linearity of the $\ln[k(m_c)/k(m_{c=0})]$ vs. molality of the co-solvent which is the essential criteria for determining the pair wise interactions is not retained for [Bmim][SCN], [Bmim]I and [Bmim][NO_3]. During this set of experiments, varied the anions have been varied keeping pace with the Hofmeister series keeping the cation [Bmim] constant.

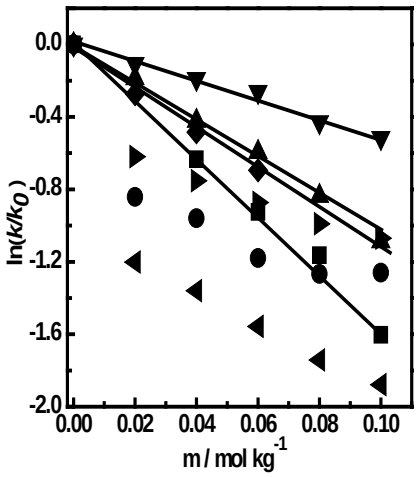

Figure 4: The $\ln(k/k_0)$ plotted against the concentrations for [■] [Bmim]I, [●] [Bmim][NO_3], [▲] [Bmim][SCN] at very low concentration region of these ionic liquids.

The effect seen in these observations is that though the anions follow a specific relationship in terms of their surface tensions if associated with alkali cations viz. Na^+, K^+ etc. but their association with organic cation to produce ionic liquid observes no clear relationship with the Hofmeister series.[37] Again present studies suggests that the kind of associations with the reactants and the transition state vary from one ionic liquid to another depend solely the nature of the anions associated with the same cation.

In order to get the quantitative idea about the range of the aforesaid ionic-liquids, the reaction have been performed (Scheme **1**) at lower molal range (not more than m = 0.015) of [Bmim]I, [Bmim][NO_3], [Bmim][SCN]. At lower value of the concentrations, these ionic liquids (Figure 4) show that the $\ln\left[\frac{k_{m_c}}{k_{m_{c=0}}}\right]$ vs. molality plots trail linearity. But from the previous graph (Figure 3), parabolic variation of the points clarifies the fact that these three ionic liquids adopt bulk interactions along with the pair wise interactions. [38, 17]

Tabular form of the data of the G_c values (Table 2) of various ionic liquids proclaim the fact that with increase in the polarity of the water by the addition of ionic liquids with higher polarity the reactivity of the ionic liquid–water system decreases very sharply. Though the nature of the transition state of the Diels-Alder reaction assumes somewhat polar but hydrophobicity plays the principal role in occurrence of such type of the reactions[2, 3] which decreases with the addition of the more polar ionic liquids in water as co-solvent. It is notable that for the ionic liquids having highly polarizable surface area do not act as supporting surface for the semi polar transition state of the reaction also. means this short range one to one interaction occurring between the groups of the ionic liquids and the corresponding group presents in the substance mainly apolar in nature i.e. the presence of the polar groups in the ionic liquids and that of in the substance do not contribute too much to overshadow the interactions among apolar moieties.

5.3.1.3 Effect of Aromatic Ring Based Cation of Ionic Liquid

In these set of experiments, we have focused on the influence of the planer aromatic cation based ionic liquid in comparison to their nonaromatic and non-planer counterparts. Here, imidazolium based ionic liquid has been chosen as aromatic one and the pyrrolidinium based ionic liquid as the non aromatic one.

Delocalization of electron in cation has very small effect on the cation – anion interactions of the ionic liquids but the difference in bond orders of imidazolium and pyrrolidinium based ionic liquids as well as the steric hindrance manipulate the thermodynamic interactions with surrounding.[39]

Table 2: The G_c values calculated for the [Bmim] based ionic liquids with different anions

Ionic liquids	**G_c (kJ mol^{-1})**
[Bmim]Ac	-6.00
[Bmim]Cl	-13.35
[Bmim]BF_4	-14.19
[Bmim]Br	-19.74
[Bmim]NO_3	-72.62
[Bmim]I	-74.86
[Bmim]SCN	-83.14

Table 3: The G_c values of interactions due to the presence of aromatic and non-aromatic ionic liquids during the reaction between **1** and **2**

Ionic liquids	**G_c (kJ mol^{-1})**
[Bpyrr]Br	-11.748
[Bmim]Br	-19.176

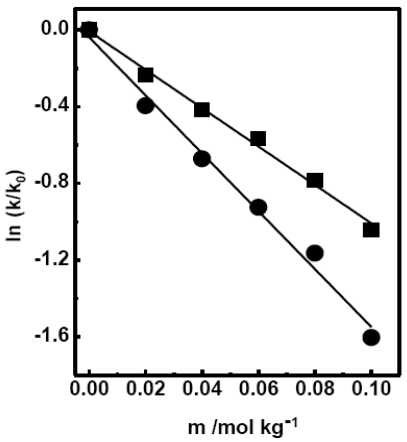

Figure 5: The comparative rate plots for ionic liquids [■] [Bpyrr]Br, [●] [Bmim]Br.

The comparison of the graph (Figure 5) and the G_c values (Table 3) for [Bmim]Br and [Bpyrr]Br justifies our view of the nature of the pairwise interactions. As nonaromatic ionic liquids are less polarizable than aromatic ionic liquids, [Bpyrr]Br interacts more strongly with apolar reactants than their corresponding transition state.[40]

As well as, the hydrophobicity of the water–ionic liquid system decreases here with introduction of the less polarizable non- aromatic ionic liquid.

5.3.1.4 Consequence of Replacing Aprotic Ionic Liquid with Protic One

Result obtained (Figure 6) from the comparison of the protic and aprotic ionic liquids stress on the fact that protic ionic liquids being more polar in comparison to their aprotic counterpart due to the presence of proton in the cation contribute more to decrease the reactivity of the water promoted Diels-Alder reactions.

As the protic ionic liquids possess more polarity in comparison to their aprotic counterpart due to the presence of proton in the cation, they contribute more to decrease the reactivity of the water promoted Diels-Alder reactions.

If one is curious to follow the effect of these two types of ionic liquids, the graphical plot (Figure 6) of the data results in a parabolic nature at near 0.02 molal of the protic ionic liquid. On the other hand, the pairwise interaction prevails up to 0.10 molal concentration of its aprotic counterpart. From the equation **7** it is clear that the introduction of the bulk interactions along with pairwise interactions contributes to the curvature of the graphical plot for the protic ionic liquids.

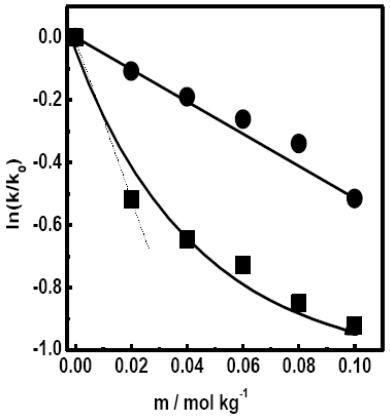

Figure 6: The graph showing the dependence of ln (k/k_0) on the variation in concentration for [■] [H-mim] Ac (Protic ionic liquid); [●][Bmim] Ac (Aprotic ionic liquid). The dotted line is to help the reader to note the nature of straight line for calculating pairwise interactions.

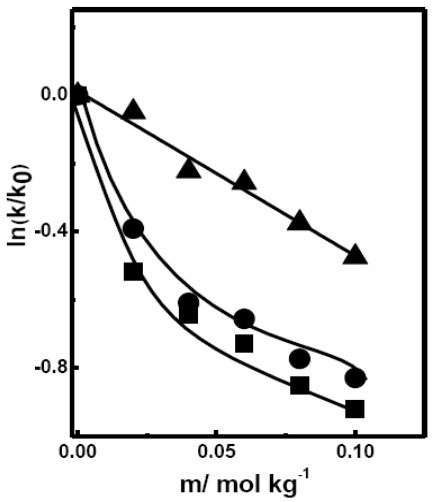

Figure 7: The comparative rate plot for protic ionic liquids viz. [▲][H-py][CH_3COO], [●][H-mim] [CH_3COO] ,[■][H-bpyrr] [CH_3COO]

From the above graphical plot (Figure 6), it is obvious that the presence of acidic proton at the cation helps in suppressing the rate constants of the water promoted reactions. Assessing the strength of the molecular interactions among the protic ionic liquids with varying properties is the present interest.

[H-mim][CH_3COO], [H-bpyrr][CH_3COO] and [H-py][CH_3COO] ionic liquids have been chosen for comparison, which varied from each other in terms of aromaticity and the size of the ring in the cations. The graph regarding the kinetic analysis with several protic ionic liquids in Figure 7 emphasizes that [H-py][CH_3COO]is less interacting with the reacting substrates in the reaction between anthracene-9-carbinol **1** and *N*-ethyl maleimide **2** than other two protic ionic liquids i.e. [H-mim][CH_3COO], [H-bpyrr][CH_3COO] due to stable aromatic structure of the pyridine. The one to one interaction prevails for a sufficient range of the molality of [H-py][CH_3COO] (Figure7). To validate the presence pairwise interaction with the introduction of the ionic liquids we have carried out temperature dependent study upon varying the molality of the [Bmim]Br ionic liquid.

5.3.1.5 Mixture of Ionic Liquids as Co-solvent

To determine whether there is more potentiality in ionic liquids, we repeated the reaction with a variety of ionic liquids. By keeping cationic part fixed, anion has been varied from Br^- to $[BF_4]^-$. The G_c value implies that these water/ionic-liquid mixtures under highly dilute conditions remain as normal non-interacting mixtures. However,

when the cation is changed and the anion is fixed, the mixture appears to possess additional interactions and this is reflected by the G_c value of 16.09 kJ mol^{-1}.

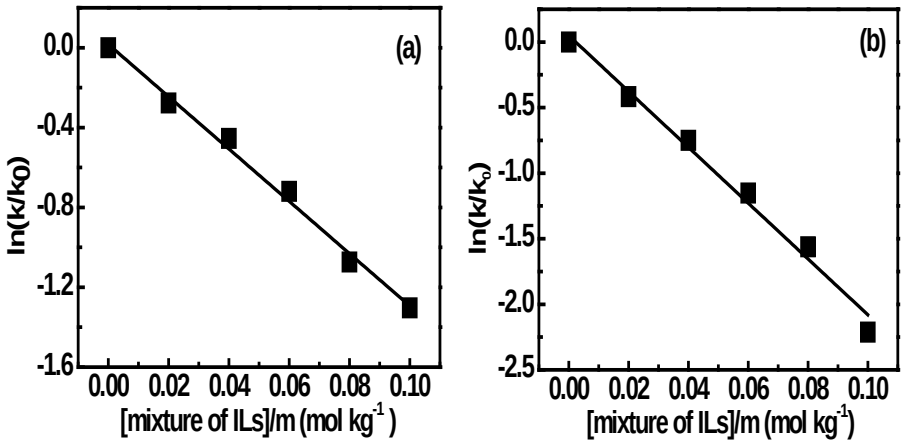

Figure10: The dependence of ln(k/k_0) on the molaities of the mixtures of ionic liquids (1:1 w/w) : (a) mixture of [Bmim]Br and [Bmim][BF_4] and (b) [Bmim]Br and [BMpyrr]Br.

It was shown that water formed hydrogen bonds with the anions in the ionic liquid mixture when the cation was kept unchanged (Figure 10).[36] Although there is no direct evidence of the use of a dilute water/ionic-liquid mixtures, we varied the cation of the ionic liquid (G_c= 24.31 kJ mol^{-1}) and our results can be correlated with recent findings, showing that the rate of hydrolysis becomes faster as a result of decreased hydrogen bonding in the water/ionic liquid mixture.

5.3.1.6 Temperature Dependent Study

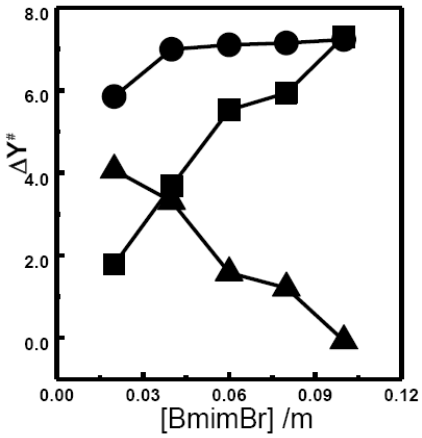

Figure 11: A plot showing the excess thermodynamic properties of the water and [Bmim]Br mixture. Where, $\Delta Y^{\#}$ refers to [●] $\Delta^{\#}$ G i.e excess molal Gibbs energy, [▲] $-T\Delta^{\#}S$ i.e. excess molal entropy and [■] $\Delta^{\#}H$ i.e. excess molal enthalpy.

By simply dividing the Gibbs potential with respect to temperature, one can obtain pairwise enthalpy and entropy. These values will provide deeper insights into the solvent – solute interactions. The graph (Figure 11) of thermodynamic activation parameters with respect to the molality of added [Bmim]Br reveals the fact that with the increase in the molal concentration of the ionic liquid ($-T\Delta S$) decrease whereas enthalpy of the system increases. It means the system tends to more endothermicity.

5.4 Discussions:

The peculiar trend in the activation parameters on molality attracts our attention to the molecular arrangement of ionic liquids around the apolar reactants and the activated complex.

Table 4: The G_c values for different ionic liquids with varying alkyl chain length with imidazolium cation

Ionic liquids	**G_c (kJ mol^{-1})**
[Omim]Br	-19.74
[Hmim]Br	-13.22
[Bmim]Br	-9.89

Table 5: Surface pressure data for [Bmim] cation based ionic liquids:

Ionic Liquids	**m (mol kg^{-1})**	**Surface Pressure with [a] (mN/m) ± 0.2**
[Bmim][SCN]	0.02	49.4
	0.1	42.9
[Bmim]I	0.02	49.1
	0.1	47.4
[Bmim]Br	0.02	45.1
	0.1	39.4
[Bmim][NO_3]	0.02	50.5
	0.10	47.2
[Bmim]Cl	0.02	53.3
	0.1	47.5
[Bmim][CH_3COO]	0.02	49.8
	0.1	40.6

[a] surface area of the LB tray was 1.594 x 10^{-2} m^2.

Ionic liquids composed of purely ions have both ionic and non-ionic roles to play in the reaction medium. The values in Table 4 emphasize that with added hydrophobicity in cation, van der Waals interactions predominate over the ionic interactions of the ionic liquids after certain concentration of the ionic liquids. If we consider the change in the structure of imidazolium cation based ionic liquids moving from butyl to hexyl and then to octyl, we find that in each case [CH_3-CH_2] group adds with their immediate precursor. From Table 4, the change in the G_c values do not follow a regular trend.

With the addition of the [CH_3-CH_2] to [Hmim]Br ionic liquid for making [Omim]Br ionic liquid, the change in the pairwise interaction value becomes almost double i.e. - 6.52 kJ mol^{-1} in comparison to that of - 3.33 kJ mol^{-1} noted while going from [Bmim]Br to [Hmim]Br. It implies that the addition of the alkyl group to the ionic liquid cation not only increase the van der Waals interactions but also the spatial arrangement of the alkyl groups control the degree of the interactions with the reactants and transition state during the reaction. For this reason the separation of the cumulative pairwise interactions into group contribution is not effortless exercise. The change in the surface pressure data (Table 5) with respect to the concentration of each ionic liquid follows an order in their magnitudes. [41] The data represented in Table 5 are the surface pressures of the ionic liquid-water mixtures. This suggests that the surface pressure decreases as the molality of the ionic liquid increases in water. This also suggests that on increasing the molality of the ionic liquid, the ionic liquid will remain more and more at the surface under our condition of experiments. But a correlation of the G_c values tabulated in the Table 5 with the corresponding series of surface tension data of ionic liquids in the order of Hofmeister series does not find any trend in the values of the pairwise interactions. It reveals the fact that pairwise interaction does not solely depend on the molecular arrangement of the surface of the solvent and co-solvent residing around the reaction solutes. A change in the bonding and nature of the surface of the ionic-liquids contribute significantly towards the pairwise interactions. A closer look on the Pairwise interaction values of [Bpyrr] Br and [Bmim] Br supports our view in the way that introduction of electron delocalization as well as planarity towards the ionic liquids in the ring of cation have noteworthy effect to facilitate the reaction dynamics. As previously from the experiment with ionic liquids having varying alkyl chain length we have concluded that the spatial arrangement of the ionic liquids is also a governing factor to calculate

the pairwise interactions. However, the planarity of the ionic liquids as well as their polarizability significantly suppress the reaction rate though both [Bpyrr]Br and [Bmim]Br have the cation with five member carbon rings. Polarity of the co-solvents appears to be the main guiding property to characterize the solubility of the reactants and the activated complexes. Protic ionic liquids at the same concentration with aprotic ionic liquids adopt complex forms of pairwise interactions whereas $\ln\left[\frac{k_{m_c}}{k_{m_{c=0}}}\right]$ vs. molality trend for aprotic ionic liquids follow clear straight line (Figure 6). As the anions for the both protic and aprotic ionic liquids are the same in our case, it can be concluded from the graph (Figure 6) that the higher order interactions at very low molality of the protic ionic liquids emerge from their structure and bonding in the cationic part of the ionic liquids. [42]

To know the role of the cation of the protic ionic liquid in guiding the interactions during reactions efforts have been made to find out an explanation by carrying out experiments with protic ionic liquids having varying spatial and configurational arrangement. It is known that a six membered ring is highly stable than its five member counterpart. A cursory view of the nature of the comparative data points in Figure 7 represents us an insight into the origin of higher order interactions with five membered cation based-protic ionic liquids in comparison to their six membered counterparts.

The π-electrons in the pyridinium cation follow a more stable electron cloud on the six- membered ring than in comparison to imidazolium based protic ionic liquid which have five-member ring. [39,43] Consequently in comparison to imidazolium based protic ionic liquid pyridinium based ionic liquid imparts less amount of catalytic interaction to change the reaction co-ordinate. It clears the fact that if the constituent cation or anion is energetically stabilized by itself due to impartial distribution of electrons throughout the structure then it has little tendency to interact with another molecule. It is well established spectroscopically and theoretically that ionic liquids remain as ion-pairs in very dilute solution and impart effect more like apolar moiety rather than dissociation into constituent ions like normal salts viz. NaCl, $MgSO_4$ etc. [44]

Our experiment of enthalpy and entropy compensation (Figure 11) guides us to visualize the arrangement of ionic liquids and reformation in bonding environment around the reactants during the reaction. This compensation can be directly analyzed

by the arrangement of water molecules around apolar solutes during hydrophobic hydration. The solvation of reactants in dilute solution of ionic liquids must follow two steps as in the case of dissolution of apolar groups in water. Firstly, the creation of cavity in the solvent going against the cohesive energy density of the solvent to accommodate the incoming solute molecule, which is followed by the reorganization of the bonding arrangement among the solute and solvent to stabilize the solute. In connection to hydrophobic hydration, Lee emphasized on the reorganization of the hydrogen bonds contribute mostly towards the entropy enthalpy contribution[45]. A scrutiny to our data suggests that with an increase in the molality of ionic liquid in water, the entropy decreases and the enthalpy increases and this enthalpy contributes more towards the activation free energy. Here the value of activation enthalpy moves towards more endothermic while the activation entropy moves towards more positive values with increase in the molality of the ionic liquids in water. From the behavior of the entropy it is clear that in our system one of the constituents is achieving higher degree of freedom as a consequence of the breaking of bonds as indicated by the endothermic nature of the activation enthalpy values with the addition of more ionic liquid in the reaction system.

Our result can be supported by the finding of Janado et al that the spontaneous transfer of apolar molecules likes biphenyl from water to sugar solution when sugar is added as co-solvent to the solution.[45c] This is also supported by the endothermic nature of the enthalpy. [45c] It is discussed that ionic liquid behave like as apolar moiety in its dilute solution. Therefore upon increasing the molality of the ionic liquid in the reaction medium, more apolar environment was introduced in the reaction medium. The decrease in the rate constants with introduction of ionic liquid in water implies the stabilization of reactants in ionic liquid throughout this investigation. This enthalpy- entropy compensation is the direct consequence of the transfer of the reactants from water by breaking hydrophobic arrangement from to apolar ionic liquid co-solvents. Following Lee[45] and other authors[43], the compensation behaviour cannot be fully described as the consequence of the rearrangement of H-bonding as ionic liquids do posses hydrogen bonding but the same is not too extensive to contribute fully towards compensation. Again it can be safely attributed that the size of ionic liquids disfavors the easy reorientation of ionic liquids around the solute molecule as like water do in case of hydrophobic hydration.

5.5 Conclusions:

Finally, through this paper that a simplistic attempt to calculate one to one molecular interactions between an ionic liquid has been presented and the substrates during the reaction progress. Though in all cases the reactions undergo through slower pathway than without presence of the ionic liquid co-solvent, the use in minute amount will multiply the width of the solubility window of water. A wide variety of ionic liquids here have been exercised as co-solvents during carbon - carbon bond formation reaction. Here from above analysis, it is clear that the high viscosity and long range interactions between cation and anions of the ionic liquids determine the interaction strategy among ionic liquids and the organic reactants. These comparative studies will help the researchers to tailor ionic liquids specific for specific reactions. The use of ionic liquid as the co-solvent in water-driven reactions will encourage the researchers to go for replacing conventional volatile organic solvents during complex organic synthesis. Further a systematic investigation including both long and short range interactions offered by ionic liquids during reactions will lead to better appreciation of structure-activity relationships.

5.6 References:

1. (a) Franks, F. Water. *A Comprehensive Treatise*; Franks, F. (ed.); Plenum; New York Vol.1, Chapter 1, **1979**.; (b) Anastas, P.; Warner, J. ed. *Green Chemistry: Theory and Practice*, Oxford University Press, New York, **1998**.

2. (a) Narayan, S.; Muldoon, J.; Finn, M. G.; Fokin, V. V.; Kolb, H. C.; Sharpless, K. B. *Angew. Chem., Int. Ed.* **2005,** *44***,** 3275**.** (b) Klijn, E.; Engberts, J. B. F. N. *Nature* **2005**, *435*, 746.

3. (a) Acevedo, O.; Armacost, K. *J. Am. Chem. Soc.* **2010**, *132*, 1966. (b) Tiwari, S.; Kumar, A. *J. Phys. Chem. A* **2009**, *113*, 13685. (b) Jung, Y.; Marcus, R. A. *J. Am. Chem. Soc.* **2007**, *129*, 5492.

4. For reviews, see: (a) Butler, R. N.; Coyne, A. G. *Chem. Rev.* **2010**,*110*, 6302. (b) Chanda, A.; Fokin, V. V. *Chem. Rev.* **2009**, *109*, 725.

5. (a) Pirrung, M. C.; Sarma, K. D.; Wang, J. *J. Org. Chem.* **2008**, *73*, 8723. (b) Pirrung, M. C.; Sarma, K. D. *Tetrahedron* **2005**, *61*, 11456. (c) Pirrung, M. C.; Sarma, K. D. *J. Am. Chem. Soc.* **2004**, *126*, 444.

6. (a) Cozzi, P. G.; Benfatti, F.; Zoli, L. *Angew. Chem., Int. Ed.*, **2009**, *48*, 1313. (b) Cozzi, P. G. ; Zoli, L. *Angew. Chem., Int. Ed.*, **2008**, *47*, 4162.

7. Rideout, D. C.; Breslow, R. *J. Am. Chem. Soc.*, **1980**, *102*, 7816-7817.

8. (a) Grieco, P. A.; Ferrino, S.; G. Vidari, Total Synthesis of dl-Quassin. *J. Am. Chem. Soc.*, **1980**, *102*, 7586-7587. (b) Vidari, G.; Ferrino, S.; Grieco, P. A. Quassinoids: Total Synthesis of dl-Quassin. *J. Am. Chem. Soc.*,**1984**, *106*, 3539. (c) Grieco, P. A. *Organic Synthesis in Water*, Ed. Blackie Academic & Professional, London, **1998**.

9. (a) Blake J. F.; Jorgensen, W. L. *J. Am. Chem. Soc.*, **1991**, *113***,** 7430. (b) Blake, J. F.; Lim D.; Jorgensen, W. L. *J. Org. Chem.***, 1994**, *59***,** 803.; (c) G. K. Van der Wel, J. W. Wijnen and J. B. F. N. Engberts, *J. Org. Chem.*, **1996**, *61*, 9001.; (d) Manna, A.; Kumar, A. *J. Phys. Chem. A*, 2013, **117**, 2446.

10. (a) Breslow, R.; Guo, T. *J. Am. Chem. Soc.*, **1988**, *110*, 5613. (b) Muller, N. *Acc. Chem. Res.* **1990**, *23*, 23. (c) Wijnen, J. W.; Engberts, J. B. F. N. Retro-Diels-Alder *J. Org. Chem.* **1997**, *62*, 2039. (d) Pindur, U.; Lutz, G.; Otto, C. *Chem. Rev.*, **1999**, *93*, 741. (e) Nagayama, S.; Kobayashi, S. A. *J. Am. Chem. Soc.*, **2000**, *122*, 11531. (f) Hayashi, T.; Inoue, K.; Taniguchi, N.; Ogasawara, M. *J. Am. Chem. Soc.*, **2001**, *123*, 9918. (g) Kumar, A. *Chem. Rev.* **2001**, *101*, 1. (h) Li, C-J. *Chem. Rev.*, **2005**, *105*, 3095.

11. (a) Blandamer, M. J.; Burgess, J.; Engberts, J.B.F.N. *Chem. Soc. Rev.*, **1986**, *14*, 237. (b) Engberts, J.B.F.N. *Water, A Comprehensive Treatise*, Franks, F. (ed.), Plenum; New York; Vol.6, Chapter 4 , **1979**.

12. (a) Blokzijl, W.; Engberts, J. B. F. N.; Blandamer, M. J. *J. Am. Chem. Soc.*, **1991**, *113*, 4241.

13. (a) Welton, T.; Wasserscheid, P. *Ionic Liquids in Synthesis*, VCH-Wiley, Weinheim, **2007**. ; Plechkova, N. V.; Seddon, K. R. *Chem. Soc. Rev.*, **2008**, *37*,123. (b) Chauvin, Y. Olefin Metathesis: The Early Days (Nobel Lecture) *Angew. Chem., Int. Ed.*, **2006**, *45*, 3740.

14. (a) Urahata, S. M.; Riberiro, M. C. C. *J. Chem. Phys.*, **2004**, *120*, 1855.(b) Hardacre, C.; Holbrey, J. D.; McMath, S. E. J.; Bowron, D. T.; Soper, A. K. *J. Chem. Phys.*, **2003**, *118*, 273.

15. (a) Poliakoff, M.; Fitzpatrick, J. M.; Farren, T. R.; Anastas, P. T. *Science*, **2002**, *297*, 807.(b) Seddon, K. R.; Stark, A. ; Torres, M.-J. *Pure Appl. Chem.*, **2000**, *72*, 2275.

16. French, H.T. *J. Chem. Thermo.*, **1989**, *21*, 801.

17. Goldammer, E.V.; Hertz, H.G. *J. Phys. Chem.*, **1970**, *74*, 3734.

18. Bowers, K. J.; Dror, R. O.; Shaw, D. E., *J. Chem. Phys.*,**2006**, *124*, 184109.

19. (a) Blandamer, M. J.; Burgess, J.; Engberts, J. B. F. N. *Chem. Soc. Rev.*, 1985, **14**, 237. (b) Burma, N. J.; Pastorello, L.; Blandamer, M. J.; Engberts, J. B. F. N. *J. Am. Chem. Soc.*, **2001**, *123*, 11848. (c) Burma, N. J. *Ph.D. Thesis*, University of Groningen, The Netherlands, **2003**.

20. (a) Savage, J. J.; Wood, R. H. *J. Solution Chem.*, **1976**, *5*, 733. (b) Bowers, K. J.; Dror, R. O.; Shaw, D. E. *J. Comput. Phys.*, **2007**, *221*, 303. (c) Dongarra, J. J.; Du Croz , J.; Hammarling, S.; Duff, I. S. *ACM Trans. Math. Soft.*,**1990**, *16*, 1. (d) Duan, Y.; Kollman, P. A. *Science*, **1998**, *282*, 740.

21. (a) Dill, K.A. *Science*, 1990, **250**, 297.; (a) Wood, R. H.; Thompson, P.T. *Proc. Natl. Aca. Sci.* **1990**, *87*, 946.

22. Koppel, I. A.; Palm, V.A. in *Advances in Free Energy Relationships*; Chapman, N.B.; Shorter-, J. (eds.), Plenum, New York, Chapter 2, **1972**.

23. Glasstone, S.; Laidler K. J.; Eyring, H. in *The Theory of Rate Processes*, McGraw-Hill, New York, **1941**.

24. (a) Friedman, H. L.; Ramanathan, P. S. *J. Phys. Chem.***1970**, *74*, 3756.; (b) Ramanathan, P. S.; Friedman, H. L. *J. Chem. Phys.***1971**, *54*, 1086.; (c) Ramanathan,P. S.; Krishnan, C. V. ; Friedman, H. L. *J. Solution Chem.***1972**, *1*,237.; (d) Gurney, R. W. in *Ionic Processes in Solution*, McGraw-Hill: New York, **1953**.

25. (a) Harris, A. L.; Thompson, P. T., Wood, R. H. *J. Solution Chem.* **1980**, *9***,** 305. (b) Kent, H. E.; Lilley, T. H.; Milburn, P. J. M. Bloemendal and G. Somsen, *J. Solution Chem.*, **1985**, *14***,** 101.; (c) Suri, S**.** K.; Wood, R. H. *J. Solution Chem.*, **1986**, *15***,** 705. (d) Wu, J. Z.; Prausnitz, J. M. *Proc. Natl. Acad. Sci. USA*, **2008**, *105*, 9512.

26. Garrod, J. E.; Harrington, T.M. *J. Phys. Chem.*, **1969**, *73*, 1877.

27. (a) Garrod , J. E.; Herrington, T. M. *J. Chem. Educ.*, 1969, **46,** 165. (b) Graziano, G. *J. Chem. Soc., Faraday Trans.*, **1998**, *94*, 3345.

28. McMillan, W. G.; Mayer, J. E. *J. Chem. Phys.*, **1945**, *13*, 276.

29. Kirkwood, J. G.; Buff, F.P. *J. Chem. Phys.* **1951**, *19*,774.

30. Newman, K. E. *J. Chem. Soc. Faraday Trans.1*., **1988**, *84*, 1387 - 1391.

31. (a) Ben-Naim, A. *J. Chem. Phys.* **1977**, *67***,** 4884.;(b) Ben-Naim, A. *Cell. Biophys.* **1988**, *12*, 255.

32. Cassel, R. B.; Wood, R. H. *J. Phys. Chem.***1974**, *78*, 2460.

33. (a) Huddleston, J. G.; Visser, A. E.; Reichert, W. M.; Willauer, H. D.; Broker, G. A.; Rogers, R. D. *Green Chemistry*, **2001**, *3*, 156.;

34. (a) Tiwari, S.; Kumar, A. *Angew. Chem., Int. Ed.* **2006**, *45*, 4824.; (b) Roland, C. M.; Bair, S.; Casalini, R. *J. Chem. Phys.*, **2006**, *125*, 124508-1.

35. (a) Sauer, J.; Sustmann, R. *Angew.Chem; Int. Ed. Eng***, 1980**, *19***,** 779.; (b) Jung, M. E.; Gervay, J. *J. Am. Chem. Soc.*, **1991**, *113*, 224.

36. (a) Pratt, L. R.; Chandler, D. C. *J. Chem. Phys.*, **1977**, *67*, 3683. (b) Choudhury, N. *J. Chem. Phys.*, **2009**, *131*, 014507-1.

37. (a) Kropman, M. F.; Bakker, H.J. *J. Chem. Phys.*, **2001**, *115*, 8942.(a) Gurau, M. C.; Lim, S. M.; Castellana, E. T.; Albertorio, F.; Kataoka S.; Cremer, P. S. *J. Am. Chem. Soc.*, **2004**, *126*, 10522.

38. Kozak, J. J.; Knight, W. S.; Kauzmann, W. *J. Chem. Phys.* **1968**, *48*, 675.

39. (a) Khupse N. D.; Kumar, A. *J. Phys. Chem. B,* **2011**, *115*, 10211.; (a) Shimizu, Y.; Ohte, Y.; Yamamura, Y.; Tsuzuki, S.; Saito, K. *J. Phys. Chem. B,* **2012**, *116*, 5406.

40. Mandal, P. K.; Samanta, A. *J. Phys. Chem. B,* **2005**, *109*, 15172.

41. (a) Freire, M. G.; Carvalho, P. J.; Fernandes, A. M.; Marrucho, I. M.; Queimada, A. J.; Coutinho, J. A. P. *J. Colloid Interface Sci.,* **2007**, *314*, 621.; (b) Torrecilla, J. S.; Rafione, T.; Garcia, J.; Rodrı´guez, F. *J. Chem. Eng. Data.*, **2008**, *53*, 923.; (c) Bresme, F.; Chacón, E.; Tarazona, P.; Wynveen, A. *J. Chem. Phys.*, **2012**, *137*, 114706-1.

42. (a) Carmichael, A. J.; Seddon, K. R. *J. Phys. Org. Chem.* **2000**, *13*, 591. (b) Anderson, J. L.; Ding, J.; Welton, T.; Armstrong, D. W. *J. Am. Chem. Soc.,* **2002**, *124*, 14247 (c) Reichardt, C. *Green Chem.***, 2005**, *7*, 339.

43. (a) Duan, Z. Y.; Gu, Y. L.; Zhang, J.; Zhu, L. Y.; Deng, Y. Q. *J. Mol. Catal. A: Chem.*, **2006**, *250*, 163. (b) Raabe, G.; Köhler, J. *J. Chem. Phys.*, **2008**, *128*, 154509.; (c) Fernandes, A. M.; Rocha, M. A. A.; Freire, M. G.; Marrucho, I. M.; Coutinho, J. A. P. Santos, L. M. N. B. F. *J. Phys. Chem. B.* **2011**, *115*, 4033.

44. (a) Mele, A.; Tran, C. D.; Lacerda, S. H. D. *Angew. Chem., Int. Ed.*, **2003**, *42*, 4364.; (b) Triolo, A.; Russina, O.; Arrighi, V.; Juranyi, F.; Janssen, S.; Gordon, M. C. *J. Chem. Phys.*, **2003**, *119*, 8549.; (c) Zhang, L.; Xu, Z.; Wang, Y.; Li, H. *J. Phys. Chem. B.*, **2008**, *112*, 6411.; (d) Graziano, G. *Chem. Phys. Lett.* **2009**, *483*, 67.

45. (a) Lee, B. *J. Chem. Phys.*, **1985**, *83*, 2421.; (b) Lee, B. *Biopolymers*, **1985**, *24*, 813.; (c) Janado, M.; Yano, Y. *Bull. Chem. Soc. Jpn.***1985**, *58*, 1913.

Chapter 6

Excited State Intramolecular Proton Transfer Reactions in Protic Ionic Liquids

"The world of chemical reactions is like a stage, on which scene after scene is ceaselessly played. The actors on it are the elements." Clemens A. Winkler

The comprehension of hydrogen dynamics is of decisive significance in chemistry and molecular biology. Excited state intramolecular proton transfer (ESIPT) is in particular well suited to understand the role of transferring hydrogen due to its intramolecular character ESIPT can be investigated under well defined conditions and it can be directly initiated by absorption of photons from a laser pulse. Changes in the electronic transition/energy levels and consequent modulations in the ESIPT process of 1, 8-dihydroxy-9,10-anthraquinone (18DHAQ) dye in protic ionic liquids (PILs) were investigated using both steady-state (SS) and time-resolved (TR) fluorescence measurements. SS fluorescence studies show large modulation in the intensities for normal (N) and tautomeric (T*) emissions on changing the solvent viscosity. Interestingly, T* emission increases largely with solvent viscosity at the expense of N* emission, which seems apparently unusual, as the dye is photoexcited to N* first converts to T*. Observed results suggest that subsequent to initial ultrafast forward ESIPT, there is a relatively slower backward ESIPT process whose propensity decreases with solvent viscosity as it is guided by diffusive solvent relaxation of the PILs and the resulting differential stabilizations of N* and T* energies as their dipole moments are largely different. Evidence of both forward and backward ESIPT has been obtained from femtosecond fluorescence up-conversion studies. While forward ESIPT is evident in all the PILs studied, backward ESIPT is observed only in the lower viscosity PILs, where diffusive solvent relaxation is relatively faster. Qualitative PE diagrams have been presented to envisage the solvent relaxation guided ESIPT process for the studied dye.*

6.1 Introduction:

Transfer of proton from acid to base, one of the most basic reaction, draws considerable attention for its crucial role in many important processes spanning from chemistry to biology.[1] The present understanding of proton transfer reactions deeply rooted on the inferences drawn on the basis of a few time honoured achievements viz. Bronsted relation, Eigen mechanism, Westheimer's postulate, Swain-Schaad relations etc.[1e,1f] All these postulates are based on the comparative analysis of proton transfer rates in various solvents and known time scale associated to the solvents under study. Excited state intramolecular proton transfer (ESIPT) reactions have drawn enormous interests among researchers, since studies of ESIPT provide intrinsic view that how solvents directly response to PT reactions following dynamics from the perspective of reactants and products.[2-4] ESIPT attracts attention because this process has served as an alternate tool to get rid of the radiation less deactivation of many essential organic luminescent compounds viz. photo stabilizers,[1b] bio imaging and labelling,[1c] fluorescent molecular probes,[2c] ultraviolet stabilizers,[2d] proton as well as metal ion sensors and so forth.[1b] Representative compound that exhibit ESIPT, such as 3 flavones, 4 imidazoles,5 or imidazo[1,2-a]pyridines, hydroxyphenylbenzoxazoles etc. possess proton donating (PD) and proton accepting (PA) substituent in the same molecule and show large stokes's shift.[5] Essential criteria for most of cases to exhibit ESIPT is the presence of strong intramolecular hydrogen bond between C=O groups (or pyridinic nitrogen) and O-H groups (or N-H), in which involvement of $^1\pi\pi^*$ state during intrinsic proton transfer follows very low or barrier less activation energy pathway in nonpolar solvent.[5] ESIPT may continue for the period of low frequency, large amplitude vibrational motions associated with the pre-existing hydrogen bond, or coherently as proposed by Elsaesser, and in recent times by Tahara and co-workers.[6]

Following excitation of the chromophoric probe dye, the acid-base character of the PD and the PA groups commonly endures a turnaround , i.e. PD becomes PA and vice versa, causing the initially photoexcited normal (N*) form at higher energy than the conjugate excited tautomeric (T*) form and accordingly ESIPT process takes place along the preexisting hydrogen bond, converting N* to T*.[7-12] During most of the cases emission spectra from both N* and T* shows significant contributions in the observed emission spectra, it is hence possible to associate the shorter or lower

wavelength emission band (LWEB) as originated from the locally excited or normal excited form (N*) and the red shifted higher wavelength emission band (HWEB) with the product of the proton transfer i.e. excited tautotomeric form (T*).[8,9] Due to excited state charge transfer property, the equilibrated normal ground state (N) possess a significantly different dipole moment (magnitude and orientation of dipole) with respect to that of excited normal state (N*). Thus ESIPT is an energetically favorable process at the Frank-Condon excited N*, and rate of ESIPT process is competitive in comparison to the solvation relaxation process.[10] The relative intensities of HWEB and LWEB as well as the dynamics of ESIPT can be modulated upon varying the solvent parameters like polarity, viscosity, experimental temperature, and so forth.

In the present chapter, efforts have been made to present and discuss the results of the study on ESIPT process in room temperature protic ionic liquids (PILs) by using 1, 8-dihydroxy-9,10-anthraquinone (18DHAQ) dye as a chromophoric probe molecule. Our choice of quinines stems from their extensive prevalence in many forms in nature and their wide range of applicability in biology especially during energy conversion in living organism. Dihydroxy derivatives of anthraquinones draw interest among researchers for liquid crystal displays as well as the parent molecules for anthracycline antitumor drugs.[13] Even though intersystem crossing (ISC) has noticeable relevance to the overall photophysics of hydroxyanthraquinone, during our study we will neglect the involvement of ISC since timescales involved in singlet state proton transfer are well separated from those contributed due to ISC. The anthraquinone nucleus of 18DHAQ is suitable probe for investigating ESIPT, since prevalent intramolecular hydrogen bond between –OH group and C=O group in anthraquinone frame work leads to near planarity structure in the ring.[13-14] Steady state fluorescence of 18DHAQ exhibits dual emission. A number of experiments have been carried out to understand the spectroscopic properties as well as time resolved characteristics of the photochemical processes adhering to 18DHAQ. However, all these experimental studies mainly limited to involvement of organic solvents only. In the present work, we have engrossed ourselves to investigate the ESIPT process of 18DHAQ in room temperature protic ionic liquids (PILs). Although room temperature protic ionic liquids posses many similar properties like high viscosity, low vapor pressure, moderate polarity etc. which are common characteristics of room temperature ionic liquids (RTILs), presence of exchangeable proton in protic ionic liquids (PILs) makes a distinct class for PILs.[19] Since PILs are entirely composed of

cations and anions, these solvents can offer intrinsic conductivity with wide potential windows. Thus PILs can offer as suitable substitution to water for proton conduction in polymer-membrane based fuel cells or in Li-ion based battery.[20-21] Again solvation dynamics study in ionic liquids indicates wide distribution of solvation time scales. Simulation study of RTILs advocated that the fastest component of time dependent dynamics can be attributed to translational motions of ions in the vicinity of solute molecules. However, prevalence of strong Coulombic interactions among constituents of ionic liquids inhibits correct picture of electronic distribution of a solute in ionic liquids through theoretical approach (QM/MM).[19,20] Amid scenario, we have tried to delineate the femtosecond time resolved fluorescence dynamics of 18DHAQ in PILs in relation to kinetics as well as energetic course of ESIPT processes.

Our preliminary studies on 18DHAQ dyes in different ionic liquids ranging from aprotic to protic ones clarifies the fact that relative intensities of LWEB and HWEB do not show any perceptible alterations on varying the nature of aprotic ionic liquids. On the contrary, significant variations in the intensities of both the emission bands were found in protic ionic liquid solvents possessing differences in viscosities and polarities. Inspiring from our preliminary observations, we have carried out detailed investigations of ESIPT process of 18DHAQ in different PILs and PIL mixtures with the aim to comprehend the effect of both polarity and viscosity of PILs on kinetics and energetics of ESIPT process.

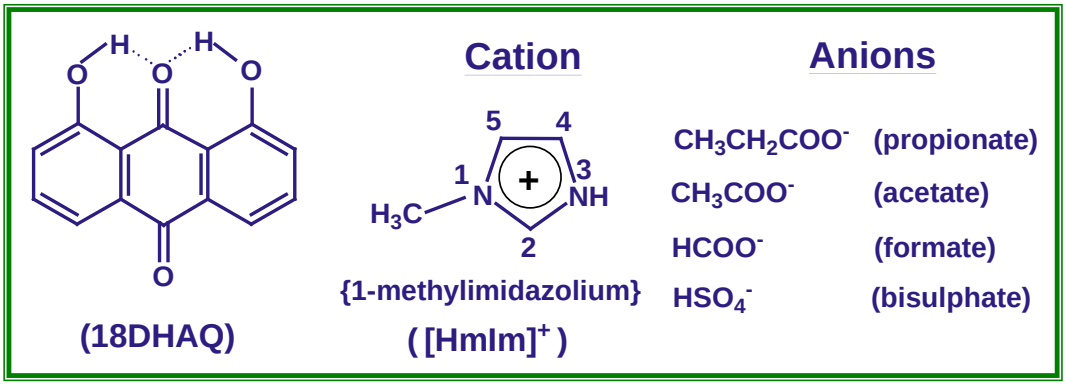

Scheme 1: Chemical structures of 18DHAQ dye and the PILs used in the present research work.

6.2 Experimental Section:

6.2.1 Compounds

18DHAQ dye had been obtained from Tokyo Kasei Kogyo (TCI), Japan. The dye was purified through repeated crystallization from cyclohexane.[22] Purity of the crystal

of 18DHAQ was established by comparing the absorption and emission fluorescence spectra of the dye in standard organic solvent.[23-26]

1-methylimidazole and acetic acid were purchased from M/s. Sigma Aldrich Co. 1-Methylimidazole was distilled under reduced pressure prior to use. Propionic acid, formic acid, sulphuric acid were procured from M/s. Merck Co. All the acids were of GR grade and used in the synthesis of PILs were purchased from the commercial form.

6.2.2 Synthesis of PILs

Following the single step atom economic reaction condition[21] the protic ionic liquids (PILs) were synthesized by adding equimolar quantities of the appropriate Bronsted acid in a drop wise fashion to the Bronsted base, 1-Methylimidazolium (HmIm), taken in a round bottom flask. During this addition, the round bottom flask containing the Bronsted base was placed in an ice bath. After addition of the acid to the base, the reaction mixture was stirred for 6 hrs vigorously. Thereafter the volatile impurities were removed from the product by using a rotary evaporator. Traces of water were removed by keeping the prepared PILs under high vacuum for 12 h. The PILs synthesized and used in this work are, [HmIm] propionate, [HmIm] acetate, [HmIm]formate, and [HmIm]bisulphate, where the abbreviation [HmIm] refers to the 1-Methylimidazolium cation.

The ^{1}H-NMR spectra were recorded to characterize the PILs synthesized and used in this work. These measurements were carried out using a 200 MHz and 400 MHz (as per suitable for the samples) NMR spectrometer from Bruker India Pvt. Ltd.

6.2.3 Determination of Polarity and Viscosity of Ionic Liquids

Wherever available, the polarity and viscosity values of the studied PILs were obtained from the published literatures.[20,21] In the other cases these values were independently estimated in the present work. Thus, the viscosity values for the required solvents and solvent mixtures were measured by using a Brookfield ultra rheometer, keeping the temperature constant at 298 K by using a Julabo Water bath. Each measurement was repeated three times to check the reproducibility, which is found to be within 1% of the average value noted. For solvent mixtures their polarity parameters ($E_T{}^N$) were estimated using the following relation,

$$E_T{}^N(MS) = f_A E_T{}^N(A) + f_B E_T{}^N(B) \qquad (1)$$

where f_A and f_B are the volume fractions and $E_T{}^N(A)$ and $E_T{}^N(B)$ are the polarity parameters of the co-solvents A and B, respectively.[23,27] The organic solvents used in the present study were of spectroscopic grade, obtained either from Spectrochem (Mumbai, India) or Fluka (Buchs, Switzerland), and used as received.

6.2.4 Spectroscopic Measurements

Absorption spectra were recorded using a JASCO UV-vis spectrophotometer (model V-530, Tokyo, Japan). Steady-state (SS) fluorescence spectra were recorded using a Hitachi spectrofluorimeter (model F-4010, Tokyo, Japan). Fluorescence decays of 18DHAQ dye in different PILs and PIL mixtures were measured using a time-resolved (TR) spectrofluorimeter (Horiba Jobin Yvon IBH, Scotland, UK) that works on the time-correlated-single-photon-counting (TCSPC) principle.[28] In the present study a 445 nm diode laser (~100 ps, 1 MHz repetition rate) was used as the excitation source and a special photomultiplier tube (PMT)-based detection module supplied by Horiba Jobin Yvon IBH was used for the fluorescence detection. All the measurements were carried out at magic angle configuration to eliminate the effect of rotational anisotropy on the observed fluorescence decays. Measured decays were analyzed using a re-convolution procedure.[28] Instrument response function (IRF) for the TCSPC setup was obtained by replacing the sample cell with a dilute scatterer solution (suspended TiO_2 particles in water). In the decay analysis the reduced chi-square (χ^2) values (close to unity) and the distribution of the weighted residuals (random distribution among the data channels) were used to judge the goodness of the fits.[28] The full-width at half-maximum for a typical IRF for the present TCSPC setup is ~140 ps. The shortest fluorescence lifetime (τ_f) thus measurable using the present setup following re-convolution analysis is about 30 ps. In the fluorescence measurements, the absorbance of the sample solution at the excitation wavelengths was always kept quite low, only about 0.1, to avoid any self absorption or inner filter effect. All the absorption and fluorescence measurements in the present study were carried out at ambient temperature (298±1 K).

Ultrafast fluorescence kinetic traces in the sub-picosecond to picosecond time domain were measured using a femtosecond fluorescence up-conversion instrument (model FOG 100, from CDP Inc., Russia). The details of this experimental setup are given elsewhere.[29, 30] Briefly, the second harmonic light (400 nm) of a 50 fs Ti:sapphire laser is used for the excitation of the sample taken in a thin (0.4 mm)

rotating cell and the residual fundamental (800 nm) of the Ti:sapphire laser is used as the gate pulse to up-convert the fluorescence light in a 0.5 mm BBO crystal. The up-converted light is detected using a Hamamatshu PMT (model 5000U-09) operated in the photon counting mode. The IRF of the present setup is found to have a Gaussian intensity profile with a FWHM of about 220 fs.

6.3 Results and Discussion:

6.3.1 Ground State Absorption and Steady State Fluorescence Studies

The absorption and steady-state fluorescence emission spectra of 18DHAQ in different PILs (used in this study) have been shown in Figure 1.

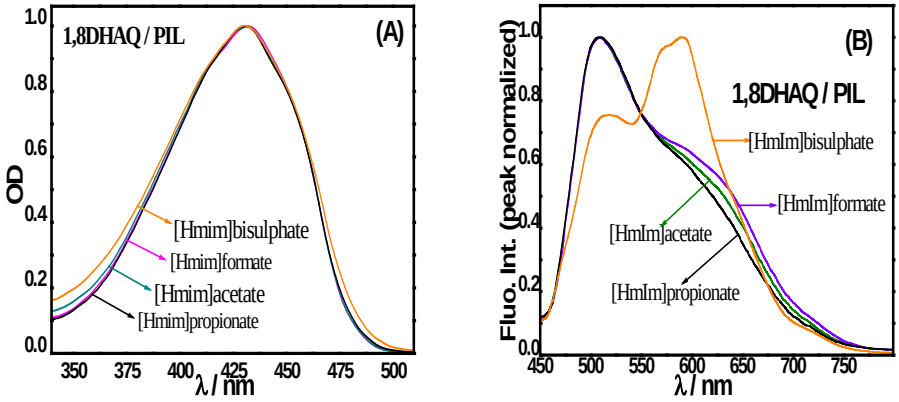

Figure 1: (A) Ground state absorption spectra and (B) Steady-state Fluorescence Spectra of 18DHAQ dye in different PILs studied: [HmIm]propanoate (Black), [HmIm]acetate (Magenta), [HmIm]formate (Green) and [HmIm]bisulphate (Orange).

From Figure 1A, it is obvious that lowest energy absorption bands in different PILs are almost similar to each other and all the absorption spectra of the dye show peak around 430nm which is analogous to observations in many conventional organic solvents for 18DHAQ.This absorption band can be assigned to $S_0 \rightarrow S_1$ charge transfer type transition with dominant π-π^* character. A study of polarization with stretched polymer signifies that this transition is polarized along the longer axis of the molecule.[22b-24, 31, 32]

In Figure 2B, steady state fluorescence emission spectra of 18DHAQ in different PILs excited at 430nm are shown. From the Figure 2B, it is evident that there is no mirror image relationship between absorption and emission spectra. It is known to us that presence of mirror image symmetry between absorption and emission bands signifies that the nuclear configuration of the probe molecule and

surrounding solvent does not exhibit change with respect to that of ground state within the timescale of excited state lifetime.[10-12]

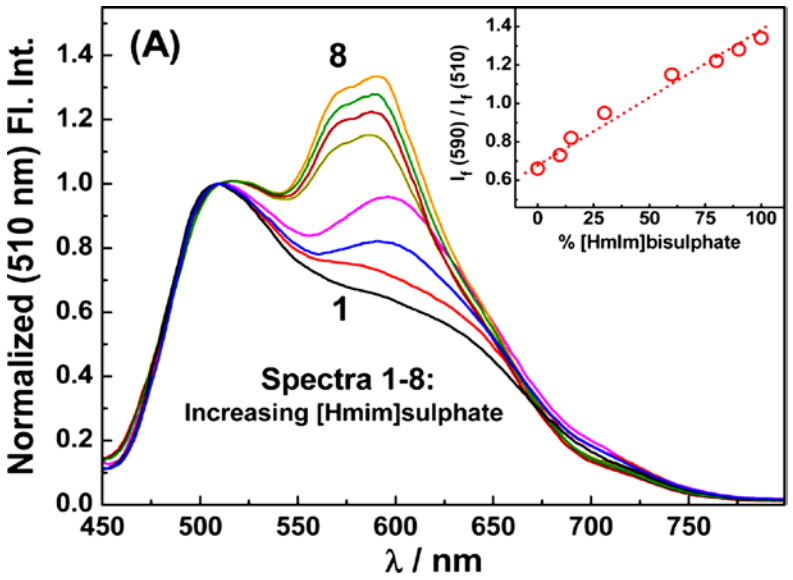

Figure 2: Changes in the Steady-State Fluorescence Spectra of 18DHAQ dye in the mixtures of [Hmim]Formate and [Hmim]Bisulphate solvents. Spectra 1-8 correspond to 0%, 10%, 15%, 30%, 60%, 80%, 90% and 100% [HmIm]bisulphate In the solvent mixtures, Respectively. Inset shows the variation in the intensity ratios for the HWEB to LWEB as a function of volume percentage of [HmIm]bisulphate in the solvent mixtures.

Quite identical nature of the absorption spectra in all the PILs implies that the dye exclusively exist in a single conformation in the ground state i.e. the dye remains at normal form (N) in which the quinonoid oxygen at 9-position is hydrogen bonded to the hydroxyl groups at 1 and 8 positions of the dye through intramolecular hydrogen bond. (Scheme2). However, the consequences of the excited state proton transfer on the Frank-Condon factors are significant enough to remove the mirror image symmetry and to cause a substantial red shift of the fluorescence spectra with respect to absorption band. Dual emission i.e. one with peak at around 505-515nm and the other one having peak at around 580-615nm, hereafter assigned as the LWEB and HWEB, respectively, by 18DHAQ in PILs is obvious from figure 1B.[2-3, 26] From the perspective of observed results in figure 1B as well as on the basis of inferences drawn in the related reports, following mechanism of ESIPT of 18DHAQ can be safely proposed.

Upon photo excitation, the dye initially attains excited normal state (N*) from normal ground state (N). Thereafter, N* undergoes very fast ESIPT to produce excited state tautomeric form (T*).

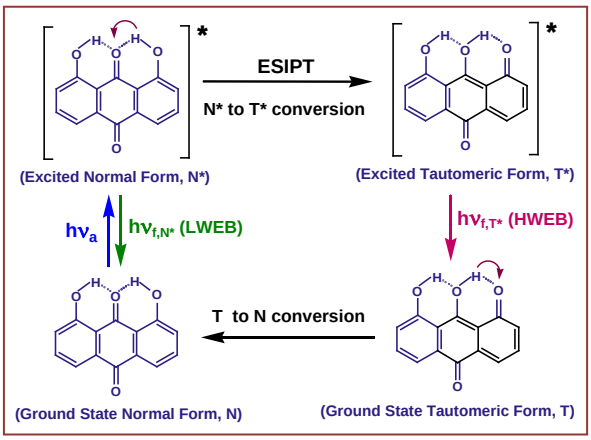

Scheme 2: ESIPT in 18DHAQ occurring along the pre-existing hydrogen bond in the ground state between the phenolic OH group and the quinonoid oxygen of the dye.

Table 1: The solvent polarity and viscosity parameters of the PILs and PIL mixtures used in the present study.

Protic Ionic Liquids	**Polarity (E_T^N)[b]**	**Viscosity (cP)[c]**
[HmIm]propanoate	0.50[b]	5.5
[HmIm]acetate	0.61[b]	5.6
[HmIm]formate	0.78[b]	6.7
[HmIm]bisulphate	1.02[b]	406
10% [HmIm]bisulphate[a]	0.804	36
15% [HmIm]bisulphate[a]	0.816	68
30% [HmIm]bisulphate[a]	0.852	175
60% [HmIm]bisulphate[a]	0.924	276
80% [HmIm]bisulphate[a]	0.972	350
90% [HmIm]bisulphate[a]	0.996	385

During this process, one of the hydroxyl hydrogen (either from position 1 or from 8 of the dye) is transferred from the hydroxyl group to quinonoid oxygen through the co-ordinate of preexisting hydrogen bond.[2-3, 26, 31]

Following ESIPT process, the T* form relaxes to ground state of the tautomeric form (T) by emitting at HWEB. In the SS spectra (Figure 1B), the emission band from the N* form of the dye has been ascribed as LWEB. A cursory view of the emission spectra (Figure 1B) reveals that the intensities of LWEB and HWEB of dye vary with the variation of PILs. It implies that solvent relaxation process in different PILs causes substantial modulation in the population of N* and T* forms of the dye through invoking largely different stabilization for both the excited form. A conscious attempt to justify the variation in stabilization of the excited isomers of the dye in different PIL solvents directs us to correlate the observations with two most important properties viz. polarity and viscosity of PILs.

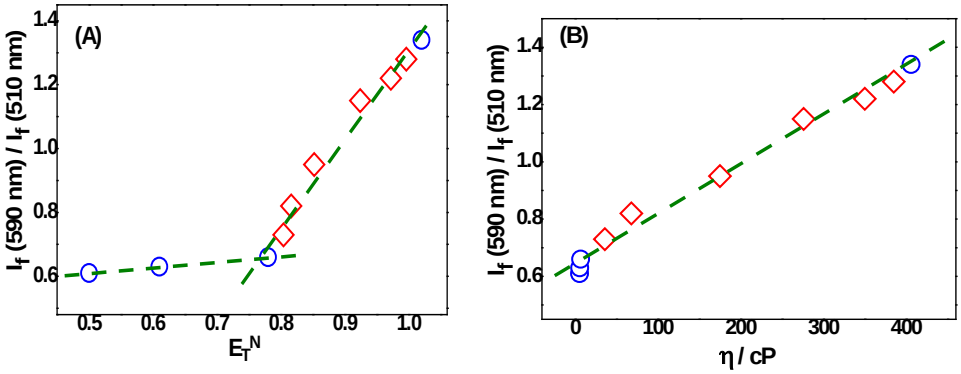

Figure 3: Variation in the relative intensity of the HWEB to LWEB for 18DHAQ dyes as a Function of (A) the E_T^N values and (B) the viscosities of the PILs and PIL mixtures studied. [Open Circles Keep up a correspondence to the pure PILs and closed diamonds correspond to the [HmIm]formate and [HmIm]bisulphate solvent mixtures (*cf*. Table **1**).

Comparing the observation in Figure 1B with values presented in Table 1, it can be concluded that increase in the intensity of HWEB as well as consequential decrease in LWEB seems to have a concurrence with both increasing trend of polarity and viscosity of PILs. To validate this concurrence SS fluorescence measurements have been carried out in a series of [Hmim]formate and [Hmim]bisulfate solvent mixtures with 18DHAQ dye, where both the parameters i.e. viscosity and polarity have shown a systematic variation in their values. The SS fluorescence emission spectra for the mixtures of [Hmim]formate and [Hmim]bisulfate has been shown in Figure 2.

From the Figure 2, it is obvious that with the increase in the % volume of [Hmim] bisulfate in the mixture studied here, intensity of HWEB gradually increases at the expenses of the intensity of LWEB. Upon comparison with the polarity and viscosity values of the mixtures (Table 1), it is ambiguous to emphasize on one of the properties responsible for such differential stabilization of the isomers since both the polarity and viscosity of the PILs mixtures varies concurrently. To distinguish the effect of solvent polarity (E_T^N) and solvent viscosity (η) on intensities of HWEB and LWEB, intensity ratio i.e. (I_{590} /I_{510}) of two emission band has been plotted with respect to solvent polarity (E_T^N) and solvent viscosity (η) separately (Figure 3).

Figure 3A depicts the variation of (I_{590} /I_{510}) ratio with respect to polarity (E_T^N) of the studied PILs and their mixture. From Figure 3A, it is obvious that the intensity ratio shows a nominal change with change in the polarity at earlier values of polarity of the solvents but ahead of a critical polarity value (~0.8) there is a steep rise in the intensity ratio with respect to (E_T^N). Presence of such switching point in the Figure 3A seems to be only possible if there is a polarity dependent huge change in the configuration of dye at either of the excited forms (N* or T*). From the reported literature on stability and conformation of 18DHAQ and the emission spectra obtained during our study, it can be safely concluded that predicted change in the configuration at the excited state from Figure 3A is impossible. In addition to that solvent dependent stabilization of both the excited forms (N* and T*) of the dye is expected to guide population in both the states such that emission contribution of both N* and T* would follow smooth linear relationship with solvent polarity. Again according to the previous reports, N* possesses higher dipole moment compared to T* of the dye.[31, 32] Correlating the observations with this fact, it can be inferred that N* form will be much more stabilized than T* form at the excited state with the increase in the E_T^N values of the PILs and their mixture. It implies that the intensity of LWEB should increase at the expense of HWEB *i.e.* a reverse proportionality relationship between (I_{590} /I_{510}) with E_T^N should be observed if solvent polarity plays pivotal role in guiding population ratio in the excited state of the dye in this study. Experimental observations justifies that solvent polarity is not playing the central role in guiding the difference in population at the excited state.

Figure 3B displays the variation of the intensity ratios (I_{590} /I_{510}) with respect to the viscosity values (η) of the PILs and mixture of PILs studied here. A cursory

view of the variation shown in the Figure 3B reveals that there is a linear relationship among intensity ratios with respect to viscosity values of the solvents studied. It univocally implies that the population distribution at both the excited states is a diffusion controlled phenomena. Salient feature of this correlation is that relative population of the excited tautomeric form (T*) of the dye raises upon increase in the viscosity of the solvent. From the normal viewpoint, it can be anticipated that the rate of ESIPT i.e. conversion from N* to T* would be retarded with the enhancement of viscosity of the solvent if solvent diffusive motions have been coupled with the forward ESIPT process, which is contrary to the observed fact. To justify the observed results, thus, one should consider that subsequent to the forward ESIPT process there seems to be some back transfer from T* to N* by the participation of a back ESIPT process and the latter process is actually controlled by the solvent diffusive motions than the former. This in other words suggest that the forward ESIPT occurs with an unusually fast rate and hence without any influence of the solvent diffusion.[2c-d, 9] The back ESIPT process, however, occurs with a relatively slower rate, influenced largely by the solvent diffusive motions and accordingly the extend of the back ESIPT reduces largely on increasing the solvent viscosity, resulting in an increase in the contribution of the T* form, as indicated in Figure 2 and 3B.

As one can appreciate that the directing force for the back ESIPT process will actually be the differential solvent stabilizations (PE stabilizations) for the N* and T* forms, caused by the diffusive solvent relaxations, the latter being known to be convincingly slow for ionic liquids.[35-37,41] Since the dipole moment of N* is higher than that of T*,[31-32] as long as the solvent relaxation rate is competitive with the de-excitation rates of N* and T*, the former will cause a more time-dependent stabilization for N* than T*, sustaining the back ESIPT process. The basis behind this assertion is that for ILs the solvent relaxation process in general occurs for a very long period of time span, with time constants for the relaxation components ranging from picoseconds to nanoseconds, and the longer components in these cases are found to be strongly dependent on the viscosity of the solvent used.[35-37] Therefore, one world expect that while in lower viscosity PILs the back ESIPT will be quite efficient (due to faster diffusive solvent relaxation), in very high viscosity PILs the back ESIPT process will be practically improbable (due to very slow diffusive solvent relaxation) leading to a large increase in the relative population of T*. A support for this proposition is in fact obtained from fluorescence up-conversion results for the dye in

different PILs and will be discussed later. In the present milieu, however, it is evident that the solvent viscosity plays a pivotal role in determining the relative population of N* and T* forms of the dye, though a minor role of the solvent polarity on this aspect cannot be overlooked entirely.

6.3.2 Time Resolved Fluorescence studies with TCSPC

The fluorescent lifetimes of 18DHAQ dye in PILs and in their mixtures were measured using a picosecond time correlated single photon counting (TCSPC) setup. From measured fluorescent decay traces it can be observed that a long decay trail as well as contribution from unusually fast decay component constitutes the whole decay traces for all the solvent studied here. Point to be mentioned here that all the PILs used in this study had shown a weak inherent fluorescence for the timescale of observation in the TCSPC measurements, due to the presence of imidazolium cation as one of the constituents of the PILs.[37, 38] However, this inherent fluorescence being too weak cannot cause any significant modulations in the spectral feature of the dye. Nevertheless, this inherent fluorescence evidently introduces additional decay components in the observed fluorescence decays. To distinguish fluorescence shown by dye in PILs from the decay components shown by PILs alone, we have also carried out time resolved fluorescence studies with PILs alone without adding any dye. Non-exponential fluorescence decays along with long tail shown by PILs alone were almost similar to that observed in case of 18DHAQ dye in PILs solvents. Therefore, it is obvious that long decay tail observed during experiments with 18DHAQ in PIL solvents are actually due to the inherent decay of PILs. Accordingly, it has been inferred that for the dye in the ionic liquids the observed decays are due to the combination of the unusually fast fluorescence decay component of 18DHAQ and the relatively long fluorescence decay components from the ionic liquids alone.

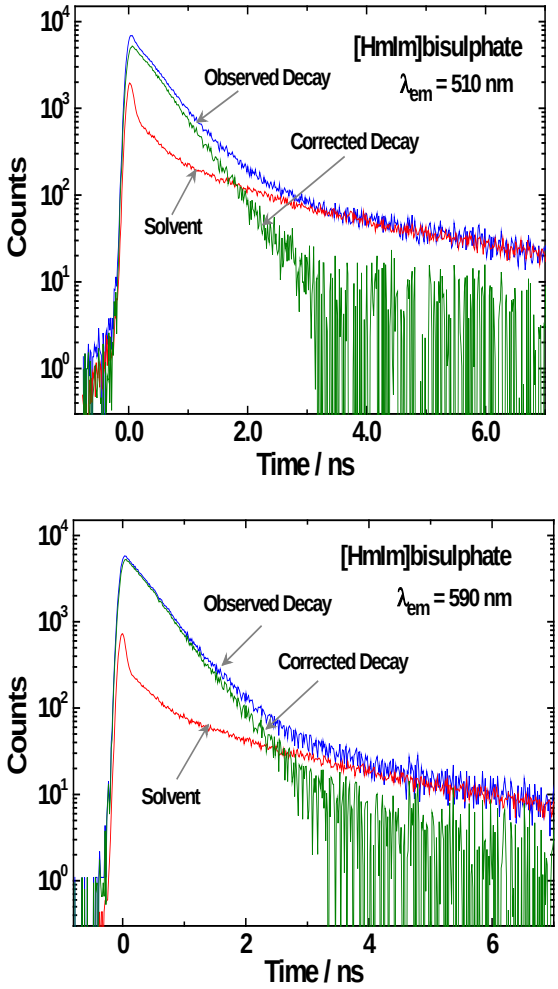

Figure 4: Fluorescence decays for 18DHAQ dye in different PILs and PIL mixtures (indicated in the panels) as measured at 510 nm (LWEB) and 610 nm (HWEB) using TCSPC technique. The inherent fluorescence decays for the PILs and PIL mixtures at the respective wavelengths are also shown in the respective panels. The true fluorescence decays for the dye at 510 nm (LWEB) and 610 nm (HWEB) were obtained by the subtracting the tail-matched solvent decays from the sample decays and are shown in the respective panels in this figure.

Table 2: Fluorescence lifetimes (τ_f) of 18DHAQ estimated at the HWEB (515 nm) and LWEB (590 nm) of the dye in different PILs used using TCSPC Measurements. Samples were Excited with 445 nm Diode Laser.

Solvent	η / cP	λ_{em} / nm	τ_f (pS)
[HmIm]propanoate	5.5	515	59
		590	64
[HmIm]acetate	5.6	515	66
		590	62
[HmIm]formate	6.7	515	70
		590	65
15% [HmIm]bisulphate	55	515	114
		590	113
30% [HmIm]bisulphate	120	515	146
		590	150
60% [HmIm]bisulphate	255	515	286
		590	290
[HmIm]bisulphate	406	515	422
		590	430

Therefore, the true fluorescence decays of 18DHAQ dye in different ionic liquids were obtained by subtracting the tail-matched decays of the ionic liquids alone from the observed decays of the dye solution at two selected wavelengths, namely 510 nm and 610 nm, corresponding to the lower wavelength emission band (LWEB) and the higher wavelength emission band (HWEB) of the dye. The two panels in Figure 4 show the representative fluorescence decays of 18DHAQ dye, tail-matched decays of the ionic liquids alone and the true fluorescence decays of the dye obtained in [Hmim]bisulphate ionic liquid, recorded at 510 nm and 610 nm emission wavelengths, respectively, as obtained in the present study. The actual fluorescence decays (both LWEB and HWEB), obtained following the subtraction of the tail matched inherent decays of the PILs from that of the dye in the respective PIL solvents, are shown in Figure 5A and 5B, respectively, for the emission wavelengths of 510 nm and 610 nm. These decays could be fitted well with a single exponential function and the fluorescence lifetime values thus estimated are listed in Table 2.

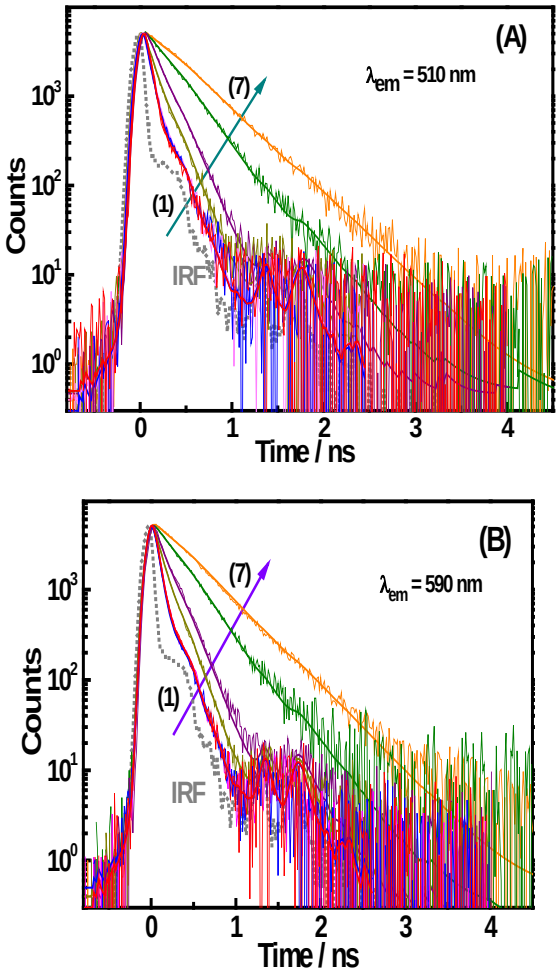

Figure 5: Comparison of the fluorescence decays at (A) the LWEB (measured at 510 Nm) and (B) the HWEB (measured at 510 Nm) Of 18DHAQ dye in different PILs and PIL Solvent Mixtures, As measured using TCSPC technique (*Cf*. Section S2 Of SI). The decays 1 to 7 correspond to [Hmim] propanoate, [Hmim] acetate, [Hmim] formate, 15% [Hmim] bisulphate, 30%[Hmim]bisulphate, 60% [Hmim]bisulphate, and [Hmim] bisulphate (*Cf*. Table 1). The Instruments Response Functions (IRF) are also shown in the respective Panels.

From Figure 5 and Table 2 it is vivid that the fluorescence decays for both the LWEB and HWEB of the dye are very fast. It implies that like many other hydroxyl- and amino-substituted quinines, the deexitation process of both N* and T* forms of 18DHAQ dye are unusually fast due to the involvement of very efficient non-radiative deexcitation arising through the fast IC process, which is strongly coupled to the motions associated to the intramolecular and intermolecular hydrogen bonds present in these molecules.[22b-25a] The true fluorescence decays of dye in all the PILs and mixture of PILs after recovery from solvents' impurity were fitted with reasonable

accuracy with a single-exponential function. Closeness of the τ_f values (in Table 2) at both the LWEB (510nm) and HWEB (590nm) of the dye implies a kind of kinetic equilibrium between the two forms i.e. N* and T* forms of the excited dye within the timescale probed by the TCSPC measurements. Substantial changes in the τ_f values with the changing PILs and their mixtures incited us to plot these τ_f values at both LWEB and HWEB of the dye as a function of polarity (E_T^N) and viscosity (η) values of the solvents studied to find any physically meaningful correlation. The plots thus obtained for the changes in the τ_f values with the changing E_T^N and η values of the solvents are shown in Figure 5A and 5B, respectively.

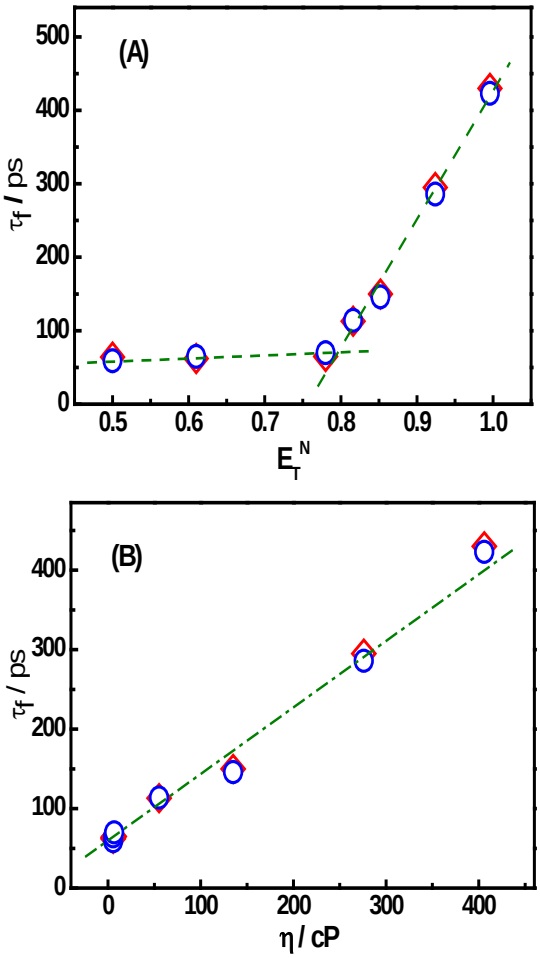

Figure 6: Variation in the τ_f Values for 18DHAQ Dye with (A) the E_T^N Values and (B) the viscosities of the PILs and PIL mixtures studied. The symbols O and ◇ represent the τ_f values estimated at the LWEB and HWEB of 18DHAQ dye.

Variation of τ_f values with respect to E_T^N values of the PILs and their mixtures shows a deviation from expected linearity but displays a sudden break at an intermediate

polarity solvents used. Observation of such a break in Figure 6A which is quite similar to that observed in Figure 3A and is of no physical significance because the variation of polarity of the solvents cannot induce any major conformational change in the structure of studied dye to lead to such a break in the τ_f values.[30b-c] However, the changes of τ_f values as a function of viscosity of the studied PILs and their mixtures follow a linear correlation (Figure 6B) which is quite similar to the trend shown by Figure 3B. At this juncture, it can be safely concluded from the combined observations of both Figure 5B and Figure 3B that diffusion component of the solvent not only guide the population distribution at both the excited states i.e. N* and T* but also the decay kinetics of these states. Our proposition is being supported by the observation of Smulevich et al.[39] where it had been examined in conventional organic solvents that while the steady-state emission spectra of the dye at room temperature have a much higher intensity for LWEB, the spectra almost exclusively exhibit the HWEB in Spolski matrix at very low temperature (10 K) with very negligible emission for LWEB. Therefore, both the excited isomers of 18DHAQ dye undergo time dependent modulation, guided by solvent diffusive relaxation, before attaining a steady state situation with in the timescale of the TCSPC measurements

6.3.3 Up-conversion Measurements to Study Ultrafast Component of the Fluorescence Decay

Femtosecond time resolved fluorescence kinetic traces were measured for 18DHAQ dye in different PILs, recorded using femtosecond fluorescence up-conversion measurements, to realize the time-evolutions of N* and T* forms of the dye at real time scales. The kinetic traces thus obtained for the dye measured at LWEB and HWEB in different PILs are shown in Figure 6A and B, respectively.

In all the cases, at least a tri-exponential function was necessary with appropriate decay and growth components to satisfactorily fit the kinetic traces. The time constants (τ_i) of the three components and their respective contributions (A_i) as obtained from the tri-exponential analysis of the kinetic traces measured at LWEB and HWEB of the dye in different PILs are listed in Table 3.

Table 3: Time constants (τ_i), corresponding relative contributions (a_i) for 18DHAQ dye estimated at LWEB and HWEB in different PILs using fluorescence Up-Conversion Measurements. Samples were excited with 400 nm LASER Pulses.

Ionic Liquids	λ_{em} nm	A_1	τ_1 (ps)	A_2	τ_2 (ps)	A_3 (ps)	τ_3 (ps)[a]
[HmIm]propanoate	510	112.1	0.22	39.4	3.4	46.6	60
	590	-27.9	0.20	51.6	3.4	83.9	60
[HmIm]acetate	510	105.4	0.21	41.9	3.3	48.1	60
	590	-18.1	0.19	51.3	3.5	83.6	60
[HmIm]formate	510	85.6	0.24	38.8	3.3	54.1	60
	590	-25.8	0.29	49.8	3.9	84.7	60
15% [HmIm]bisulphate	510	95.2	0.24	39.4	3.3	52.5	90
	590	-24.8	0.23	27.1	5.2	101.6	90
30% [HmIm]bisulphate	510	83.2	0.26	43.0	3.5	54.6	135
	590	-21.8	0.25	24.1	8.5	103.2	135
60% [HmIm]bisulphate	510	62.7	0.26	25.2	3.4	78.7	290
	590	-19.9	0.27	2.5	18	123.0	290
[HmIm]bisulphate	510	48.5	0.27	26.5	3.2	83.4	425
	590	-19.0	0.27	2.4	22	122.3	425

In all the cases, a tri-exponential function was uniformity used to analyze the observed traces. To be mentioned here that in these analyses we justifiably kept the longest time constant (τ_3) fixed as equal to the average τ_f values estimated from TCSPC measurements (*cf.* Table 2). As indicated from Table 3, for all the kinetic traces recorded at 510 nm, irrespective of the solvents used, there is an ultrafast decay component τ_1, having time constant in the range of 0.2-0.3 ps.

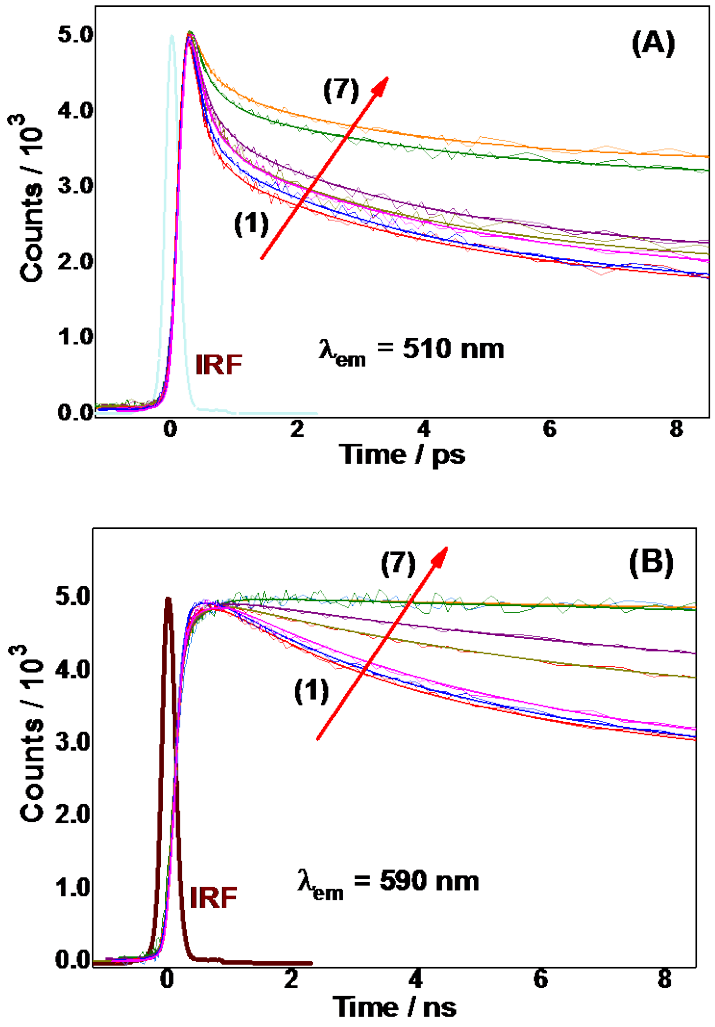

Figure 7: Comparison of the fluorescence kinetic traces (for shorter time span) as measured at (A) the LWEB (recorded at 510 nm) and (B) the HWEB (recorded at 590 nm) of 18DHAQ dye in Different PILs and PILs mixtures using Up-conversion technique. The Traces 1 to 7 Correspond to [HmIm] propanoate, [HmIm] acetate, [HmIm] formate, 15% [HmIm] bisulphate, 30% [HmIm]bisulphate, 60% [HmIm]bisulphate, and [HmIm] bisulphate (*cf*. Table 1). The Instruments Response Functions (IRF) are also shown in the respective panels.

Based on the reports that in most ESIPT dyes the process occurs with an unusually fast rate, the τ_1 decay component observed at 510 nm is justifiably assigned to ultrafast forward ESIPT process (conversion of initially photo produced N* to T*).[2c-d, 3a] These results thus are in accordance with our proposition of the presence of an unusually fast component for the forward ESIPT process. Another point to be noted from Table 3 is that apparently there is a small increase in the τ_1 values as the

solvent viscosity is increased (*cf.* Table 1). Though we cannot give much of emphasis to this increase as the changes are almost within the time-resolution of the present experimental setup, yet a small effect of viscosity of the PIL solvents on the ultrafast forward ESIPT process cannot be ruled out. The presence of the unusually fast forward ESIPT components in the studied systems suggests that the conversion N* to T* of 18DHAQ dye essentially occurs along a barrierless PE surface. [2c-d,3a]

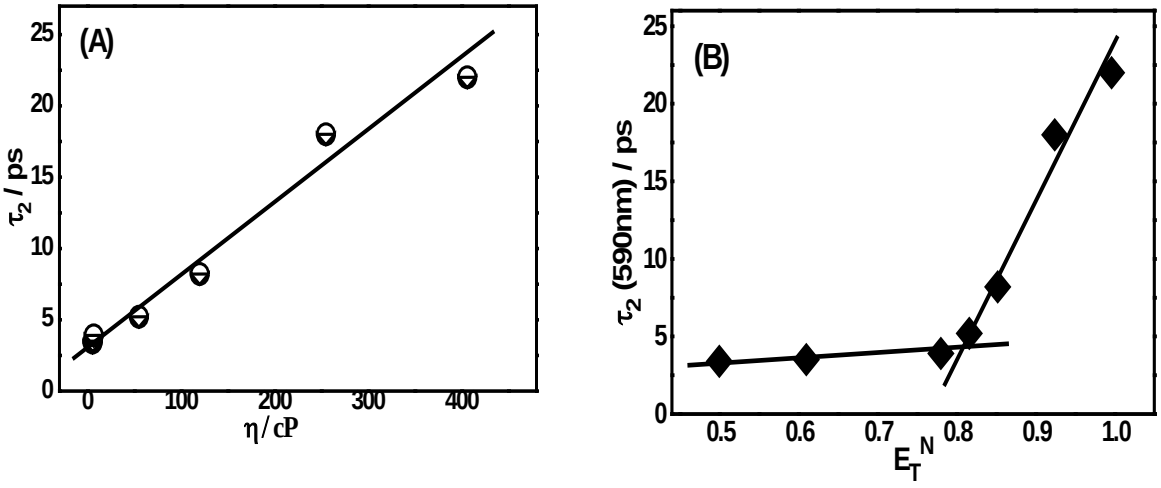

Figure 8: Correlation of the τ_2 decay component at 590 nm with (A) the viscosity (η) and (B) the polarity (E_T^N) of the solvents studied. While the τ_2 correlates more or less linearly with the solvent viscosity, it does not show a single correlation for the whole range of the solvent Polarities Studied.

For the 510 nm kinetic traces, in addition to the ultrafast τ_1 decay component, there is a second relatively slower decay component τ_2 with time constants in the range of 3.2-3.5 ps, in all the solvents studied. Presence of this τ_2 decay component at 510 nm clearly advocates that in the studied PILs the forward ESIPT process in 18DHAQ dye is not a single-step ultrafast process (corresponding to τ_1) but actually occurs following a non-single-exponential kinetics that can effectively be fitted in terms of the two decay components τ_1 and τ_2. Interesting point to note from the up-conversion results is that relating to the τ_2 decay component at 510 nm there is no corresponding growth component present in the kinetic traces at 590 nm. In the contrary, we actually find a distinctly different decay component τ_2 in the traces at 590 nm which clearly does not match with the τ_2 component observed at 510 nm. Moreover, unlike the τ_2 component at 510 nm, the τ_2 component at 590 nm shows a clear and significant increase on increasing the viscosity of the solvents. In fact a plot

of these τ_2 values at 590 nm with the viscosity of the solvents shows a reasonably linear correlation, as shown in Figure 8A, suggesting that the diffusive solvent motion has a direct influence on the observed τ_2 component at 590 nm. However, τ_2 values at 590 nm with the polarity of the solvents (Figure 8B) follow the trend observed in case of Figure 3B and Figure 6A. It implies that polarity of the PILs is not playing any direct or crucial role in guiding the energy stabilization of the excited tautomeric states as a consequence of very fast ESIPT in 18DHAQ.

The viscosity dependent differential stabilizations of the excited state arises out of forward and reverse ESIPT can schematically be presented as in Figure 9 depending upon the time constants obtained from the up-conversion studies.

In Figure 9, the topmost curves in both the left and right panels (*left panel for lower viscosity solvents and right panel for very high viscosity solvents*) qualitatively represent the PE changes for the excited dye as a function of the ESIPT coordinate as it happens just immediately after the ultrafast ESIPT process, irrespective of the viscosity of the solvent. The PE curves for the excited dye in the left and right panels, however, represent different extent of relaxation for the N* and T* states, in the lower and higher viscosity solvents, as are elaborated above. In relation to the presentation in Figure 9, following photoexciation the dye is initially placed at a very high PE configuration of N*, wherefrom the excited dye undergoes quick relaxation along the ESIPT coordinate sliding down the barrierless PE curve, eventually converting to the T* conformation, causing the forward ESIPT process to be ultrafast in nature. Subsequent to this initial effect, however, there could be more time-dependent evolutions for the N* and T* forms if the nature of the PE changes with time.

As reported in the literature, [31-32] the N* form of the dye possess a higher dipole moment than its T* form. Thus, one would expect that with progresses of time, subsequent to the ultrafast forward ESIPT, there will be more stabilization for the energy of the N* form than T* form, as would be caused by the time-dependent diffusive relaxation of the solvent around the excited dye. Such a differential stabilization in the energies of the N* and T* forms can thus eventually make the energy of the N* form to become lower than T* and thus driving a back ESIPT process that will convert part of T* population formed by the ultrafast forward ESIPT to return back to N*. Such a situation can be represented by the differentially lowering the energies corresponding to the N* and T* forms, as qualitatively shown

by the lower PE curves for the excited state in the left and right panels of Figure 9 for low viscosity and high viscosity solvents, respectively. According to this presentation, subsequent to the ultrafast forward ESIPT, there will be a continuous time-dependent modulation in the populations of the N* and T* forms in the intermediate time scales, before attaining a kind of steady-state situation for the relative populations of the two forms as accessed by the TCSPC measurements.

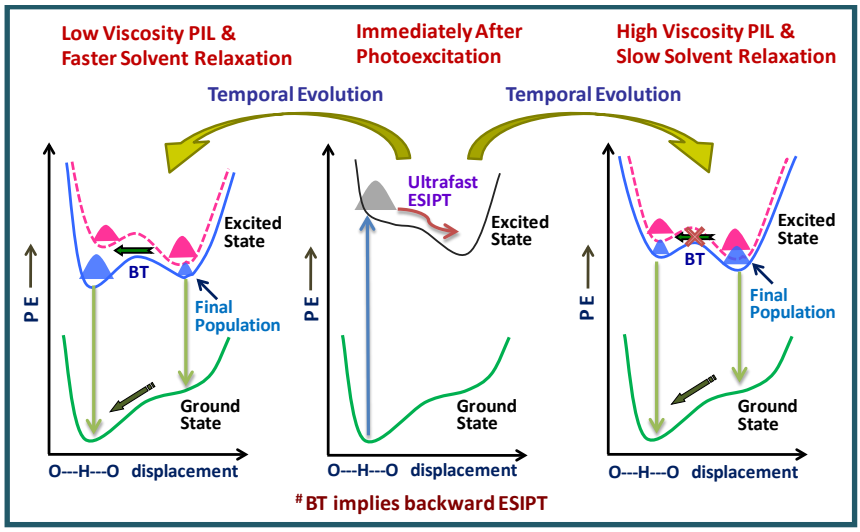

Figure 9: Qualitative potential energy diagrams to represent the solvent relaxation guided differential stabilization of the excited N* And T* forms of 18DHAQ dye and the consequent involvement or non-involvement of the back ESIPT Process. Left panel shows The Situation prevailing to the lower viscosity PILs and the right panel shows the situation prevailing to the high viscosity PILs.

From the observed fluorescence up-conversion results, it is quite intuitive to assume that during the initial ultra-short time span representing τ_1 component, there is not much of modulation in the PE surfaces for the excited dye, which is in accordance with the fact that the ultrafast inertial solvation component contributes only to a small extent in the overall solvent relaxation dynamics in IL solvents.[33-37] In other words, it is expected that during the ultrafast forward ESIPT process the energy of N* essentially remains higher than that of T* and most of the modulations in the excited state energies of the dye in effect occurs during the diffusive component of the solvent relaxation, which is known to be quite slow in the ILs. Thus, the PE diagrams in Figure 9 in corroboration with the ultrafast fluorescence up-conversion results nicely explains all the ESIPT results obtained for 1,8DHAQ dye in PIL solvents.

6.4 Conclusions:

Steady-state (SS) and time-resolved (TR) fluorescence studies of 1,8-dihydroxyanthraquinone (18DHAQ) dye in protic ionic liquid (PIL) solvents unravel the interesting aspects of excited state intramolecular proton transfer (ESIPT) kinetics of the dye that could not be observed unambiguously in the earlier studies using time-resolved fluorescence or absorption measurements. The fact that the intensity ratios for tautomeric (T*) to normal (N*) forms of the excited dye increases with increasing solvent viscosity, as observed in SS fluorescence measurements, and is apparently unusual as the N* is the initial photoexcited state that converts to T*, impelled us to invoke the participation of a relatively slower backward ESIPT process following the initial ultrafast forward ESIPT. Interestingly, the evidence for both ultrafast forward ESIPT and relatively slower backward ESIPT has been convincingly obtained from the kinetic traces recorded using femtosecond fluorescence up-conversion measurements. From the observed results it is clearly indicated that the backward ESIPT process can contribute efficiently in lower viscosity PILs but the process cannot simply take part in very high viscosity solvents. Based on the experimental finding and the literature reports on the viscosity dependent changes in the solvent relaxation dynamics, it is proposed that the backward ESIPT process is actually guided by the differential stabilization of the energies for N* and T* forms during the progress of the diffusive solvent relaxation, subsequent to the ultrafast forward ESIPT, as the dipole moments of N* and T* forms are largely different. Due to a relatively faster diffusive solvent relaxation, the potential energy (PE) of N* form can quickly come down below that of T* in lower viscosity PILs, triggering the backward ESIPT process. In very high viscosity PILs, an extremely slow diffusive solvent relaxation can never bring down the PE of N* below T* and hence backward ESIPT becomes improbable. Accordingly, qualitative PE diagrams have been proposed to represent the solvent relaxation guided stabilizations of the N* and T* forms and the consequent involvement or non-involvement of the backward ESIPT depending on the viscosity of the PILs studied. Present study clearly demonstrates the participation of the backward ESIPT process for 18DHAQ dye from the direct measurements of the N* and T* emissions, which could not be unambiguously established in any of the earlier studies in common organic solvents, though resonant pump third-order Raman spectroscopy indirectly indicated the presence of this process. It is evident from the present study that not only the ultrafast forward ESIPT but also a reasonably fast

backward ESIPT plays a role in determining the relative contributions of the N* and T* forms of the excited dye, especially in lower viscosity solvents, and this backward ESIPT is the main cause for the unusually higher N* emissions observed in most of the conventional solvents, including organic solvents, even if the forward ESIPT for the dye is understood to be unusually fast in all these cases.

6.5 References:

1. (a) Jaramillo, P.; Coutinho, K.; Canuto, S. *J. Phys. Chem. A.* **2009**, *113*, 12485. (b) Malmstrom, B. G. Cytochrome C *Chem. Rev*. **1990**, *90*, 1247. (c) Cui, G.; Lan, Z.; Thiel, W. *J. Am. Chem. Soc.* **2012**, *134*, 1662. (d) Paul, B. K.; Guchhait, N. *J. Phys. Chem. B.* **2010**, *114*, 12528. (e) Elsaesser, T; Bakker, H. J. *Ultrafast Hydrogen Bonding Dynamics and Proton Transfer Processes in the Condensed Phase.* Springer Pub. , **2002.** (f) Kuznetsov, A. M. *Charge Transfer in Chemical Reaction Kinetics* PPUR Presses Polytechniques, **1997.**

2. (a) Wu, J. S.; Liu, W. M.; Ge, J. C.; Zhang, H. Y.; Wang, P. F. *Chem. Soc. Rev.*, **2011**, *40*, 3483. (b) Deperasinska, I.; Gryko, D. T.; Karpiuk, E.; Kozankiewicz, B.; Makarewicz, A.; Piechowska, J. *J. Phys. Chem. A.* **2012**, *116*, 2109. (c) Zhao, J.; Ji, S.; Chen, Y.; Guo, H.; Yang. P. *Phys. Chem. Chem. Phys.*, **2012**, *14*, 8803. (d) Park, S.; Kwon, J. E.; Park, S. Y. *Phys. Chem. Chem. Phys.*, **2012**, *14*, 8878.

3.(a) Landge, S. M.; Tkatchouk, K.; Benitez, D.; Lanfranchi, D. A.; Elhabiri, M.; Goddard III, W. A.; Aprahamian, I. *J. Am. Chem. Soc*. **2011**, *133*, 9812. (b) Klymchenko, A. S.; Demchenko, A. P. *J. Am. Chem. Soc.* **2002**, *124*, 12372. (c) Zamotaiev, O. M.; Postupalenko, V. Y.; Shvadchak, V. V.; Pivovarenko, V. G.; Klymchenko, A. S.; Mely, Y. *Bioconjugate Chem*. **2011**, *22*, 101. (d) Kim, T.; Kang, H. J.; Han, G.; Chung, S. J.; Kim, Y. *Chem. Commun*. **2009**, 5895.

4. Mutai, T.; Tomoda, H.; Ohkawa, T.; Yabe, Y.; Araki, K. *Angew. Chem., Int. Ed.*, **2008**, *47*, 9522.

5. (a) Mordziński, A.; Grabowska, A.; Kuhnle, W.; Krówczyński, A. Chem. Phys. Lett. 1983, 101, 291−296. (b) Nickel, B.; Rodríguez Prieto, M. F. Chem. Phys. Lett. 1988, 146, 125−132. (c) Rodríguez Prieto, M. F.; Nickel, B.; Grellmann, K. H.; Mordziński, A. Chem. Phys. Lett. 1988, 146, 387.

6. (a) Elsaesser, T.; Kaiser, W. *Chem. Phys. Lett.*, **1986**, *128*, 231.; (b) Takeuchi, S.; Tahara, T. *J Phys Chem A* **1998**,*102*, 7740.

7. (a) Rode, M. F.; Sobolewski, A. L. *J. Phys. Chem. A.* **2010**, *114*, 11879. (b) Tang, K.; Chang, M.; Lin, T.; Pan, H.; Fang, T.; Chen, K.; Hung, W.; Hsu, Y.; Chou, P.

Fine *J. Am. Chem. Soc.* **2011**, *133*, 17738. (c) Kwon, J. E.; Park, S. Y. *Adv. Mater*. **2011**, *23*, 3615. (d)Yang, P.; Zhao, J.; Wu, W.; Yu, X.; Liu, Y. *J. Org. Chem*. **2012**, *77*, 6166.

8. Keck, J.; Kramer, H. E. A.; Port, H.; Hirsch, T.; Fischer P.; Rytz, G. J. *J. Phys. Chem*. **1996**, *100*, 14468.

9. Hsieh, C. C.; Chou, P. T.; Shih, C. W.; Chuang, W. T.; Chung, M. W.; Lee, J. H.; Joo, T. H. *J. Am. Chem. Soc*. **2011**, *133*, 2932.

10. (a) Hojniak, A. S.; Wisniewski, L.; Deperasinska, I.; Makarewicz, A.; Jerzykiewicz, L.; Puszko, A.; Erez, Y.; Huppert, D. *Phys. Chem. Chem. Phys.*, **2012**, *14*, 8147. (b) Barroso, M.; Arnaut, L.G.; Formosinho, S.J. *J. Phys. Chem. A.* **2007**, *111*, 591.; (c) Ishikawa, H; Iwata, K.; Hamaguchi, H. Picosecond *J. Phys. Chem. A.* **2002**, *106*, 2305.

11. Wu, Y.; Lawson, P. D. V.; Henary, M. M.; Schmidt, K.; Bredas, J. L.; Fahrni, C. J. *J. Phys. Chem. A.* **2007**, *111*, 4584.

12. Huang, J.; Peng, A. D.; Fu, H. B.; Ma, Y.; Zhai, T. Y.; Yao, J. N. *J. Phys. Chem. A.* **2006**, *110*, 9079.

13. (a) Yushchenko, D. A.; Shvadchak, V. V.; Klymchenko, A. S.; Duportail, G.; Pivovarenko, V. G.; Mely, Y. *J. Phys. Chem. A.* **2007**, *111*, 10435.; (b) Das, K.; English, D. S.; Petrich, J. W. *J. Am. Chem. Soc*. **1997**, *119*, 2763. 19.; (c) Huang, Q.; Lu, G.; Shen, H. -M.; Chung, M. C. M.; Choon, N. O. *Med. Res. Rev*. **2007**, *27*, 609.; (d) Doi, A. M.; Irwin, R. D.; Bucher, J. R. *J. Toxicol. Environ. Health, Part-B,* **2005**, *8*, 109.

14. (a). R. H. Garrett, C. M. Grisham, *Biochemistry*, 3rd ed.; Thomson Brooks/Cole: Belmont, CA, **2005**; pp 645-657 & pp. 681.; (b) Rich, P. R. A. *FEBS Lett.* **1981**, *130*, 173.

15.(a) Quan, M.; Sanchez, D.; Wasylkiw, M. F.; Smith, D. K. *J. Am. Chem. Soc*. **2007**, *129*, 12847.; (b) M. Hattori in *Kirk-Othmer Encyclopedia of Chemical Technology*, 5th edition. Vol. 9 (Ed. A. Seidel), John Wiley & Sons: Hoboken, NJ, **2004**, pp. 300.

16. (a) Miyazaki, K.; Tabata, I.; Hori, T. *Coloration Tech.* **2012**, *128*, 51.

17. Rembold, M. W.; Kramer, H. E. A. *J. Soc. Dyers Colour*. **1980**, *96*, 122.

18. (a) Abhayawardhana, A. D.; Sutherland, T. C. *J. Phys. Chem*. C. **2009**, *113*, 4915.; (b) Campos-Martin, J. M.; Blanco-Brieva, G.; Fierro, J. L. G. *Angew. Chem. Int. Ed*. **2006**, *45*, 6962.

19. Eul, M.; Moeller, A.; Steiner, N. In *Kirk-Othmer Encyclopedia of Chemical Technology*, 5th ed.; Seidel, A., Ed.; *John Wiley & Sons: Hoboken*, NJ, **2004**; Vol. 14, pp. 42-51.

20.(a) Gao, H. X.; Han, B. X.; Li, J. C.; Jiang, T.; Liu, Z. M.; Wu, W. Z.; Chang, Y. H.; Zhang, J. M. *Synth*. *Commun*. **2004**, *34*, 3083; (b) Hangarge, R. V.; Jarikote, D. V.; Shingare, M. S. Knoevenagel Condensation Reactions in an Ionic liquid. *Green Chem.* **2002**, *4*, 266; (c) Greaves, T. L.; Weerawardena, A.; Fong, C.; Drummond, C. J. *J. Phys. Chem. B.* **2007**, *111*, 4082.; (d) T. Welton, P. Wasserscheid, Eds. *Ionic Liquid Synthesis*, 2nd ed. Chapter-2; Wiley VCH: Weinheim, **2008**. (e) Yoshizawa, M.; Xu, W.; Angell, C. A. *J. Am. Chem. Soc.* **2003**, *125*, 15411.

21. (a) Ohno, H.; Yoshizawa, M. *Solid State Ionics*, **2002**, *154*, 303.; (b) Xu, W.; Angell, C. A. *Science*, **2003**, *302*, 422.; (c) Zhao, C.; Burrell, G.; Torriero, A. A. J.; Separovic, F.; Dunlop, N. F.; MacFarlane, D. R.; Bond, A. M. *J. Phys. Chem. B.* **2008**, *112*, 6923.; (d) Shukla, S. K.; Khupse, N. D.; Kumar, A. *Phys. Chem. Chem. Phys*., **2012**, *14*, 2754.; (e) MacFarlane, D. R.; Pringle, J. M.; Johansson, K. M.; Forsyth, S. A. Forsyth, M. *Chem. Commun.* **2006**, 1905.

22.(a) Lavie, G.; Barliya, T.; Mandel, M.; Blank, M.; Ron, Y.; Orenstein, A.; Livnat, T.; Friedman, N.; Weiner, L.; Sheves, M.; Weinberger, D. *Photochem. Photobiol.* **2007**, *83*, 1270.; (b) Flom, S. R.; P. F. Barbara, *J. Phys. Che*m. **1985**, *89*, 448.

23. Palit, D. K.; Pal, H.; Mukherjee, T.; Mittal, J. P.; *J. Chem. Soc. Faraday Trans.* **1990**, *86*, 3861.

24. Yatsuhashi, T.; Inoue, H. M *J. Phys. Chem. A*, **1997**, *101*, 8166.

25.(a) Dahiya, P.; Kumbhakar, M.; Maity, D. K.; Mukherjee, T.; Tripathi, A. B. R.; Chattopadhyay, N.; Pal, H. *J. Photochem. Photobiol. A: Chem*. **2006**, *181*, 338.; (b) Dahiya, P.; Kumbhakar, M.; Mukherjee, T.; Pal, H. *J. Mol. Str*. **2006**, *798*, 40.

26.(a) Marzocchi, M. P.; Mantini, A. R.; Casu, M.; *J. Chem. Phys*. **1998**, *108*, 534. (b) S. Y. Arzhantsev, S. Takeuchi, T. Tahara, *Chem. Phys. Lett*. **2000**, *330*, 83.

27. Nad S.; Pal H. *J. Phys. Chem. A,* **2003**, *107*, 501.

28. O'Connor, D. V.; Philips, D. *Time Correlated Single Photon Counting.* Academic Press, New York, **1984**.

29. Singh, P. K.; Nath, S.; Bhasikuttan, A. C.; Kumbhakar, M.; Mohanty, J.; Sarkar, S. K.; Mukherjee, T.; Pal, H. *J. Chem. Phys*. **2008**, *129*, 114504.

30.(a) Kumbhakar, M.; Singh, P. K.; Nath, S.; Bhasikuttan, A. C.; Pal, H. *J. Phys. Chem. B.* **2008**, *112*, 6646.; (b) Dahiya P.; Kumbhakar M.; Mukherjee T.; Pal H.

Chem. Phys. Lett. **2005**, *414*, 148.; (c) Barik A.; Kumbhakar M.; Nath S.; Pal H. *Chem. Phys.* **2005**, *315*, 277.

31. (a) Schmidtke, S. J.; Underwood, D. F.; Blank, D. A. *J. Am. Chem. Soc.* **2004**, *126*, 8620.; (b) Schmidtke, S. J.; Underwood, D. F.; Blank, D. A. *J. Phys. Chem. A.* **2005**, *109*, 7033.

32. Neuwahl, F. V. R.; Bussotti, L.; Righini, R.; Buntinx, G. *Phys. Chem. Chem. Phys.* **2001**, *3*, 1277.

33. Zhang, X. –X; Liang, M.; Ernsting, N. P.; Maroncelli, M. *J. Phys. Chem. B* **2013**, 117, 4291.

34. Jin, H.; Baker, G. A.; Arzhantsev, S.; Dong, J.; Maroncelli, M. *J. Phys. Chem. B.* **2007**, *111*, 7291.

35. Samanta, A. *J. Phys. Chem. Lett.* **2010**, *1*, 1557.

36. Muramatsu, M.; Nagasawa, Y.; Miyasaka, H. *J. Phys. Chem. A.* **2011**, *115*, 3886.

37. Paul, A.; Mandal, P. K.; Samanta, A. *J. Phys. Chem. B.* **2005**, *109*, 9148.

38. Mandal, P. K.; Paul, A.; Samanta, A. *J. Photochem. Photobiol. A: Chem.* **2006**, *182*, 113.

39. Smulevich, G.; Foggi, P.; Feis, A.; Marzocchi, M. P. *J. Chem. Phys.* **1987**, *87*, 5664.

40. Smith, T. P.; Zaklika, K. A.; Thakur, K.; Walker, G. C.; Tominaga, K.; Barbara, P. F. *J. Phys. Chem.* **1991**, *95*, 10465.; (c) Smith, T. P.; Zaklika, K. A.; Thakur, K.; Barbara, P. F. *J. Am. Chem. Soc.* **1991**, *113*, 4035.

Chapter 7

Bimolecular Photoinduced Electron Transfer Reactions in Ionic Liquids

"There is one simplification at least. Electrons behave ... in exactly the same way as photons; they are both screwy, but in exactly in the same way..." — Richard P. Feynman

Steady-state and time-resolved fluorescence measurements have been carried out to monitor the bimolecular electron transfer reactions between the electron acceptor coumarins in its S1 state and the donor N, N-dimethylaniline in two ionic liquids having differences in their viscosity and polarity. The Marcus inverted region (MIR) has been demonstrated from the ultrafast electron transfer (ET) quenching experiments between coumarin derivatives and dimethylaniline in the studied viscous solvent media. The intrinsic ET rates estimated for the studied systems are faster than or competitive with the solvent reorganization and do not involve any significant diffusion of the reactants. It is inferred from the observed results that the inversion for the ET rates at higher exergonicity is a general phenomenon for bimolecular ET reactions in viscous media having exceedingly slow solvent relaxation. The two dimensional ET model that considers an extremely slow relaxing solvent coordinate and a fast relaxing intramolecular coordinate to assist the ET reaction is inferred as the most appropriate mechanistic model to account for the observed facts for the ET reactions in present viscous ionic liquid media.

7.1 Introduction:

Electron transfer (ET) is one of the most important and fundamental reactions having diverse applications in biological, physical, inorganic, and organic chemical systems.[1,2] Thus, understanding and manipulating the nature and the rates of ET processes has become a very active research area in chemical sciences.[3-5] Many electron donor-acceptor pairs which do not give good ET reactions in their ground states often undergo efficient ET reactions when either of them is excited to the higher excited state.[6] ET reactions involving an excited donor or an excited acceptor are thus commonly classified as the photoinduced electron transfer (PET) processes and most of the dynamic studies on the ET reactions in fact deal with these PET reactions.[2,7] One of the plus points with the PET reactions is that the ET can be triggered by an ultra short excitation light source (ultrafast lasers) and the dynamics of the subsequent ET process can be investigated efficiently in real time.[6,7] For PET to take place between an excited donor and a ground state acceptor (or an excited acceptor and a ground state donor) in solution, the reactants are required to come within the interaction distance via diffusion process to form the encounter complex (R, also called the precursor complex). The ET then takes place in the encounter complex to form the ion-pair state (P, also called the successor complex).[9] One of the most illustrious predictions of the ET theory given by Prof. R. A. Marcus is that the rate of the ET reaction should decrease with the exergonicity ($-\Delta G^0$) of the reaction as the exergonicity is increased beyond a certain value.[8] Following the simple classical approach to obtain rate constant for chemical reactions, the rate of an ET reaction can also be expressed as,

$$k_{et} = \nu_n \, \kappa_n \, \kappa_{el} \qquad (1)$$

where, ν_n is the nuclear frequency, i.e. the frequency at which the reactant state oscillates at the transition state (TS), κ_n is the nuclear factor, which is a measure of the thermodynamic probability of the reactants of having excess energy to reach the TS and κ_{el} is the transition probability of the reactants at the TS to cross to the product energy surface. The transition probability factor κ_{el} is given as, $\kappa_{el} = \exp(-\Delta G^*/RT)$, where ΔG^* is the free energy of activation. According to Marcus ET theory, [8] $\Delta G^* = (\Delta G^0 + \lambda)^2 / 4\lambda$; where ΔG^0 is the free energy change for the ET reaction and λ is total reorganization energy. If the value of $|\Delta G^0|$ exceeds more than the value of λ, Marcus inversion region (MIR) can be observed during electron

transfer reaction. In all these cases, the distance between the donor and acceptor is assumed to be constant, thus the diffusion of reactants is avoided, making the ET reaction a unimolecular process. Unexpectedly, experiments pertaining to bimolecular electron transfer reactions where donor and acceptor are two separate entities in order to ascertain the existence of the Marcus's inverted region ends up with consequences pioneered by D. Rehm and A. Weller.[9] It has been observed that the ET rate constant *vs.* ΔG^0 plots initially increases as ΔG^0 becomes more and more negative and ultimately reach to a plateau value at the highly exergonic region (highly negative ΔG^0). Such behaviour of the k_{et} *vs.* ΔG^0 plots is commonly known as the Rehm-Weller behaviour, as shown in Figure 1. The Marcus predicted bell shaped curve is also shown in Figure 1 for a comparison with the Rehm-Weller plot. To explain the experimentally observed behaviour for the k_{et} *vs.* ΔG^0 plots, Rehm and Weller proposed an empirical expression for ΔG^*, as given in equation 2:[9]

$$\Delta G^* = \left(\frac{\Delta G^0}{2}\right) + \left\{\left(\frac{\Delta G^0}{2}\right)^2 + \left(\frac{\lambda}{4}\right)^2\right\}^{1/2} \qquad (2)$$

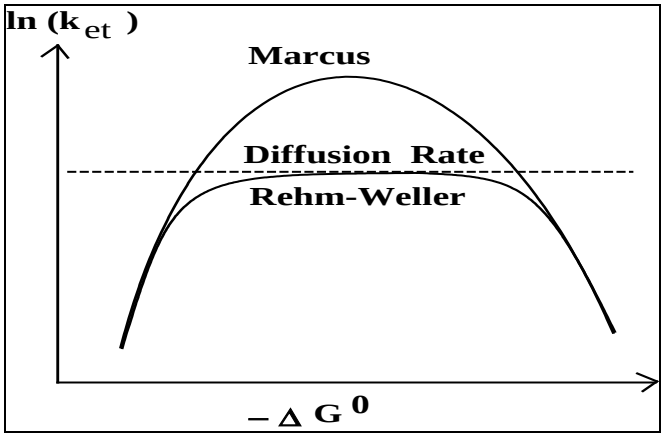

Figure 1: Conversion of the Marcus plot to the Rehm-Weller plot due to the effect of diffusion.

A cognisant attempt to circumvent the limiting situation arising from reactant diffusion as well as the non-availability of highly exergonic reactant pairs towards the observation of MIR in bimolecular ET reactions has been the judicious selection of systems with donor/acceptor distances fixed by protein frameworks, [12-14] covalent networks of rigid spacers,[10,11] frozen media,[13,14] and so on. In the cases of micelles and reverse micelles as the reaction media, due to the entanglement of the reactants with the surfactant chains and the slower solvent reorganization inside these media, or

in the excess of using electron donating solvents directly as a reactant, the availability of the donors within the reaction sphere of the excited acceptor, the MIR is interestingly found to appear at much lower exergonicity (~ 0.7 eV) than expected in conventional homogeneous solvents of similar polarity.[17,18] The results have been rationalized by invoking the two-dimensional ET (2DET) model,[19,20]where solvent and intramolecular reorganizations are suggested to occur independently to each other. To be mentioned here that in classical ET model the solvent and intramolecular reorganizations are coupled to each other and occur so fast that the reactant state is always in thermal equilibrium during the course of the ET reaction. In such cases thus, the effective reorganization energy that contributes in determining the free energy of activation (ΔG^*) for the ET reaction is the total reorganization energy λ, which is the sum of the intramolecular reorganization energy λ_i and the solvent reorganization energy λ_s, and is given as,

$$\lambda = (\lambda_S + \lambda_i) \qquad (3)$$

In the case of 2DET, however, as the solvent relaxation is considered to be slow, depending upon the propensity of this relaxation in comparison to ET rate, the λ_s can contribute only partially to the ΔG^* of the ET reaction, though λ_i contributes completely towards ΔG^*, as the intramolecular reorganization is considered to be faster than the ET reaction.

Coumarin dyes are good electron acceptors in their excited singlet states (S_1).[21,22] Since last decade, significant research has been carried out on PET reactions involving different amines as the electron donors and various coumarin dyes as the electron acceptors, enriching our knowledge on the kinetics and mechanism of ET reactions under different reaction environments. Many of these pervasive investigations on PET reactions using amine donors and coumarin acceptors have been concentrated mainly in conventional homogeneous solvents or in microheterogeneous media like micelles, reverse micelles, etc.[17,18,22,23] To comprehend the effect of highly viscous solvent media on ET reactions, ionic liquids (ILs) have been chosen as the reaction media in the present study, as the PET studies in ILs are very limited and also because these solvents have attracted remarkable attention in recent years, due to their interesting properties like, low volatility, intrinsic conductivity, high thermal stability, tailorability of the constituents, and so on.[24-26] Currently, applications of ILs as solvents permeate most fields of chemistry.

Among other applications, ionic liquids are being used as electrolytes in photovoltaic cells and super-capacitors, as green solvents for synthesis and catalysis, as separation tools for mixtures, and as media for storage and transport of toxic gases.[24a,26b] For all of these emerging applications, an understanding of the basic physical chemistry of ILs and how they behave as solvent media for chemical reactions is of utmost importance.[24c,26a] Most chemical reactions take place in solution, which makes it very important to choose a proper solvent for the given reaction. The tailorability of ILs makes them to stand out as the "designer solvents".[25] For example, the alkyl chains of the cation, or less commonly the anion, can be easily varied to make a solvent of the desired size, viscosity and polarity,[26] may be useful to modulate the reactions of our interest.

Of late, several groups have reported the MIR in bimolecular ET reactions in various organized assemblies.[27] Similar observation of MIR has also been reported by many groups in different high viscosity room temperature ILs, where solvent reorganization is generally very slow.[28] In most of these studies on bimolecular ET reactions, the fluorescence quenching kinetics is mostly applied following steady-state (SS) and time resolved (TR) time-correlated single photon counting (TCSPC) measurements.[29] In the SS data, the positive deviation from Stern-Volmer (SV) linearity is generally observed in such systems, even in the absence of any ground state complex formation, and is ascribed to the quenching involving close vicinity D-A pairs at the moment of photo-excitation. As the closely spaced D-A pairs participate in instantaneous quenching (i.e. static quenching); they gradually contribute more to the observed quenching as the quencher concentration is increased.[27a-j] Contrary to SS results, however, linear SV plots are mostly observed for the same set of the reaction pairs, where average lifetime values obtained from TCSPC measurements are correlated with the quencher concentration following SV analysis. Accordingly, such SV analysis is used to estimate the quenching constant k_q (*a measure of the ET rate in such systems*), which mainly reflects the dynamic part of the quenching process, with negligible contributions from static or transient quenching, even if the latter are not absent completely.[27a-d] In view of that, simple Smoluchowski approach for predicting effective k_q values derived from linear SV plots of the lifetime data are in general been considered to visualize the Marcus correlation (*free energy dependent changes in the ET rates*) and thus to comprehend the kinetics and energetic aspects of the studied ET reactions. In all these studies the MIR has been clearly observed and

interestingly it is found that the exergonicity for the onset of MIR in these cases is dependent on the relative propensity of the solvation relaxation dynamics and ET rates.

With the expanding theoretical approach to account for the quenching dynamics, encompassing the static quenching at early time scales to the diffusion limited conditions at the longer times, quantitative analysis of different quenching components is in principle possible as an alternative to SV analysis in a viscous media where the effect of retarded reactant diffusion would be very much pronounced on the reaction rates. Important to mention here that based on the conventional Marcus formulation coupled with differential encounter theory (DET),[30] to account for all the stages of bimolecular ET quenching in the viscous ILs and dimethyl sulfoxide (DMSO)/glycerol (GLY) mixed solvents, it has been recently concluded by Vauthey & coworkers[31] that the MIR observed in such viscous media apparently arises from (1) the neglect of different quenching regimes (i.e. static, transient and stationary regimes) in the simple SV equation and (2) the differential excited state lifetimes (τ_0) of the fluorophores considered in the donor-acceptor series. It is thus important and essential to explore the merit of these claims of the authors that counter the well studied observation of MIR in viscous media, which is also one of the goals in the present study to carryout bimolecular ET reactions in viscous IL solvents.

Though the first argument of Vauthey & coworkers[31] regarding transient effects on ET reactions is theoretically well established for long and certainly can lead to overestimation of the quenching rates following SV analysis of the sub-nanosecond resolved TCSPC data in a viscous medium and thus can influence the Marcus correlation curve to some extent when there is a broad distribution of fluorophore lifetimes, but, these aspects would necessarily not affect the intrinsic ET rate (k_0, in the static quenching regime), measured using a ultrafast technique like fluorescence up-conversion (FU), and thus will mainly be modulated by the energetics of the reacting D-A pairs. To be mentioned that with ultrafast quenching experiments, performed using FU measurements, the MIR has already been reported for k_0 in various micelles, where D and A are maintained to be at the interaction distance (*at close constant or at close proximity*) prior to the photoexcitation.[27c,27d] Such situations were realized either by using the surfactant directly as the electron acceptor, e.g. in cetyl pyridinium chloride (CPC) micelles, or using high concentration of the quencher

(amine donor) in normal micelles, e.g. in TX-100 micelle.[27c,27d] Typical results in these systems displaying clear MIR are shown in Figure 2.[27c,27d] To address the second issue, i..e. the effect of τ_0 of the fluorophores on the observed MIR, it is essential to carry out measurements involving a large number of fluorophores using both FU and TCSPC measurements and thus to see if there is in fact any correlation between the estimated ET rates and the τ_0 of the fluorophores used. Thus to explore the merit of the arguments put forward by Vauthey & coworkers[31] and also to independently investigate if MIR for bimolecular ET reactions is indeed a unique observation in viscous reaction media, in the present work we have investigated the fluorescence quenching studies involving a series of coumarin dyes (Chart 1) as the acceptors and *N*,*N*-dimethylaniline (DMAN) as the donor in two IL solvents, e.g. [Emim][NTf_2] (IL1, η~37cP) and [Hmim][NTf_2] (IL2, η~81cP). In the present study, time resolved fluorescence experiments were performed; (1) with FU measurements to explore the early stages of the quenching kinetics and (2) with TCSPC measurements to explore the longer time quenching kinetics for the studied systems, as discussed in the following sections.

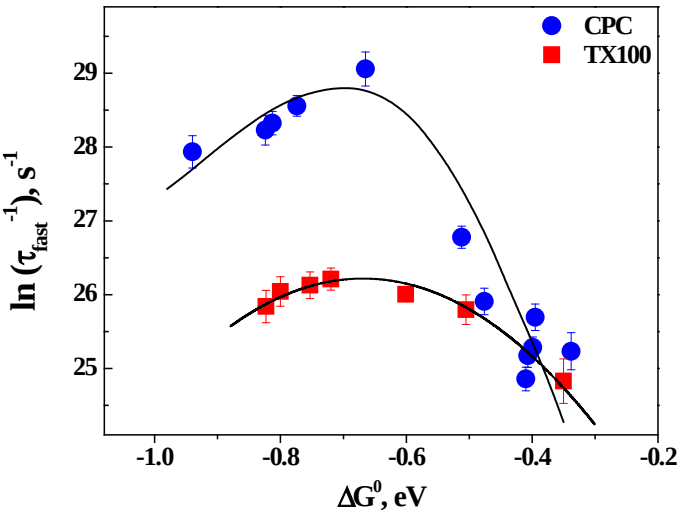

Figure 2: Marcus correlation for coumarin-DMAN systems in CPC and TX-100 micelles. Revised plot from Ref 27c, 27d.

7.2 Experimental Procedures:

7.2.1 Synthesis of Ionic Liquids

7.2.1.1 Materials

Laser grade coumarin dyes were obtained from Exciton, USA. *N*-methyl imidazole, 1-bromohexane, 1-bromoethane were procured from M/s. Sigma Aldrich and were further distilled prior to their use. $LiNTF_2$ was purchased from M/s. Sigma Aldrich and dried in vacuum for 6 hr. prior to its use.

7.2.1.2 Preparation of Ionic Liquid

Ionic liquids,[Emim][NTf_2] (IL1) and [Hmim][NTf_2] (IL2) have been synthesized following the standard procedures.[24a-b] We have followed two principle steps to synthesize these ILs. In the first step, known as quartanization, imidaziolium based organic cation has been prepared by mixing *N*-methyl imidazole and *N*-alkyl bromide at 1:1.1 molar ratios. Excess alkyl bromide was removed by washing with ethyl acetate for several times. In the second step, metathesis was followed to replace the bromide anion by bis(trifluoromethylsulfonyl)imide [NTf_2^-]. Here the organic cation synthesized during first step was mixed with $LiNTf_2$ at equimolar ratio in water. Thereafter, the mixture was subjected to 12 h stirring. The synthesized ILs were extracted in dichloromethane (DCM) and followed by the solvent removal with rotary vapour at reduced pressure. To remove the trace amount of water, the ILs were desiccated under high vacuum for 12h prior to their use. The ILs were purged with nitrogen gas during their storage. The water content, as estimated by Karl-Fischer titration, was around 20 ppm for both the ILs. Purity of the prepared ILs was ensured by ^{1}H-NMR (recorded at 200 MHz with Bruker Spectrometer).

7.2.2 Steady-State and Time-Resolved Fluorescence Measurements

Ground-state absorption spectra were recorded using a JASCO model V530 spectrophotometer (Tokyo, Japan). Steady-state fluorescence spectra were recorded using a HITACHI model F-4010 spectrofluorimeter (Tokyo, Japan).

Ultrafast fluorescence decays were recorded using the femtosecond fluorescence up-conversion (FU) measurements. Briefly, in the present FU setup (FOG 100, CDP Inc., Russia), the coumarin dyes were excited close to their absorption maxima (~390-425 nm) in IL solutions using the second harmonic (SH) of a mode locked Ti: Sapphire laser (CDP Inc., Russia, 50 fs, 82.2 MHz repetition rate), pumped by a 5W DPSS laser. The SH was generated in a type-I BBO angle-tuned phase-matched nonlinear crystal with 0.5 mm thickness. Optical delay between the

excitation and the gate pulses was varied using a delay rail (with smallest steps of 6.6 fs) at the path of the gate pulse. The up-converted signal (using a 0.5 mm Type-I BBO crystal) corresponding to the emission maxima of the dyes (~490-535 nm) was measured with a photon counter, after passing through a proper band-pass filter and a double monochromator. For each of the decays, at least three scans were taken to check the reproducibility of the decays as well as for averaging. In all these measurements, the samples were taken in a rotating cell (0.4 mm path length) to have a better heat dissipation and thus to avoid photo-degradation of the dyes. For the measurements of the fluorescence decays, the polarization of the excitation beam was set to magic angle (54.7^0) with respect to the horizontally polarized gate light pulses using the Berek wave plate arrangement[5] (CDP Inc., Russia). A cross-correlation of the fundamental and the SH displayed a full width at half maxima (FWHM) of ~210 fs for the instrument response function (IRF). Femtosecond transients were fitted by convolution analysis using a Gaussian shape for the IRF. In case of fluorescence anisotropy measurements, samples were excited with vertically and horizontally polarized SH pulses using appropriate angles for the Berek's wave plate. In the present setup, since the horizontally polarized fluorescence is mixed with the horizontally polarized gate pulses in the up-conversion crystal, the measured sum frequency signal for horizontally polarized excitation measures I_{II} and that for vertically polarized excitation measures $I_{\perp}$. Accordingly, fluorescence anisotropy decay, $r(t)$, was calculated as, $r(t)=(I_{II}-I_{\perp})/(I_{II}+2I_{\perp})$.

The nanosecond fluorescence decays for the coumarin dyes in the absence and presence of the quencher were measured using a diode laser (374 and 408 nm, <100 ps, 1 MHz) based time-correlated single photon counting (TCSPC) setup (IBH, UK). In the present work, a MCP-PMT detector (IBH, UK) was used for the fluorescence decay measurements. The instrument response function for this setup is ~130 ps at FWHM. All the experiments were carried out with magic angle configuration and at ambient temperature of 298± 1 K.

7.3. Scheme of the Study:

In the present study, our main goal is to investigate electron transfer reactions between coumarin dyes (abbreviated with C and followed by the respective numbers as used in their commercial names) and *N*,*N*-dimethyl aniline (DAMN) using [Emim][NTf_2] (1-ethyl-3-methylimidazolium bis(trifluoromethylsulfonyl)imide; IL1)

and [Hmim][NTf_2] (1-hexyl-3-methylimidazolium bis(trifluoromethylsulfonyl)imide; IL2) as the reaction media.

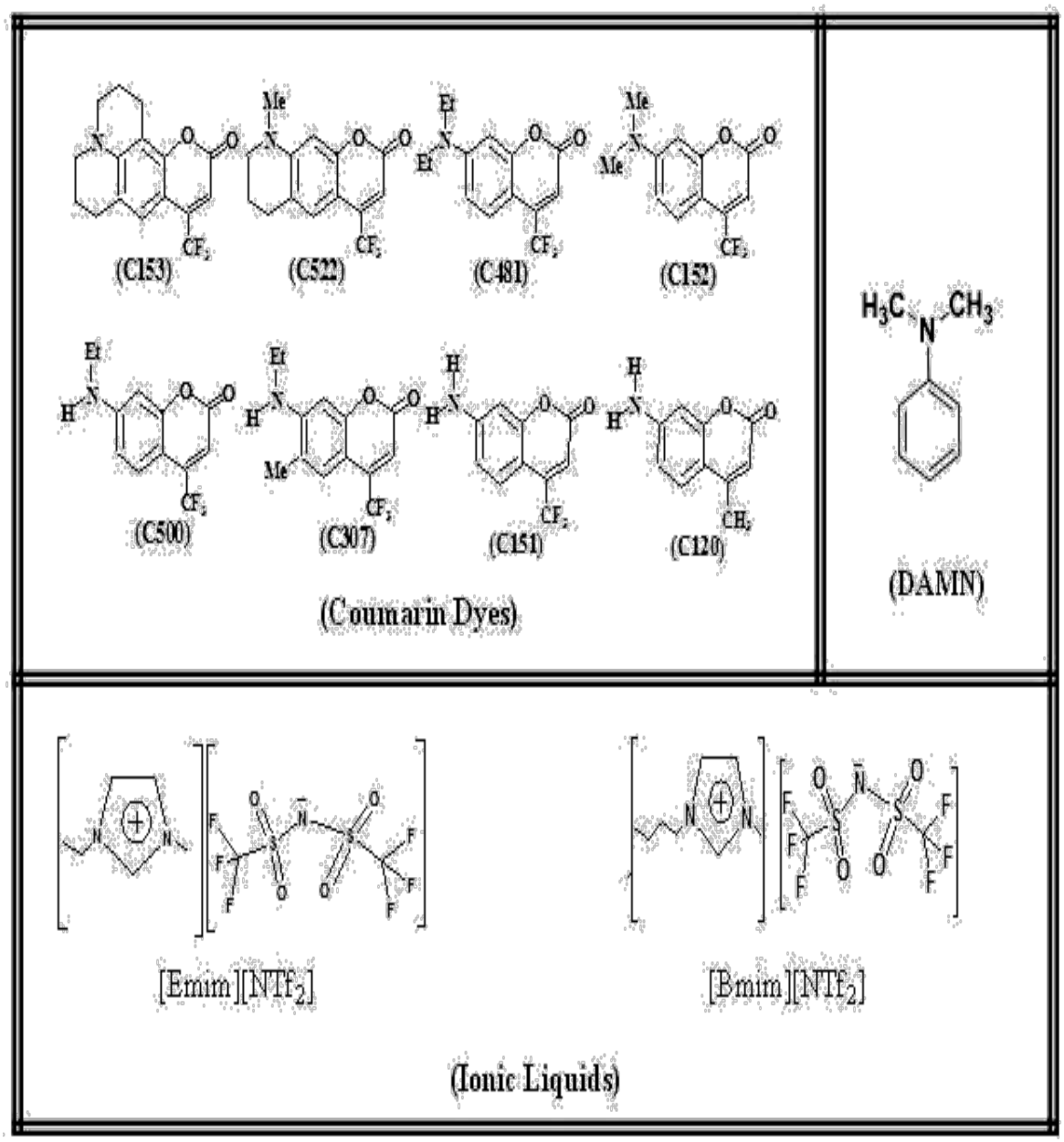

Scheme 1: Chemical structure of *N*, *N*-dimethyl aniline (electron donor), coumarin dyes (electron acceptors) and ionic liquids (solvent media) used in the present study are shown.

7.4 Results and Discussion:

7.4.1 Inversion in the Intrinsic ET Rates

Ultrafast fluorescence decays obtained from FU measurements for the coumarin dyes in the presence of DMAN in both IL1 and IL2 solvents are strongly non-exponential in nature, as shown in Figure 3 and 4, respectively.

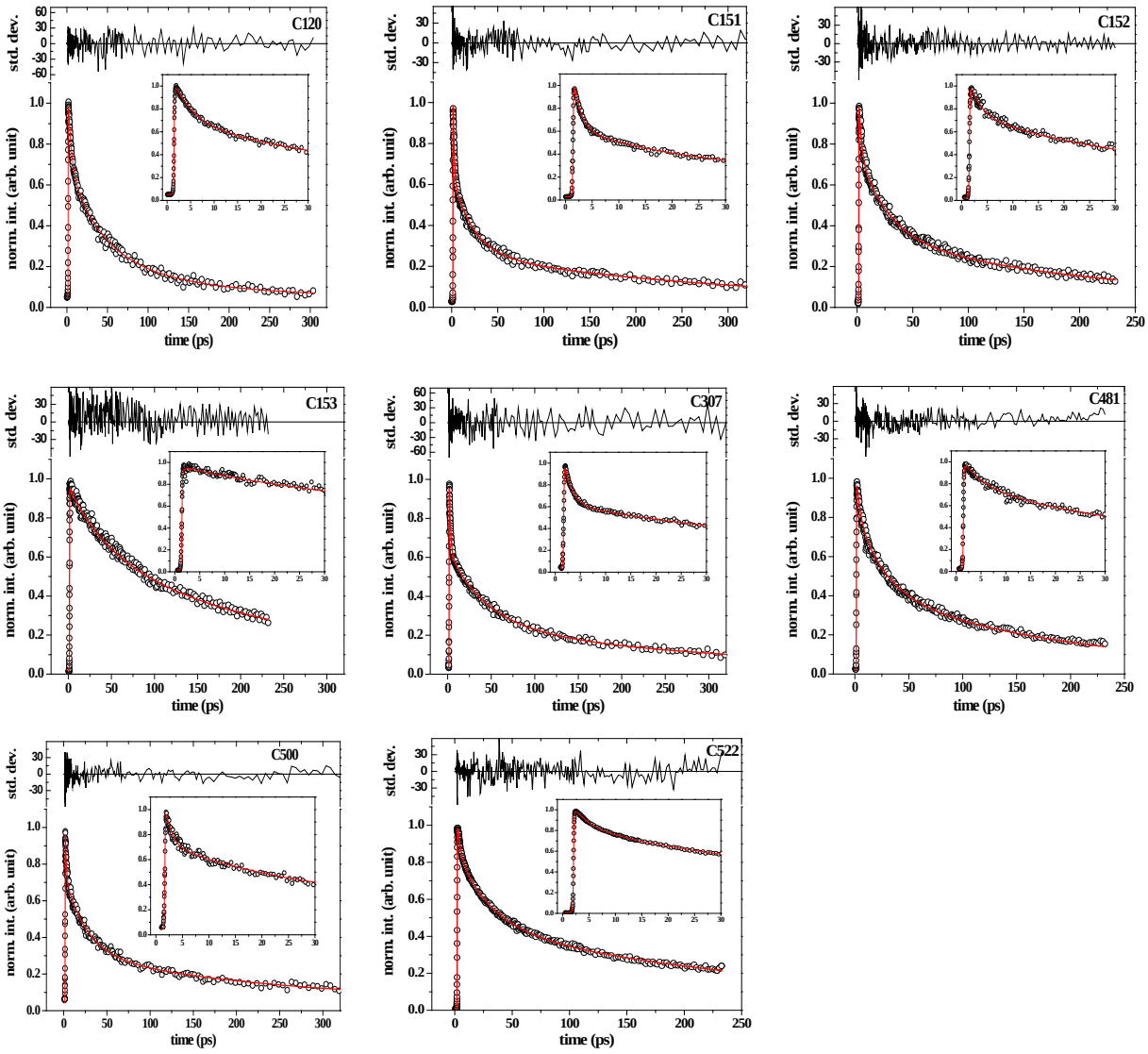

Figure 3: Ultrafast fluorescence decays of the coumarin dyes (O) in the presence of DMAN, recorded in IL1 solvent following up-conversion measurements. The tri-exponential fits (line) of these decays following convolution analysis are also shown. Insets show the expanded initial part of the decays to indicate the quality of the fits at the early time scales.

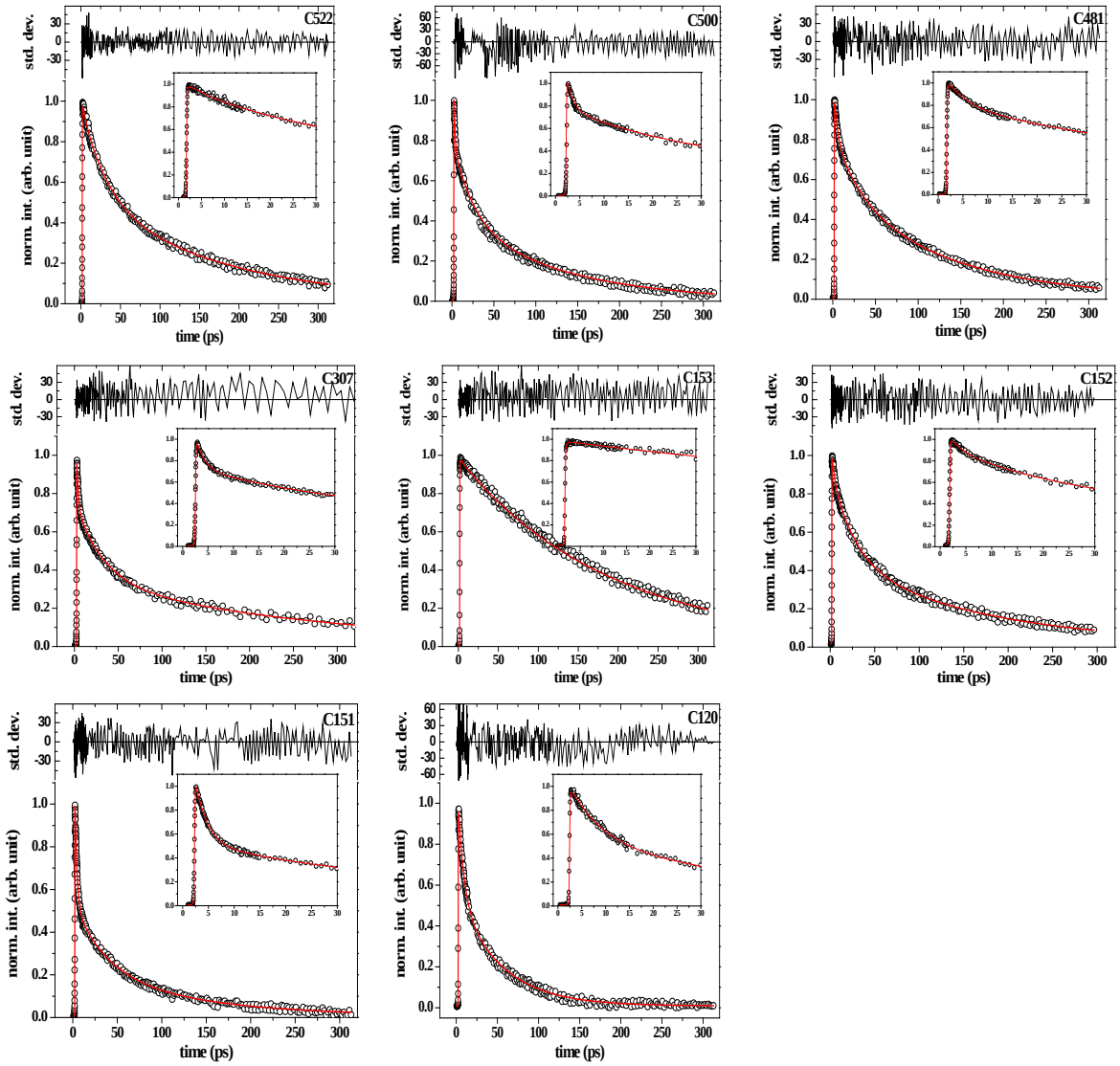

Figure 4: Ultrafast fluorescence decays of the coumarin dyes (O) in the presence of DMAN, recorded in IL2 solvent following up-conversion measurements. The tri-exponential fits (line) of these decays following convolution analysis are also shown. Insets show the expanded initial part of the decays to indicate the quality of the fits at the early time scales.

These decays were fitted by convolution method using Gaussian shape for the instrument response function (IRF, ~200 fs) and assuming tri-exponential function for the decays, expressed in general as, $I(t) = \sum A_i \exp(-t/\tau_i)$, where, τ_i is the fluorescence lifetime and A_i is the pre-exponential factor for the i-th component.[35]

The fitting parameters obtained from the analysis of the ultrafast fluorescence decays of the coumarin dyes in IL1 and IL2 are listed in Table 1. Fluorescence

lifetime (τ_0) of the coumarin dyes in the studied solvents in the absence of the DMAN quencher were estimated following TCSPC measurements and are also listed in Table 1 for a comparison. As indicated from Table 1, the shortest fluorescence lifetime components (τ_1) of the ultrafast decays for the dyes in the presence of the quencher, which ranges between 1-10 ps (*henceforth designated as* τ_{fast}), are several orders of magnitude shorter than the τ_0 of the dyes in the absence of quenchers. Though all the three time constants estimated from the ultrafast decays cannot be attributed directly to specific physical processes related to the diffusion influenced quenching dynamics, yet the observed fastest decay time constant (τ_{fast}) in the presence of DMAN quencher can safely be assigned to the ultrafast ET process, as the diffusion of the reactants would be negligible during this time scale. Consequently, the inverse of this shortest time constant is considered as the measure of the intrinsic ET rate ($k_0 = \tau_{fast}^{-1}$) for the respective donor-acceptor systems. This is similar to the earlier reports, where ET is effectively dominated by the intrinsic quenching for the initial about few ps time-spans following photo-excitation.[31,33, 36]

For the studied donor-acceptor systems in IL solvents, the reaction free energy (ΔG^0) values were estimated using the following Rehm-Weller expression, [9]

$$\Delta G^0 = E_{\left(\frac{D}{D^+}\right)} - E_{\left(\frac{A}{A^-}\right)} - E_{00} - \frac{e^2}{4\pi\varepsilon_0\varepsilon_{IL}R_0} \qquad (4)$$

where, E_{00} is the excitation energy of the coumarin dyes in the S_1 state, e is the charge of an electron; ε_{IL} is the static dielectric constants of the reaction medium.[32,34] The R_0 (=R_A+ R_D) is the center to center distance between the interacting coumarin (R_A) and DMAN (R_D). The E_{00} values were estimated from the crossing wavelength of the normalized absorption and fluorescence spectra of the dyes in the respective cases. The R_A and R_D values were estimated using Edward's volume addition method.[36] The ε_{IL} values were obtained from the reported literatures.[34] The calculated free energy values for different systems are listed in Table 1.

Table 1: Fluorescence decay and ET parameters of Coumarin-DAMN systems in ILs at 298.15±1 K, as estimated using fluorescence up-conversion measurements.

Ionic Liquid	Coumarin	τ_0, ns[a]	Decay time constants (τ_i), ps (%)[b]	E(A/A[c]), eV	E_{00}, V	ΔG^0, eV[d]	k_q x 10^8, $M^{-1}s^{-1}$ [e]
IL1	C153	5.81	10.26 (0.91), 55.42 (9.99), 298.18 (89.10)	-1.69	2.55	-0.155	4.10
	C522	5.86	2.8 (0.41), 29.23 (9.36), 294.01 (90.23)	-1.63	2.64	-0.306	7.98
	C481	1.43	3.54 (0.76), 25.63 (11.03), 185.10 (88.21)	-1.66	2.70	-0.340	4.90
	C152	2.74	2.07 (0.62), 25.56 (12.57), 218.33 (86.81)	-1.63	2.71	-0.380	9.01
	C500	4.81	1.15 (0.52), 24.91 (13.34), 239.96 (86.14)	-1.61	2.79	-0.477	9.11
	C307	5.45	1.49 (0.99), 34.63 (18.28), 220.3 (80.73)	-1.68	3.01	-0.628	3.71
	C151	5.50	1.29 (0.86), 22.52 (12.83), 249.1 (86.31)	-1.57	2.92	-0.644	6.87
	C120	3.70	3.97 (1.91), 38.69 (90.44), 302.1 (67.65)	-1.61	3.14	-0.827	1.32
IL2	C153	5.74	10.01 (0.03), 55.28 (0.17), 189.07 (99.80)	-1.69	2.57	-0.175	2.86
	C522	5.65	3.50 (0.15), 32.02 (12.92), 180.55 (86.93)	-1.63	2.64	-0.304	4.61
	C481	1.81	3.80 (0.98), 31.67 (10.93), 134.57 (88.09)	-1.66	2.69	-0.324	8.29
	C152	2.95	2.18 (0.31), 24.88 (13.03), 159.61 (86.66)	-1.63	2.70	-0.362	6.59
	C500	5.13	1.14 (0.64), 23.07 (13.58), 125.22 (85.78)	-1.61	2.80	-0.487	7.23
	C307	5.83	1.58 (0.95), 30.59 (21.97), 180.01 (77.08)	-1.68	2.98	-0.598	7.89
	C151	4.98	2.24 (2.46), 36.02 (26.86), 130.2 (70.68)	-1.57	2.93	-0.658	6.90
	C120	3.69	6.90 (6.44), 52.28 (56.33), 198.7 (37.33)	-1.61	3.12	-0.807	1.51

The variations of k_0 (= τ_{fast}^{-1}) with ΔG^0 values for coumarin-DMAN systems in two IL solvents are shown in Figure 3. It is very evident from this figure that the ET rate increases initially with an increase in the reaction exergonicity ($-\Delta G^0$), reaches a maximum value around the free energy change of about -0.5 eV and then the ET rate gradually decreases again as the reaction exergonicity is made even higher. Thus MIR and the full bell-shaped Marcus correlation curve for bimolecular ET are clearly evident for the studied electron donor-acceptor systems in the IL solvents, similar to that reported earlier for different micellar media.[18, 23, 27] Figure 5 also shows the plots of the inverse of the second fastest decay constants (τ_2) obtained for the present donor-acceptor systems in the two ILs as a function of the ($-\Delta G^0$) values of the reaction. Interestingly, the MIR and bell-shaped correlation is also clearly seen for this τ_2 component, which occur in the range of 20-60 ps and obviously are in between the static and transient regimes of the diffusion process.[31,46]

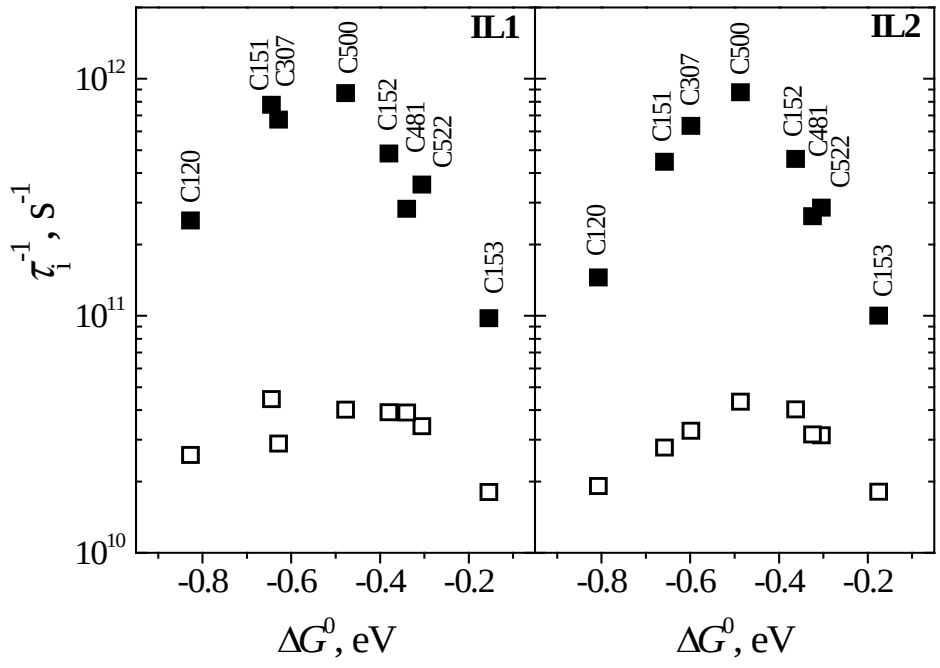

Figure 5: Plots of τ_{fast}^{-1} (=k_0) and τ_2^{-1} (=k_1) vs. ΔG_0 for coumarin-DMAN systems in the two IL solvents, represented by solid and open squares, respectively.

7.4.2 Calculation of Diffusion Coefficient and Diffusion Rate

The relative diffusion coefficients (D, m^2s^{-1}) were calculated following Stokes-Einstein relationship,

$$D = \frac{k_B T}{6\pi\eta R_h}; \qquad \text{where, } R_h = \frac{1}{R_D^{-1} + R_A^{-1}} \tag{5}$$

where, k_B is the Boltzmann constant, T is the absolute temperature, η is viscosity of the solvent and R_h is the effective hydrodynamic radius; R_D and R_A being the radii of coumarin and DMAN, respectively. The values for R_D and R_A were estimated using Edward's volume addition method.[36] The η values were taken as 37 and 81 cP for IL1 and IL2 respectively, as reported in the literature.[37,38] Considering the average R_h value for the donor-acceptor systems used in this work, the relative diffusion coefficients are estimated to be ~3.41 x 10^{-11} and ~1.56 x 10^{-11} m^2s^{-1} in IL1 and IL 2, respectively. Following Smoluchowski prediction and considering average R_h value for the donor-acceptor systems used, the diffusion-limited rate constant (k_D, $M^{-1}s^{-1}$) for present systems were estimated using the following equation,

$$k_D = \frac{4\pi N_0 R_h D}{1000\,\eta} \approx \frac{8\times10^6 RT}{3\eta} \tag{6}$$

where, N_0 is the Avogadro's number and R is the universal gas constant. Thus, the k_D values in IL1 and IL2 solvents are thus found to be ~1.8 x 10^8 $M^{-1}s^{-1}$ and ~0.8 x 10^8 $M^{-1}s^{-1}$ respectively.

The time scale for the ultrafast quenching observed for the present systems is similar to the earlier reports, where ET is effectively dominated by static quenching for the initial about few ps time-spans following photoexcitation.[39-41] The root mean square distance that a quencher can diffuse ($\sqrt{2D\tau}$,[29] where D is the relative diffusion coefficient) within 10 ps is only ~0.26 Å in [Emim][NTf_2] and ~0.18 Å in [Hmim][NTf_2]. These distances are much smaller than the average molecular diameter of the coumarin dyes used (~7.4 Å, following Edward's volume addition method[36]). Hence, the effect of reactant diffusion during the ultra-short time scale of the τ_{fast} component can simply be neglected for the present systems.

7.4.3 Fluorescence Anisotropy Decay and Reorientational Motion of Reactants

In the current perspective, it is also important to see if the reorientational motion of the reactants can have any possible influence in modulating the estimated intrinsic ET dynamics (k_0) estimated from ultrafast fluorescence measurements.[33] Thus, rotational correlation times (τ_r) of the coumarin dyes were estimated in the two IL solvents, using both FU measurements for the faster time scales and TCSPC measurements for the slower time scales. Typical of these anisotropy decays for C153 dye in IL1 solvent

is shown in Figure 6, where faster part was measured using FU and latter part was measured using TCSPC technique.

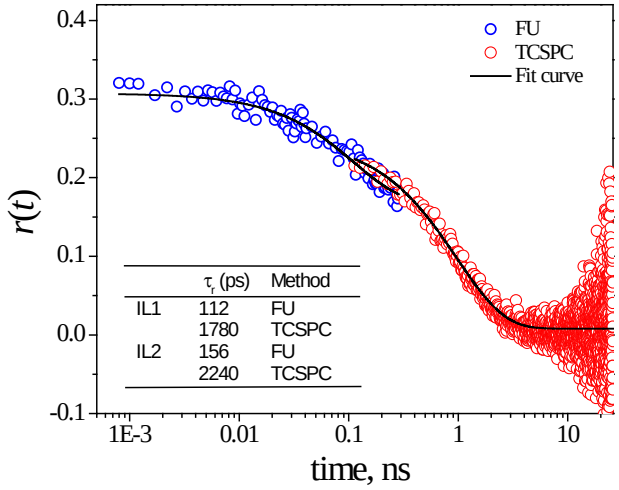

Figure 6: Fluorescence anisotropy decay of C153 in [Emim][NTf_2] (IL1). The faster part of the decay (blue) was measured using FU technique and the latter part of the decay (red) was measured using TCSPC technique.

Both the initial and the latter parts of the anisotropy decays, as measured by FU and TCSPC techniques, respectively, are seen to independently fit well with a single-exponential function. Accordingly, the faster and the slower components of the rotational time constants are estimated as τ_{r1} ~100-150 ps and τ_{r2} ~1800-2200 ps, respectively. Thus, considering the rotational time constants as estimated in the present work for the coumarin dyes in the studied ILs (*cf.* Figure 6), it is evident that even the shortest τ_{r1} values are orders of magnitude longer than the fastest ET components (k_0) observed for the studied donor-acceptor systems. These results clearly suggest that in high viscous media like the ones used in the present study an excited fluorophore undergoes an ultrafast ET reaction with one of the closely placed pre-existing quencher molecules that gives a sizable donor–acceptor electronic coupling and this ultrafast interaction effectively occurs under the non-diffusive conditions, without involving any translational and rotational motions of the reactants.[27c]

In addition to the MIR observed in the present cases, the other interesting observation is that the inversion appears at a much lower exergonicity than one would expect considering the conventional Marcus ET model, where solvent relaxation is

considered to be very fast. Solvent reorganization time in ILs is known to span from sub-ps to few ns and the contribution of the ultrafast solvation component with <10 ps relaxation time is only around 10-20% of the total solvent relaxation.[45] As a consequence, in ILs the slow diffusive solvent reorganization has to compete with ultrafast ET dynamics. Moreover, since this solvent relaxation is very slow, according to 2-DET model its role towards the free energy of activation (ΔG^*) for the ET reaction will be less effective than one would expect from the the conventional ET theory, where due to very fast solvent relaxation the reactant will always be in thermal equilibrium along the solvent coordinate. It implies that in the slow solvent relaxation cases, the ET has to occur along the *q* coordinate, from a large distribution of temporally evolving non-equilibrated reactant states in the *X* coordinate, as schematically presented in Figure 7.[21,48] Therefore, it is evident that not only the time-dependent donor-acceptor separation as it evolves by the diffusional motion of the reactants, but also the temporal evolution of the solvent configuration plays an immense role in determining the bi-molecular ET dynamics in a viscous media, where diffusion of reactants as well as solvent reorganization are retarded very largely.

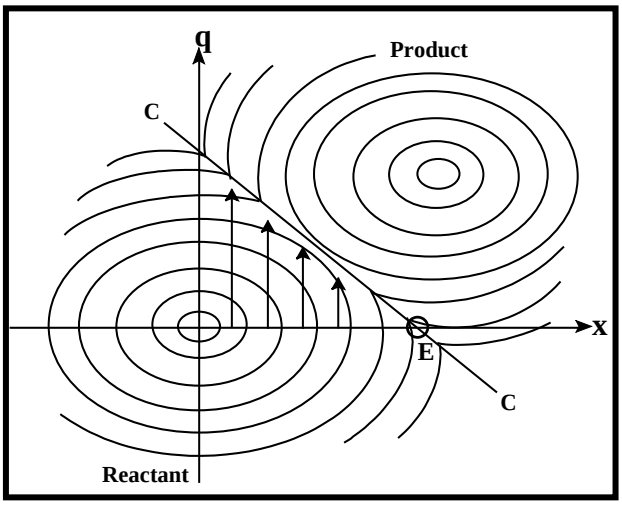

Figure 7: Isoenergy contours of the potential energy surfaces drawn in a two-dimensional plane for the reactant and product states in relation to the two-dimensional ET model. In this scheme, *X* representing the solvent coordinate and *q* representing the nuclear coordinate. The line C-C represents the transition state curve corresponding to the crossing of the reactant and product state potential energy surfaces. ET occurs along the *q* coordinate for any solvent configuration (*X*), as are shown by arrows parallel to *q* coordinate. The point E corresponds to the single crossing point of the reactant and product state potential energy surfaces along the *X*

axis and represents the unique transition state as to be consideered following the conventional ET theory.

It is pertinent at this juncture to compare the observation of MIR as we made in this study in high viscous and slow relaxing media with the one of the recent result reported on Marcus inversion behaviour for bimolecular ET interaction in normal fast relaxing solvent like ACN.[46] In this latter case, the intrinsic ET rates (static quenching) have been theoretically estimated by fitting of the ultrafast fluorescence decays incorporating the diffusion assisted conventional Marcus ET model but using the finite dielectric response of the solvent. However, with an average solvation time of 260 fs[46] and the derived fastest ET time of ~ 250 fs (approximately corresponding to k_0 value of 40×10^{11} $M^{-1}s^{-1}$ at ~1 M quencher concentration [46]) under non-adiabatic condition (V_{el} ~ 72 cm^{-1}), the ET reaction is certainly competitive with solvation process. Hence, Sumi-Marcus 2-DET model would have been better equipped to illustrate such ET reaction, as discussed earlier, than the semi-classical Marcus ET model used in reported study. Besides, the inability of the model to fit the initial part of the ultrafast decays (*i.e. about initial 1 ps of the data*) perhaps also suggests the possibility of even faster ET rate than solvation rate, as considered under 2DET model.

7.4.4 Sumi-Marcus 2DET Model and Observation of MIR in the Present ET Systems

Although a brief theoretical foundation has been discussed in the introduction part of the thesis, yet a logical approximation of the system parameters can certainly be obtained to appreciate the insights of the ET dynamics and even to attain a semi-quantitative relationship among the ET results in the viscous ionic liquids solvents. Following the Marcus ET theory, the rate constant k_{et} for an outer sphere ET reaction under non-adiabatic condition can be given by the following general quadratic equation,

$$k_{et}(NA) = \frac{2\pi}{\hbar} \frac{V_{el}^2}{\sqrt{4\pi\lambda_S T k_B}} exp\left(\frac{\Delta G^*}{k_B T}\right) \quad (7)$$

where each term corresponds to their standard meaning. In the 2DET model, the free energy of activation $\Delta G^*(X)$ for the ET reaction becomes a function of the non-equilibrium solvation coordinate X and can be expressed as [21,22,49]

$$\Delta G^{*}(X) = \frac{\left[\Delta G^{0}(X) + \lambda_s(1-2X) + \lambda_i\right]^2}{4\lambda_i} \qquad (8)$$

In the present photoinduced ET reactions, it is obvious that the initial X coordinate for the reactant state produced through photo-excitation, say X_g, would be quite away from the equilibrium X coordinate (X=0) for the reactant, as the dipolar nature of the fluorophore changes very substantially in the excited state compared to that in the ground state. Let this non-equilibrium X coordinate is X_g. Under the present situation, if the solvent relaxation process is significantly slow, as would be the case in relation to the ultrafast ET component in ILs, only the $(1-2X_g)$ fraction of λ_s {i.e. $\lambda_s^{eff} = (1-X_g)\lambda_s$} can contribute to $\Delta G^*(X)$. Accordingly MIR would show its onset at a much lower exergonicity ($|\Delta G^0| << \lambda_s$) than what it would have been under the conventional ET model ($|\Delta G^0| >> \lambda_s$).

The value of X_g for the studied D-A systems can roughly be estimated from the observed differences in the Stokes shifts ($\Delta\nu$) for the coumarin dyes between the concerned IL media and a nonpolar reference solvent (e.g. hexane), where the dielectric solvation can be assumed negligible. The $\Delta(\Delta\nu)$ and X_g values are related by the following equation,[21-23]

$$\Delta(\Delta\nu) = 2\lambda_s X_g^2 \qquad (9)$$

An estimate of the average X_g parameter thus obtained as ~0.29 for the present ET systems (*cf.* Table 2) which translates the contribution of λ_s towards the free energy of activation for the initially prepared reactant state following photo excitation as about 0.42 eV in the two studied ILs, much lower than the total solvent reorganization energy of ~1 eV. Interestingly, this value is slightly lower than the effective exergonicity (~ 0.5 eV) indicated for the onset of MIR for the studied systems (*cf.* Fig. 4). This small difference, we propose is due to the contribution of the intramolecular reorganization energy λ_i. From the above considerations it is therefore quite justified to assume that the ultrafast component (τ_{fast}) of the ET process in the studied ILs is mainly governed by the 2DET mechanism where solvent reorganization contributes only partially to the effective free-energy of activation.

Table 2: Average 2DET parameters for the coumarin-DMAN systems studied in IL solvents.

	$\langle\lambda_s\rangle$, cm^{-1}	$\Delta\langle\Delta\nu\rangle$, cm^{-1}	X_g	λ_s^{eff}, cm^{-1}
ILs	8067 (1 eV)	1367 (0.17 eV)	0.29	3370.7 (0.42 eV)

In the present context, mention should be made that the conventional Marcus ET model can also not justify the observation of MIR reported in the literature for ET reactions between intercalated dye and the nucleobases in a DNA scaffold at ΔG^0 ~ -0.4 eV,[50] although the observation can be justifiably explained by using the Sumi-Marcus 2-DET model. Moreover, the later model, can also in principle justify the observation of MIR at much lower exergonicity than expected from the value of solvent reorganization energy, as observed in the present study and also reported earlier for bimolecular ET reactions in micelles, reverse micelles, vesicles, supramolecular aggregates and other ionic liquids.[17,18,22,23,27,28,43]

7.4.5 Differential Lifetimes of the Probes and Observed MIR

As stated earlier, the influence of transient (or non-stationary) contribution on the ET reaction can possibly lead to a higher estimate for the k_q values obtained from the simple Stern-Volmer (SV) analysis of the TCSPC and/or SS data. However, the extent of this influence will depend upon the observed time-window for which the quenching data have been collected using a fluorescence probe. As it is indicated from Table 1 that the range of the fluorescence lifetime (τ_0) values for the coumarin dyes used in this study is not very narrow but is spreading over ~1.4 - 5.8 ns. Consequently one may argue that a somewhat higher ET rate can be exhibited by the dyes having shorter lifetime values (e.g. C481 & C152) compared to those having longer lifetimes. To look into this aspect critically and thus to ensure that the observed MIR in viscous media is genuinely stems from the energetics of the ET reactions than due to the differences in the τ_0 values of the dyes, we plotted the τ_0^{-1} values of the studied coumarin dyes against ΔG^0 values for the concerned ET systems, as shown in Figure 8. As observed from this figure, the τ_0^{-1} vs. ΔG^0 plot lacks any resemblance to the bell-shaped Marcus correlation shown in Figure 5 as obtained by plotting the k_0 values against the ΔG^0 values.

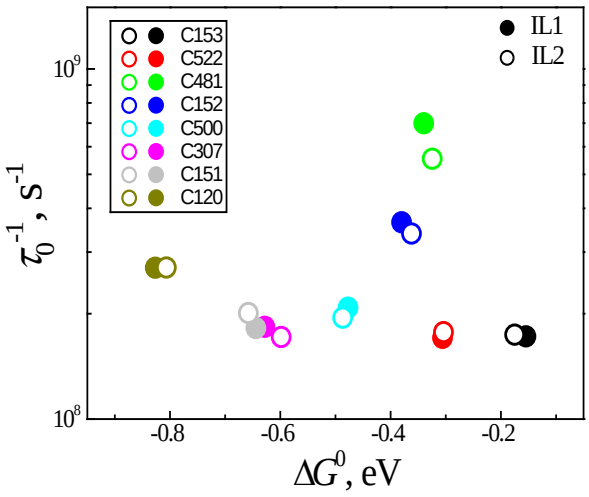

Figure 8: Plot of natural fluorescence decay rate (τ_0^{-1}) in absence of quencher as a function reaction free energy for coumarin-DMAN systems.

For the present ET systems, the k_q values were also estimated using the time-resolved fluorescence quenching data obtained from TCSPC measurements where the average fluorescence lifetime ($<\tau>$) of the dyes in the presence of DMAN quencher were correlated with DMAN concentration following the usual SV analysis as,[29]

$$\frac{\tau_0}{<\tau>} = 1 + k_q \tau_0 [DMAN] \qquad (10)$$

Figure 9 shows the plots of the k_q values thus estimated from the SV analysis of the TCSPC data against ΔG^0 values of ET systems. As indicated from this figure, a clear bell shaped correlation is also indicated for the k_q values in both IL1 and IL2 solvents, similar to those reported by many groups in number of restricted reaction environments (*with respect to reactant diffusion & solvent relaxation*).[17,18,22,23,27,28,43] Comparison of the correlation plots in Figure 5, Figure 8 and Figure 9 it is quite evident to conclude that the energetics of the ET reaction actually play the dominant role in the observation of MIR in viscous media. Interesting to mention here that even though the lifetime of C481 dye ($\tau_0 \approx 1.4$ ns) is much shorter than that of C500 ($\tau_0 \approx 5.0$ ns), the later dye encounters quite a comparable or a higher value for k_q and k_0, respectively, in the two IL solvents studied. This observation is in stark contrast to the argument of Vauthey and co-workers,[31] suggesting the differential lifetimes of the probe dyes as the reason for the observed MIR in viscous media.

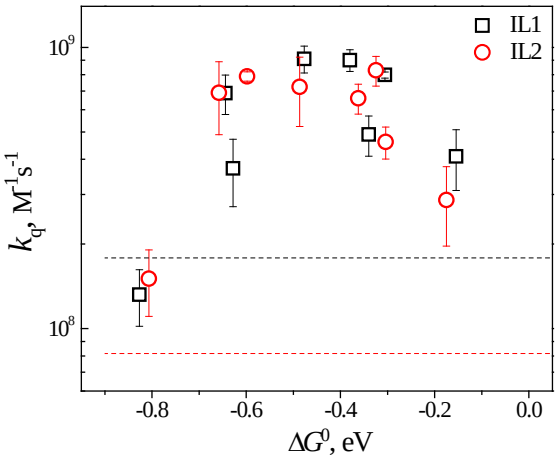

Figure 9: Plot of the k_q values estimated from the TCSPC data against the free energy changes of the ET systems in the IL1 and IL2 solvents studied. The dashed lines represent the diffusion rate expected from the viscosity of the IL1 and IL2 solvent media.

With respect to the present study, following a conservative approach, the diffusion limited rate constant (k_d) can approximately be estimated as ~1.8x10^8 $M^{-1}s^{-1}$ in IL1 and 0.8x10^9 $M^{-1}s^{-1}$ in IL2 solvents, which are much smaller than the k_q values noted at the maxima of the Marcus correlation plots shown in Figure 9. Considering that the k_q values for the present coumarin-DMAN systems in the two IL solvents are in the range of about (1-10) x 10^9 $M^{-1}s^{-1}$, assuming a typical quencher concentration of one molar, which is the highest DMAN concentration range used in the present study, the span of the quenching times ($\tau_q = \{k_q[DMAN]\}^{-1}$) for the present systems is expected to be in the range of 1-10 ns. This range of the τ_q values is well within the observation time window using the TCSPC measurements (*from ~100 ps to around five times of τ_0 values*), even for the shortest lifetime dye (τ_0 =1.43 ns) used in the present study. Therefore, it is understandable that the major part of the non-stationary regime will certainly be monitored by all the fluorophores used in this study, giving a reasonably accurate estimate of the average k_q values. To be mentioned that the contribution of the small portion of the quenching in the non-stationary quenching regime, which is monitored additionally by the longer lifetime coumarin probes at the boundary of non-stationary and stationary regimes, but possibly be missed by using the shorter lifetime dyes, will be quite nominal and hence cannot influence the estimated average k_q values any significantly. This is in fact quite evident from a comparison of Figure 8 and Figure 9, demonstrating beyond

doubt that the shallow distribution of the fluorescence lifetimes of the coumarin dyes used in this study does not obscure the observation of Marcus inversion under restricted reaction environment of the viscous IL solvents used in this investigation. Furthermore, the absence of any clear correlation in the plot of k_0 *vs.* τ_0^{-1}, as shown in Figure 10, also substantiates that the ultrafast ET component is completely independent of the fluorophore lifetimes.

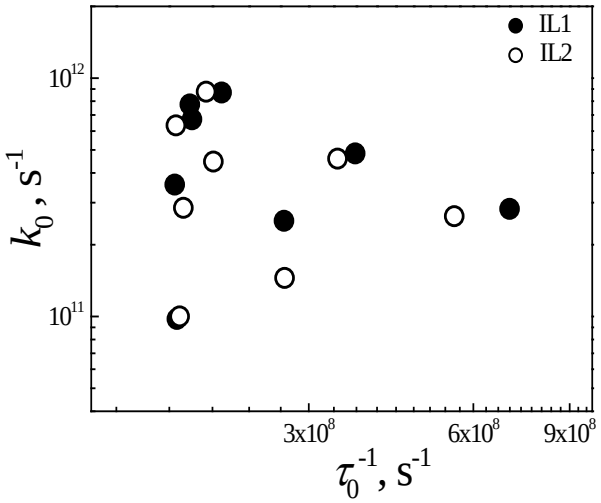

Figure 10: Plot of the k_0 values for the ET systems studied against the τ_0^{-1} values of the coumarin dyes. There is no obvious correlation between the two parameters.

Therefore, it we strongly feel that the distribution of fluorophore lifetimes (at least for the studied coumarin dye systems) does not have any significant influences on the observed MIR for the studied ET reactions in the present IL solvents. It is to be mentioned here that no pronounced influence of the chemical structures of two types of coumarin dyes used in this study, one with unsubstituted amino groups (C500, C307, C151 & C120) and the other with alkyl or julolidinyl substitutions (C153, C522, C481 & C152), could also been observed on the estimated ET/quenching rates in the studied systems. It is thus evident that the observed MIR in the present ET systems certainly arises due to the energetic and kinetic reasons of the ET reactions, which can be well understood and correlated on the basis of the 2DET model, as the ET reaction in the present cases occur under the constrained condition of the viscous IL media where both reactant diffusion and solvent relaxation are exceedingly slow.

7.5 Conclusion:

In conclusion, present study demonstrates with conviction that the MIR for bimolecular ET reactions in viscous media using ultrafast fluorescence up-conversion

measurement, where ET rates are measured directly as the static quenching component, is a genuine observation. Observed results convincingly establish that the MIR for the ET reactions in the studied IL solvents arises mainly due to the energetics and dynamics of the ET reactions and is not influenced any significantly by the differential fluorescence lifetimes of the probe dyes used in the study. It is understood that as the solvation dynamics in the viscous IL solvents are significantly slow, in these solvents the ET reaction actually follows a 2DET model, where the reactant state converts to the product state along the intramolecular vibrational coordinate keeping quite a non-equilibrium situation for the reactants along solvent coordinate, as the thermal equilibration along this coordinate is slower than the ET reaction. Evidently, the conventional Marcus ET model, where the reactant state maintains a thermal equilibrium for both solvent and intramolecular coordinates (*due to exceptionally fast relaxation along both coordinates*), cannot explain the easy observation of MIR in constrained media, especially its appearance at an unusually lower exergonicity ($-\Delta G^0$), much lower than the solvent reorganization energy. In regard to the theoretical modelling of the ET kinetics in viscous media, as adopted by Vauthey and co-workers[31] raising a doubt on the observation of MIR, is understood to be clearly due to the improper choice of the conventional Marcus ET formulation into the diffusive reaction equation. From the observations of the present study we strongly feel that the incorporation of the 2DET formulation into the spherically symmetric diffusion equation will probably be able to theoretically model the ET kinetics properly in viscous media and thus would be able to apprehend the observation of MIR as well as its appearance at exceedingly lower exergonicity, as observed experimentally for the ET reactions in viscous media like ionic liquids and in constrained organized assemblies like micelles, reverse micelles, and so on.

7.6 References:

1. Balzani, V. *Electron Transfer in Chemistry*, Wiley-VCH Publishers Inc., New York, **2001** Vol. I-V.
2. Jortner, J.; Bixon, M. (Eds.), *Electron Transfer from Isolated Molecules to Biomolecules, Adv. Chem. Phys.*, **1999** Wiley, New York, Vol. 106 & 107.
3. Weinberg, D. R.; Gagliardi, C. J.; Hull, J. F.; Murphy, C. F.; Kent, C. A.; Westlake, B. C. Paul, A.; Ess, D. H.; McCafferty, D. G.; Meyer, T. J. *Chem. Rev.***2012**, *112*, 4016.

4. Bolton, J. R.; Mataga, N.; Mc Lendon, G. L. *Electron Transfer in Inorganic, Organic and Biological systems*, Am. Chem. Soc., Washington, DC, **1991**.

6. Fox, M. A.; Chanon, M. *Photoinduced Electron Transfer*, Elsevier, Amsterdam, **1988**.

7. Gray, H. B.; Winkler, J. R. *PNAS*, **2005**, *102*, 3534.

8. (a) Marcus, R. A. *J.Chem.Phys.* **1956**, *24*; (b) Marcus, R. A. *J.Chem.Phys.* **1956**, *24*; (c) Marcus, R. A. *Annu. Rev. Phys.Chem.* **1964**, *15*.

9. (a) Rehm, D.; Weller, A. *Isr. J. Chem.* **1970**, *8*, 259. (b) Rehm, D.; Weller, A. *Ber. Bunsen-Ges. Phys. Chem.***1969**, *73*, 834.

10. Miller, J. R.; Calcaterra, L. T.; Closs, G. L. *J. Am. Chem. Soc.*, **1984**, 106, 3047.

11. Miller, J. R.; Beitz, J. V.; Huddleston, R. K. J. Am. Chem. Soc.,**1984,** 106, 5057.

12. Mataga, N.; Chosrowjan, H.; Shibata, Y.; Yoshida, N.; Osuka, A.; Kikuzawa, T.; Okada, T. *J. Am. Chem. Soc.* **2001**, *123*, 12422.

13. Porter, G. *Chemistry in Microtime*; Imperial College Press: London, **1997**.

14. (a) Rubstov, I. V.; Shirota, H.; Yoshihara, K. *J. Phys.Chem. A* **1999**, *103*, 1801.; (b) Yoshihara, K. In *Electron Transfer: From Isolated Molecules to Biomolecules*; Jortner, J., Bixon, M., Eds.; John Wiley: New York, **1999**; Vol. 107, pp 371.

15. (a) Morandeira, A.; Fürstenberg, A.; Gumy, J.-C.; Vauthey, E. *J. Phys. Chem. A* **2003**, *107*, 5375.; (b) Morandeira, A.; Fürstenberg, A.; Vauthey, E. *J. Phys.Chem. A* **2004**, *108*, 8190.

16. (a) Guldi, D. M.; Asmus, K.-D. *J. Am. Chem. Soc.***1997**, *119*, 5744. (b) Fukuzumi, S.; Yoshida, Y.; Urano, T.; Suenobu, T.; Imahori, H. *J. Am. Chem. Soc.* **2001**, *123*, 11331.

17. Kumbhakar, M.; Nath, S.; Pal, H.; Sapre, A. V.; Mukherjee, T. *J. Chem. Phys.* **2003**,*119*, 388.

18. (a) Satpati, A. K.; Kumbhakar, M.; Nath, S.; Pal, H. *J. Photochem. Photobiol. A* **2008**, *200*,270; (b) Kumbhakar, M.; Dey, S.; Singh, P. K.; Nath, S.; Satpati, A. K.; Gangully, R.; Aswal, V. K.; Pal, H. *J. Phys. Chem. B* **2011**, *115*, 1638.

19. Sumi, H.; Marcus, R. A. *J. Chem. Phys.* **1986**, *84*,4894.

20. (a) Jortner, J.; Bixon, M. *J. Chem. Phys.* **1988**, *88*,167. (b) Bixon, M.; Jortner, J. *Chem. Phys.* **1993**, *176*,467.

21. Pal, H.; Shirota, H.; Tominga, K.; Yosihara, K. *J. Chem. Phys.* **1999**, *110*,11454.

22. Shirota, H.; Pal, H.; Tominga, K.; Yosihara, K. *J. Chem. Phys.* **1998**, *102*,3089.

23. Pal, H.; Nagasawa, Y.; Tominaga, K.; Yoshihara, K. *J. Phys.Chem.* **1996**, *100*, 11964.

24. (a) Welton, T.; Wasserscheid, P. *Ionic Liquids in Synthesis*, VCH-Wiley, Weinheim, **2007**. ; Plechkova, N. V.; Seddon, K. R. *Chem. Soc. Rev.*, **2008**, *37*,123. (b) Chauvin, Y. Olefin Metathesis: The Early Days (Nobel Lecture) *Angew. Chem., Int. Ed.*, **2006**, *45*, 3740.

25. (a) Urahata, S. M.; Riberiro, M. C. C. *J. Chem. Phys.*, **2004**, *120*, 1855.(b) C. Hardacre, J. D. Holbrey, S. E. J. McMath, D. T. Bowron, and A. K. Soper, *J. Chem. Phys.*, **2003**, *118*, 273.

26. (a) Poliakoff, M.; Fitzpatrick, J. M.; Farren, T. R.; Anastas, P. T. *Science*, **2002**, *297*, 807.(b) Seddon, K. R.; Stark, A. ; Torres, M.-J. *Pure Appl. Chem.*, **2000**, *72*, 2275.

27. (a) Kumbhakar, M.; Nath, S.; Mukherjee, T.; Pal, H. *J. Chem. Phys.* **2004**, *120*, 2824; (b) Kumbhakar, M.; Nath, S.; Mukherjee, T.; Pal, H. *J.Chem. Phys.* **2005**, *123*, 034705; (c) Kumbhakar, M.; Singh, P. K.; Nath, S.; Bhasikuttan, A. C.; Pal, H. *J. Phys. Chem. B* **2008**, *112*, 6646; (d) Kumbhakar,M.; Singh, P. K.; Satpati, A. K.; Nath, S.; Pal, H. *J. Phys. Chem. B* **2010**, *114*, 10057; (e) Chakraborty, A.; Chakrabarty, D.; Hazra, P.; Seth, D.; Sarkar, N. *Chem.Phys.Lett* **2003**, *382*, 508; (f) Chakraborty, A.; Seth, D.;Chakrabarty, D.; Hazra, P.; Sarkar, N. *Chem. Phys. Lett.* **2005**, *405*, 18; (g) Ghosh, S.; Mondal, S. K.; Sahu, K.; Bhattacharyya, K. *J. Phys. Chem. A* **2006**, *110*, 13139; (h) Ghosh, S.; Sahu, K.; Mondal, S. K.; Sen, P.; Bhattacharyya, K. *J. Chem. Phys.* **2007**, *126*, 204708; (i) Mandal, U.; Ghosh, S.; Dey, S.; Adhikari, A.; Bhattacharyya, K. *J. Chem. Phys.* **2008**, *128*,164505 ;(j) Sarkar, S.; Mandal, S.; Ghatak, C.; Rao, V. G.; Ghosh, S.; Sarkar, N. *J. Phys. Chem. B* **2012**, *116*, 1335; (k) Tablet, C.; Matei, I.; Hillebrand, M. *J. Mol. Liq.* **2011**, *160*, 57; (l) Fukuzumi, S.; Nishimine, M.; Ohkubo, K.; Tkachenko, N. V.; Lemmetyinen, H. *J. Phys. Chem. B* **2003**,*107*, 12511.

28. (a) Das, A. K.; Mondal, T.; Mojumdar, S. S.; Bhattacharyya, K. *J.Phys. Chem. B* **2011**, *115*, 4680; (b) Yuan, S.; Zhang, Y.; Lu, R.; Yu, A. *J.Photochem. Photobiol. A* **2013**, *260*, 39; (c) Sarkar, S.; Pramanik, R.; Ghatak,C.; Rao, V. G.; Sarkar, N. *J. Chem. Phys.* **2011**, 074507; (d) Sarkar, S.;Pramanik, R.; Ghatak, C.; Rao, V. G.; Sarkar, N. *Chem. Phys. Lett.* **2011**,*506*, 211.

29. Lakowicz, J. R. *Principle of fluorescence spectroscopy*; 3 ed.;Spinger: New York, **2006**.

30. Dudko, O. K.; Szabo, A. *J. Phys. Chem. B* **2005**, *109*, 5891.

31. (a) Rosspeintner, A.; Koch, M.; Angulo, G.; Vauthey, E. *J. Am.Chem. Soc.* **2012**, *134*, 11396; (b) Koch, M.; Rosspeintner, A.; Angulo,G.; Vauthey, E. *J. Am. Chem. Soc.* **2012**, *134*, 3729.

32. The Born correction for the solvent dependence, which takes into account the differences between the driving force in IL compared to that in the reference solvent, e.g., acetonitrile (ε = 37.5), used for redox potential measurements, has not been considered, as various experiments and simulations have shown that electrostatic solvation energies in ILs are typically close to those in high polarity solvents like acetonitrile. The consideration of ε values of these two ILs (7 and 11.5 for [Emim][NTf_2] and [Hmim][NTf_2], repectively) in the Born correction factor only leads to a positive shift of ΔG^0 value by ~0.13 and ~0.25 eV for [Emim][NTf_2] and [Hmim][NTf_2], respectively.

33. (a) Castner, J. E. W.; Kennedy, D.; Cave, R. J. *J. Phys. Chem.A.* **2000**, *104*, 2869; (b) Guldi, D. M.; Luo, C.; Prato, M.;Troisi, A.; Zerbetto, F.; Scheloske, M.; Dietel, E.; Bauer, W.;Hirsch, A. *J. Am. Chem. Soc.* **2001**, *123*, 9166.

34. Horng, M. L.; Gardecki, J. A.; Papazyan, A.; Maroncelli, M. *J. Phys. Chem.* **1995**, *99*, 17311.

35. The quality of the fits were judged by the reduced chi-square (χ^2) values and the distribution of the weighted residuals among the data channels. For good fits the χ^2 values were close to unity and the weighted residuals were distributed randomly among the data channels.

36. Edwards, J. T. *J. Chem. Educ.* **1970**, *47*, 261.

37. McHale, G.; Hardacre, C.; Ge, R.; Doy, N.; Allen, R. W. K.; MacInnes, J. M.; Brown, M. R.; Newton, M. I. *Anal. Chem.* **2008**, *80*, 5806.

38. Yu, G.; Zhao, D.; Wen, L.; Yang, S.; Chen, X. *AIChE Journal* **2012**, *58*, 2885.

39. Liang, M.; Kaintz, A.; Baker, G. A.; Maroncelli, M. *J. Phys. Chem. B* **2012**, *116*, 1370.

40. (a) Rosspeintner, A.; Kattnig, D. R.; Angulo, G.; Landgraf, S.; Grampp, G.; Cuetos, A. *Chem. Eur. J.* **2007**,*13*, 6474. (b) Angulo, G.; Kattnig, D. R.; Rosspeintner, A.; Grampp, G.;Vauthey, E. *Chem. Eur. J.* **2010**, 16, 2291.

41. Tunitskii, N. N.; Bagdasaryan, K. S. Opt. Spektrosk. **1963**, *15*, 100.

42. Jin, H.; Baker, G. A.; Arzhantsev, S.; Dong, J.; Maroncelli, M. *J. Phys. Chem. B* **2007**, *117*,7291.
43. Adhikari, A.; Sahu, K.; Dey, S.; Ghosh, S.; Mandal, U.; Bhattacharyya, K. *J. Phys. Chem. B* **2007**, *111*, 12809.
44. Ingram, J. A.; Moog, R. S.; Ito, N.; Biswas, R.; Maroncelli, M. *J. Phys. Chem. B* **2003**, *107*, 5926.
45. (a) Funston, A. M.; Fadeeva, T. A.; Wishart, J. F.; E. W. Castner, J. *J. Phys. Chem. B* **2007**, *111*, 4963; (b) Zhang, X.-X.; Liang, M.; Ernsting, N. P.; Maroncelli, M. *J. Phys. Chem. B* **2013**, *117*, 4291; (c) Jin, H.; Li, X.; Maroncelli, M. *J. Phys.Chem. B* **2007**, *111*, 13473; (d) Ingram, J. A.; Moog, R. S.; Ito, N.; Biswas, R.; Maroncelli, M. *J. Phys. Chem. B* **2003**, *107*, 5926; (e) Lang, B.; Angulo, G.; Vauthey, E. *J. Phys. Chem. A* **2006**, *110* 7028; (f) Samanta, A. *J. Phys. Chem. Lett.* **2010**, *1*,1557.
46. Rosspeintner, A.; Angulo, G.; Vauthey, E. *J. Am. Chem.Soc.* **2014**, *136*, 2026.
47. Horng, M. L.; Gardecki, J. A.; Papazyan, A.; Maroncelli, M. *J. Phys. Chem.* **1995**, *99*, 17311.
48. Barbara, P. F.; Meyer, T. J.; Ratner, M. A. *J. Phys. Chem.***1996**, *100*, 13148.
49. (a) Heitele, H. *Angew. Chem. Int. Ed. Engl.* **1993**, *32*, 359. (b) Zusman, L. D. *Chem. Phys.* **1980**, *49*, 295; (c) Zusman, L. D. *Chem. Phys.* **1983**, *80*, 29. (d) Barbara, P. F.; Walker, G. C.; Smith, T. P. *Science* **1992**, *256*, 975.
50. Fukuzumi, S.; Nishimine, M.; Ohkubo, K.; Tkachenko, N. V.; Lemmetyinen, H. *J. Phys. Chem. B,* **2003**, *107*, 12511.

Chapter 8

Conclusions

“Reasoning draws a conclusion, but does not make the conclusion certain, unless the mind discovers it by the path of experience.” Roger Bacon

8. Conclusion:

The studies presented in the thesis focused on the effect of solvent on organic reactions and photo-physical reactions in water and ionic liquids. The solvents have been chosen since their ecological impact of chemical methodologies stresses upon their economical viability and environmental affability. The method of investigations pursued kinetic and photo physical studies which facilitated estimation of crucial thermodynamic and kinetic parameters.

From initial studies on the mechanism of 'on water' reactions in heterogeneous condition it has been experimentally proved that the interface created due to vigorous stirring due to the formation of bubbles of reactions in water plays pivotal role in promotion of 'on water' type reaction. Moreover delineation of the responsible physical forces present at the oil/water interface has emphasised on the role of accessible hydrogen bonding offered by the dangling OH groups present at the water surface in stabilizing both reactants and transition states of Diels-Alder and Wittig reaction and thereby decreasing the activation energy.

While water has been emerged as a better reaction medium, immiscibility reactants as well as the absence of hydrogen bonding capability of most of the organic reactants in water logically encouraged us to use ionic liquids as co-solvents to overcome the limited solubility of the reactants. In addition to this instead of using carcinogenic and volatile organic co-solvents, the introduction of ionic liquids as co-solvents is justifiable in terms of maintaining the greenness of medium water. To address selection of apposite ionic liquids as co-solvents for appropriate organic reactions, investigations have been directed to calculate ionic liquid- reactants and ionic liquids–activated state interactions in terms of pairwise interactions. The value of pairwise interactions parameter (G_c) with respect to structural variation of ionic liquids obtained from the present study described in the thesis can act as yardstick for using ionic liquids as co-solvents in future.

The study of excited state proton transfer reactions (ESIPT) in protic ionic liquids has revealed the role of ionic liquids during intramolecular proton transfer reactions. Careful observations of associated energetics and kinetics of proton transfer reactions confirmed the viscosity guided reverse proton transfer along with forward movement of proton. In addition to this emphasis has been given on slow and unusual dynamics of ionic liquids throughout the intra molecular proton transfer study. A qualitative diagram has been given to portray the change in the stability of the excited

states during transfer of proton to facilitate tautomerism reaction in protic ionic liquids based on the estimated kinetic parameters obtained through spectroscopic investigations.

Investigations of bimolecular electron transfer (ET) reactions in ionic liquids having variation in the viscosity values address the role of chemical activation energy over solvent diffusion components. On the basis of estimated results, it has been concluded that not only is the appearance of Marcus Inversion Region particularly indisputable but also the mechanistic model essential to elucidate the observed evidence for the bimolecular ET reactions in a viscous medium is the two-dimensional ET description, which deals with an extremely slow relaxing solvent coordinate and a fast relaxing intramolecular coordinate to describe the ET reactions.

The methodical investigations of solvent effects offer the twin advantages of expansion of the fundamental understanding of the subject and assuring better 'solution' for practical applications in near future.

Appendix A

NMR Spectra

A1 The NMR spectra of the product of the reaction of cyclopentadiene with methyl acrylate: Methyl bicyclo [2.2.1] hept-5-ene-2-carboxylate ^{1}H-NMR (200 MHz, CDCl3): 1.22 (d, 1H), 1.39 (m, 2H), 1.67 (m, 1H), 2.78 (m, 2H), 3.14 (s, 1H), 3.57 (s, 3H), 5.97 (bs, 2H).

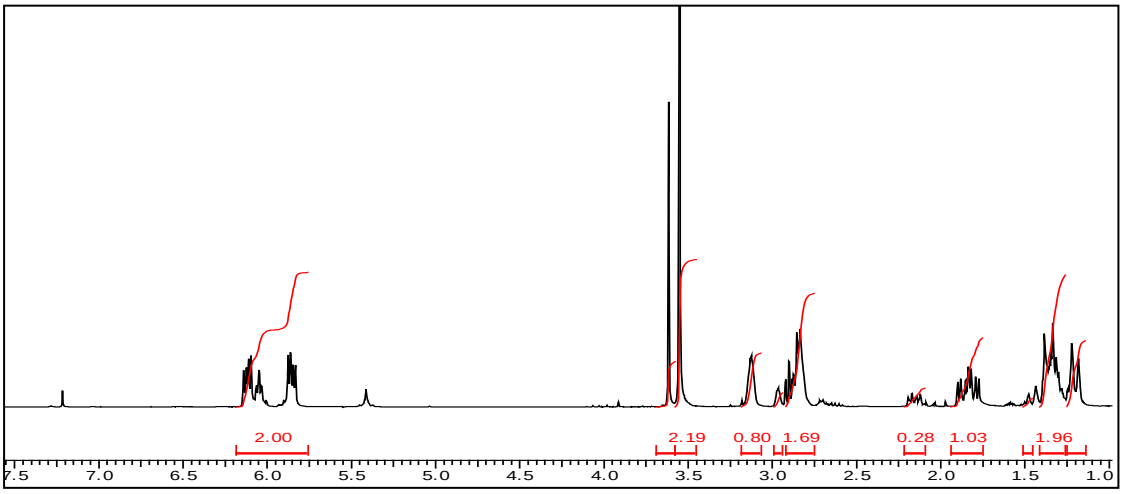

A2 The NMR spectra of the product of Anthracene-9-carbinol (4) with N-ethyl maleimide (5) : adduct (6) ^{1}H-NMR (200 MHz, CDCl3): δ 7.61 (d, 1H), 7.39 (d, 1H), 7.11−7.33 (m, 6H), 5.16 (d, 1H), 4.98 (d, 1H), 4.77 (d, 1H), 3.34 (m, 1H), 3.17 (q, 2H), 0.41 (t, 3H)

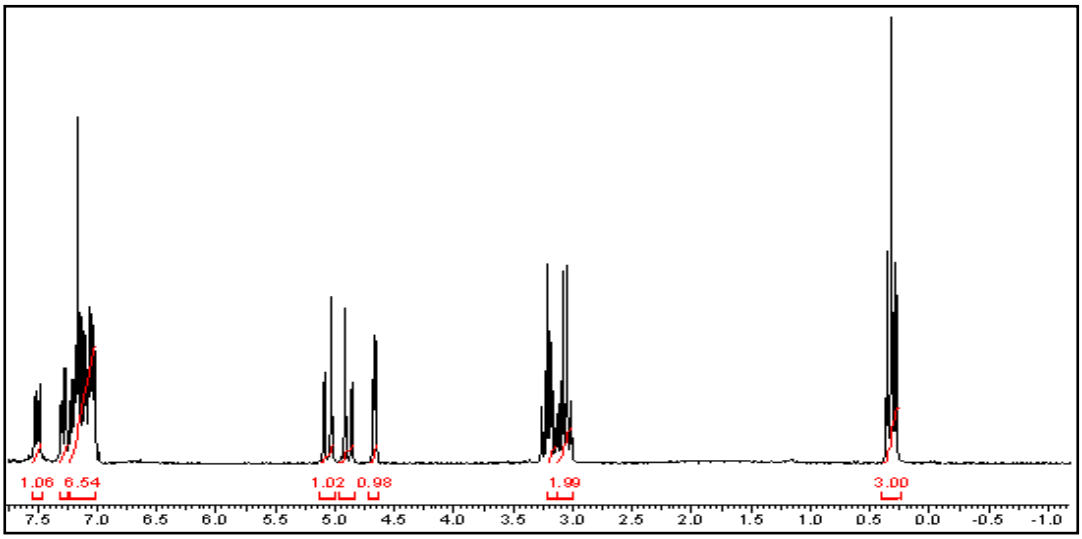

A3 The ^{1}H-NMR spectra of [HmIm]propionate in CDCl3 at 200 MHz

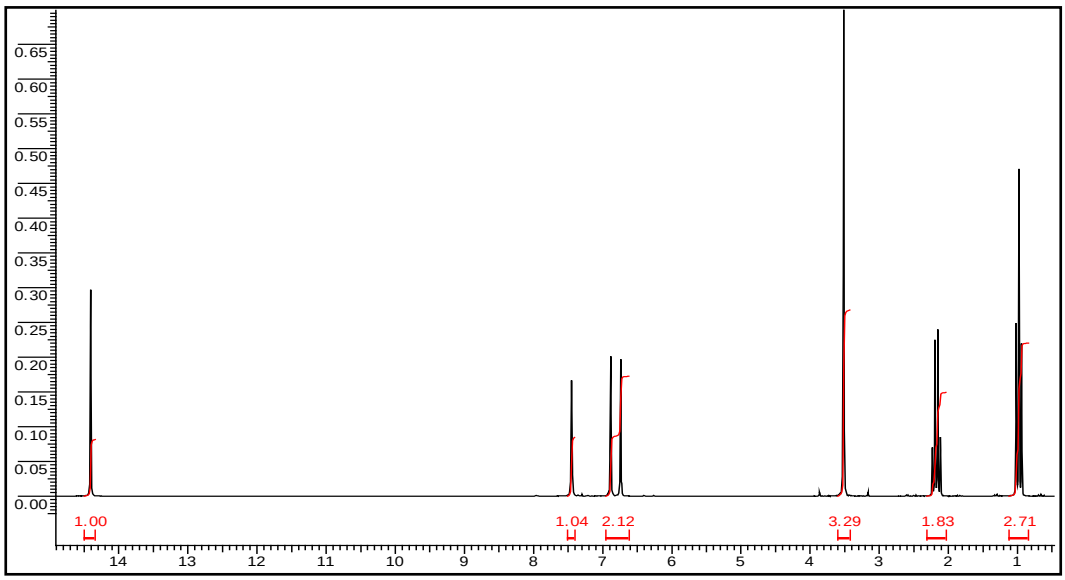

A4 The ^{1}H NMR spectra of [HmIm]acetate in $CDCl_3$ at 200 MHz

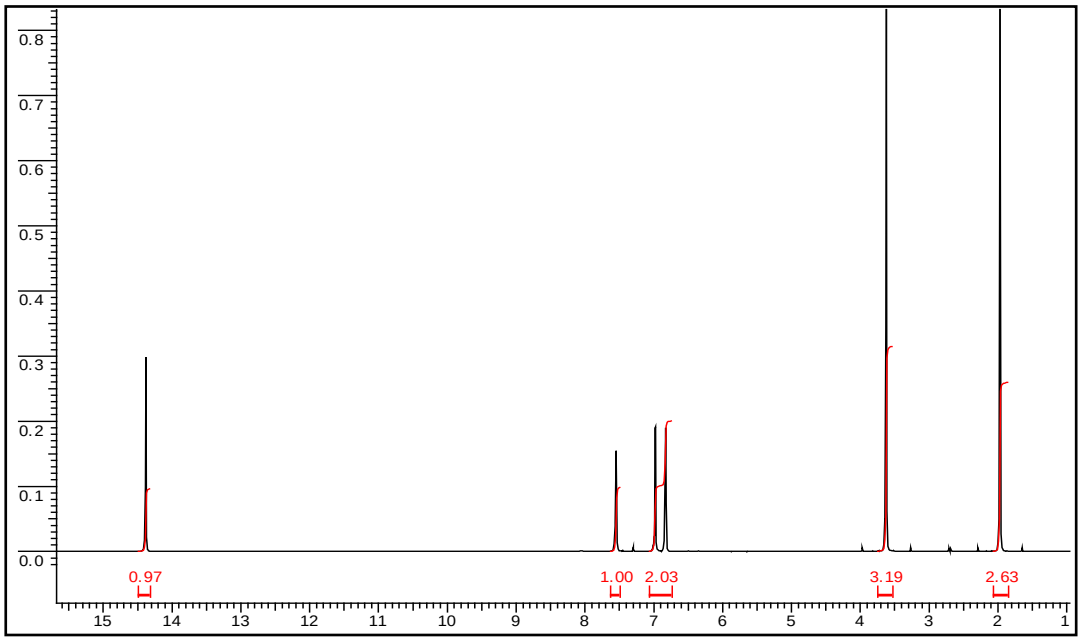

A5 The ^{1}H NMR spectra of [HmIm]formate in $CDCl_3$ at 200 MHz

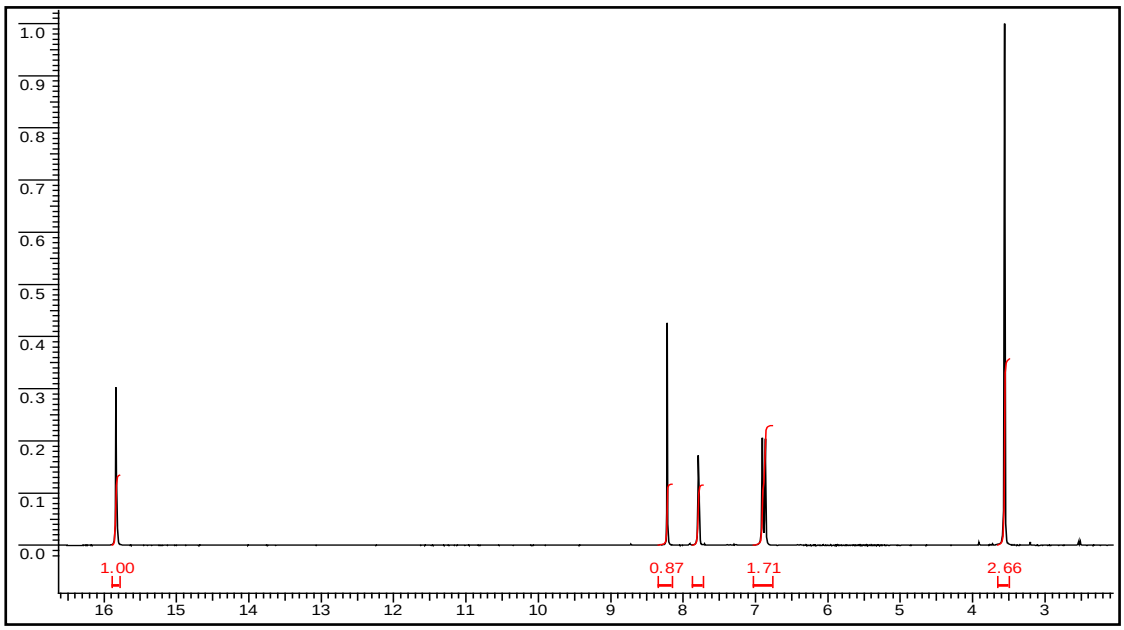

A6 The ^{1}H NMR spectra of [HmIm] bisulfate in DMSO-d^{6} at 200 MHz

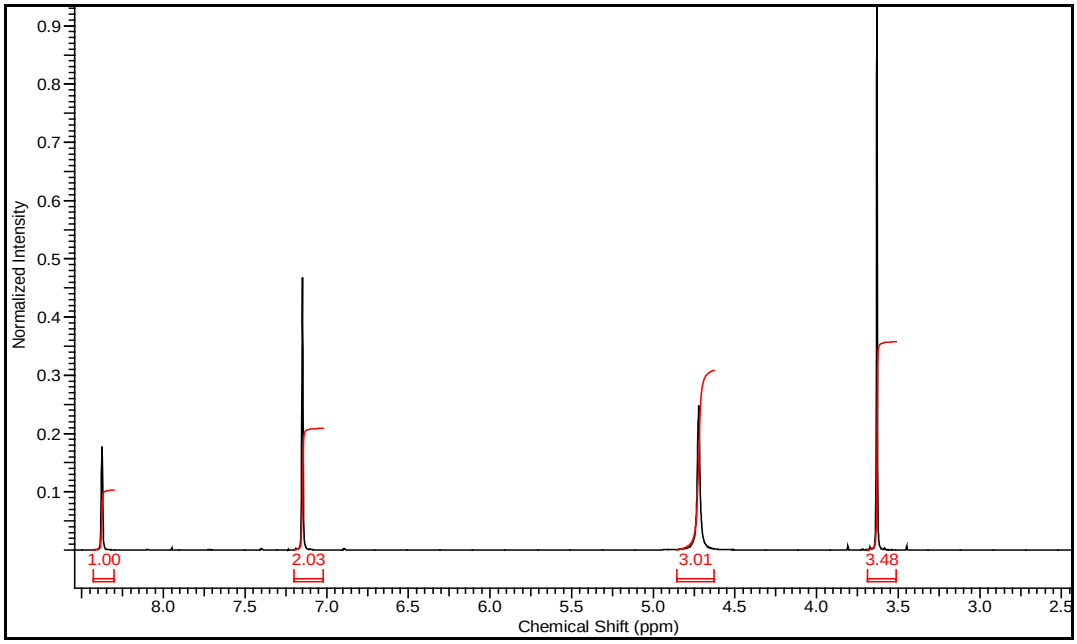

A7 The ^{1}H NMR spectra of [Emim]NTf_2 in $CDCl_3$ at 200 MHz

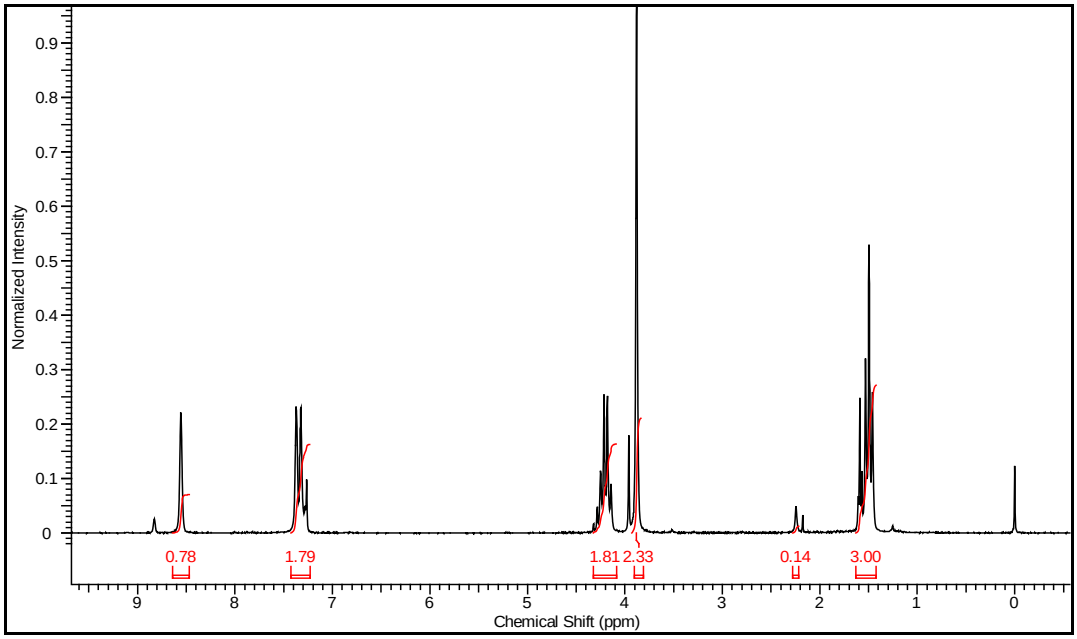

A8 The ^{1}H NMR spectra of [Hmim]NTf_2 in $CDCl_3$ at 200 MHz

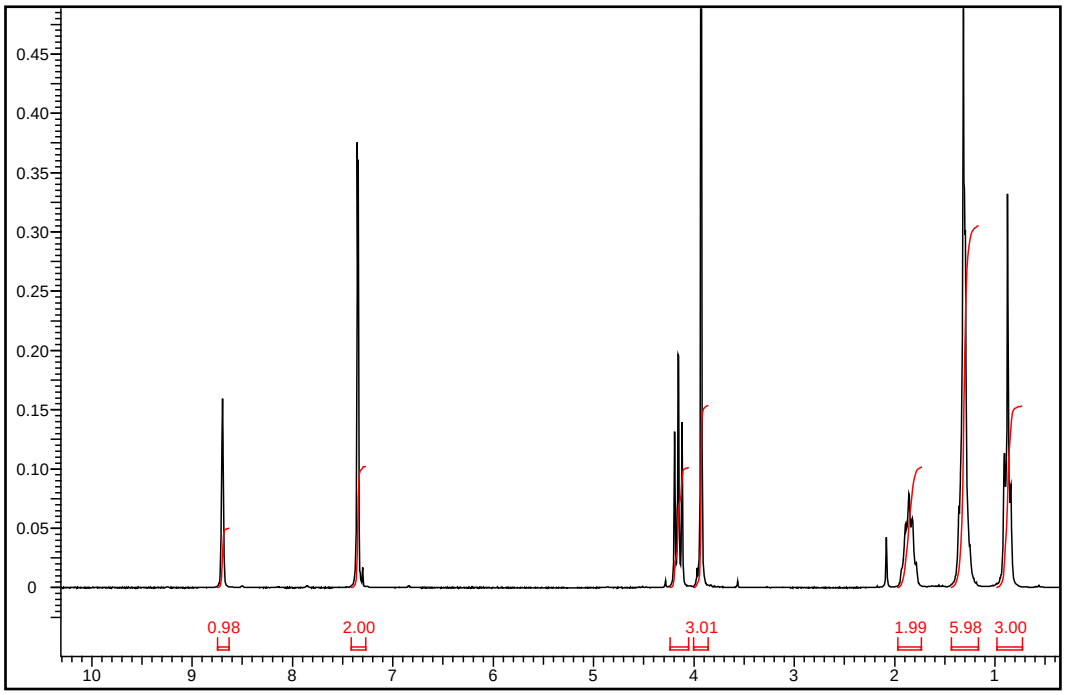

A9 The ^{1}H NMR spectra of [Bmim]BF_4 in $CDCl_3$ at 200 MHz

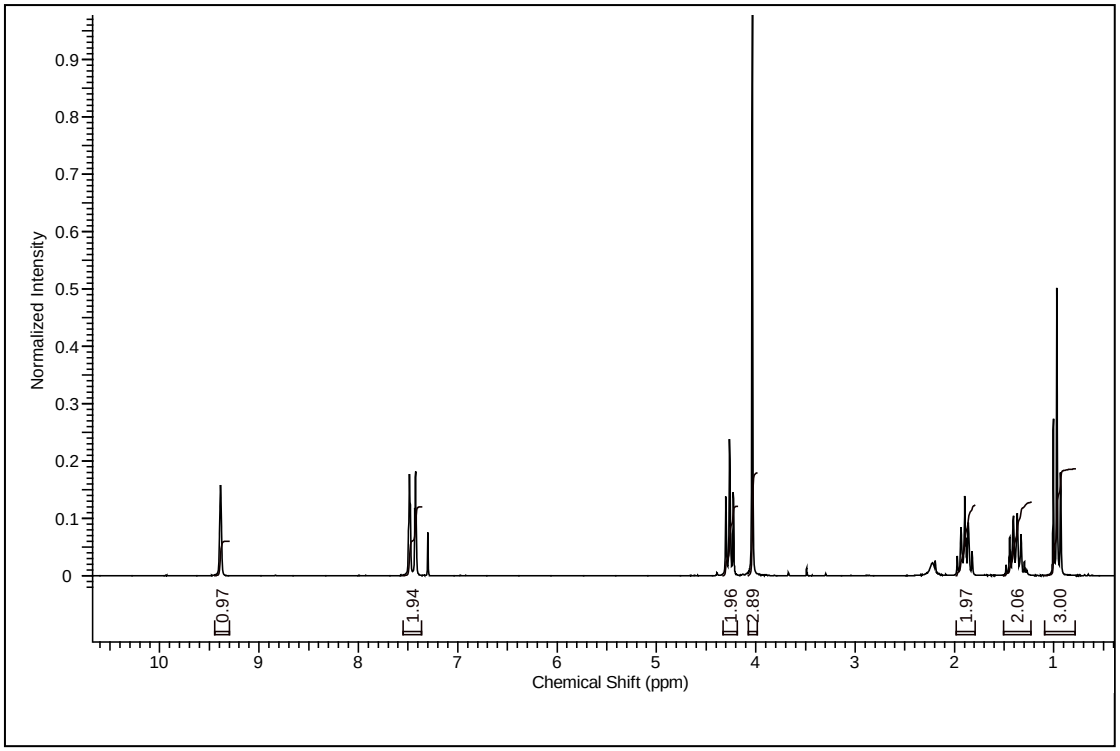

A10 The ^{1}H NMR spectra of [Bmim]NO_3 in $CDCl_3$ at 200 MHz

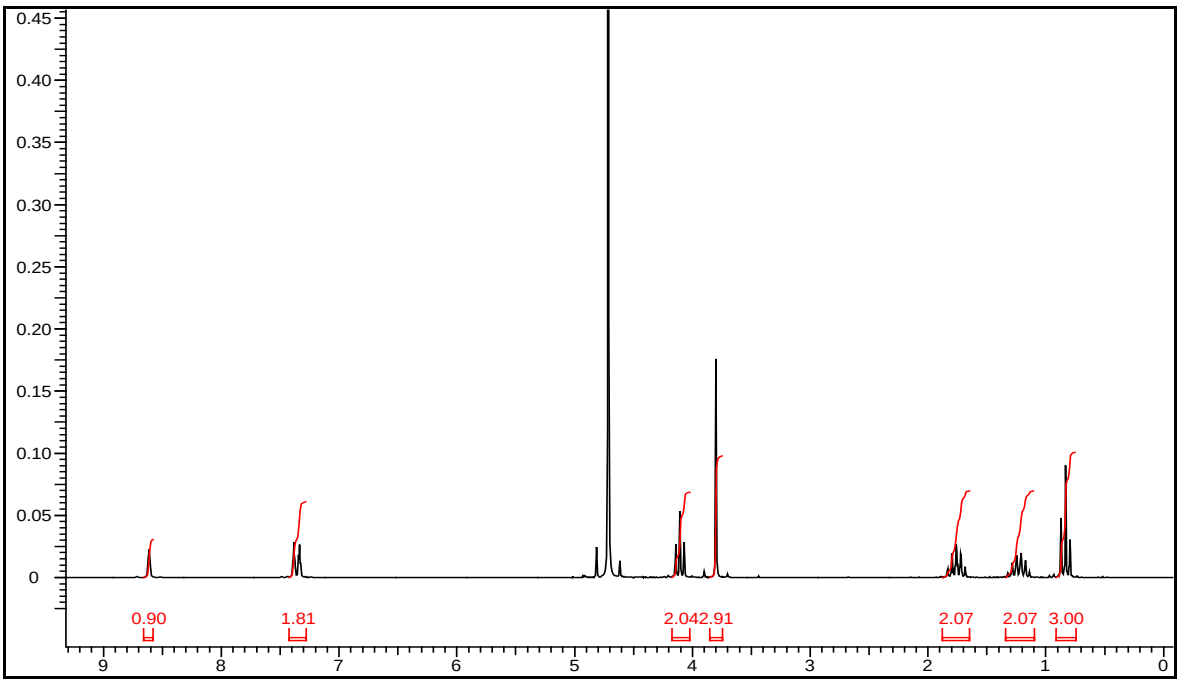

A11 The ^{1}H NMR spectra of [Bmim]Br in $CDCl_3$ at 200 MHz

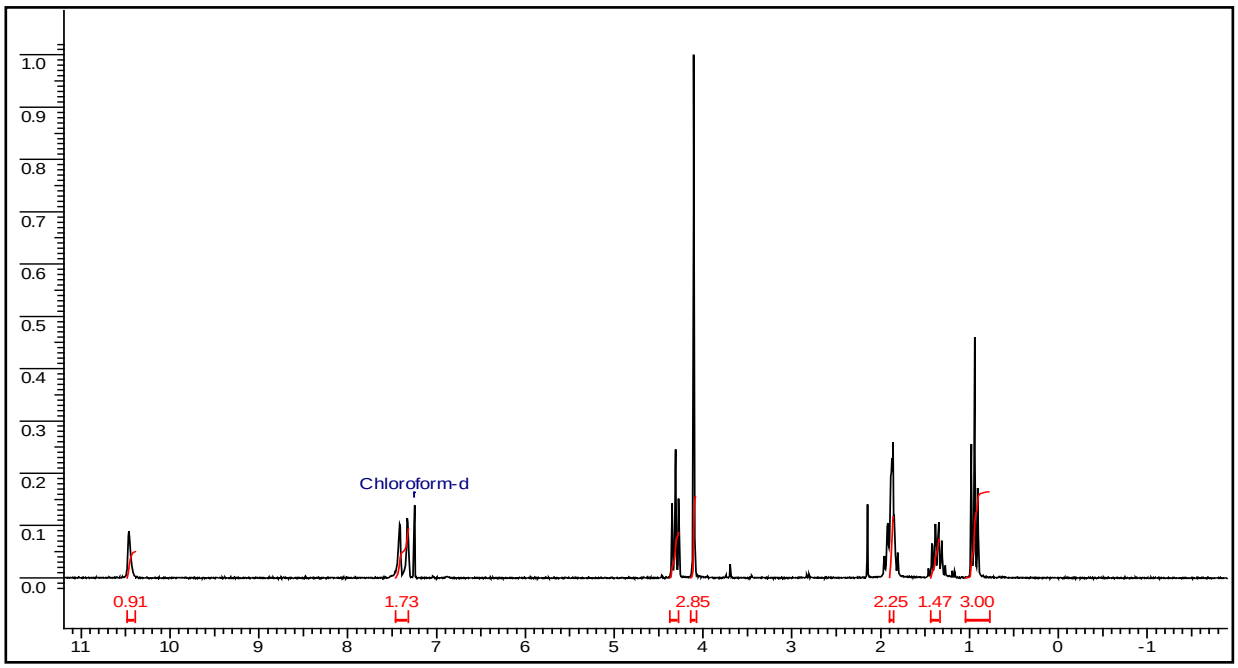

Appendix B
Gas Chromatography Parameters

B. The Detailed GC Method:

The following parameters were set for a typical kinetic analysis for the product methyl acrylate methyl acrylate:Methyl bicyclo [2.2.1] hept-5-ene-2-carboxylate reaction of cyclopentadiene with methyl acrylate methyl acrylate

Column make: CP SIL 5CB
Column length: 15m
Internal diameter: 0.25 mm
Film thickness: 0.25-micron
Flow rate: 0.8 ml/min of nitrogen
Injector temperature: 200^{o}C
Detector temperature: 250^{o}C.
Total run time 18.51 min (Hold at 70^{o}C for 5 min., ramp at 4^{o}C, then maintain at 100^{o}C for 0 min., ramp at 79^{0}C and then maintain at 180^{0}Cfor 5 min.)

Internal Standard (IS): Chlorobenzene

The following parameters were set for a typical kinetic analysis for The NMR spectra of the product of Anthracene-9-carbinol (4) with N-ethyl maleimide (5) : adduct (6)

Column make: CP SIL 5CB
Column length: 15m
Internal diameter: 0.25 mm
Film thickness: 0.25-micron
Flow rate: 0.8 ml/min of nitrogen
Injector temperature: 200^{o}C
Detector temperature: 280^{o}C.

The GC method was calibrated with respect to the product concentrations using pure samples of the products. The amount of product formed as a function of time gave the extent of the reaction (x).

Appendix C

List of Publications

1. "Why Does Water Accelerate Organic Reactions under Heterogeneous Condition?" Arpan Manna and Anil Kumar *J. Phys. Chem. A* **2013** *117*, 2446-2454

2. "Atypical Energetic and Kinetic Course of Excited-State Intramolecular Proton Transfer (ESIPT) in Room-Temperature Protic Ionic Liquids" Arpan Manna, Mhejabeen Sayed, Anil Kumar, and Haridas Pal *J. Phys. Chem. B* **2014,** *118*, 2487-2498

3. "Invoking Pairwise Interactions in the Water-Promoted Diels-Alder Reactions Using Ionic Liquid as a Co-solvent" Arpan Manna, Anil Kumar *Chem. Phys. Chem* DOI: 10.1002/cphc.201402338

4. "Observation of Marcus Inverted Region for Bimolecular Photoinduced Electron Transfer Reactions in Viscous Media" Arpan Manna, Manoj Kumbhakar, Mhejabeen Sayed, Anil Kumar, and Haridas Pal *J. Phys. Chem. B* **2014**, *118, 10704−10715.*

5. * "Investigation of Facile C-C bond Formation Organic Reactions in Natural Supersaturated Media at Ambient Condition " Arpan Manna, Amit Nagare, Anil Kumar *Manuscript submitted for review.*
6. * "Delineation of Forces at Ionic Liquid-Organic Solvent Interface in Promotion of Organic Reactions" Vijay Beniwal, Arpan Manna, Anil Kumar *Manuscript under preparation.*

* **Works have not been included in the present thesis.**

Appendix D

Posters and Oral Presentations

1. Poster presented at “Trombay Symposium for Radiation and Photochemistry” organized by Bhabha Atomic Research Centre, Mumbai, India from 6-9 January, 2014
2. Poster presented at “National Science Day” celebration event organized by National Chemical Laboratory, Pune from 27-28 February 2012.
3. Poster presented at Diamond Jubilee Symposium on Recent Trends in Chemistry event organized by Indian Institute of Technology, Kharagpur from 21-22 October, 2011.
4. Delivered an oral presentation at RSC West India PhD symposium organized by RSC from 03-04 September, 2010.

Erratum